

AD-A073 297

ROCKWELL INTERNATIONAL EL SEGUNDO CA LOS ANGELES DIV  
MECHANICAL POWER SYSTEM FOR AIRCRAFT INTERMITTENT UTILITY FUNCT--ETC(U)

F/G 1/3

APR 79 C W HELSLEY

F33615-75-C-2011

UNCLASSIFIED

RI/LAD-NA-79-64

AFAPL-TR-79-2028

NL

1 OF 3  
AD  
A073297







AFAPL-TR-79-2028

**MECHANICAL POWER SYSTEM FOR AIRCRAFT  
INTERMITTENT UTILITY FUNCTIONS**

C. W. Helsley

Rockwell International Corporation  
Los Angeles Division  
Los Angeles, California 90009

April 1979

Final Report March 1975 - February 1979

Approved for public release; distribution unlimited.

AIR FORCE AERO PROPULSION LABORATORY  
AIR FORCE WRIGHT AERONAUTICAL LABORATORIES  
AIR FORCE SYSTEMS COMMAND  
WRIGHT-PATTERSON AIR FORCE BASE, OHIO 45433

2

LEVEL

AD A 073297

DDC FILE COPY

DDC  
RECEIVED  
AUG 30 1979  
A

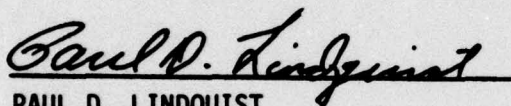
79 08 30 045

NOTICE

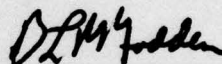
When Government drawings, specifications, or other data are used for any purpose other than in connection with a definitely related Government procurement operation, the United States Government thereby incurs no responsibility nor any obligation whatsoever; and the fact that the government may have formulated, furnished, or in any way supplied the said drawings, specifications, or other data, is not to be regarded by implication or otherwise as in any manner licensing the holder or any other person or corporation, or conveying any rights or permission to manufacture, use, or sell any patented invention that may in any way be related thereto.

This report has been reviewed by the Information Office (OI) and is releasable to the National Technical Information Service (NTIS). At NTIS, it will be available to the general public, including foreign nations.


This technical report has been reviewed and is approved for publication.



PAUL D. LINDQUIST  
Project Engineer  
Power Systems Branch  
FOR THE COMMANDER



B. L. MCFADDEN  
Acting Chief  
Power Systems Branch

  
JAMES D. REAMS  
Chief, Aerospace Power Division

If your address has changed, if you wish to be removed from our mailing list, or if the addressee is no longer employed by your organization please notify AFAPL/POP-1, W-PAFB, OH 45433 to help us maintain a current mailing list.

Copies of this report should not be returned unless return is required by security considerations, contractual obligations, or notice on a specific document.



UNCLASSIFIED

SECURITY CLASSIFICATION OF THIS PAGE (When Data Entered)

| REPORT DOCUMENTATION PAGE   |                       | READ INSTRUCTIONS<br>BEFORE COMPLETING FORM  |
|---|-----------------------|--|
| 1. REPORT NUMBER<br>AFAPL-TR-79-2028  | 2. GOVT ACCESSION NO. | 3. RECIPIENT'S CATALOG NUMBER  |
| 4. TITLE (and Subtitle)<br>Mechanical Power System for Aircraft<br>Intermittent Utility Functions,<br>(Final Technical Report)  |                       | 5. TYPE OF REPORT & PERIOD COVERED<br>Technical Report<br>March 1975 - February 1979 |
| 6. AUTHOR(s)<br>C. W. Helsley   |                       | 7. PERFORMING ORG. REPORT NUMBER<br>NA-79-647  |
| 8. PERFORMING ORGANIZATION NAME AND ADDRESS<br>Rockwell International Corporation<br>Los Angeles Division, P.O. Box 92098<br>Los Angeles, California 90009  |                       | 9. CONTRACT OR GRANT NUMBER(s)<br>F33615-75-C-2011                                   |
| 10. CONTROLLING OFFICE NAME AND ADDRESS<br>Air Force Aero Propulsion Laboratory (POP)<br>Air Force Systems Command<br>Wright-Patterson AFB, Ohio 45433  |                       | 11. PROGRAM ELEMENT, PROJECT, TASK<br>AREA & WORK UNIT NUMBERS<br>3145 30 16         |
| 12. MONITORING AGENCY NAME & ADDRESS (if different from Controlling Office)<br>2291p.   |                       | 13. REPORT DATE<br>April 1979  |
|   |                       | 14. NUMBER OF PAGES<br>272   |
|   |                       | 15. SECURITY CLASS. (of this report)<br>Unclassified                                 |
|   |                       | 15a. DECLASSIFICATION DOWNGRADING<br>SCHEDULE  |
| 16. DISTRIBUTION STATEMENT (of this Report)<br>Approved for public release, distribution unlimited.   |                       |  |
| 17. DISTRIBUTION STATEMENT (of the abstract entered in Block 20, if different from Report)<br>Approved for public release; distribution unlimited.  |                       |  |
| 18. SUPPLEMENTARY NOTES   |                       |  |
| 19. KEY WORDS (Continue on reverse side if necessary and identify by block number)<br>Flywheel<br>Energy Storage<br>Traction Drive  |                       |  |
| 20. ABSTRACT (Continue on reverse side if necessary and identify by block number)<br>→ The program reported upon herein is designed to develop a satisfactory method for utilizing flywheel energy in an aircraft control system. To attain this objective, the program will design, fabricate and demonstrate a mechanical power package (MPP) for controlling and powering a high-horsepower utility actuation function. The MPP will consist of a hydraulic motor, a flywheel, an adapter gearbox, a controller, and a screwjack actuator, and will be designed to replace an existing hydraulic actuator. |                       |  |

DD FORM 1 JAN 73 1473 EDITION OF 1 NOV 65 IS OBSOLETE

UNCLASSIFIED  
SECURITY CLASSIFICATION OF THIS PAGE (When Data Entered)

410665

y/B

## PREFACE

This report presents the results of a development test program for a mechanical power package (MPP), U. S. Air Force Contract F33615-75-C-2011. This test program was performed by the Los Angeles Division (LAD) of Rockwell International (Rockwell). The program was administered by the Air Force Aero Propulsion Laboratory (AFAPL), Wright-Patterson Air Force Base, Ohio. The Air Force project engineer for the program was Mr. Paul Lindquist, AFAPL/POP-3.

The tasks described in this report were performed from March 1975 to February 1979. The program manager was C. W. Helsley, and laboratory tests were conducted by B. J. Call.

|                              |  |
|------------------------------|--|
| Accession For                |  |
| REF ID: A6441                | <input checked="checked" type="checkbox"/><br><input type="checkbox"/><br><input type="checkbox"/> |
| DOC TAB                      |  |
| Unannounced<br>Justification |  |
| By _____                     |  |
| Distribution/                |  |
| Availability Codes           |  |
| Dist                         | Avail and/or<br>special  |
| A                            |  |

79 08 30 045

# TABLE OF CONTENTS

| Section    |  | Page |
|------------|--|------|
| I          | INTRODUCTION AND SUMMARY   | 1    |
|            | General  | 1    |
|            | Mechanical Power Package Program                                     | 1    |
| II         | TECHNICAL DISCUSSION   | 3    |
|            | Task I - Analysis  | 3    |
|            | Task IA  | 3    |
|            | Task IB  | 10   |
|            | Task II - Design and Fabrication                                     | 26   |
|            | Original Design Concept  | 26   |
|            | MPP System Design  | 28   |
|            | MPP Power Flow Analysis  | 31   |
|            | Energy Analysis  | 43   |
|            | MPP System Procurement   | 46   |
|            | Component Design   | 46   |
|            | Task III - System Tests  | 188  |
|            | Mechanical Power Package Test Plan                                   | 188  |
| III        | CONCLUSIONS AND RECOMMENDATIONS                                      | 205  |
| APPENDIX A | SPECIFICATION POWER TRANSMISSION GEARBOX<br>MECHANICAL POWER PACKAGE | 209  |
| APPENDIX B | MECHANICAL POWER PACKAGE TEST REQUIREMENTS                           | 255  |



# LIST OF ILLUSTRATIONS

| Figure |   | Page |
|--------|---|------|
| 1      | Schematic - Mechanical Power Package . . . . .  | 2    |
| 2      | B-1 Aircraft Hydraulic Load Profile . . . . .   | 4    |
| 3      | 747 Aircraft Hydraulic Load Profile . . . . .   | 5    |
| 4      | L1011 Aircraft Hydraulic Load Profile . . . . .   | 6    |
| 5      | Flow Demand Profile for Systems No. 1 and 2 (C5A) . . . . .   | 7    |
| 6      | Main Landing Gear . . . . .   | 11   |
| 7      | Main Landing Gear Cylinder Extending Cycle (No<br>Airload Vs 280 Knots, $\mu = 0.20$ ) . . . . .      | 13   |
| 8      | Main Landing Gear Cylinder Retracting Cycle (No<br>Airload Versus 280 Knots, $\mu = 0.20$ ) . . . . . | 14   |
| 9      | Main Landing Gear Cylinder Air Vehicle on Jacks<br>(No Airload) . . . . .                             | 15   |
| 10     | Main Landing Gear Cylinder Extending Cycle (No<br>Airload Versus 280-Knot Airload) . . . . .          | 16   |
| 11     | Main Landing Gear Cylinder Retracting Cycle (No<br>Airload Versus 280-Knot Airload) . . . . .         | 17   |
| 12     | Main Landing Gear Cylinder (No Airload) . . . . .   | 18   |
| 13     | Main Landing Gear Cylinder Retracting Cycle<br>(190 Knot Airload) . . . . .                           | 19   |
| 14     | Main Landing Gear Cylinder Composite Cycle . . . . .  | 21   |
| 15     | Wheel Well Compartment Temperature - Main Gear . . . . .  | 22   |
| 16     | Mechanical Power Package . . . . .  | 27   |
| 17     | MPP Power Flow . . . . .  | 32   |
| 18     | Flywheel Speed Reduction Versus Energy Storage . . . . .  | 34   |
| 19     | Ball Screw Loss Characteristics . . . . .   | 35   |
| 20     | Screwjack Reduction Gear Train Losses (63.28:1 Ratio) . . . . .                                       | 37   |
| 21     | Mechanical Controller Loss Characteristics . . . . .  | 38   |
| 22     | Roller Toroid Type Mechanical Valve . . . . .   | 39   |
| 23     | Gearbox Loss Characteristics . . . . .  | 41   |
| 24     | Flywheel Loss Characteristics . . . . .   | 42   |
| 25     | Early Flywheel Design . . . . .   | 48   |
| 26     | Flywheel Shapes . . . . .   | 52   |
| 27     | Flight Operations . . . . .   | 56   |
| 28     | Ground Operations (On Jacks) . . . . .  | 56   |
| 29     | Critical Crack Length . . . . .   | 58   |
| 30     | Cycles to Critical Flaw Size . . . . .  | 59   |
| 31     | Typical Hydrodynamic Bearing . . . . .  | 63   |
| 32     | Typical Hydrostatic Bearing . . . . .   | 65   |

| Figure | LIST OF ILLUSTRATIONS (continued)   | Page |
|--------|---|------|
| 53     | Proposed Series (Hydrodynamic-Hydrostatic)<br>Bearing . . . . .   | 60   |
| 54     | Proposed Series - Hybrid Bearing . . . . .  | 67   |
| 55     | Flywheel Centrifugal Forces (Ball Bearing Radial<br>Runout Omitted) . . . . .   | 72   |
| 56     | Flywheel Shaft Detail . . . . .   | 74   |
| 57     | Bearing Loads Versus Radial Clearance and No Oil<br>(Duplex 9103WO Bearings, 40-Pound Preload . . . . .                             | 82   |
| 58     | Shaft Bending Stresses Versus Radial Clearance and<br>No Oil (Duplex 9103WO Bearings, 40-Pound Preload) . . .                       | 83   |
| 59     | Precession Load Effects . . . . .   | 87   |
| 40     | Rotating Load Diagram . . . . .   | 96   |
| 41     | Ball Path Characteristics Under Load . . . . .  | 100  |
| 42     | Bearing Deflection - Radial Load at Ball Liftoff<br>Versus Preload in Duplex Sets (Load-Sharing =<br>(i) <sup>0.7</sup> ) . . . . . | 105  |
| 43     | Bearing Deflection Rate Versus Radial Load Only<br>( $\beta_0 = 0^\circ$ ) (Duplex Bearing) . . . . .                               | 107  |
| 44     | Bearing Deflection Rate Versus Preload (Axial<br>Thrust Only) . . . . .   | 108  |
| 45     | Bearing Deflection Under Pure Thrust Load Only . . . . .  | 109  |
| 46     | Typical Duplex Bearing Arrangement (Face-to-Face<br>Mounting) . . . . .   | 111  |
| 47     | Deflection Rate Versus Radial Load, 9103-WI,<br>Duplex Bearing . . . . .  | 115  |
| 48     | Bearing Friction Torque Versus Speed and Preload<br>at Mean Radial Load . . . . .   | 119  |
| 49     | Bearing Friction Torque Versus Speed and Preload<br>at Mean Radial Load . . . . .   | 120  |
| 50     | Bearing Friction Power Loss Versus Speed and<br>Preload at Mean Radial Load . . . . .   | 121  |
| 51     | Bearing Friction Power Loss Versus Speed and<br>Preload at Mean Radial Load . . . . .   | 122  |
| 52     | Cooling Oil Required Versus Speed and Preload . . . . .   | 124  |
| 53     | Apparent Bearing Life Versus Speed and Preload,<br>9103 Duplex . . . . .  | 127  |
| 54     | Apparent Bearing Life Versus Speed and Preload,<br>9104 Duplex . . . . .  | 128  |
| 55     | Apparent Bearing Life Versus Speed and Preload,<br>9305 Duplex . . . . .  | 129  |
| 56     | Ball Centrifugal Force Action . . . . .   | 151  |

| Figure | LIST OF ILLUSTRATIONS (continued)  | Page |
|--------|--|------|
| 57     | Normal Approach of Race Curvatures . . . . .   | 133  |
| 58     | Contact Angle Change Due to Preload and<br>Centrifugal Force . . . . .   | 135  |
| 59     | Axial Shift Due to Preload and Centrifugal Force<br>at High Speeds, Bearing Size 9103-WI . . . . .                 | 137  |
| 60     | Apparent Decrease in Bearing Preload Due to<br>Centrifugal Force at High Speeds, Bearing<br>Size 9103-WI . . . . . | 138  |
| 61     | Flywheel Bearing Assy - 88,000 RPM . . . . .   | 141  |
| 62     | Friction Torque Versus Radial Clearance . . . . .  | 144  |
| 63     | Friction Horsepower Versus Radial Clearance . . . . .  | 145  |
| 64     | Ferro Fluid Seal . . . . .   | 152  |
| 65     | Flywheel Assembly . . . . .  | 155  |
| 66     | MPP Lubrication and Cooling System Schematic . . . . .   | 158  |
| 67     | Gear Drive Assembly . . . . .  | 161  |
| 68     | Controller Assembly . . . . .  | 164  |
| 69     | Controller . . . . .   | 165  |
| 70     | Infinitely Variable Traction Section . . . . .   | 166  |
| 71     | Ratio Change Forces . . . . .  | 168  |
| 72     | Bidirectional Planetary Gear Set . . . . .   | 170  |
| 73     | Controller Control System . . . . .  | 172  |
| 74     | Controller Assembly . . . . .  | 175  |
| 75A    | Controller Design Tab Run, Sheet 1 . . . . .   | 179  |
| 75B    | Controller Design Tab Run, Sheet 2 . . . . .   | 180  |
| 75C    | Controller Design Tab Run, Sheet 3 . . . . .   | 181  |
| 76     | Screwjack Actuator Assembly, Sheet 1 . . . . .   | 185  |
| 77     | Screwjack Actuator Assembly, Sheet 2 . . . . .   | 185  |
| 78     | MPP Assembly for Test . . . . .  | 189  |
| 79     | Controller Loss Characteristics . . . . .  | 192  |
| 80     | MPP Assembly Fit Check - Inboard View . . . . .  | 200  |
| 81     | MPP Assembly Fit Check - Outboard View . . . . .   | 201  |



# LIST OF TABLES

| Table |  | Page |
|-------|--|------|
| 1     | Endurance Test Load Duty Cycle . . . . .                 | 23   |
| 2     | Actuation System Speeds . . . . .                        | 31   |
| 3     | MPP Flywheel Bearing Load Summary (Lb) at 88,235 RPM . . | 92   |
| 4     | Bearing Characteristics . . . . .                        | 101  |
| 5     | SN 1 Controller Losses (HP) . . . . .                    | 191  |
| 6     | MPP Controller Changes to Eliminate Rumble . . . . .     | 194  |
| 7     | Controller Losses (HP) . . . . .                         | 195  |
| 8     | MPP Controller Stability Tests . . . . .                 | 197  |

## SECTION I

### INTRODUCTION AND SUMMARY

#### GENERAL

This program was conducted in recognition of the fact that the power requirements for present-day aircraft hydraulic systems are frequently determined by the peak power demands of utility functions on the aircraft. These power demands occur for time durations of less than one minute and are repeated only one or two times a flight. Previous programs (Reference 1) had demonstrated that an aircraft hydraulic power generation system's size and weight could be significantly reduced by using stored energy to meet the peak power demand. Those programs also demonstrated that flywheels were a practical energy storage device for providing the required energy. However, practical power extraction methods had not been established for utilizing flywheels. The basic objective of this program was to demonstrate, through actual hardware development and test in a realistic application, that practical power extraction methods were available. A secondary objective was to show that large power demand utility functions, which have historically been powered exclusively by hydraulics, could be powered electrically.

#### MECHANICAL POWER PACKAGE PROGRAM

To achieve its objectives, the program evaluated various large power demand work functions, associated with existing aircraft, and selected one to be used as the basis for test and development. This was the B-1 aircraft's main landing gear actuation function. The program also designed, fabricated, and partially demonstrated a mechanical power package unit. The mechanical power package (MPP) consisted of a hydraulic motor, a flywheel, a gearbox, a controller, and a screwjack actuator arranged as shown in Figure 1.

The MPP unit was designed to be a direct physical replacement for the existing hydraulic actuator. It was also designed to extend and retract the main landing gear against the same loads and in the same operating times as the existing actuator but to do it through energy stored in the flywheel, using only one-fifth the power (flow) of the existing system.

The program was accomplished in four tasks, as follows:

- Task I - Analysis
- Task II - Design and Fabrication
- Task III - Test
- Task IV - Reporting

Reference 1. Call, B.J., Helsley, C.W., Jr., and Cruther, C.A., "Energy Storage Concepts for Aircraft Actuation Functions," AFAPL TR-66-29, April 1966

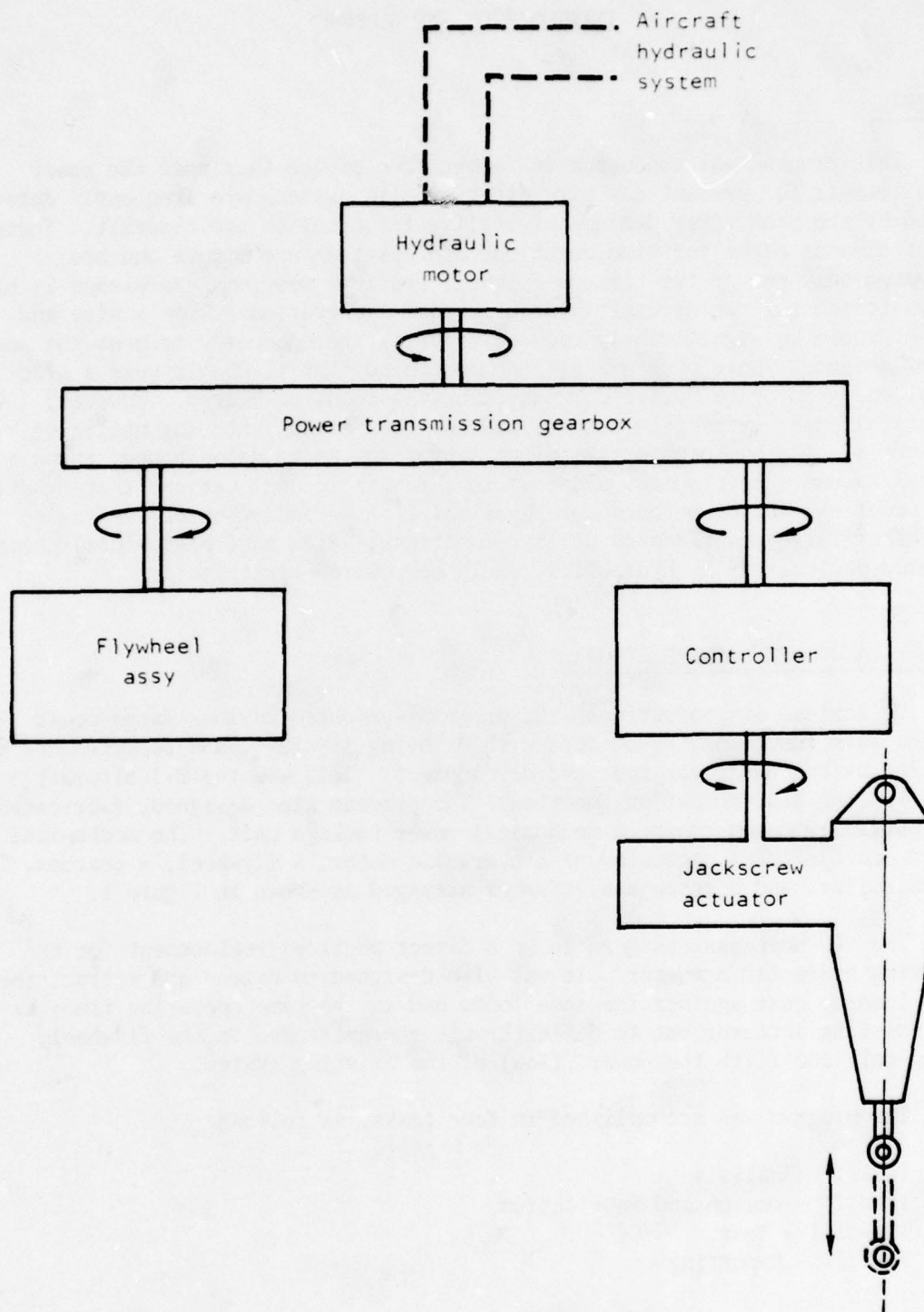


Figure 1. Schematic - Mechanical Power Package



## SECTION II

### TECHNICAL DISCUSSION

#### TASK I - ANALYSIS

Task I was accomplished in two subtasks, which were as follows:

Task IA - Selection of utility work function

Task IB - Establishment of power requirements and duty cycle

#### TASK IA

The requirements for this task were to involve the selection of a utility work function that was performed by conventional hydraulic techniques on a present-day aircraft. The input power level (peak) of the work function was to be over 50 hp in order to indicate that there was a potential for application of MPP's to a wide range of future high-performance aircraft. The selected work function was also to be adaptable to rotary input power.

To accomplish this task, a range of aircraft was studied including fighters, bombers, and transport types. The specific aircraft studied were the B-1, 747, L1011, C5A, and Rockwell's proposals for the F-14 and F-15 aircraft. From these studies, two important facts emerged. These were as follows:

- 1) Utility function type MPP's will save considerable weight when applied to large subsonic aircraft.
- 2) Utility function type MPP's must be supplemented by flight control function type MPP's if weight is to be saved in high-performance, supersonic-type aircraft.

The verification of these two statements may be seen by examining Figures 2, 3, 4, and 5. Figure 2 is the hydraulic system 2 load profile for the B-1 aircraft. This figure shows that three subsystems contribute to the peak loads experienced by the hydraulic power system with the magnitude of each subsystem's contribution being shown by the crosshatched areas. Two of the subsystems are of the utility function type (landing gear and wing sweep), while the third system is of the flight control type (horizontal stabilizer). If MPP's were applied only to the two utility functions, the overall weight

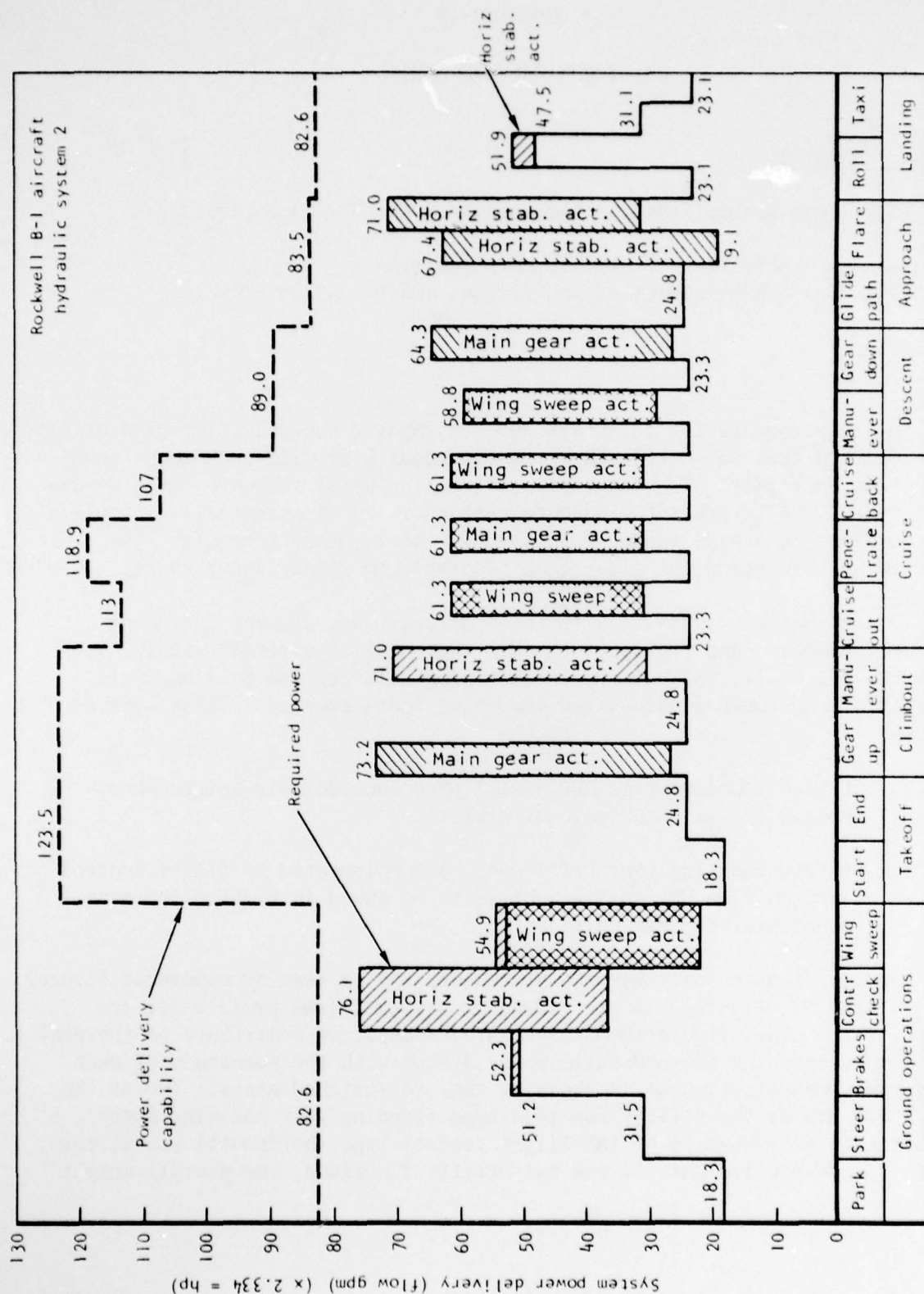


Figure 2. B-1 Aircraft Hydraulic Load Profile

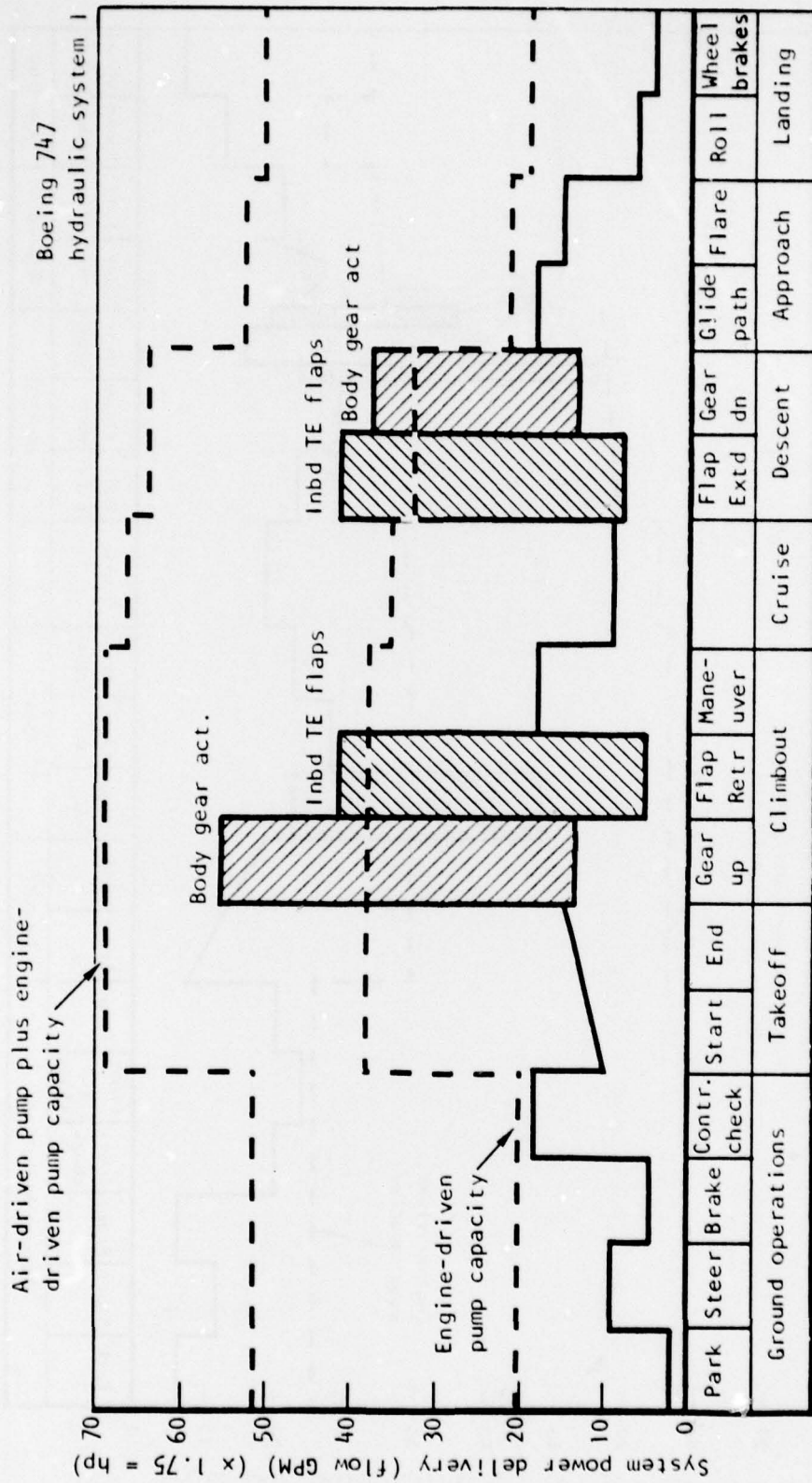


Figure 3. 747 Aircraft Hydraulic Load Profile



# Lockheed L1011 hydraulic system C

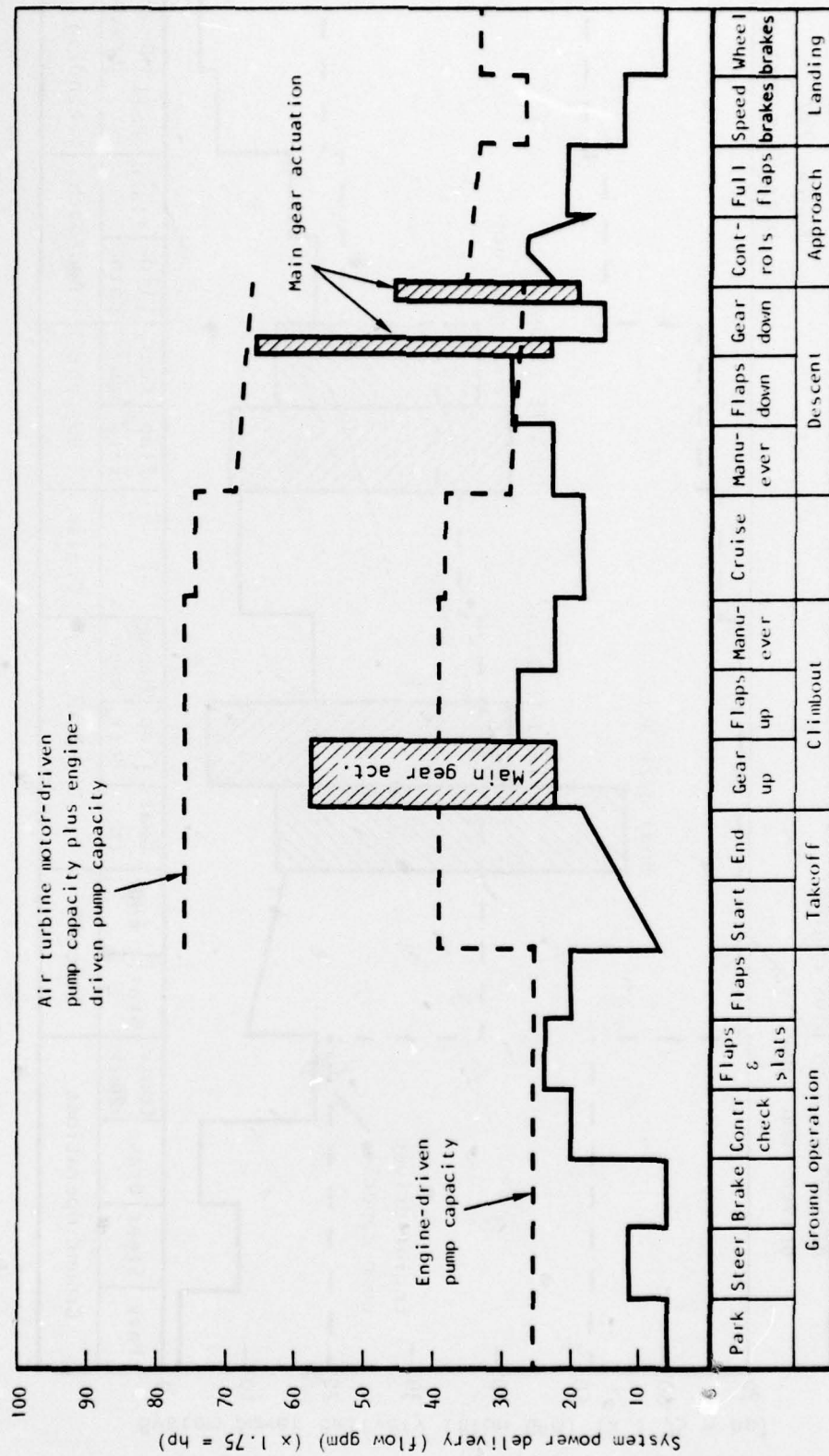


Figure 4. L1011 Aircraft Hydraulic Load Profile

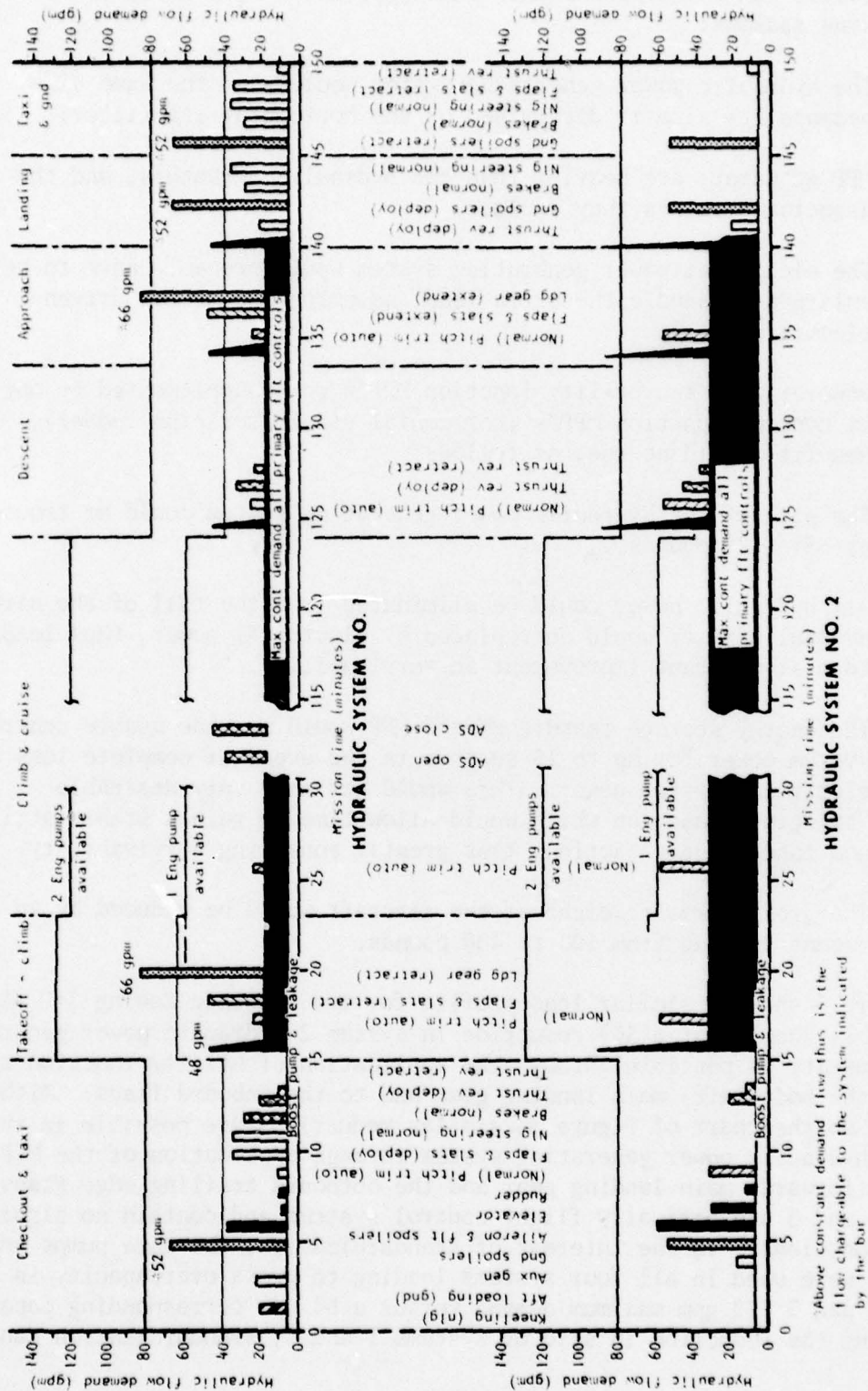


Figure 5. Flow Demand Profile for Systems No. 1 and 2 (C5A)



of the aircraft would increase rather than decrease. This would be true for the following reasons:

- 1) The hydraulic power generating system would stay the same size because its size is determined by the horizontal stabilizer.
- 2) MPP actuators are heavier than the hydraulic actuators, and the associated valves they replace.
- 3) The electrical power generating system would probably have to be enlarged to handle the extra load (assuming the MPP is driven electrically).

If, however, the two utility function MPP's were supplemented by one or more flight control function MPP's (horizontal stabilizer plus rudder), numerous benefits would accrue, as follows:

- 1) The size of the hydraulic power generating system could be reduced by 33% (425 pounds).
- 2) All hydraulic power could be eliminated from the tail of the aircraft. Hydraulic power would be replaced by electrical power, thus leading to a significant improvement in survivability.
- 3) The energy storage feature of the MPP would provide usable control system power for up to 15 seconds in the event of complete loss of electrical system power. This would act as a very desirable "bridging" function which would allow time to gain a stable attitude and take remedial action, thus greatly enhancing survivability.
- 4) The gross takeoff weight of the aircraft would be reduced by an amount ranging from 100 to 400 pounds.

Figure 3 shows a similar load profile for the subsonic Boeing 747 aircraft. This shows that a 50% reduction in system 2 hydraulic power generating system capacity is possible through the application of utility function type MPP's to the body (aft) main landing gear and to the inboard flaps. Although not shown on the chart of Figure 3, similar reductions are possible in the system 4 hydraulic power generating system through application of the MPP to the wing (forward) main landing gear and the outboard trailing edge flaps. Systems 2 and 3 are basically flight control systems and contain no significant utility functions. In the interest of standardization, the same pumps and gearboxes were used in all four systems leading to gross overcapacity in systems 2 and 3 (30 gpm maximum demand versus a 64 gpm corresponding capacity). By allowing the reduction in size of systems 1 and 4, standardization can

still be maintained with none of the systems being grossly oversized. In view of this system peculiarity, the use of MPP's on the 747 aircraft would allow an exceptionally large reduction in gross takeoff weight.

Figure 4 is the load profile for hydraulic system "C" on the Lockheed L1011 aircraft. It can be seen that the application of the MPP to the landing gear only is sufficient to reduce the size of the pumping system by slightly more than 56%.

Hydraulic flow demand profiles for systems 1 and 2 on the C5A aircraft are shown in Figure 5. It will be noted that the profiles differ considerably with system 1 exhibiting large utility function demands and system 2 having large flight control function demands. Although not shown, system 3 is essentially similar to system 2 (i.e., large flight control function demands), and system 4 is essentially identical to system 1.

Examining system 1 more closely, it can be seen that if the ground spoiler and landing gear system demands (both utility functions) can be reduced to one-third of their present values (i.e., 17.3 and 22 gpm, respectively) through the use of MPP's, the size of the pumping system (for both systems 1 and 4) can be cut in half. It is true that the descent, approach, and landing flight control system demand spikes will momentarily exceed capacity (48 gpm demand versus 40 gpm capacity). However, it will also be noted that in system 2, as presently designed and sized, flight control system demand spikes exceed capacity by at least that much. It is also true that flap-slat system (utility system) demand would also exceed capacity during approach (47 versus 40 gpm). However, in system 1, as it is presently designed and sized, landing gear extend demand exceeds capacity by nearly as much. These overdemand are taken care of in the present system through inherent system accumulator action supplemented by power transfer units, and would be taken care of in the reduced size MPP-type system in the same manner.

Data obtained from the Rockwell International proposal on the F-14 and F-15 (supersonic high-performance aircraft) were also examined. In common with the B-1 aircraft, these aircraft indicated the need for the development of a flight control type MPP before significant aircraft weight reductions can be made in these types of aircraft. The reason that this is true is that on high-performance, supersonic aircraft, a flight control surface (usually the horizontal tail) tends to become the major power user, whereas on subsonic aircraft, the landing gear and/or flaps (utility functions) are usually the prime power users. The reason for the shift in power demand arises from the fact that the power demand of the landing gear and/or flaps is a function of aircraft weight and the "Q's" associated with landing. These "Q's" vary only slightly between a subsonic or a supersonic aircraft. On the other hand, the power demand of a primary flight control surface is also a function of

aircraft weight and "Q", but in this case, the maximum "Q" varies by several orders of magnitude, dependent upon whether the aircraft is subsonic or supersonic.

As a general "rule of thumb," if the size of the power generation and distribution system can be reduced by half through the application of an MPP to a single function (say, the landing gear), the weight saving in the whole system (generation, distribution, and utilization) will be about 18% to 20%. If, to accomplish the same power generation and distribution size reduction, the MPP must be applied to two functions (such as the ground spoilers and landing gear in the C5A), the weight saving per system will drop to 9% to 10%. Since the MPP approach can be applied to only systems 1 and 4 in the C5A, the overall hydraulic system weight saving (counting all four systems) will be in the 4% to 5% bracket (i.e., 200 to 250 pounds).

The work function selected was the B-1 main landing gear (MLG) retract-extend function. This work function was selected for the following reasons:

- 1) It was the highest energy (power) demand utility function on the B-1 aircraft (see Figure 2).
- 2) It was typical in terms of cycle time, peak power (35 hp per gear), and total energy demand relative to most large utility function applications on all the large subsonic and supersonic aircraft studied in this program.
- 3) The contractor had existing test facilities which were well instrumented and equipped to duplicate the load-stroke characteristics and thermal environment conditions of the B-1 MLG.

Figure 6 illustrates the B-1 aircraft's MLG and flags out the hydraulic actuators with which it is extended and retracted. The entire MLG actuation system (including the two actuators and the plumbing, valves, and contained fluid) weighs 305.2 pounds, or 151.6 pounds per strut. The maximum hinge moment during gear retraction is 1,035,515 inch-pounds, and the maximum actuator output force is 107,100 pounds at that hinge moment. The total energy which must be delivered at the output of the actuator to retract the gear (retract is the maximum energy requirement) is 942,200 inch-pounds. The power delivered to the actuator by the hydraulic system to achieve a 7.5-second retraction is 36.87 hp (15.86 gpm at 4,000 psi).

#### TASK IB

This task concerned itself with determining the loads and duty cycles associated with the work function selected in task IA. It also concerned itself with establishing the design requirements for the MPP assembly.



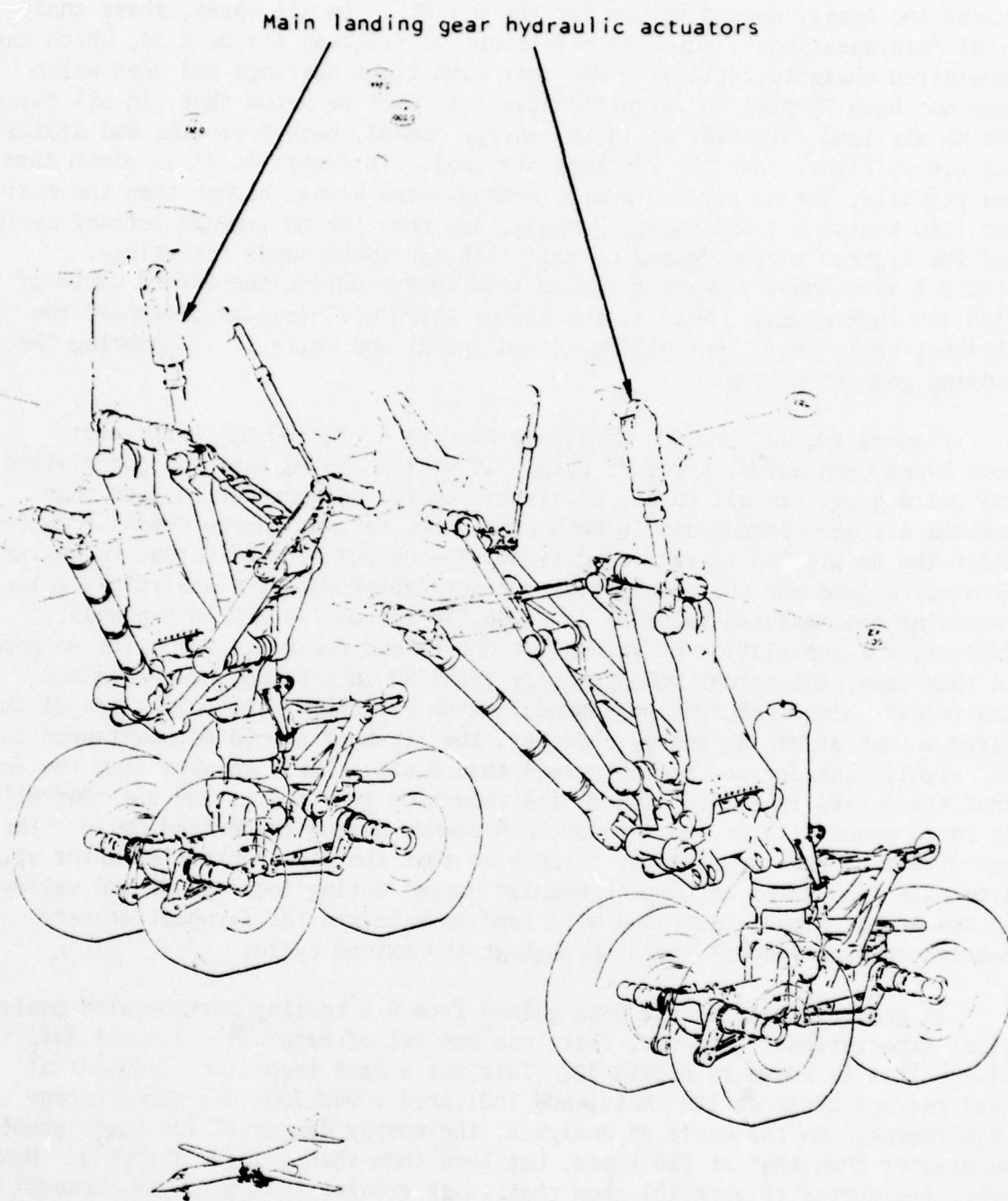


Figure 6. Main Landing Gear

## Load Stroke Curves

Figures 7, 8, and 9 show the analytically determined load stroke curves and energy demand values for the B-1 MLG. In all cases, these analytical determinations assumed a coefficient of friction ( $\mu$ ) of 0.20, which was considered characteristic of a new gear with tight bearings and ones which have not been "broken in" significantly. It will be noted that, in all cases, the no air load (aircraft on jacks) energy demand, both resisting and aiding, was always higher than the 280 knot air load. In Figure 8, it is shown that, analytically, the no airload energy demands were always higher than the maximum (280 knots) airload energy demands, and that the no airload retract cycle had the highest energy demand of all (-786,550 inch-pounds resisting). Figure 8 also shows a maximum aiding load energy during the extend cycle of +486,400 inch-pounds. This is the energy which will tend to overspeed the flywheel while it is controlling extend speed, and while it is snubbing the landing gear to a stop.

Figures 10, 11, and 12, duplicate Figures 7, 8, and 9, except they were based upon actual aircraft data. It will be noted that the correlation was quite good. In all cases, no airload energy demands were higher than maximum airload demands and in both cases, the maximum energy demand occurred under the no airload retract condition. The correlation of actual values was also quite good for the comparative retract cycles with the analytical value exceeding the measured value by 5% (-786,550 versus 746,200 inch-pounds). However, the correlation of values for the extend cycle was not quite so good. In this case, the actual aiding energy (589,250 inch-pounds) exceeded the analytical value (486,400 inch-pounds) at no airload by 17%. In spite of this large amount of aiding energy, however, the flywheel should not overspeed to any significant degree (probably less than 0.05%). This results from the fact that the losses in the screwjack, its reduction gear train, and the controller at rated speed will exceed 600,000 inch-pounds during the extend cycle. The net effect of this near-energy balance is that the flow controlled motor will alternate from motor to pump (hydraulic brake) during local peaks and valleys in the energy demand curve and will tend to maintain the flywheel at very nearly constant (rated) speed throughout the extend cycle.

In general, most of the data gained from B-1 testing corroborated analytical expectations. However, there was one set of data which did not fall in line. This is shown in Figure 13. This was a data recording of an actual gear retract cycle at 190 knots, and indicated a 942,200-inch-pound energy requirement. On the basis of analysis, the energy demand at 190 knots should be greater than that at 280 knots, but less than that at zero airspeed. However, the curves (Figure 13) show that it is greater than both and exceeds that at zero airspeed by 21% (196,000 inch-pounds). Although there was some doubt about the validity of the instrumentation in terms of stroke position (note that the ramp position occurs at 3.3 inches rather than at the 4.1-inch

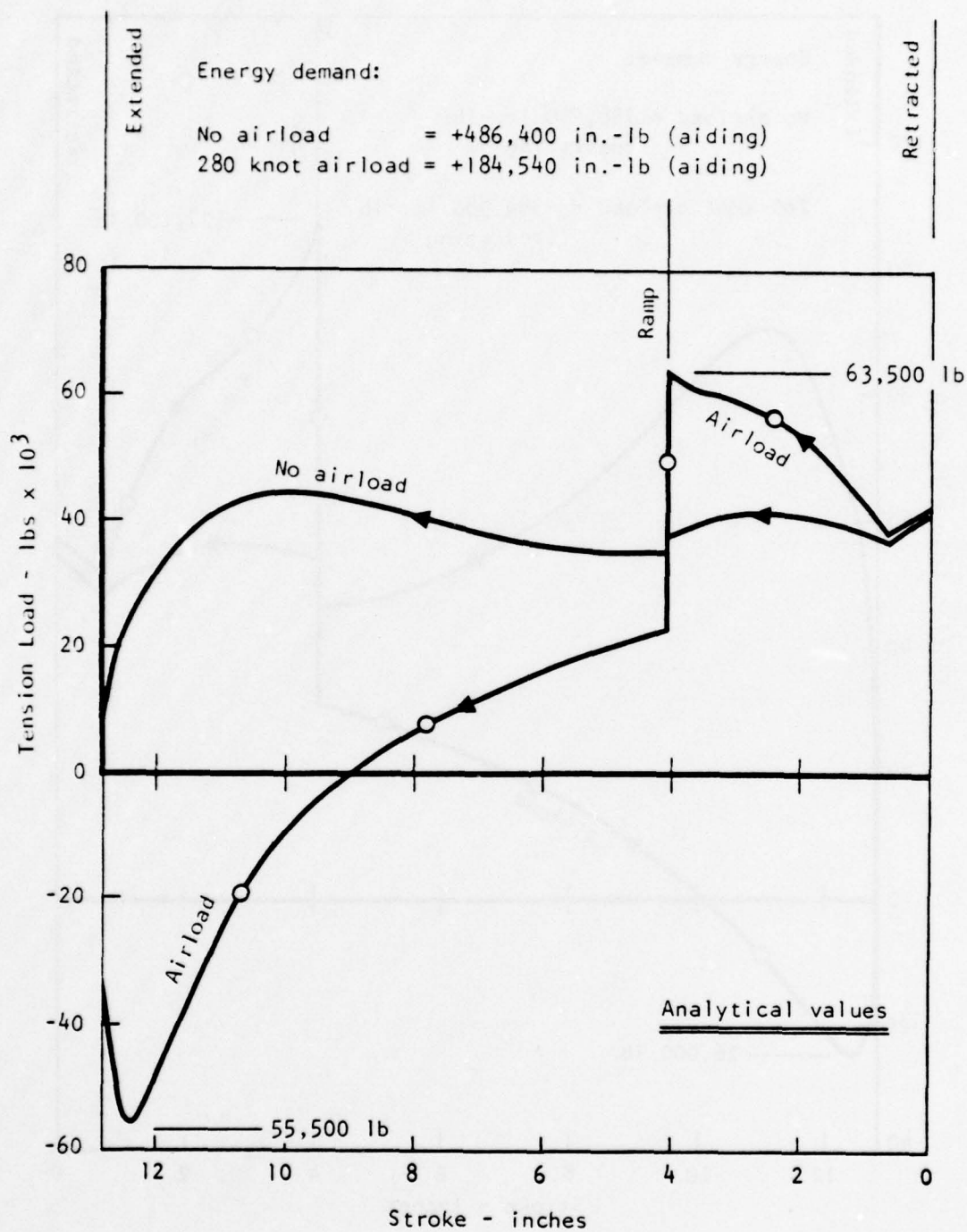


Figure 7. Main Landing Gear Cyclinder Extending Cycle  
(No Airload Versus 280 Knots,  $\mu = 0.20$ )



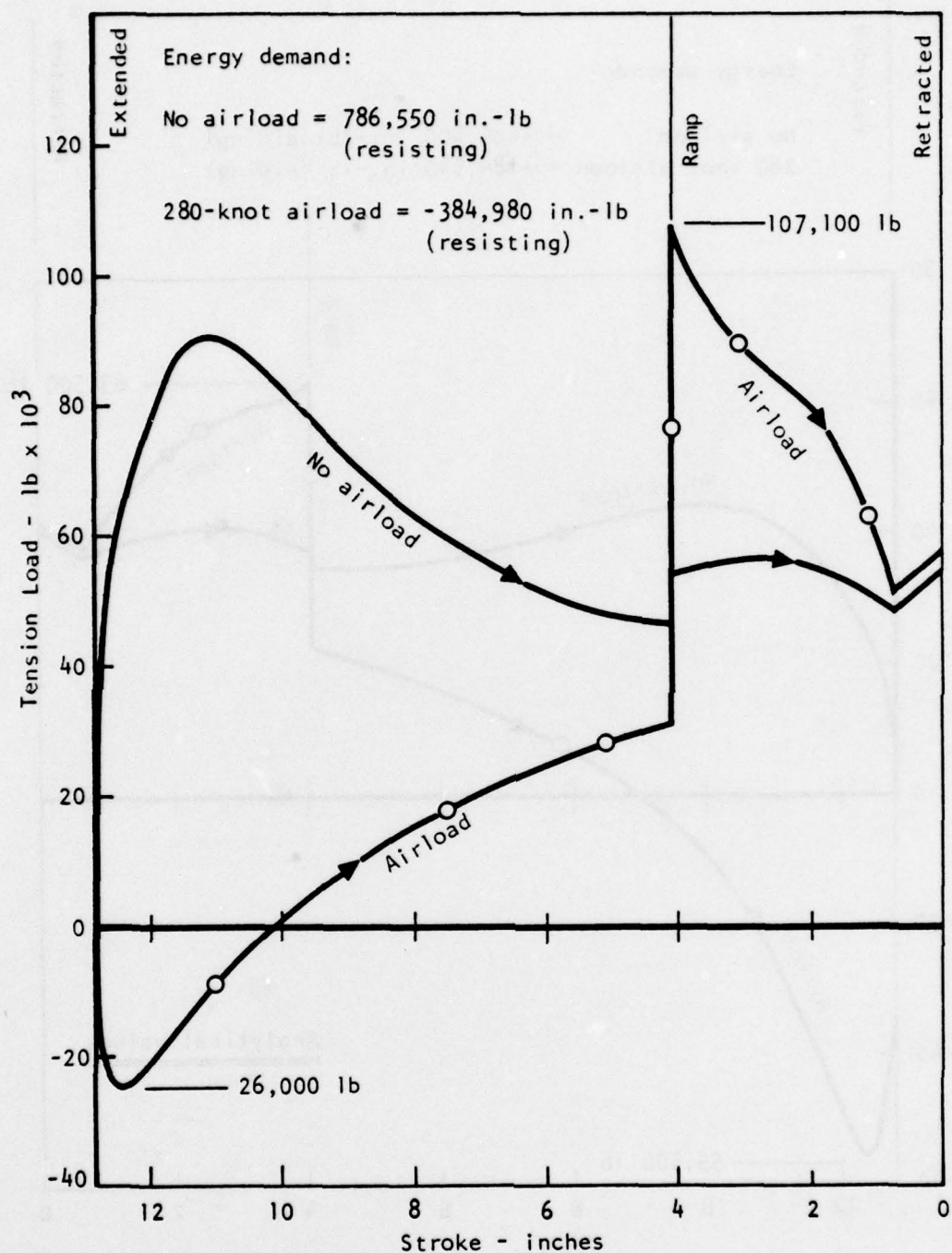


Figure 8. Main Landing Gear Cyclinder Retracting Cycle  
(No Airload Versus 280 Knots,  $\mu = 0.20$ )

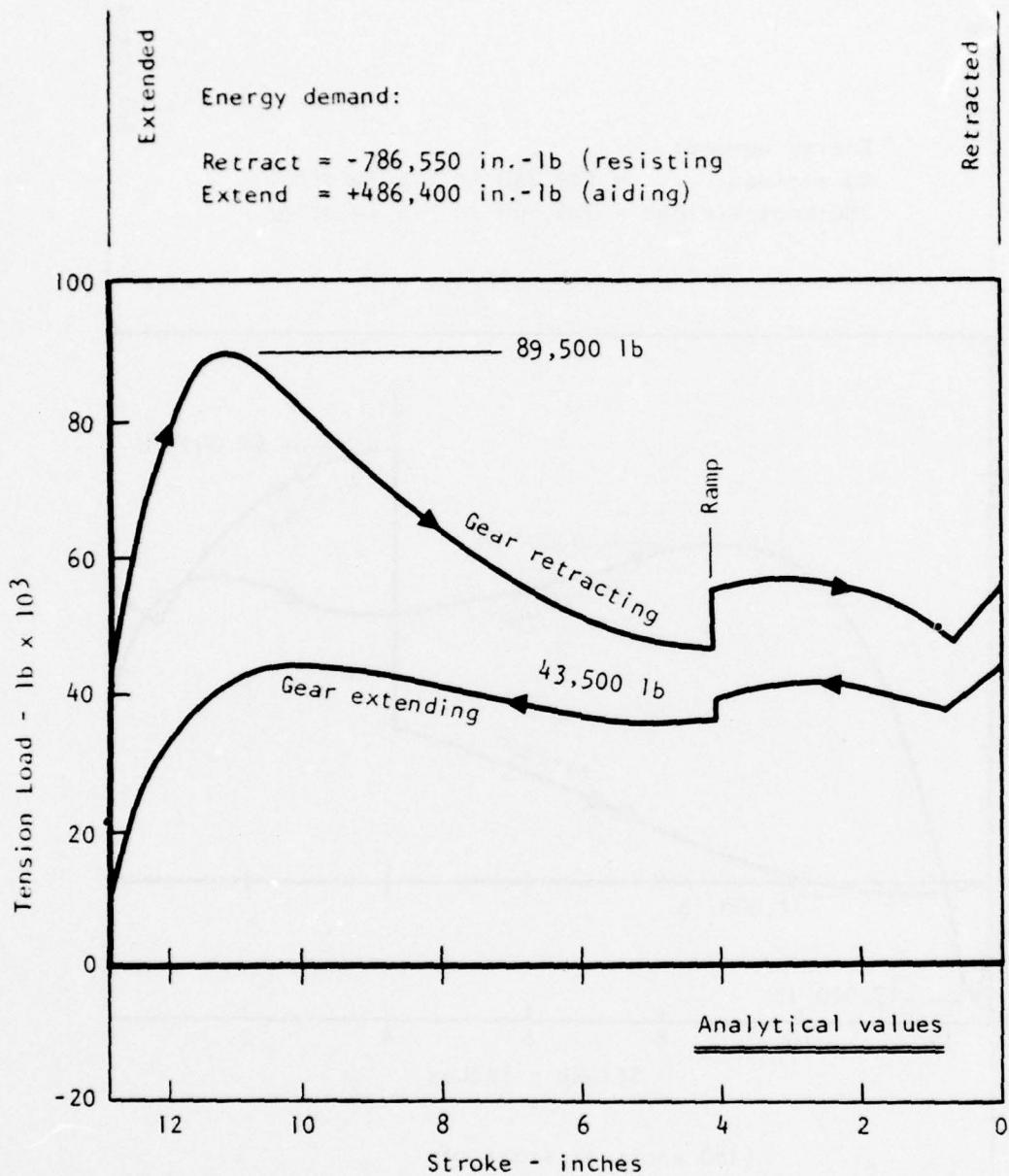


Figure 9. Main Landing Gear Cyclinder, Air Vehicle on Jacks (No Airload)



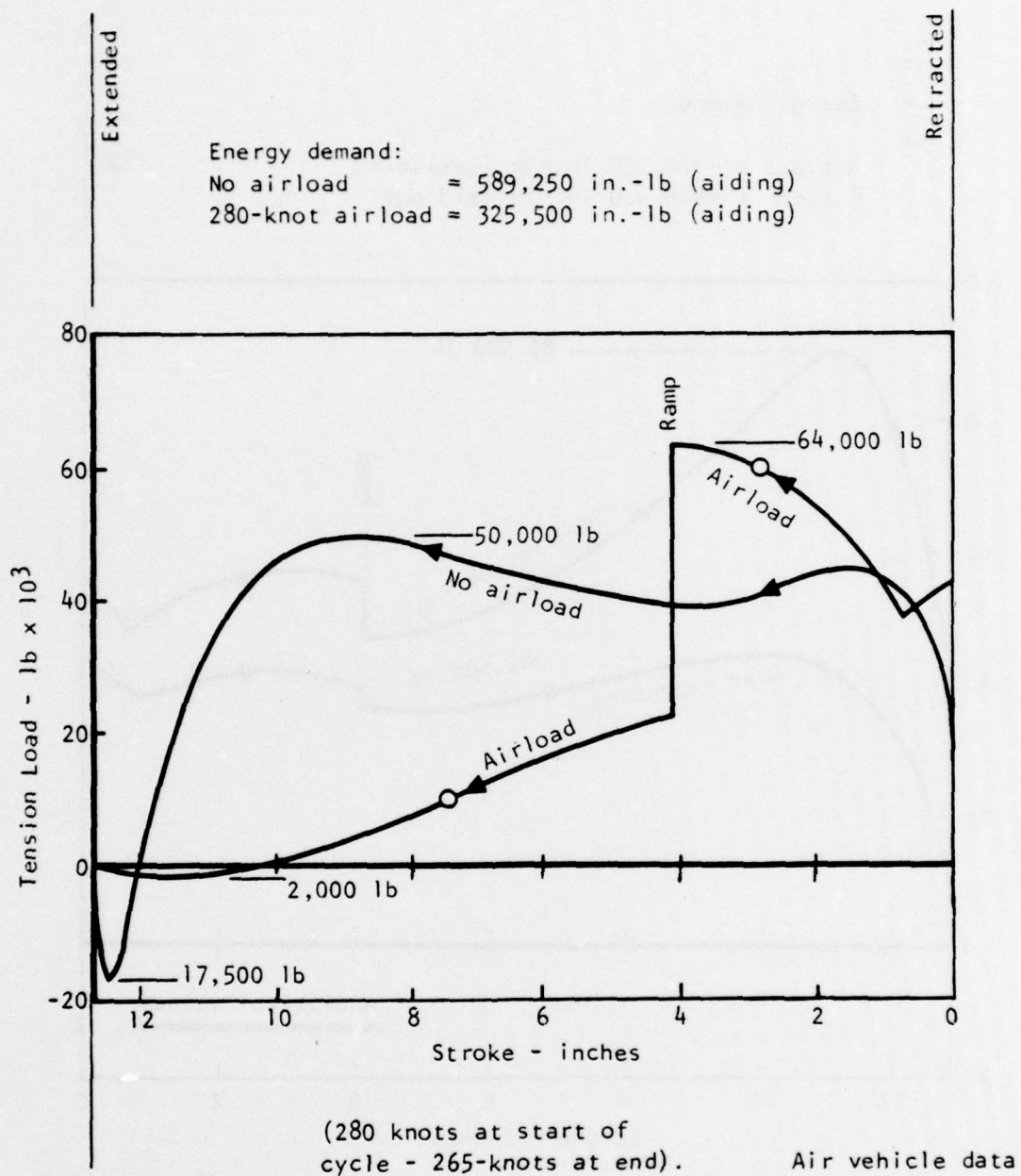


Figure 10. Main Landing Gear Cylinder Extending Cycle (No Airload Versus 280-Knot Airload)

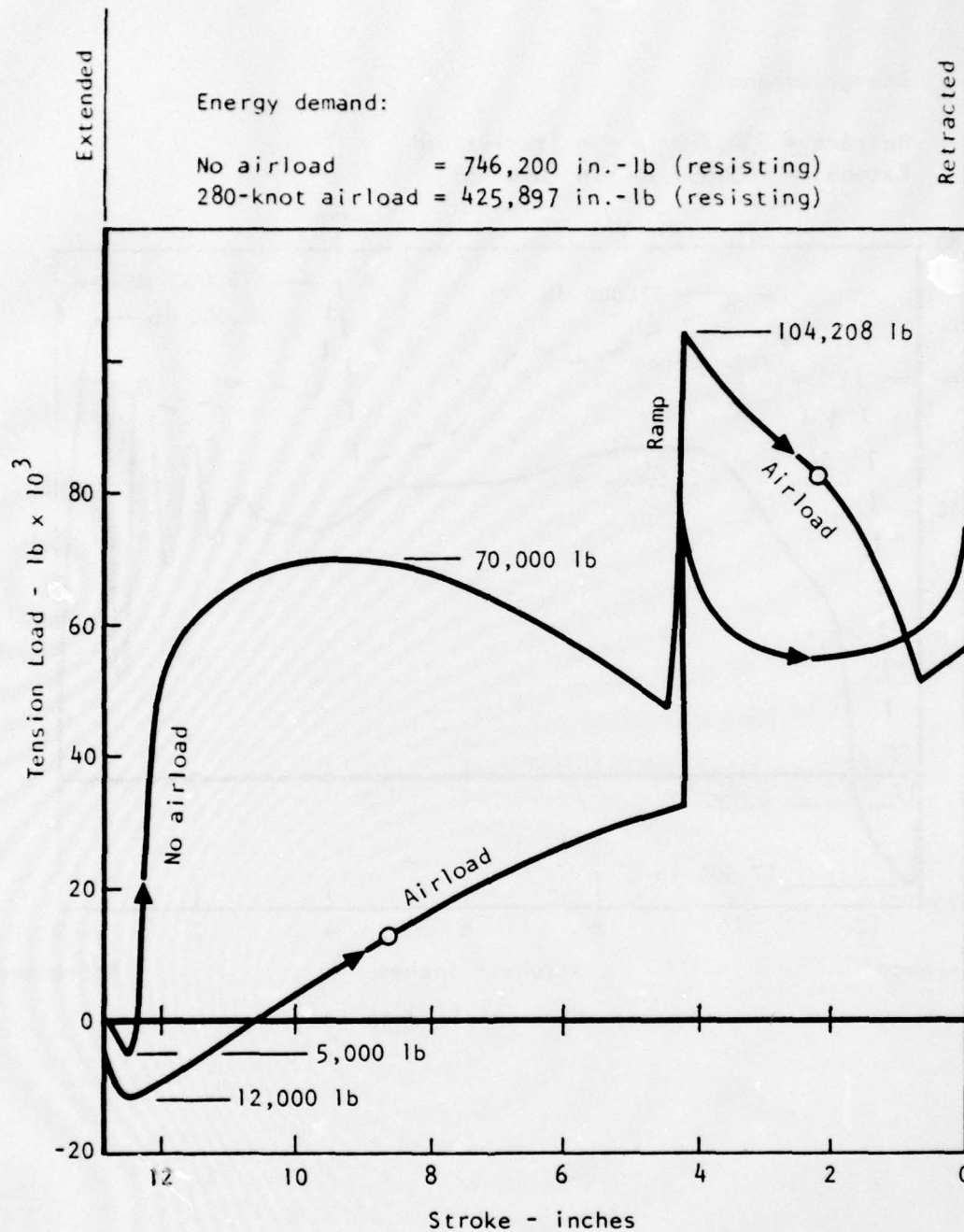


Figure 11. Main Landing Gear Cylinder Retracting Cycle (No Airload Versus 280-Knot Airload)

Energy demand:

Retract = 734,750 in.-lb (resisting)

Extend = 463,850 in.-lb (aiding)

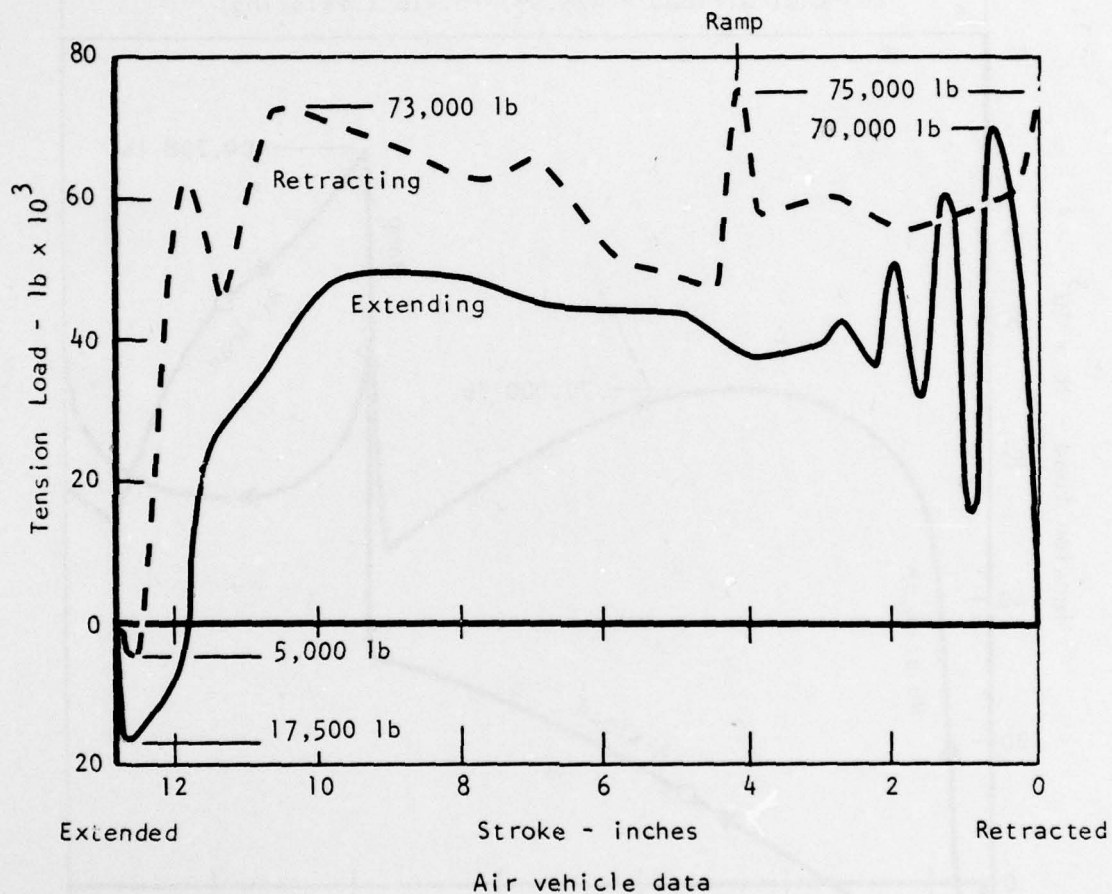


Figure 12. Main Landing Gear Cylinder (No Airload )

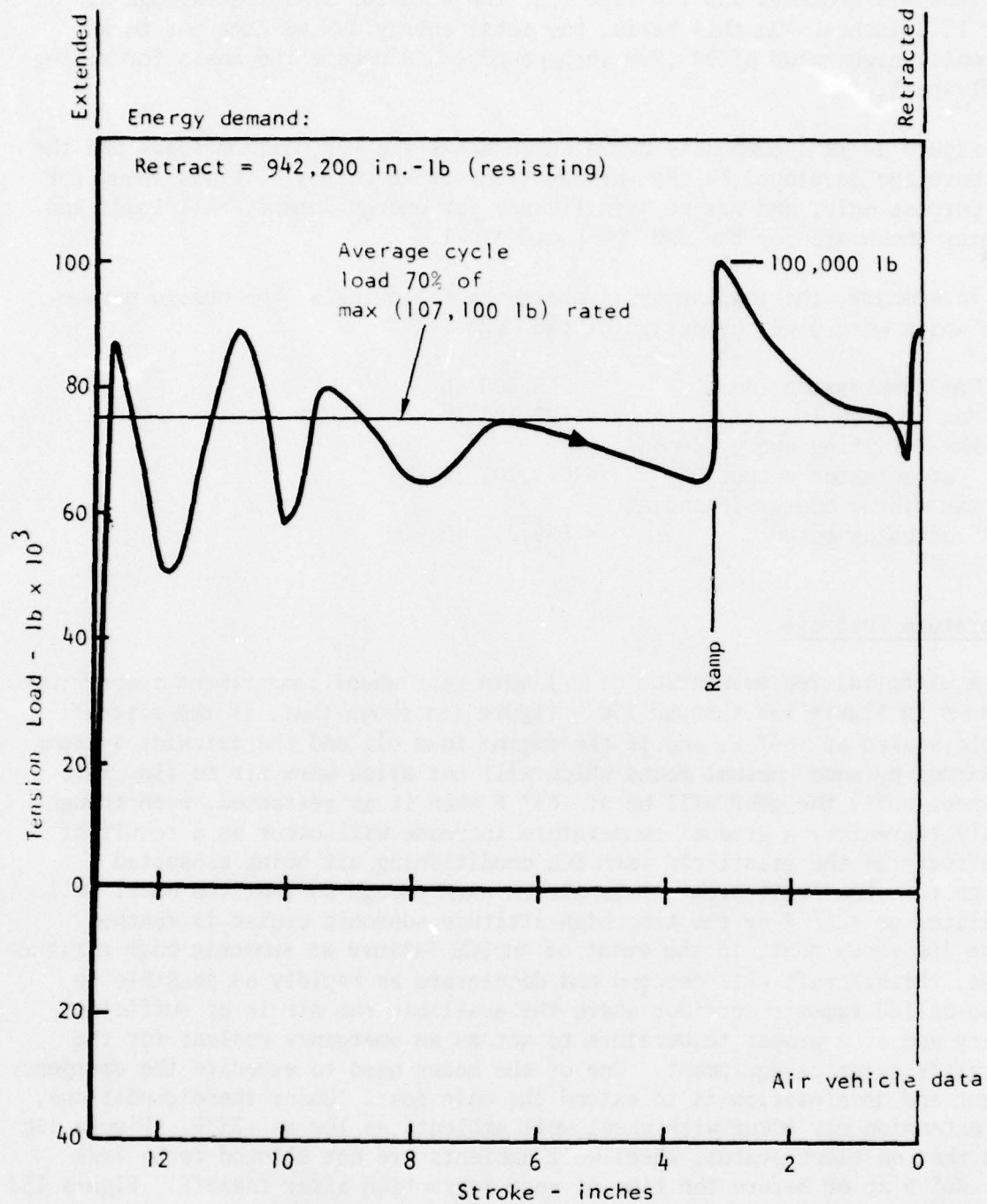


Figure 13. Main Landing Gear Cylinder Retracting Cycle (190-Knot Airload)



characteristic of all other data), there was no reason to doubt the load amplitude measurements and the fact that the actuator traveled through at least 12.8 inches. On this basis, the total energy demand came out to an abnormally high value of 942,200 inch-pounds, and became the basis for sizing the flywheel.

Figure 14 is a composite curve which shows the key maximum loads and the load envelope developed by the various load stroke curves. It was shown for this purpose only, and has no significance for energy demand. All loads and energies shown are for the 390,000-pound A/C-1.

In summary, the load analysis shows the following as the design parameters which were used for design of the MPP:

|   |                  |
|---|------------------|
| Max compression load                              | = 55,500 lb      |
| Max tension load                                  | = 107,100 lb     |
| Max resisting energy demand<br>at actuator output | = 942,200 in.-lb |
| Max aiding energy demand at<br>actuator output    | = 589,250 in.-lb |

#### Temperature Analysis

A pictorial representation of B-1 main gear wheel compartment temperatures is shown in Figure 15a through 15e. Figure 15a shows that, if the aircraft is cold-soaked at  $-65^{\circ}\text{F}$ , and if the engine lube oil and the avionics systems are warmed by some unusual means which will not allow warm air to flow into the wheel well, the gear will be at  $-65^{\circ}\text{F}$  when it is retracted, even though shortly thereafter a gradual temperature increase will occur as a result of the effects of the relatively warm ECS conditioning air being exhausted through the wheel well area. This air is warm enough so that the wheel well stabilizes at  $+20^{\circ}\text{F}$  by the time high-altitude subsonic cruise is reached. Figure 15b shows that, in the event of an ECS failure at subsonic high-altitude cruise, the aircraft will descend and decelerate as rapidly as possible to the so-called ram-air corridor where the available ram air is of sufficient density and of a proper temperature to act as an emergency coolant for the aircraft's avionics equipment. One of the means used to expedite the emergency descent and deceleration is to extend the main gear. Under these conditions, gear extension may occur with wheel well ambients as low as  $-55^{\circ}\text{F}$ . Figure 15c shows that on alert status, wheel well ambients are not allowed to be less than  $-30^{\circ}\text{F}$  at or before the time of gear retraction after takeoff. Figure 15d shows a temperature condition in direct contrast to that of Figure 15b. In this case, ECS failure occurs during a supersonic dash, and by the time the gear must be extended, the wheel well ambient is  $+200^{\circ}\text{F}$ . Figure 15e shows the

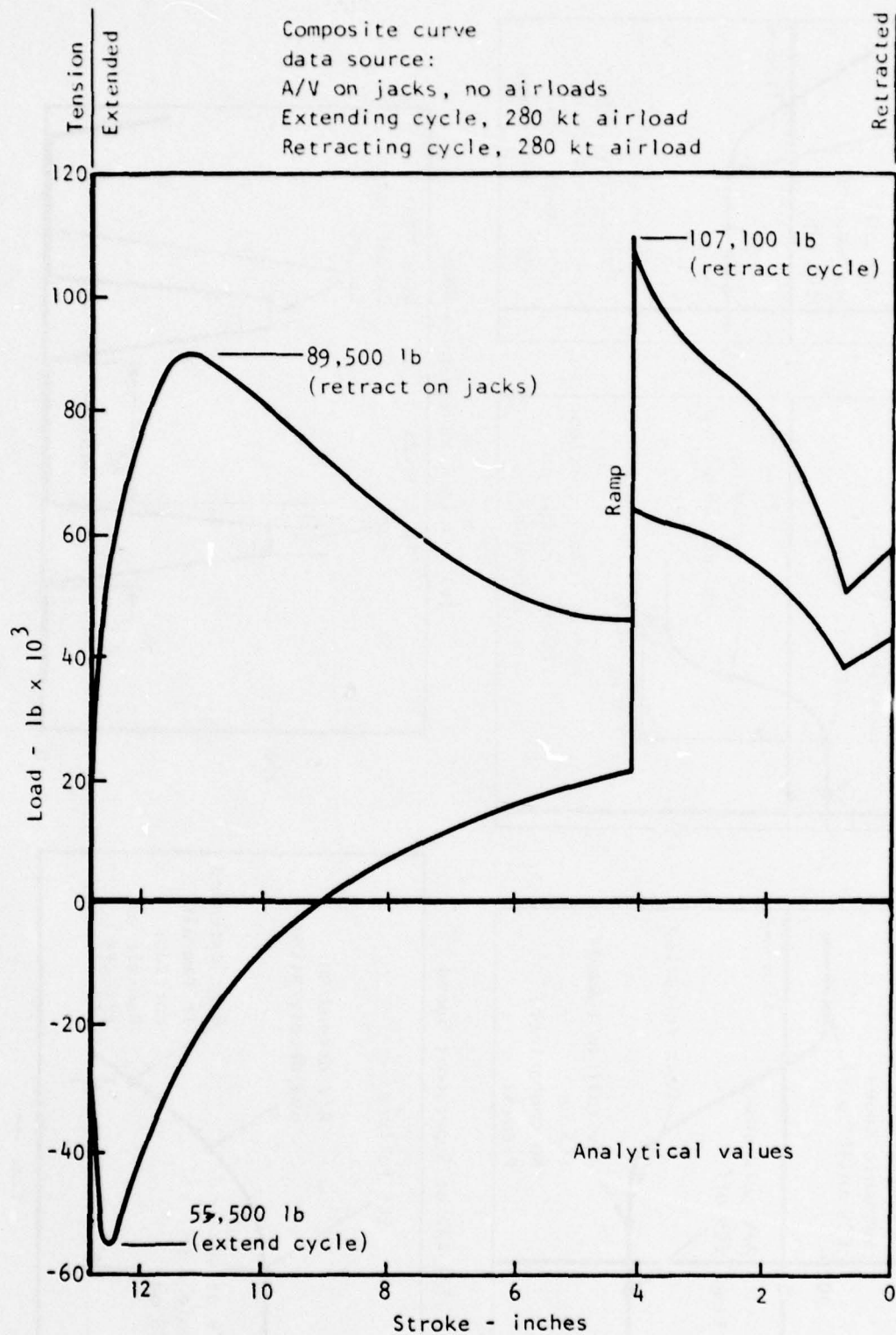
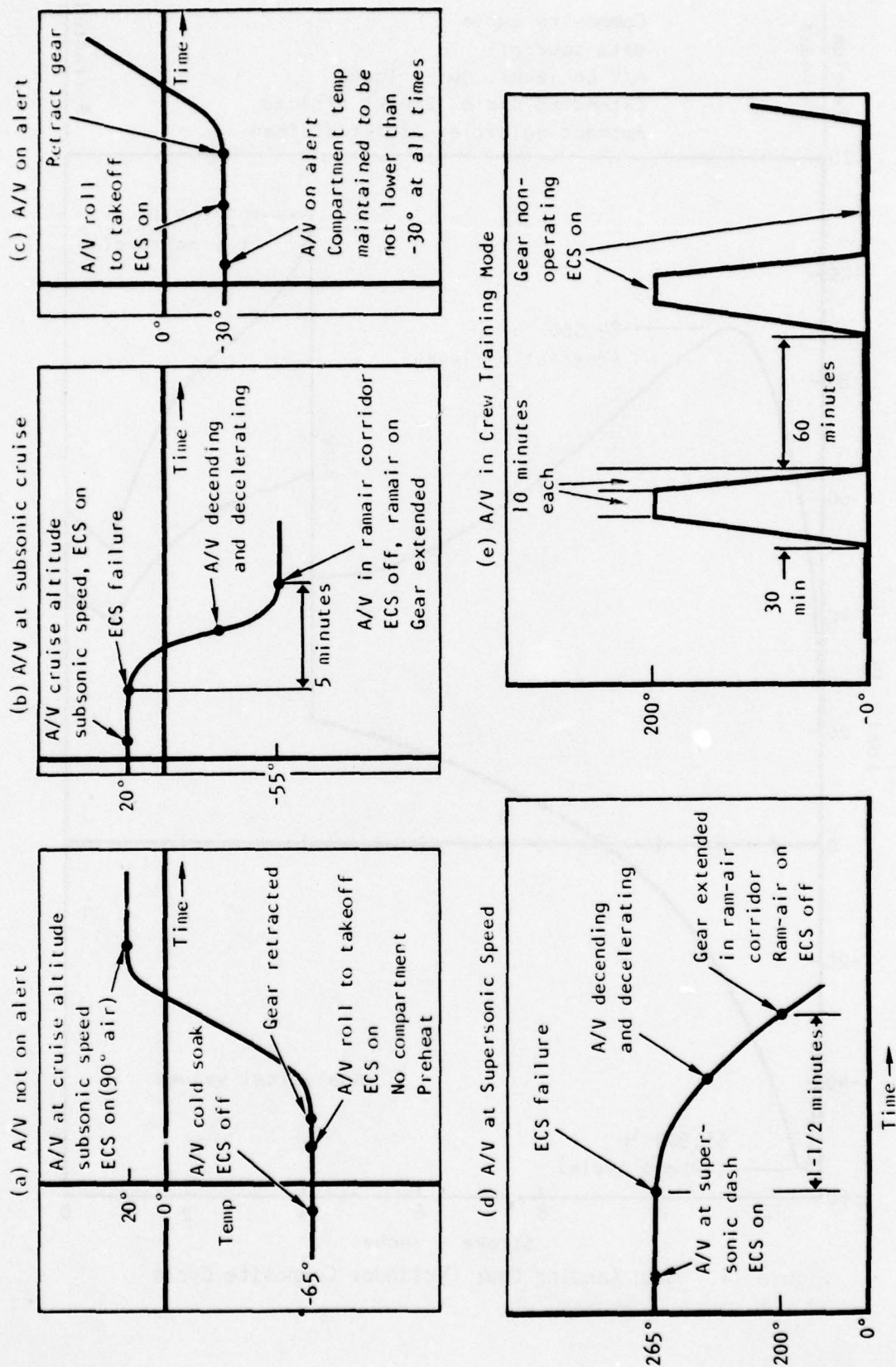


Figure 14. Main Landing Gear Cyclinder Composite Cycle





wheel well ambient temperature variations during a crew training mission. Although the gear would not normally be operated during this mission, it could occur and would thus experience operation at any of the temperatures along the profile. From the data presented in Figure 15 and general B-1 aircraft requirements, the following were concluded about gear operating requirements in terms of ambient temperatures:

1) Gear retraction

Minimum temperature -65° F  
 Minimum temp - full rate -39° F  
 Maximum temperature +200° F

2) Gear extension

Minimum temperature -55° F  
 Minimum temp - full rate -30° F  
 Maximum temperature +200° F

3) Nonoperating soak temperature

Minimum -80° F  
 Maximum +265° F

### Load and Thermal Duty Cycles

Based upon the load and thermal analyses of task IB, the duty cycle listed in Table 1 was established for the endurance test. Code letters have been used in Table 1 to describe load and temperature conditions. These codes, their descriptions, and the reason for their selection are discussed as follows:

TABLE 1. ENDURANCE TEST LOAD DUTY CYCLE

| Number of Load Cycles | Type of Load Cycle | Temperature Conditions |
|-----------------------|--------------------|------------------------|
| 2                     | A                  | A                      |
| 60                    | A                  | B                      |
| 1000                  | A                  | C                      |
| 988                   | B                  | C                      |



Load Cycle (Code A). Load per load stroke curve as shown in Figure 9. This load cycle represents the "high average" energy requirement, both aiding and resisting, which would be representative of most of the landing gear's actuation cycles. Therefore, this cycle was used for slightly over 50 percent of the total endurance.

Load Cycle (Code B). Load per "airload" curve as shown in Figure 8 for retract cycle, and "airload" curve as shown in Figure 7 for extend cycle. This cycle generates the highest tensile loads (retract) and compression loads (extend) which will occur during gear operation even though the "resisting" energy extraction and "aiding" energy inputs are relatively low. Because of its high reversing loads, this cycle tends to fatigue the screwjack, controller, and gearing to a maximum; therefore, it is used for just under 50% of the cycles.

Temperature Condition (Code A). Cold temperature cycle at  $-30^{\circ}$  and  $-65^{\circ}$  F. The MPP shall first be cold-soaked at  $-40^{\circ}$  F for 1 hour, after which the temperature shall be brought up to  $-30^{\circ}$  F and held for 1 hour. The MPP shall be started and brought up to speed (11,968-rpm hydraulic motor speed) within 2 minutes. Thirty seconds later, the retract portion of the gear cycle shall be initiated, and shall be completed within 8.5 seconds. Two minutes after the completion of retract, the extend portion of the cycle shall be initiated and completed within 8.5 seconds. The hydraulic fluid supplied to the hydraulic motor shall have warmed to at least  $60^{\circ}$  F by the time the retract cycle has been initiated.

Following the  $-30^{\circ}$  F test, the MPP shall be cold-soaked to  $-80^{\circ}$  F for 1 hour, after which the temperature shall be brought up to  $-65^{\circ}$  F. The MPP shall be started and brought up to rated speed within eighteen minutes. Two minutes after rated speed has been achieved, the retract portion of the gear cycle shall be initiated. The retract portion shall be completed within 16 seconds. Four minutes after the completion of retract (and only if the screwjack thermocouple records temperatures warmer than  $-55^{\circ}$  F), the extend portion of the cycle shall be initiated and completed within 10 seconds.

Operations analysis of the B-1 bomber indicates that there is no requirement for  $-65^{\circ}$  F gear retraction in actual operational use. However, in spite of this fact, a design requirement was imposed upon the B-1 to demonstrate  $-65^{\circ}$  F gear operation capability. In view of this, and the fact that some military aircraft in which the MPP might be used will have a real  $-65^{\circ}$  F gear cycling requirement, a  $-65^{\circ}$  F gear cycle is included in the test program to show capability.

Temperature Condition (Code B). Operate MPP at  $275 \pm 10^\circ$  F ambient (after 2-hour soak) with  $210 +0 -30^\circ$  F lubrication and cooling oil supply. Although the main gear well in flight never exceeds  $265^\circ$  F (see Figure 15d), and the gear is never asked to operate at temperatures higher than  $200^\circ$  F, the design requirements for the B-1 aircraft specify  $275 \pm 10^\circ$  F ambient. Therefore, this ambient temperature is used for the MPP program. As previously indicated, task I studies have determined that a utility function MPP without the backing of a flight control type MPP cannot save weight on a supersonic aircraft, and is confined to applications on subsonic aircraft. Under these conditions (i.e., in subsonic aircraft), maximum wheel well temperatures will range between  $140^\circ$  and  $184^\circ$  F. The lower limit is more typical of most high-performance, subsonic aircraft flying close to the deck (500-foot altitude) over the desert on a hot day. The upper limit is the temperature in the B-1 wheel well under the same conditions. The difference lies in the fact that avionics cooling exhaust air is dumped into the wheel well on the B-1 and causes the additional temperature rise. The ultimate objective of the MPP design will be to reject the MPP's self-generated heat in its immediate area. Depending upon the installation, the means used can vary widely as illustrated in the following:

- 1) In the normal high-altitude, high-subsonic aircraft (707, DC10, C5A, etc), reject heat directly to the wheel well ambient by conduction, radiation, and self-induced convection.
- 2) In the low-altitude, high subsonic aircraft (i.e., penetration missions for B-1 or F-111), or the high-altitude, low-supersonic (M 1.7) aircraft, reject heat by means of oil to fluid heat exchanger, if hydraulically driven, or by means of an integral fan-cooled heat exchanger, if electrically driven, or by means of avionics cooling exhaust air, if available, or by any combination of the aforementioned.
- 3) In high-altitude, long-range, high-supersonic (M 2.0) aircraft reject heat remotely, such as to an oil to fuel heat exchanger, or design for extreme high-temperature operation ( $450^\circ$  F or greater) so that heat rejection can be done locally.

For the purposes of this program, it is assumed that the MPP will be designed to fully meet the requirements of the aforementioned items 1 and 2, and the remote heat exchanger portion of item 3. On this basis, oil supply temperatures in the  $180^\circ$  F range give a high enough mean temperature in the unit ( $230^\circ$  to  $260^\circ$  F, with  $300^\circ$  F maximum at any point in the MPP) to reject heat directly in the item 1 case, and with fan assistance in the item 2 case. It is also a compatible temperature for use in the fuel heat exchanger of item 3.

Temperature Condition (Code C). Operate the MPP at  $70^{\circ} \pm 20^{\circ}$  F ambient temperature with  $180^{\circ} \pm 10^{\circ}$  F lubrication and cooling oil supply. This will be the temperature range used in the greater portion of the testing. It represents the average conditions which should exist during a majority of takeoffs and landings, and because it allows tests to be conducted outside the thermal control chamber, simplifies testing.

## TASK II - DESIGN AND FABRICATION

### ORIGINAL DESIGN CONCEPT

The general arrangement of the MPP, as originally conceived, is shown in Figure 16. Although the specific relationship of the components had to be revised to fit in the space available surrounding the existing B-1 MLG hydraulic actuating cylinder, the operating principles and power flow directions did not change throughout the program. The basic components making up the MPP, and a brief description of their function, is as follows. Note that various speeds, dimensions, and loads are listed with various component descriptions. In all cases, the number preceding the slash is the original concept value and that following is the final design value.

- 1) A conventional axial piston type hydraulic motor - This motor's power delivery is one-fifth that of the hydraulic actuator currently used for retracting and extending the main landing gear. The motor supplies the power to wind up the flywheel and assists the flywheel in driving the main landing gear during extension and retraction.
- 2) An adapter gearbox - The adapter gearbox performs several functions:
  - a) It transmits power between the motor, the flywheel, and the input to the controller.
  - b) It steps up speed from the motor (24,000/11,968 rpm) to the flywheel (100,000/88,235 rpm) and to the controller input (25,000/15,000 rpm).
  - c) It delivers lubricating and cooling oil to the flywheel and the controller as well as meeting its own internal demands.
- 3) A high-strength steel flywheel - The flywheel stores energy in a high-speed (100,000/88,235 rpm) small-diameter (6/7.125-inch) spinning disk of optimized cross section and makes it available for extending and retracting the gear.



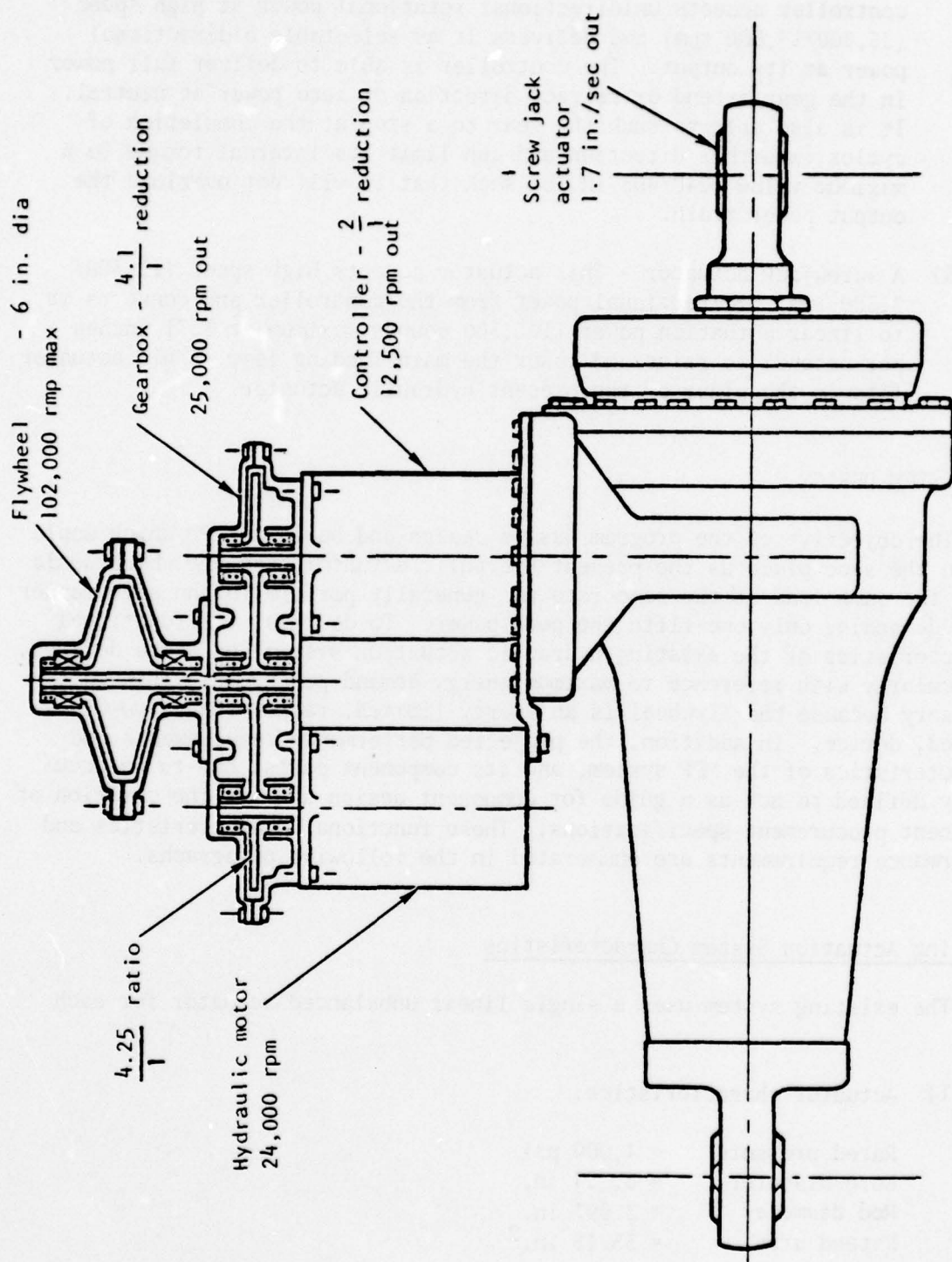


Figure 16. Mechanical Power Package

- 4) An infinitely variable traction transmission type controller - The controller accepts unidirectional rotational power at high speed (25,000/15,000 rpm) and delivers it as selectable bidirectional power at its output. The controller is able to deliver full power in the gear extend or retract direction or zero power at neutral. It is also able to snub the gear to a stop at the completion of cycles in either direction and can limit its internal torque to a maximum value (240/405 in.lb) such that it will not overload the output power train.
- 5) A screwjack actuator - This actuator accepts high speed (12,500/7,500 rpm) bidirectional power from the controller and converts it to linear actuation power (107,500 pounds maximum at 1.71 inches per second) to raise and lower the main landing gear. This actuator fits in the place of the present hydraulic actuator.

#### MPP SYSTEM DESIGN

The objective of the program was to design and build an MPP which would fit in the same place as the present hydraulic actuator, and one which would carry the same load at the same rate and generally perform in the same manner while demanding only one-fifth the peak power. To do this, the functional characteristics of the existing hydraulic actuation system had to be defined, particularly with reference to maximum energy demand per cycle. This was necessary because the flywheel is an energy-limited, rather than a power-limited, device. In addition, the projected performance requirements and characteristics of the MPP system, and its component parts, had to be accurately defined to act as a guide for component design and for the creation of component procurement specifications. These functional characteristics and performance requirements are enumerated in the following paragraphs.

#### Existing Actuation System Characteristics

The existing system uses a single linear unbalanced actuator for each gear.

##### 1) Actuator characteristics:

|                |                          |
|----------------|--------------------------|
| Rated pressure | = 4,000 psi              |
| Bore diameter  | = 6.724 in.              |
| Rod diameter   | = 2.997 in.              |
| Extend area    | = 55.15 in. <sup>2</sup> |

|                                  |                                       |
|----------------------------------|---------------------------------------|
| Retract effective area           | = 28.46 in. <sup>2</sup>              |
| Stroke                           | = 12.841 in.                          |
| Maximum actuator load            |                                       |
| (Assumes $\mu = 0.2$ in linkage) | = 107,100 lb (Retract) (See Figure 8) |

## 2) System characteristics:

|                          |                    |
|--------------------------|--------------------|
| Maximum hinge moment     | = 1,035,515 in.-lb |
| Maximum energy required: |                    |

|                  |                  |
|------------------|------------------|
| Theoretical      | = 786,550 in.-lb |
|                  | (See Figure 9)   |
| Maximum measured | = 942,200 in.-lb |
|                  | (See Figure 13)  |

|  |             |
|--|-------------|
| Maximum flow rate to actuator                            | = 15.79 gpm |
| Power input to actuator                                  | =           |
| $\frac{15.79 \text{ GPM} \times 4000 \text{ PSI}}{1714}$ | = 36.85hp*  |

\*Power computed is that generated at the hydraulic system pumps

Weight (lb):

|                 |               |
|-----------------|---------------|
| Actuators       | = 235.0       |
| Control valve   | = 12.0        |
| Fluid           | = 28.0        |
| Flow regulators | = 5.0         |
| Plumbing        | = <u>23.2</u> |

|       |         |
|-------|---------|
| Total | = 303.2 |
|-------|---------|

|          |                |
|----------|----------------|
| Per gear | = <u>151.6</u> |
|----------|----------------|

|                |               |
|----------------|---------------|
| Actuation time | = 7.5 Seconds |
|----------------|---------------|

## Replacement System (MPP) Characteristics

The replacement system was generally configured as shown in Figure 16. The following data provided a basis for system analysis and the preparation of initial drawings and specifications.



1) System characteristics:

|                                       |                      |
|---------------------------------------|----------------------|
| Maximum hinge moment ( $HM_m$ )       | = 1,035,515 in.-lb   |
| Maximum energy required ( $E_m$ )     | = 942,200 in.-lb     |
| Maximum power input to MPP ( $HP_m$ ) | = $36.85/5 = 7.4$ hp |
| Actuation time ( $t_a$ )              | = 7.5 Seconds*       |

\*For purposes of design, it was assumed that the system output accelerated linearly to operational speed at the beginning of the stroke in 1 second and decelerated to 0 at the end of the stroke in a similar manner. It was assumed that, in between acceleration and deceleration, the output moved at uniform speed for 5.5 seconds.

2) Actuator characteristics:

|                                    |              |
|------------------------------------|--------------|
| Ball screw type screwjack actuator |              |
| Ball circle diameter ( $B_{CD}$ )  | = 4.000 in.  |
| Ball diameter ( $B_D$ )            | = 0.750 in.  |
| Ball turns ( $B_T$ )               | = 3.50 turns |
| Lead ( $L$ )                       | = 1.00 in.   |
| Stroke ( $S$ )                     | = 12.841 in. |
| Maximum operating load ( $P_L$ )   | = 107,100 lb |
| Maximum end stop load ( $PSL$ )    | = 115,185 lb |
| Screwjack output speed ( $N$ )     | = rpm        |

$$N = \frac{60 \text{ sec/min} \times \theta_s}{\frac{t_{aA}}{2} + t_{au} + \frac{t_{aD}}{2}}$$

$$\text{Where: } \theta_s = \frac{S}{L} = \frac{12.841 \text{ in/stroke}}{1 \text{ in/rev}} = 12.841 \text{ rev/stroke}$$

$$t_{aA} = \text{Time to accelerate} = 1 \text{ second}$$

$$t_{au} = \text{Time at uniform speed} = 5.5 \text{ seconds}$$

$$t_{aD} = \text{Time to decelerate} = 1 \text{ second}$$

$$N = \frac{60 \times 12.841}{1/2 + 5.5 + 1/2} = \frac{770.46}{6.5} = 118.53 \text{ rpm}$$

$$\text{Maximum input torque to ballscrew } (T_B) = \text{in.-lb}$$

$$T_B = \frac{P_L L}{2\pi e_B}$$

Where:  $e_B$  = Ballscrew efficiency = 0.909

$$T_B = \frac{107,100 \text{ lb} \times 1.00 \text{ in}}{2\pi \times 0.909} = 18,751.92 \text{ in.-lb}$$

Using the known hydraulic motor speeds as an input and the assumed output actuator characteristics shown in item 2) above, a set of speed requirements for the other elements of the MPP was established. Originally, these speeds were those shown before the "slash mark" (see pages 26 and 28), but gradually, through continued analysis, and negotiations with potential component suppliers, they changed to become those shown in Table 2. The Table 2 values very closely approached the final speed values used in the delivered components (i.e., the "after slash" values shown on pages 26 and 28), and were the speeds used for system analysis.

TABLE 2. ACTUATION SYSTEM SPEEDS

| Component                | Minimum speed (RPM)<br>(50% energy)<br>(70% speed) | Average speed (RPM)<br>(75% energy)<br>(86% speed) | Rated speed (RPM)<br>(100% energy)<br>(100% speed) | Ratio | Over-Speed<br>(105%) |
|--------------------------|--|--|--|-------|----------------------|
| Hydraulic motor          | 8,400  | 10,320   | 12,000   | 7.35  | 12,600               |
| Flywheel                 | 61,764   | 75,882   | 88,235   |       | 92,647               |
| Controller in            | 10,500   | 12,900   | 15,000   | 5.88  | 15,750               |
| Controller out ( $\pm$ ) | 5,250  | 6,450  | 7,500  | 2.00  | 7,875                |
| Ballscrew in ( $\pm$ )   | 82.97  | 101.94   | 118.53   | 63.28 | 124.22               |

#### MPP POWER FLOW ANALYSIS

Once the component speeds had been tentatively established it became apparent that a fairly detailed power analysis, including parasite losses for all components upstream of the screwjack, would be required before adequate procurement specifications for the controller and adapter gearbox could be prepared. The MPP is particularly sensitive to the validity of the results of this type of analysis since it is an energy storing unit operating with minimum available input power rather than being a conventional power transfer unit with adequate input power. Parasite losses, of a magnitude which would be barely noticeable in a conventional power transfer arrangement, could be disastrous to an energy storing unit.

Figure 17 is a condensed summary of a whole series of power system analyses, each of which represented incremental refinements to its predecessor as more was learned about the probable design approach which would be used for each component. Figure 17 works backward from the known output requirements (i.e., the known maximum load  $P_L$  and retract cycle time ( $t_a$ ) established by B-1 aircraft requirements) through important interface points of the various components to the input power sources (i.e. to the hydraulic motor and fly-wheel). The computation of the full load torque and power characteristics

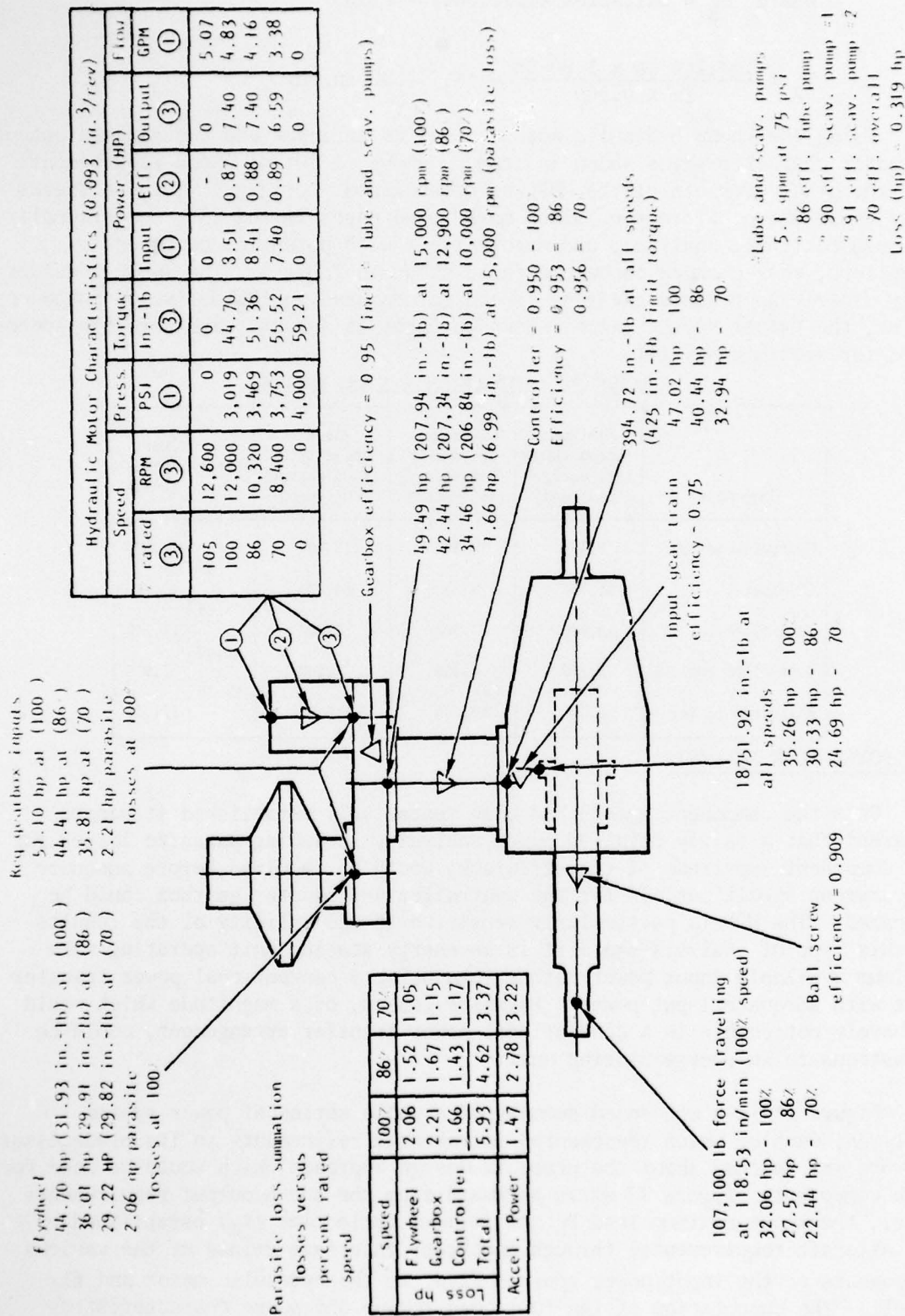


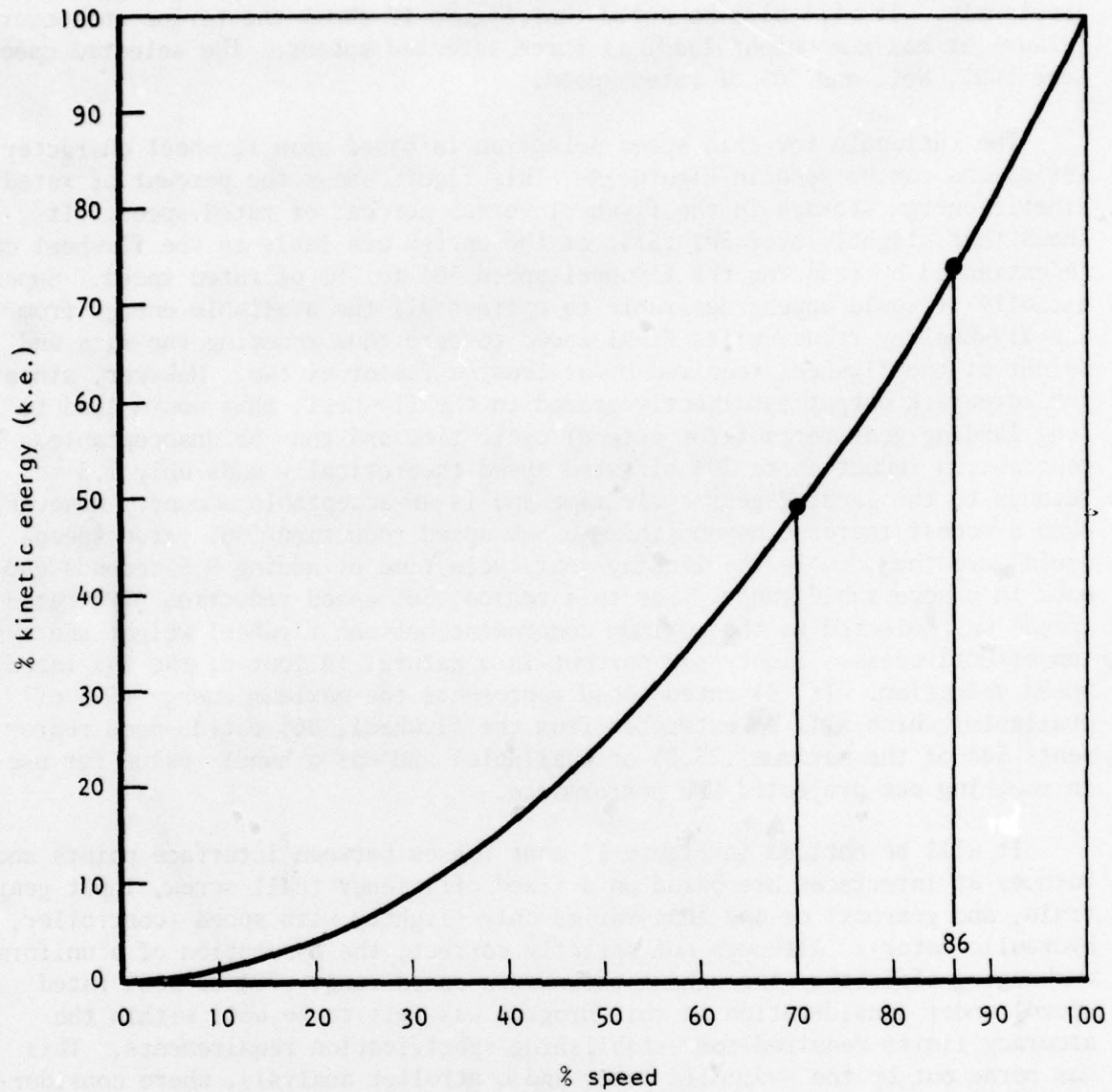
Figure 17. MPP Power Flow



were fairly straightforward up to the controller output pad. These computations have already been illustrated under actuator characteristics listed previously. It will also be noted that Figure 17 shows the torque and power (always at maximum output load) at three selected speeds. The selected speeds were 100%, 86%, and 70% of rated speed.

The rationale for this speed selection is based upon flywheel characteristics and can be seen in Figure 18. This figure shows the percent of rated kinetic energy storage in the flywheel versus percent of rated speed. It shows that slightly over 50% (51%) of the energy available in the flywheel can be extracted by reducing the flywheel speed 30% to 70% of rated speed. Superficially it would appear desirable to extract all the available energy from the flywheel by reducing its final speed to zero thus reducing the size and weight of the flywheel required by at least a factor of two. However, since the screwjack output is directly geared to the flywheel, this would lead to long landing-gear retract (or extend) cycle time and thus be unacceptable. In contrast, a reduction to 70% of rated speed theoretically adds only 1.5 seconds to the landing-gear cycle time and is an acceptable amount. However, even a modest increase beyond this to 50% speed reduction (50% rated speed) would more than double the landing-gear cycle time by adding 9.5 seconds and is back in unacceptable range. For this reason, 30% speed reduction (70% rated speed) was selected as the optimum compromise between flywheel weight and system effectiveness. Eighty-six percent is a natural fallout of the 70% rated speed selection. If 70% rated speed represents the maximum energy (51% of available) which will be extracted from the flywheel, 86% rated speed represents 50% of the maximum (25.5% of available) and was a handy value for use in roughing out projected MPP performance.

It will be noticed in Figure 17 that losses between interface points and torques at interfaces are based on a fixed efficiency (ball screw, input gear train, and gearbox) or one that varies only slightly with speed (controller, hydraulic motor). Although not strictly correct, the assumption of a uniform unchanging efficiency throughout the narrow speed range (70% to 100% rated speed) under consideration in this program was felt to be well within the accuracy limits required for establishing specification requirements. This was borne out by the hydraulic motor and controller analysis, where considerably more effort was expended in trying to predict probable losses and efficiencies in the belief that they might vary in a highly nonlinear way with respect to speed. In the case of the hydraulic motor (Figure 17), even though the torque and speed varied significantly, the efficiency only varied  $\pm 1\%$  from a mean efficiency of 88 percent. In the case of the controller (Figure 17), the variation was even less ( $95.3\% \pm 0.3\%$ ). The ball screw loss characteristics used to assist in determining specification requirements is shown in Figure 19. As indicated in Figure 17, this curve (Figure 19) is based on a 90.9% full load efficiency derived from Saginaw ball screw performance data. An input gear train efficiency of 75 percent was used for creating the loss curves



% speed reduction

% K.E. used

|    |    |    |    |    |    |    |    |    |
|----|----|----|----|----|----|----|----|----|
| 10 | 20 | 30 | 40 | 50 | 60 | 70 | 80 | 90 |
| 19 | 36 | 51 | 64 | 75 | 84 | 91 | 96 | 99 |

Figure 18. Flywheel Speed Reduction Versus Energy Storage

100% ratings

Output load = 107,100 in.-lb  
Output speed = 1.9755 in./sec.  
Input torque = 18,751.92 in.-lb  
Input speed = 118.53 rpm  
Output power = 35.26 H.P.

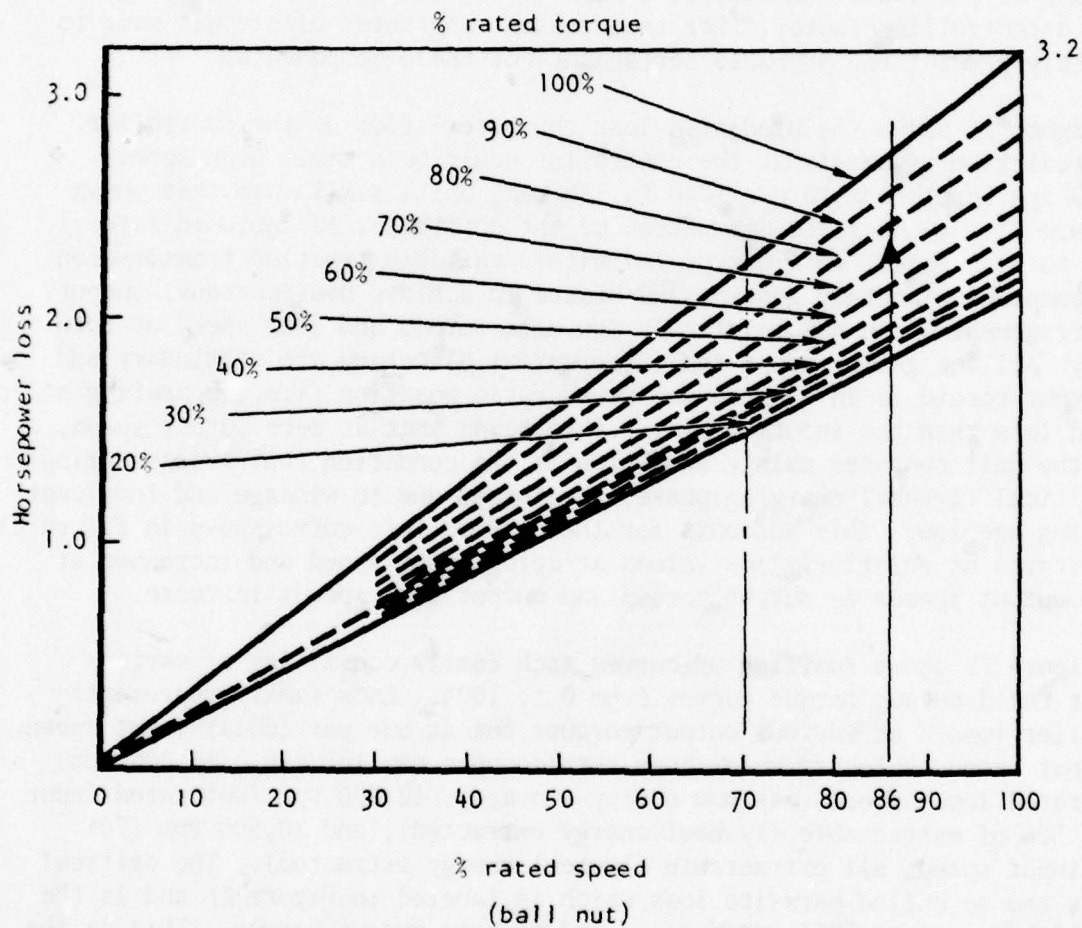


Figure 19. Ball Screw Loss Characteristics



shown in Figure 20. The use of this low efficiency value was based on the assumption that a major element of the input gear train, to achieve the overall 63.28:1 ratio required, would be a worm gear.

With these efficiencies the full load power output at 100% speed raises from 32.06 hp at the screwjack output rod end to 47.02 hp at the screwjack controller interface (Figure 17) and the controller output torque becomes 394.72 in.-lb. The screwjack controller interface represents the point in the system where parasite losses become critical. Downstream, the screwjack operates for only short bursts (9 seconds maximum) and the rest of the time is effectively disconnected from the system. When it operates, it has an essentially unlimited (assuming the flywheel is wound up to speed) source of power to draw upon. Therefore, within limits, losses are not a driving factor. Upstream, as previously indicated, the situation is reversed and losses become a controlling factor. For this reason, a greater effort was made to accurately predict the probable performance of these components.

Figure 21 shows the predicted loss characteristics of the controller. This prediction assumed that the controller would be a small high-speed (24,000 rpm input) low torque (240 in.-lb max) unit, similar to that shown in Figure 22. (A detailed discussion of the controller is included later.) It was to be a roller toroid-type infinitely variable traction transmission using compound planetary gearing and brakes to achieve bidirectional output. The arrangement shown has relatively low mean toroid and gear speed at zero output. All the gears except the differential planetary are stationary and the output toroid is in a speed decreased ratio position (i.e., operating at a speed less than the input toroid). This means that at zero output speed, where the unit operates mainly and which is the condition that exists during the critical flywheel charging phase, the losses due to windage and lubricant threshing are low. This accounts for the assumed loss curve shown in Figure 21 which starts at relatively low values at zero output speed and increases at higher output speeds as output toroid and output gear speeds increase.

Figure 21 shows families of curves each family consisting of various percent rated output torque curves from 0 to 100%. Each family represents controller losses at various output torques but at one particular input speed. The input speeds selected were those settled upon earlier i.e., 15,000 rpm (100% rated input speed, maximum energy storage), 12,900 rpm (86% rated input speed, 50% of extractable flywheel energy extracted), and 10,500 rpm (70% rated input speed, all extractable flywheel energy extracted). The critical loss is the so called parasite loss which is labeled in Figure 21 and is the loss which occurs at 100% rated speed and at zero output torque. This is the loss which, combined with the parasite losses of the other upstream components, determines the steady state power which must be put into the MPP at all times (other than when the landing gear is being actuated) if the flywheel is to be maintained at full speed and, hence, at full charge. In Figure 21

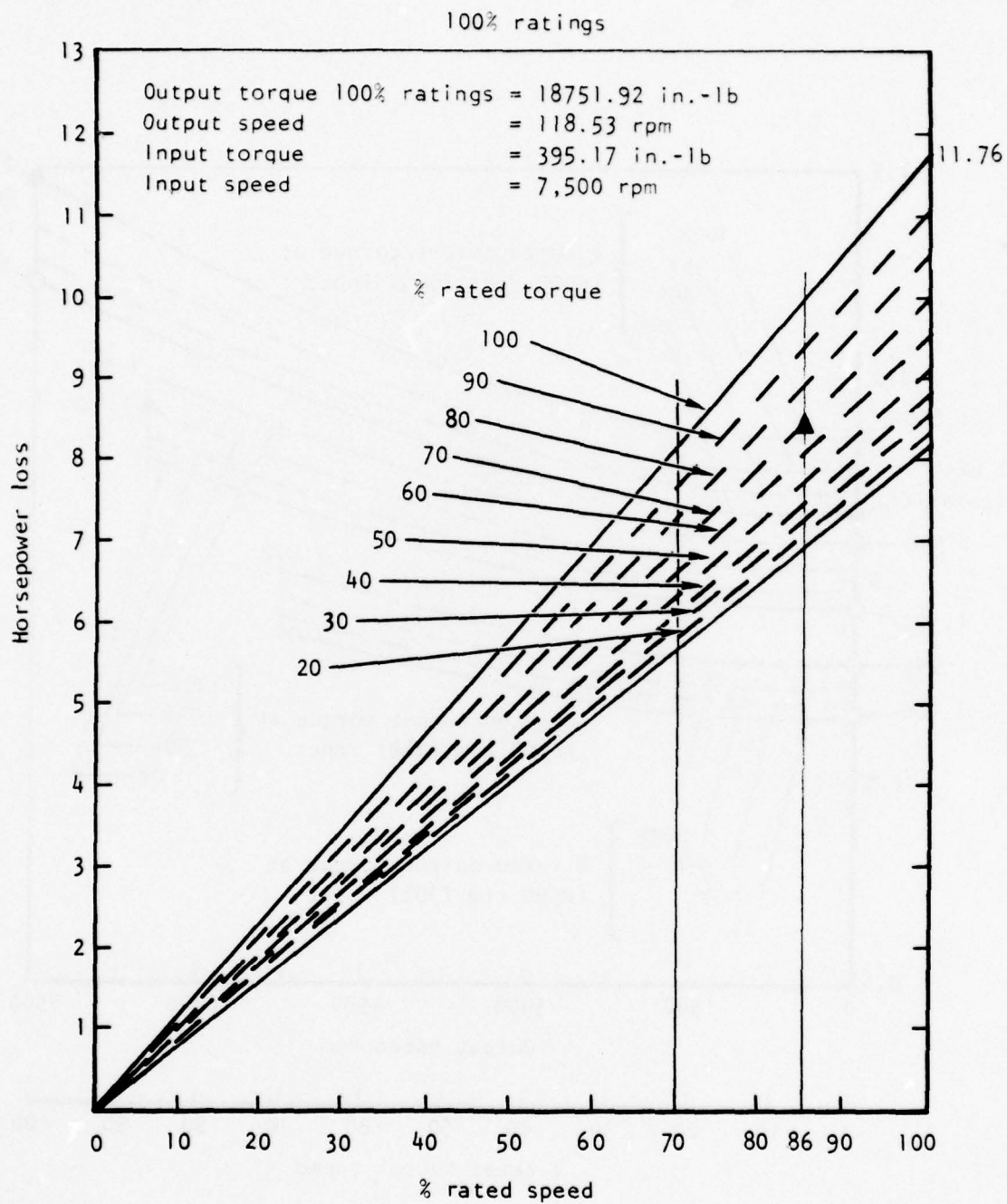


Figure 20. Screwjack Reduction Gear Train Losses (63.28:1 Ratio)

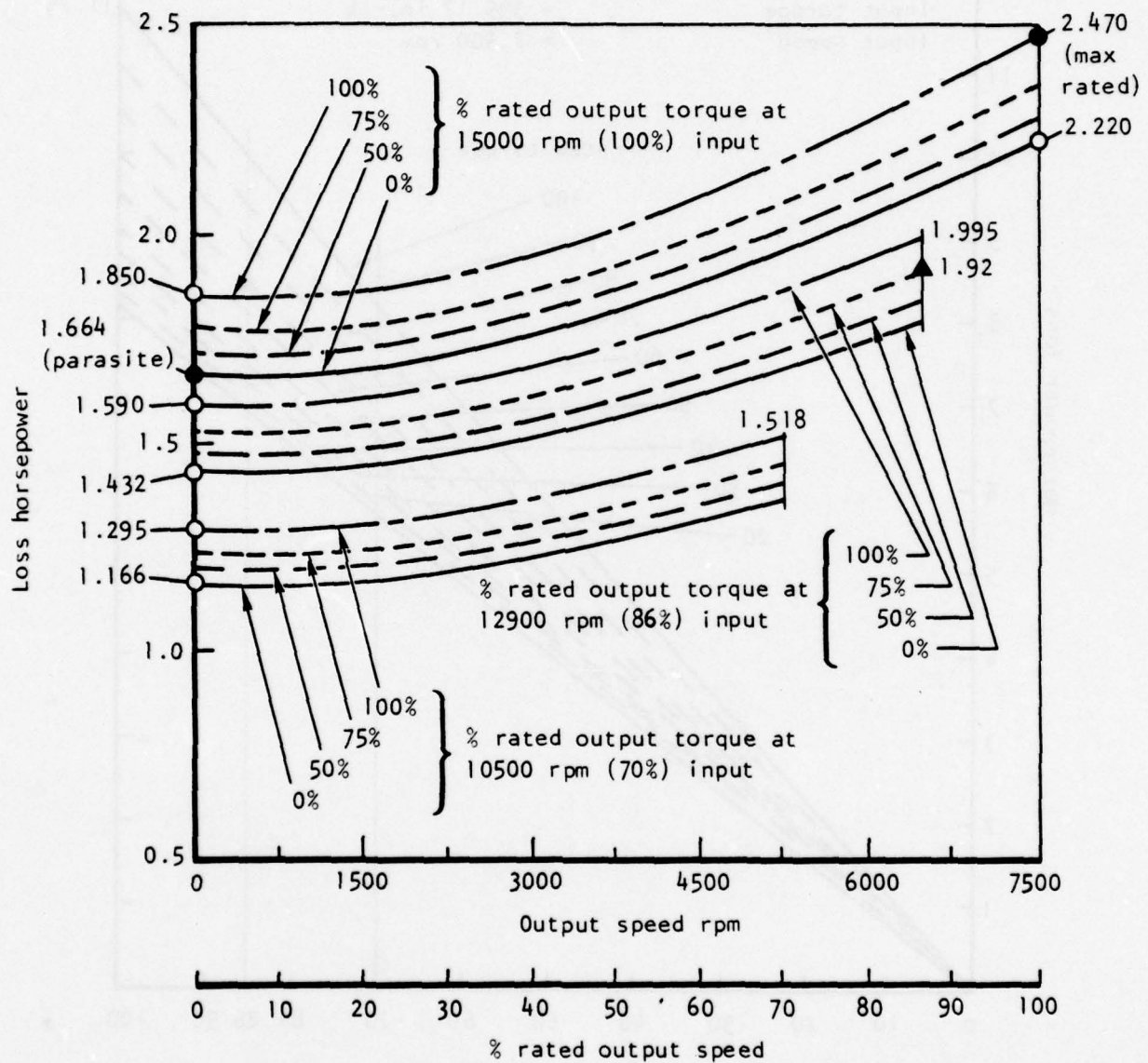


Figure 21. Mechanical Controller Loss Characteristics



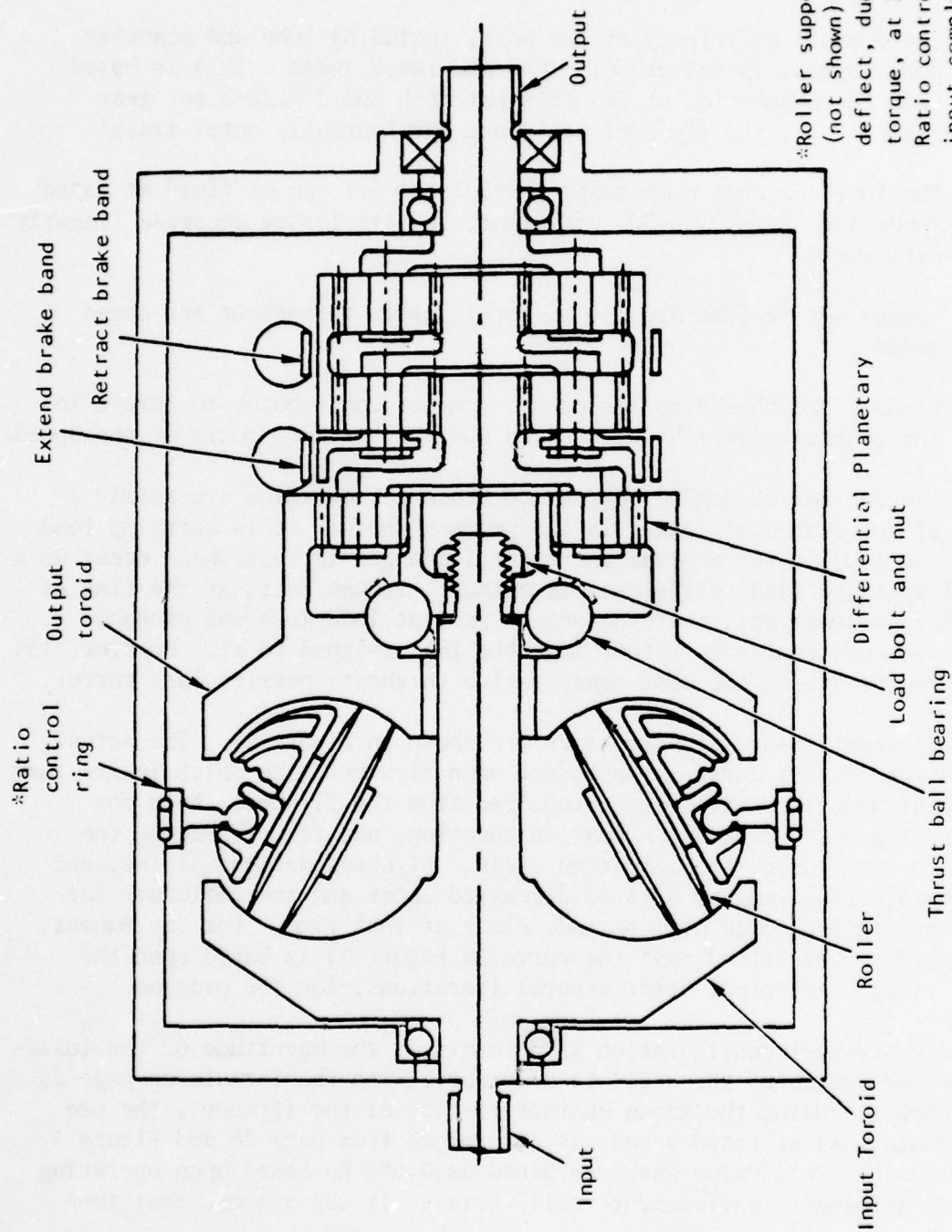


Figure 22. Roller Toroid Type Mechanical Valve

the critical loss for the controller was assumed from the curves as 1.66 horsepower while the maximum instantaneous loss was presumed not to exceed 2.47 horsepower.

The assumed gearbox losses are shown in Figure 23. These curves were constructed based upon the following assumptions:

- 1) The overall efficiency of the unit, including lube and scavenge pump losses, is 95% at full load and rated speed. This is based upon the assumption of 2+% loss per mesh and 2 meshes per gear train (i.e., the flywheel train and the hydraulic motor train).
- 2) The lube-scavenge pump system circulates 5.1 gpm of fluid at rated speed and 75 psi, is 70% efficient, and its losses decrease linearly with speed.
- 3) Losses due to load are 15% of total losses throughout the speed range.
- 4) Windage and threshing losses are a major contributor to losses in the gearbox system at high speed and vary as the square of the speed.

The windage and threshing losses are those losses which are solely a function of speed and will exist in the gearbox whether it is carrying load or not. The load losses are the incremental changes in loss which occur as a result of applying load to the gearbox output. It was felt, at the time of making these assumptions, that the actual percent load loss was probably closer to 30% of total loss rather than the 15% assigned to it. However, 15% was selected as giving the most conservative (highest) parasite loss curve.

The flywheel loss characteristics are shown in Figure 24. The actual determination of this curve is dependent upon flywheel size which in its turn is dependent upon the total energy required from the flywheel, both for performing the most demanding actuation function, and for offsetting the losses occurring during the actuation cycle. Flywheel design, sizing, and energy storage requirements will be discussed later and the rationale for determining flywheel size will be made clear at that time. For the moment, it only need be understood that the curve in Figure 24 is based upon the flywheel finally selected, after several iterations, for the program.

Once a flywheel configuration is determined, the magnitude of the losses varies as the square of the speed in accordance with the formula on page 26 of Reference 1. Using the known characteristics of the flywheel, the probable windage loss at rated speed was determined from page 26 and Figure 4 of Reference 1. This value was determined as 0.688 hp based upon operating in 1/100th atmosphere environment (0.147 psia). It was assumed that the

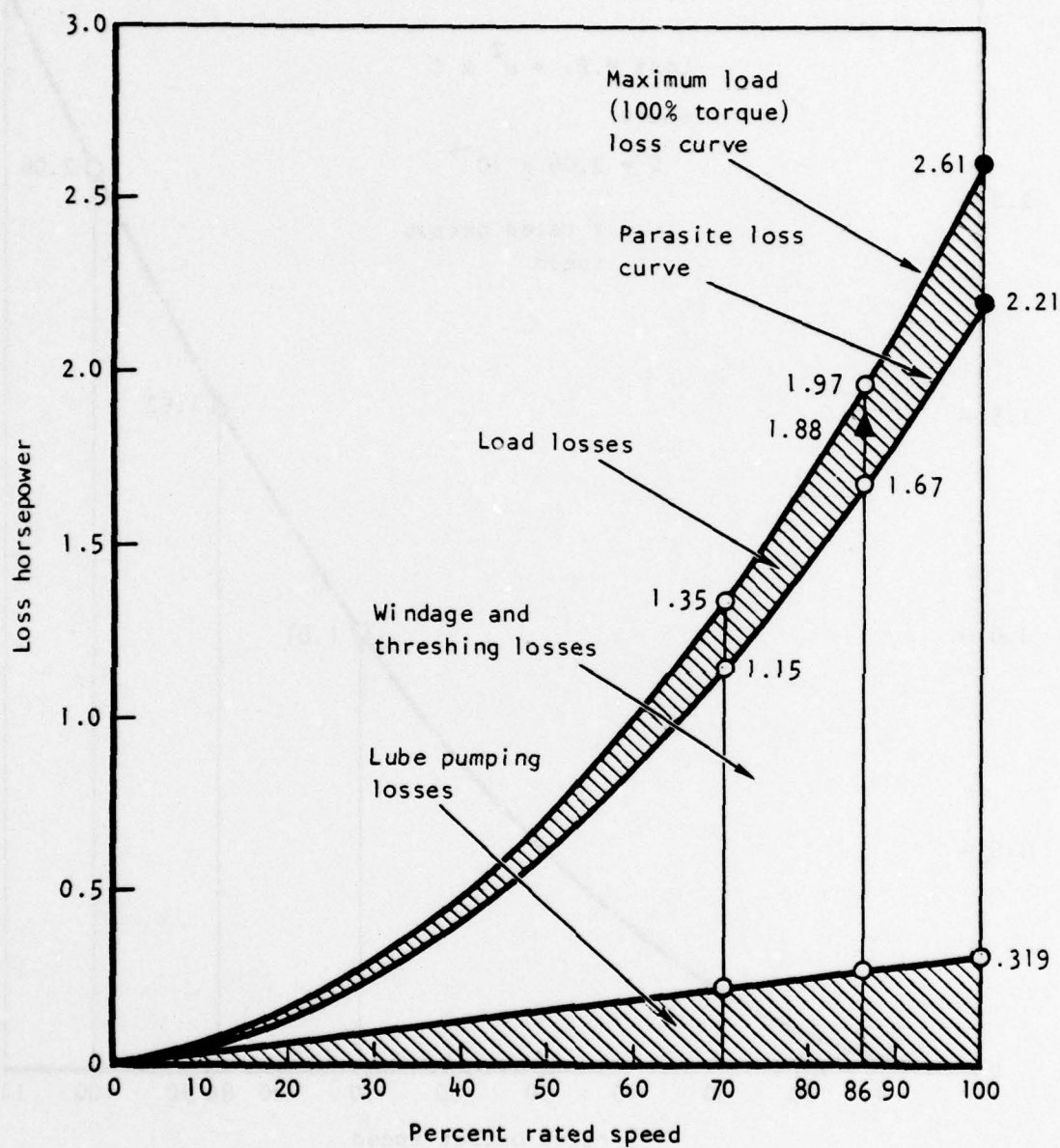


Figure 23. Gearbox Loss Characteristics



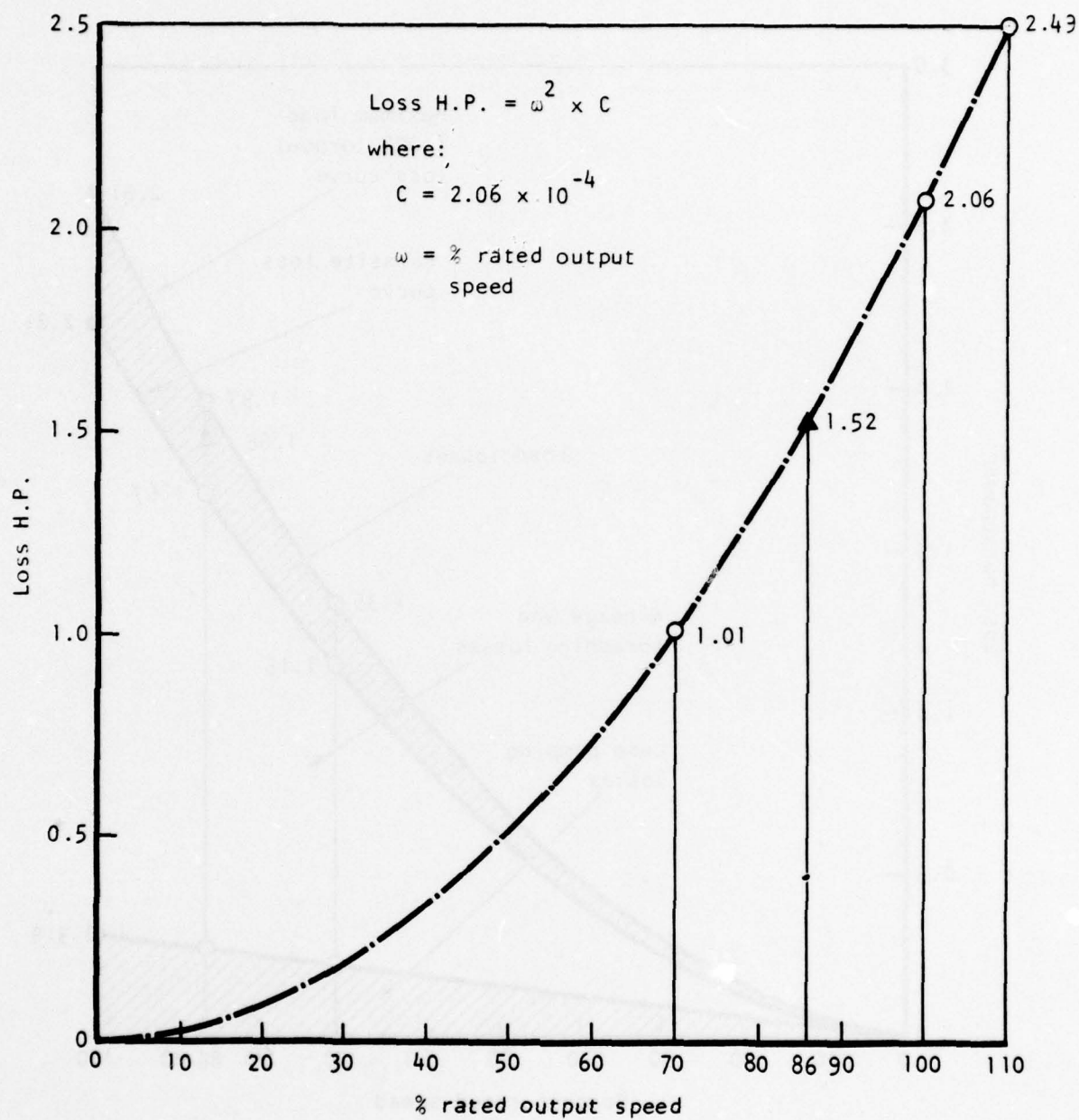


Figure 24. Flywheel Loss Characteristics

flywheel disk losses would be one-third of the total losses, with the other two-thirds being generated by the bearings and seals. This lead to the assumption of 2.06 hp as the total loss for the flywheel system at rated speed. Using the formula shown in Figure 24, a curve was plotted to give the projected loss values at other speeds (percent rated speed) from which it was assumed that the loss at 86% rated speed would be 1.52 hp and the loss at 70% rated speed would be 1.01 hp. This plot further assumed that bearing and seal losses would show the same second-power relationship with respect to speed as that shown by the flywheel.

The last component involved in the power flow analysis is the hydraulic motor. Unlike the rest of the components, the hydraulic motor was an existing fixed displacement 4,000 psi rated unit (ABEX AM05C) whose performance could be predicted quite accurately. The performance data are tabulated in the upper right portion of Figure 17. These data show that hydraulic motor efficiency increases slowly with decreasing speed over the normal operating speed range (70 to 100% rated speed). Comparing the output power of the hydraulic motor shown in Figure 17 to the required gearbox inputs tabulated in the upper center of Figure 17 shows that the motor should meet the one-fifth power requirement (i.e., the hydraulic motor should supply no more than 20% of the total power requirement of the whole MPP unit) stated in the contract. At rated speed, the motor is projected to supply 14.5%, at average speed 16.7%, and at minimum speed 18.4% of the total power requirement. Data which can be derived from the tabularized data in Figure 17 (hydraulic motor and parasite loss data) show that the motor is projected to operate at pressures well below 3,000 psi for most of its life. When operating in the charged standby condition, the operating pressure should be less than 2,105 psi.

### ENERGY ANALYSIS

One of the most important factors involved in completing the system definition phase was to determine the energy which must be stored in the flywheel and through it define the flywheel size. The energy needed in the flywheel will be the energy required for the worst-case actuation function, plus the losses occurring in the actuation system, minus the energy supplied by the hydraulic motor during the actuation cycle. This may be stated in equation form as follows:

$$E_F = E_O + E_L - E_M$$

where

$E_F$  = Energy available for extraction from flywheel

$E_O$  = Energy output required to perform function

$E_L$  = Sum of losses of all components in MPP downstream of hydraulic motor (i.e., flywheel, gearbox and controller)

$E_M$  = Energy supplied by hydraulic motor during actuation cycle

The load stroke curve of Figure 13 represents the worst-case energy demand condition and, as shown in the figure, has an energy demand of 942,200 in.-lb.  $E_0$ , therefore, equals 942,200 in.-lb. Certain assumptions were made to determine the other energy values (i.e.,  $E_M$  and  $E_L$ ). These assumptions were as follows:

- 1) The loss values for the various components were determined at 86% rated speed and 70% rated load. 86% rated speed was selected because this represents the average speed at which the unit will operate during a worst-case cycle. 70% load was selected because, as can be seen in Figure 13, it represents the average load (or torque) at which all components in the MPP will operate during the cycle. Triangular tic marks are placed on all loss curves (Figures 19, 20, 21, 23, and 24) to indicate the value of the average hp loss occurring during the worst-case actuation cycle.
- 2) The flywheel starts to slow down (deliver energy) at the same time that the hydraulic motor hits full load, both of which events occur 0.50 second after cycle initiation.
- 3) The flywheel energy delivery time is 6.0 seconds based upon the following:  
  
7.5 sec cycle time - 0.5 sec at beginning of cycle, 1.0 sec snub time at end of cycle = 6.0 sec net
- 4)  $E_M$  is determined based on the average of the output powers listed for the hydraulic motor in Figure 17 (i.e., 7.13 hp).

Using the preceding assumptions,  $E_M$  may be found as follows:

$$E_M = 6,600 \frac{\text{in.-lb}}{\text{sec hp}} \times 6.0 \text{ sec} \times 7.13 \text{ hp} = 282,348 \text{ in.-lb}$$

$E_L$  may be found as follows:

$$E_L = 6600 \frac{\text{in.-lb}}{\text{sec hp}} \times 6.0 \text{ sec} \times \text{HP}_L$$



where

$$\begin{aligned} \text{HP}_L &= \text{Sum of average loss horsepowers} \\ &= +2.28 \text{ hp ball screw loss (Figure 19)} \\ &\quad +8.54 \text{ hp screwjack reduction geartrain loss (Figure 20)} \\ &\quad +1.92 \text{ hp controller loss (Figure 21)} \\ &\quad +1.88 \text{ hp adapter gearbox loss (Figure 23)} \\ &\quad +\underline{1.52} \text{ hp flywheel loss (Figure 24)} \\ &= 16.13 \text{ hp total} \end{aligned}$$

therefore

$$E_L = 6,600 \times 6.0 \times 16.13 = 638,748 \text{ in.-lb}$$

Based on the foregoing, the energy which must be available for extraction from the flywheel as a result of a 30% speed reduction (i.e.,  $E_F$ ) may be found

$$\begin{aligned} E_F &= 942,200 + 638,748 - 282,348 \\ &= 1,298,600 \text{ in.-lb} \end{aligned}$$

Since the energy extractable from the flywheel ( $E_F$ ) at 30% speed reduction is 51% of the total (Figure 18), the total energy stored in the flywheel must be nearly double that used. The total energy required in the flywheel  $E_{TF}$  is found based on the following relationship:

$$\frac{E_{TF}}{E_F} = \frac{1}{0.51} \text{ or } E_{TF} = 1.961 E_F$$

$$E_{TF} = 1.961 \times 1,298,600 = 2,546,554 \text{ in.-lb}$$

Applying a safety margin of 23% gives

$$E_{TF} \times 1.23 = 3,132,261 \text{ in.-lb}$$

## MPP SYSTEM PROCUREMENT

The work completed under "MPP System Design" provided the basis for writing procurement specifications. Procurement specifications were written for the following components and are included in this report as Appendix A:

- 1) Gearbox (NA-75-363A)
- 2) Controller (NA-75-401A)
- 3) Screwjack (NA-75-527)

As previously pointed out, the system design and analysis was an iterative and refining process which continued on through the design, analysis, and procurement cycle. For this reason, all specifications, and particularly the first two issued (gearbox and controller), differ in some small details from the values given in Figure 17 and Table 2. As an example, the maximum torque loads during cycling given in the gearbox specification (NA-75-363A, Table II) is 44, 34, and 233 in.-lb for the hydraulic motor pad, flywheel pad, and controller pad, respectively, while the corresponding Figure 17 values (i.e., the final design values) are essentially equal or less, being 44.70, 31.93, and 207.94 in.-lb. In those few instances where Figure 17 values were significantly higher than the values appearing in the specification (i.e., hydraulic motor stall torque - 59.21 in.-lb in Figure 17 and 45.4 in.-lb in the specification), negotiations were conducted to determine that the predicted loads would fall well within the inherent safety factors incorporated in the component design.

Although it was intended that the gearbox contract be the first one awarded, the controller contract was actually the first. This contract was awarded to Traction Propulsion, Inc., on a competitive bid basis after three prospective suppliers had been contacted, two of whom submitted viable bids. The gearbox and screwjack contracts were also awarded on a competitive bid basis in which two viable bids were also received. The successful bidder on the gearbox was John Maddock, a consulting engineer and specialist in gearbox design. The successful bidder on the screwjack was also John Maddock.

## COMPONENT DESIGN

Once the speed, load, and loss requirements had been defined and specifications had been issued, detailed design of the various components could proceed at Rockwell and at the subcontractors. The design considerations and detailed designs of each major component are discussed in the following order:

- 1) Flywheel
- 2) Gearbox

3) Controller

4) Screwjack

### Flywheel Design

An illustration of an early flywheel design approach is in Figure 25. At that time, the design was still built around the small (6-inch-diameter) high-speed (104,784 rpm) disk. The design also incorporated, in a single sketch, two approaches to hybrid bearing design and two stub shaft sizes. Although the final design differed from this considerably in detail, Figure 25 incorporates all of the basic characteristics of the flywheel, and this was felt to provide an excellent tool for illustrating the many trade-offs necessary in reaching the final design.

Using Figure 25 as a guide, the discussion of the flywheel design is broken down into the following general categories:

- 1) Flywheel disk
- 2) Flywheel bearings
- 3) Flywheel seals
- 4) Flywheel lube, cooling, and assembly

### Flywheel Disk Design

As Figure 25 shows, the original flywheel disk design was based upon a 6-inch-diameter flywheel disk. This disk weighed 4.023 pounds and turned at 104,784 rpm on 15 mm diameter integral stub shafts weighting 0.402 pound, giving a total flywheel weight of 4.425. This design was shortly abandoned when it was found that energy requirements for actual B-1 aircraft landing gear operation were nearly double those assumed initially. A new design based on a 7.125-inch-diameter flywheel disk was selected, after several iterations, as being the optimum design.

In attempting to arrive at the optimum design, a variety of often conflicting factors had to be taken into account:

- 1) The bearing system must have the ability to resist high precessional load torques (i.e., gyroscopic effects resulting from changing the flywheel rotational axis as a result of aircraft maneuvering). This can be accomplished for a given capacity bearing by spacing the bearings wide apart.



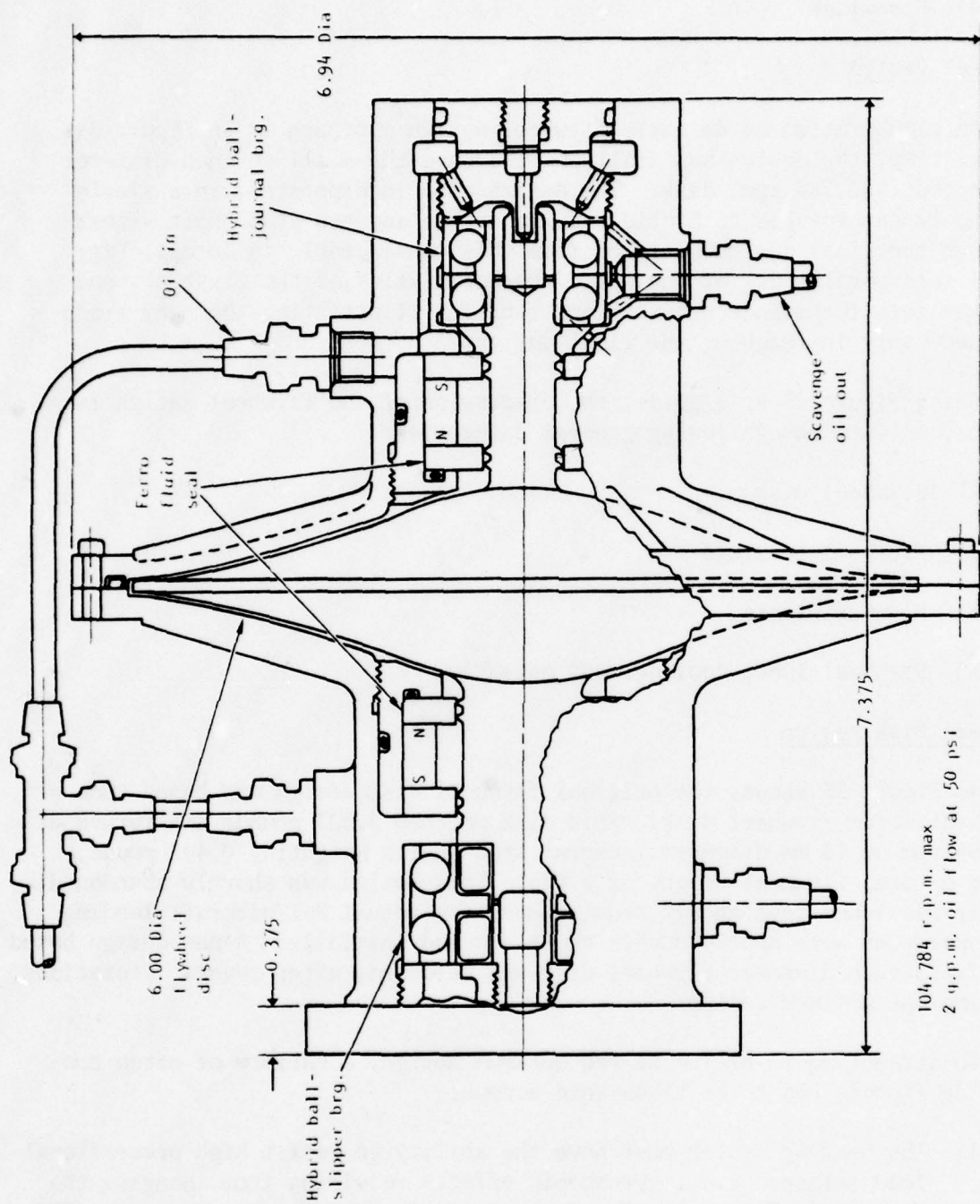


Figure 25. Early Flywheel Design

- 2) There must be a seal between the flywheel disk and its support bearings. This is necessary so that a vacuum can be maintained around the flywheel disk to reduce windage losses. To keep seal losses low, the seal diameter and, hence, the flywheel shaft diameter, must be kept small.
- 3) It is highly desirable that the rated operating speed of the flywheel be less than the first critical speed.

Item 3 is in nearly direct conflict with items 1 and 2. In order to keep the critical speed of the flywheel high, the flywheel stub shafts should be short and large in diameter, more like the section of the shaft under the seal in the left portion of Figure 25. However, since seal and bearing losses tend to increase as the square of the diameter (seal diameter for seals and journal, or mean ball diameter for bearings), the increase in shaft diameter can have a disastrous effect on losses.

Early in the design phase, a series of critical speed analysis was conducted on a flywheel design generally in accord with Figure 25 but with various shaft sizes ranging from 13 through 20 to 25 mm.

The critical speeds were computed using the Rayleigh-Ritz equation

$$\omega_c = \sqrt{\frac{g \sum \omega \delta}{\sum \omega \delta}}$$

where  $\omega$  and  $\delta$  represent the rotor masses and shaft deflections at the respective CG of their multimass system.

For this initial evaluation, the flywheel rotor system was considered as consisting of flexible shafts, concentrated masses, no bending in the region of the flywheel disk, and rigid bearing supports. It was recognized that the final design will use flexible bearings, which will tend to reduce the critical speed. However, by initially establishing a rotor geometry based on fixed supports, approximate bearing sizes could be quickly selected. The rotor system critical speeds could then be further evaluated with such a fixed geometry. The computations indicated the following critical speeds.

| Shaft Dia<br>(mm) | Critical Speed<br>(rpm) |
|-------------------|-------------------------|
| 13                | 23,700                  |
| 20                | 45,400                  |
| 25                | 69,800                  |

Because the critical speeds calculated for the various shaft diameters resulted in a speed value below the operating speeds of 70,000/100,000 rpm, it was considered desirable to examine the second critical. By selecting a shaft size whose first critical is below and second critical is above the operating speed range of the rotor, an optimum shaft/bearing design becomes feasible (i.e., optimum in the sense that a lower first critical speed makes possible a smaller shaft, which makes possible a smaller bearing and minimizes bearing and seal rotating losses).

In order to check the second and third critical speeds, the 15 mm diameter shaft was recalculated using an existing computer program. This determination considered the free mode, including spring stiffness representative of the duplex bearing and housing support, and provided the following values:

|              |            |
|--------------|------------|
| 1st critical | 23,345 rpm |
| 2nd          | 56,643     |
| 3rd          | 151,791    |

It can be seen that the first critical speed value corroborated, almost exactly, the value determined earlier by hand calculation, especially considering the small critical speed reduction which could be expected from introducing flexibility in the bearing supports. It can also be seen that the first and second critical speeds were much too low and close together to bracket the projected operating speed range of the flywheel (70,000-100,000 rpm at this stage of design development).

At this point, the flywheel was redesigned to meet the new and higher energy requirement determined under "Energy Analysis." A comparison of the "old" and "new" flywheels is as follows:

| <u>Characteristic</u>                | <u>Old</u>                    | <u>New</u>                     |
|--------------------------------------|-------------------------------|--------------------------------|
| Rated speed                          | 104,784 rpm                   | 88,235 rpm                     |
| Design stress                        | 140,000 psi                   | 140,000 psi                    |
| Wheel dia                            | 6 in.                         | 7.125 in.                      |
| Tip thickness                        | 0.09 in.                      | 0.121 in.                      |
| Base thickness                       | 1.492 in.                     | 2.011 in.                      |
| Shaft dia.                           | 15 mm                         | 17 mm                          |
| Wheel weight                         | 4.023 lb                      | 7.64 lb                        |
| Shift weight                         | 0.402 lb                      | 0.56 lb                        |
| Total weight                         | 4.425 lb                      | 8.20 lb                        |
| Nom. of inertia                      | 0.027 in.-lb sec <sup>2</sup> | 0.0513 in.-lb sec <sup>2</sup> |
| Energy storage                       | 1,648,334 in.-lb              | 3,132,261 in.-lb               |
| Available energy<br>(30% speed red.) | 824,167 in.-lb                | 1,298,600 in.-lb               |
| Bearing spacing                      | 5.000 in.                     | 5.366 in.                      |



The most significant factors are that the new flywheel is larger (7.125-inch diameter), slower (88,235 rpm), and heavier (8.20 pounds). It would have been possible to retain the 6-inch diameter and the 104,784 rpm operating speed at the higher required energy level. However, as in all trade-off situations, this would have involved certain advantages and disadvantages which analysis indicated were weighted to the disadvantage of the smaller high-speed wheel.

A comparison of the two flywheel cross sections is shown in Figure 26. Both flywheels shown weigh the same and store the same energy, even though the smaller (6-inch diameter) flywheel turns at a 19% higher speed. Both flywheels are of the optimized disk cross section and are designed to an operating stress of 140,000 psi. They were sized and proportioned in accordance to Appendix A of Reference 1.

Figure 26 shows that the small-diameter flywheel is much wider at its base (hub). This, coupled with its higher speed, leads to several advantages and disadvantages, as follows:

#### 1) Advantages

- a) The smaller diameter of the 6-inch-diameter flywheel leads to a lower volume installation and a lighter weight housing and bearing system. The lower volume results from the fact that the housing is 1.125 inches smaller in diameter, while the assembly length increases only 0.825 inch. The lower weight results not only from the lower volume, but because the housing is better shaped to react precessional load effects between ends and because (item b) the precessional loads are less.
- b) As indicated in the preceding, the precessional loads in the bearings are less, making possible a smaller and more high-speed-adaptable bearing package. All other things being equal, the precessional loads appearing in a flywheel support bearing system tend to be a function of the square of the diameter. In this case, the precession loads in the 7.125-inch-diameter wheel would be 41% greater than those in the 6.00-inch-diameter wheel.

#### 2) Disadvantages

- a) The critical speeds of the small-diameter flywheel will be lower. This results from the fact that critical speeds are a function of shaft diameter and shaft diameter is, in turn, a function of the seal surface speed tolerance. As shown in Figure 25, a seal must be used between the bearing and the flywheel disk to allow the disk to turn in a vacuum. The seal (whether ferrometic or conventional carbon face seal type) has a definite allowable differential surface speed between the static member and the rotating

| Flywheel coordinates |             |        |           |             |        |       |
|----------------------|-------------|--------|-----------|-------------|--------|-------|
| 7.125 Dia            |             |        | 6.000 Dia |             |        |       |
|                      | R           | T      | T/2       | R           | T      | T/2   |
|                      | +0.000-.005 | ±0.002 |           | +0.000-.005 | ±0.002 |       |
| 1                    | 3.562       | 0.121  | 0.061     | 3.000       | 0.171  | 0.086 |
| 2                    | 3.384       | 0.158  | 0.079     | 2.850       | 0.224  | 0.112 |
| 3                    | 3.206       | 0.206  | 0.103     | 2.700       | 0.291  | 0.145 |
| 4                    | 3.028       | 0.264  | 0.132     | 2.550       | 0.373  | 0.186 |
| 5                    | 2.850       | 0.334  | 0.167     | 2.400       | 0.470  | 0.253 |
| 6                    | 2.671       | 0.414  | 0.207     | 2.250       | 0.585  | 0.292 |
| 7                    | 2.493       | 0.508  | 0.254     | 2.100       | 0.717  | 0.358 |
| 8                    | 2.315       | 0.612  | 0.306     | 1.950       | 0.865  | 0.433 |
| 9                    | 2.137       | 0.730  | 0.366     | 1.800       | 1.031  | 0.516 |
| 10                   | 1.959       | 0.858  | 0.429     | 1.650       | 1.213  | 0.606 |
| 11                   | 1.781       | 0.995  | 0.498     | 1.500       | 1.404  | 0.702 |
| 12                   | 1.603       | 1.136  | 0.568     | 1.350       | 1.606  | 0.803 |
| 13                   | 1.425       | 1.283  | 0.642     | 1.200       | 1.809  | 0.905 |
| 14                   | 1.247       | 1.422  | 0.711     | 1.050       | 2.010  | 1.005 |
| 15                   | 1.068       | 1.561  | 0.781     | 0.900       | 2.201  | 1.101 |
| 16                   | 0.890       | 1.683  | 0.842     | 0.750       | 2.379  | 1.190 |
| 17                   | 0.712       | 1.796  | 0.898     | 0.600       | 2.533  | 1.266 |
| 18                   | 0.534       | 1.883  | 0.942     | 0.450       | 2.661  | 1.331 |
| 19                   | 0.356       | 1.955  | 0.978     | 0.300       | 2.757  | 1.378 |
| 20                   | 0.178       | 1.992  | 0.996     | 0.150       | 2.815  | 1.407 |
| 21                   | 0.000       | 2.011  | 1.006     | 0.000       | 2.836  | 1.418 |

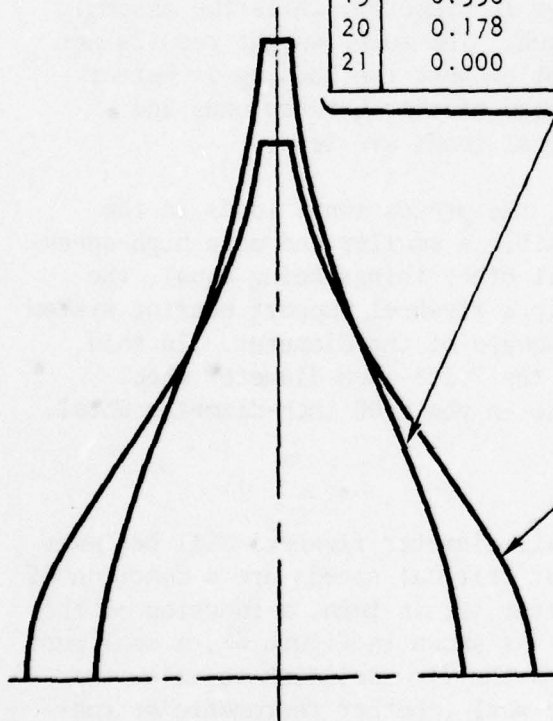


Figure 26. Flywheel Shapes

member. This means that the diameter of the shaft, associated with the 6-inch-diameter wheel, must be reduced in the area next to the flywheel disk (i.e., in the bending stiffness-critical area) by an amount proportional to the increase in speed. The increased "whipiness" which results, plus the increased operating speed level, exponentially compounds the problem of controlling the eccentricities, resonances, and loads which occur while operating through the speed range.

- b) The bearing system will tend to be designed by flywheel unbalance (even though the out of balance is extremely small) because it is amplified greatly by shaft deflection, due to the shaft flexibility of the small-diameter shaft at high speed. This phenomena is discussed more thoroughly in the following paragraphs covering bearing design. For this reason, precession loads (which the small-diameter wheel reduces) will cease to be the governing design criteria; thus, the small-diameter flywheel lost this as a potential advantage.
- c) The small-diameter flywheel is harder to inspect and has a poorer stress distribution. As discussed later, the flywheel design was based upon fracture mechanics principles. These principles determined allowable operating stress levels based on the minimum flaw size which can be detected in the area of maximum stress by the best available nondestructive test methods. The minimum detectable flaw size was a direct function of the depth of material which must be penetrated by the nondestructive test beam. The greater the depth of penetration, the larger the flaw which could escape detection and the lower the allowable operating stress. Since the maximum stress in an optimized disk flywheel occurs at the center of the hub on the axis of rotation, it can be seen that the small-diameter flywheel's wider hub required approximately 25% greater depth of penetration to reach the maximum stress point than did the larger diameter wheel. In addition to the poorer inspectability, the wide-hubbed flywheel showed a poorer stress distribution. As long as the hub width was less than 30% of the outside diameter (the 7.125-inch-diameter wheel is 28.2%), the stresses along the axis of rotation and the stresses at any other radial position in the wheel would not vary by more than +5% from the computed values (i.e., the values from Appendix A of Reference 1). However, as the width-to-diameter ratio increased significantly above 30% (the 6.00-inch-diameter wheel is 47.3%), the stress variations increased rapidly (for the 6.00-inch-diameter wheel, the variation approached +20%). The maximum stresses in excess of theoretical occur on the axis of rotation at the center of the hub, which is the hardest point to inspect.



Equating the one remaining advantage (modestly smaller volume and weight) of the small-diameter flywheel against its disadvantages (poorer critical speed characteristics, poorer inspectability, harder to balance, and poorer stress distribution), it became apparent that the larger diameter wheel should be used and was selected for the final design.

The material selected for the flywheel disk was HP9-4-20 heat treated in accordance with Rockwell material specification ST0160LB0002. This gave a material which, when forged per MIL-F-7190 and subsequently heat treated, had the following basic properties:

|  |                           |
|--|---------------------------|
| Density ( $\rho$ )                           | 0.285 lb/in. <sup>3</sup> |
| Modulus of elasticity (E)                    | 28,800,000 psi            |
| Ultimate tensile strength (F <sub>TU</sub> ) | 205,000 psi               |
| Yield strength (F <sub>TY</sub> )            | 185,000 psi               |
| Poissons ratio ( $\nu$ )                     | 0.296                     |

This material was selected because of its fracture mechanics properties (i.e., it was the best steel available in terms of fatigue properties in relation to crack propagation rate and critical flaw size).

The required fatigue properties for a device such as a flywheel are largely determined by the alternating stresses which result from actual operation. For this application, the B-1 mission profile was used to determine the number and magnitude of these alternating stresses. The determination was arrived at as follows:

- 1) There were considered to be 1,280 missions per air vehicle life.
- 2) There were 2,697 landings and 2,697 takeoffs per air vehicle life, or an average of 2.1 landings and takeoffs per mission.
- 3) For the 2,697 landings, 2,200 were full-stop landings and 497 were touch-and-go landings. For this study, it was assumed that the gear was raised and lowered between each landing for an average of 4.2 gear operations per mission, and after each gear operation the speed of the flywheel would build up to maximum speed before next gear operation or shut down.
- 4) The flywheel was considered to operate only during the takeoff and landing phases of the mission. This meant that the flywheel was started up and shut down from the 100% speed twice per mission.
- 5) The maximum (unloaded) flywheel speed was 88,235 rpm. During the gear operation, the flywheel speed reduced to 70% maximum speed or 61,765 rpm.

- 6) Ground operation consisted of operating the gear on jacks 25 times during the life of the aircraft with four gear cycles per operation.
- 7) Considering a scatter factor of 4.0, the flywheel must support 5,120 missions.

The flywheel was thus anticipated to be subject to 10,340 cycles of 0 to 100% speed variation and 21,904 cycles of 0 to 100% speed variation during the life of the B-1, with a scatter factor of 4 applied. (See Figures 27 and 28.)

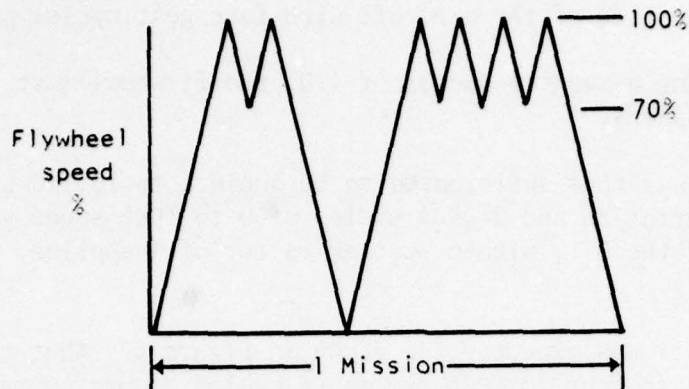
In addition, it was expected, as shown in Figure 27, that the flywheel would be subjected to four 70-105% overspeed cycles occurring randomly during the course of B-1 aircraft operations. The maximum stress in the flywheel was biaxial (radial and tangential stresses were essentially equal) and varies as the square of the speed of rotation. As indicated earlier, the normal design (maximum) stress at 100% rated speed was 140,000 psi therefore the nominal stresses existing at other speeds were as tabulated below:

| <u>Speed</u><br><u>(%)</u> | <u>Speed</u><br><u>(rpm)</u> | <u>Stress</u><br><u>(psi)</u> |
|----------------------------|------------------------------|-------------------------------|
| 105                        | 92,647                       | 154,350                       |
| 100                        | 88,235                       | 140,000                       |
| 70                         | 61,765                       | 68,600                        |
| 0                          | 0                            | 0                             |

The stress R-factors (i.e., the ratio of minimum stress to maximum stress in an alternating stress cycle) shown in Figures 27 and 28 were derived from these stress values.

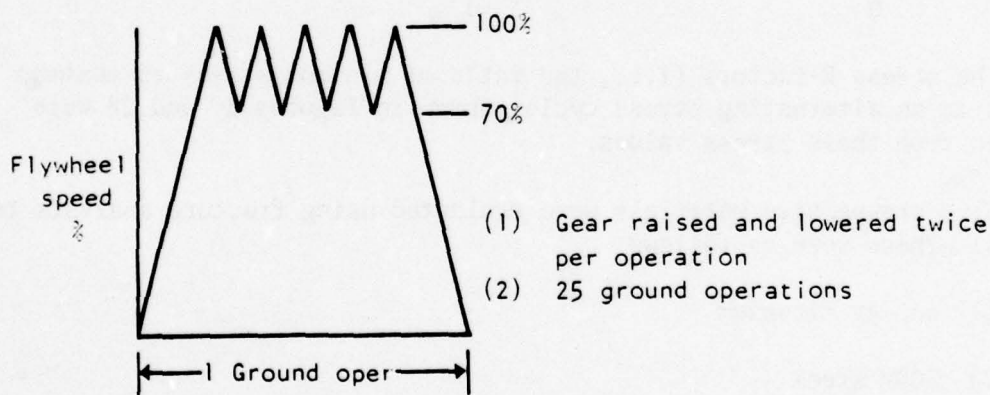
Five prospective materials were evaluated using fracture analysis techniques. These were as follows:

- 1) 6AL-4V titanium
- 2) 300M steel
- 3) HP9Ni-4C0-.20C steel
- 4) 10 Ni modified steel
- 5) HP9Ni-4C0-.30C steel



| Spectrum step no. | Item               | Max speed % | Min speed % | Stress R factor | Cycles per mission | Cycles per 1 life | Cycles per 4 lives |
|-------------------|--------------------|-------------|-------------|-----------------|--------------------|-------------------|--------------------|
| 1                 | Startup - shutdown | 100         | 0           | 0               | 2                  | 2,560             | 10,240             |
| 2                 | Gear operation     | 100         | 70          | +0.49           | 4.2                | 5,376             | 21,504             |
| 3                 | Overspeed          | 105         | 70          | +0.44           | -                  | 4                 | 4                  |

Figure 27. Flight Operations



| Spectrum step no. | Item               | Max speed % | Min speed % | Stress R factor | Cycles per 1 life | Cycles per 4 lives |
|-------------------|--------------------|-------------|-------------|-----------------|-------------------|--------------------|
| 1                 | Startup - shutdown | 100         | 0           | 0               | 25                | 100                |
| 2                 | Gear operation     | 100         | 70          | +0.49           | 100               | 400                |

Figure 28. Ground Operations (On Jacks)



Of the five, 10 Ni modified steel appeared to be the best material based on data available at the time the selection was made. However, it was a new material and there was some basic conflict in the data in several important areas. Therefore, selection was narrowed to the HP9 steels because they were clearly superior to the other two materials. Even though both of the HP9 steels were rated very closely, the 20% carbon version showed superiority when subject to a relatively few (less than 30,000) high stress cycles. As can be seen from the mission stress cycle profile established earlier, the significant stress cycles are 2,585 cycles (0-100% stress, R-factor = 0) in one lifetime or 10,340 cycles when considering a scatter factor of four. In like manner, during four lifetimes (scatter factor of four), the flywheel will be subject to 21,904 cycles (70% to 100% speed, 49% to 100% stress, R-factor = +0.49). Stressing at an R-factor of +0.49 in HP9-4-.20 steel material propagates flaws only 42.75% as fast as stressing at an R-factor of 0. Therefore, 21,904 cycles are equivalent to 9,364 when R-factor = 0 cycles. This gives a total equivalent R-factor = 0 cycles for four lifetimes of 19,704 cycles. This justified the use of HP9-4-.20 in preference to HP9-4-.30 and was very close to the 20,000 cycle life required in the contract. For the sake of convenience, therefore, the number used was 20,000 cycles.

It was expected that the flywheel would be inspected for flaw propagation at least once during the life of the aircraft or at 2,500 equivalent cycles, whichever occurs first, to gain confidence in the material and in the inspection techniques. A total of 2,500 cycles was selected because it is one-eighth the equivalent cycles of four lifetimes or one-half of one lifetime based on four lifetimes equaling 20,000 (0-100%) stress cycles.

Fracture mechanics analyses usually consider two types of flaws: surface and embedded. Surface flaws are easier to detect in smaller sizes than embedded flaws. This, plus the fact that the flywheel, unlike most structural elements, experiences its maximum stress at its geometrical center, well away from the surface, led to the embedded flaw being the determinant of flywheel's fatigue performance. Figure 29 shows the critical crack length versus stress. This graph assumes an embedded circular flaw whose diameter is twice  $a_{cr}$ . "Critical" describes a flaw which has grown to such a dimension (critical dimension) that the next application of stress to the level indicated will cause catastrophic failure. Figure 30 shows the initial flaw size which will propagate to critical size when subject to R-factor = 0 stress cycles to the peak stress and for the number of cycles indicated.

As indicated earlier, 140,000 psi was selected as the design (100%) stress for the flywheel. Based on Figure 30 an initial flaw of 0.056 radius ( $a_i$ ) or 0.112 diameter would survive for 2,500 cycles (the planned inspection period) before catastrophic failure. Figure 29 shows that the flaw will be very large (1.080 in. diameter) at failure. Since flaws 0.100 inch in diameter can be detected with a high degree of certainty in the center of a

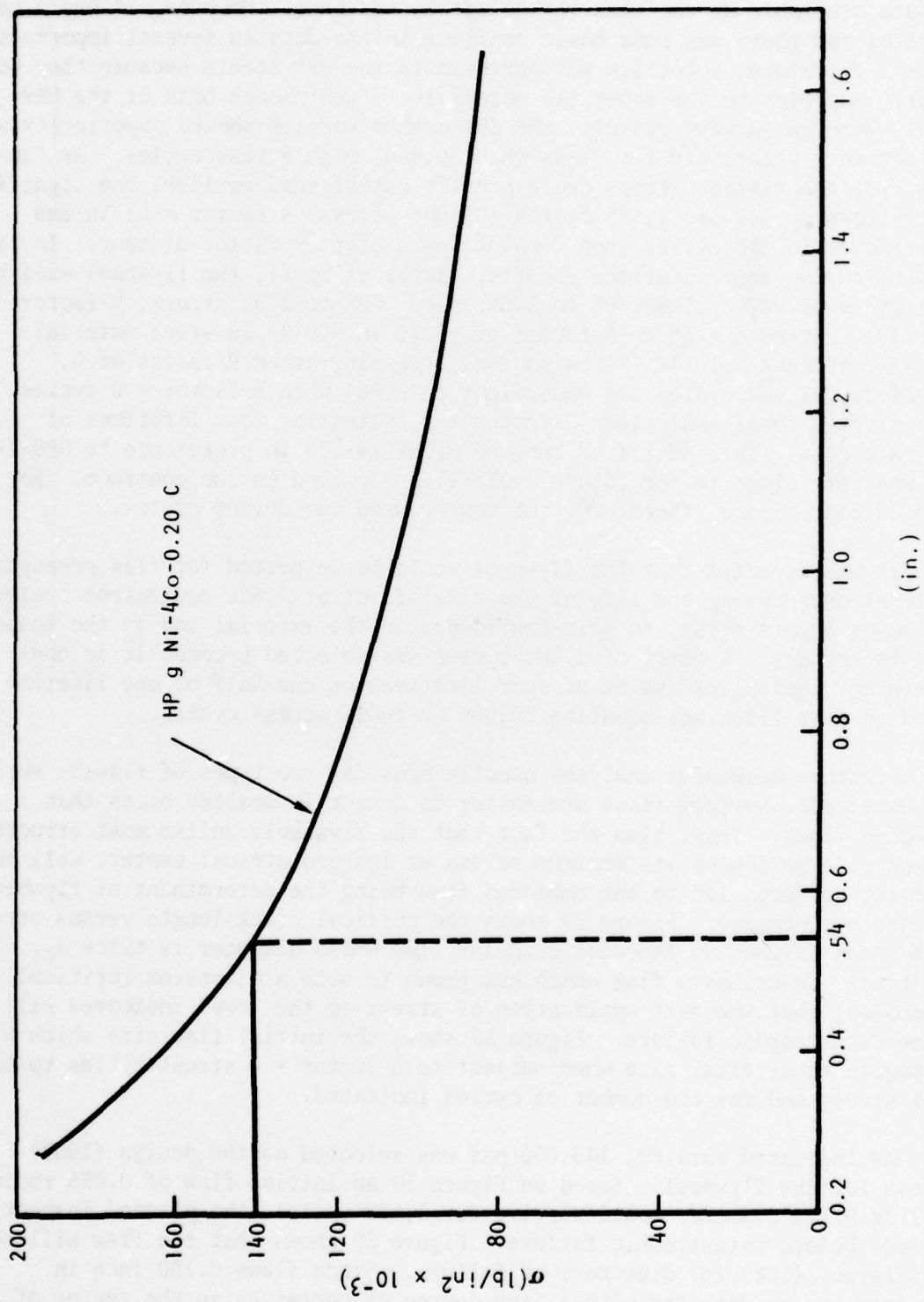


Figure 29. Critical Crack Length

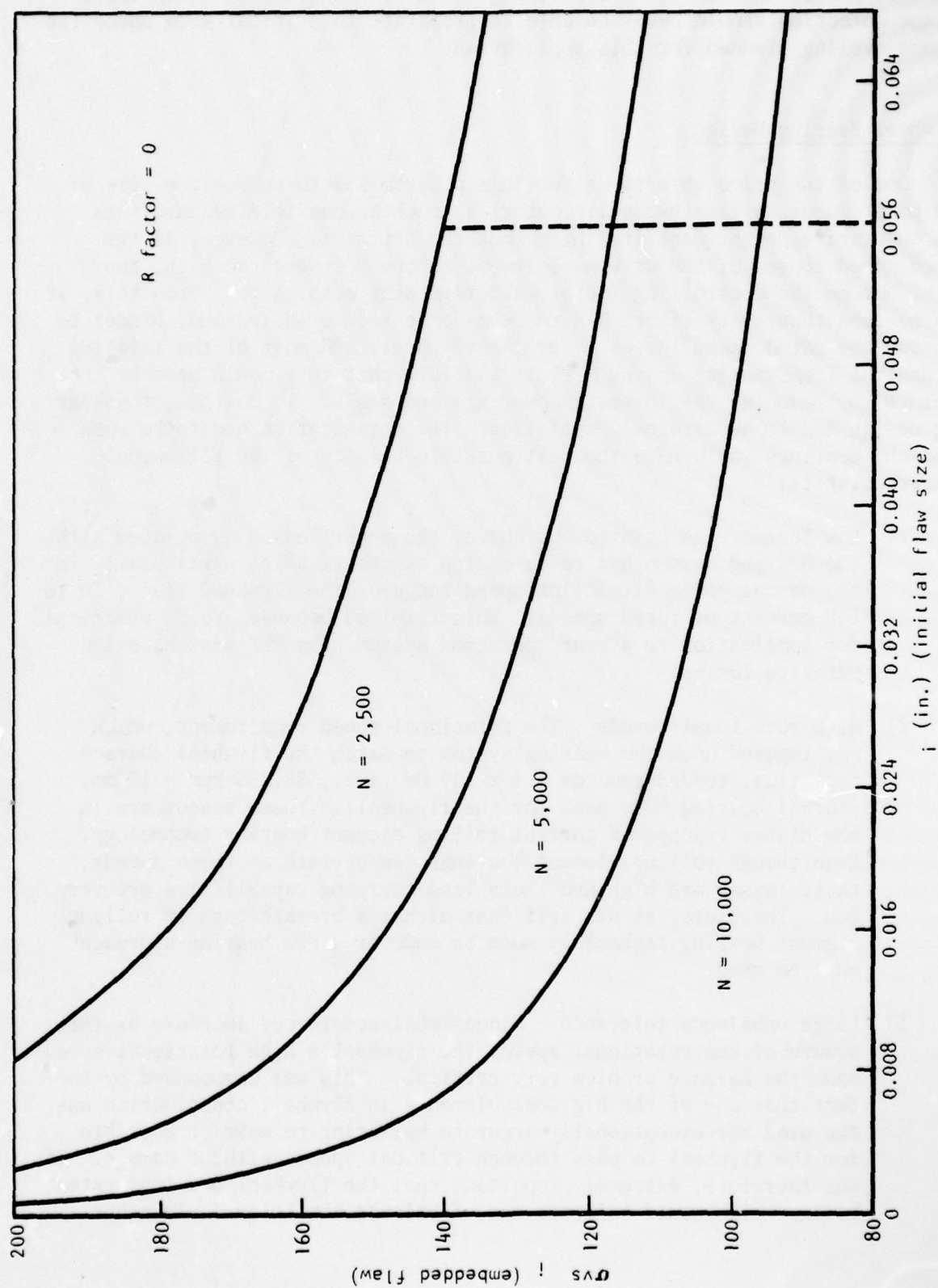


Figure 30. Cycles to Critical Flaw Size



flywheel hub of this size, it was believed that initial flaws, which could escape detection should never be able to propagate to critical size under the stress cycling planned for this application.

### Flywheel Bearing Design

One of the prime objectives for this program was to reduce the size of the power input device (hydraulic motor) as much as possible because this has cumulative weight benefits throughout the aircraft. However, if the rated speed losses of the driven equipment in the MPP were too high, they might become the controlling factor in determining motor size. From this, it can be seen that every effort had to be made to reduce losses and, hence, to improve the rated speed losses. For the flywheel, and most of the rotating mechanical items making up the MPP, it was felt that this could best be achieved by reducing the losses in bearings and seals. To do this, the bearing design had to be carefully optimized. The optimization had to be such that the bearings would have the best possible balance of the following characteristics:

- 1) Low losses - As pointed out above, the power losses associated with the bearing system had to be as low as practicable, particularly in the normal power extraction speed range of the flywheel (i.e., 70 to 100 percent of rated speed). This resulted because, to be practical for application to a gear operation system, the MPP must have low parasite losses.
- 2) High rotational speeds - The rotational speed requirement, which was imposed upon the bearing system to match the flywheel characteristics, tended towards  $1.5 \times 10^6$  DN (i.e., 88,235 rpm x 17 mm, journal bearing bore used for the flywheel). These speeds are in the higher reaches of current rolling element bearing technology. Even though rolling element bearings can operate at these speeds, their losses are high and their load carrying capabilities are very low. Therefore, it was felt that either a breakthrough in rolling element bearing technology must be made or a new bearing approach must be used.
- 3) Large unbalance tolerance - Since imbalance forces increase as the square of the rotational speed, the flywheel's high rotational speed made the balance problem very critical. This was compounded by the fact that one of the big cost elements in flywheel construction was the need for exceptionally accurate balancing to make it possible for the flywheel to pass through critical speeds without damage. It was therefore, extremely important that the flywheel bearing system be one which would tolerate out of balance conditions. In other

words, it should be one which would allow the flywheel to rotate about its mass center rather than its geometric center and, in so doing, would not transmit excessive loads through the bearing to surrounding structure.

- 4) High load capability - As previously indicated, the highest loads generated externally which, the flywheel bearing will encounter, are those generated by aircraft maneuvering. Since the flywheel is essentially a gyroscope, rotation of the platform upon which it is mounted about any axis, (other than the flywheel rotational axis or one parallel to it) will generate precessional loads in its bearings. The highest rotational maneuver rates are those which occur about the aircraft's line of flight axis (i.e., roll rates). These are 5 to 10 times as great as a typical aircraft's largest yaw and pitch rates. Therefore, if the flywheel rotational axis is oriented parallel to the aircraft roll axis so that roll rates do not generate precessional loads, the maximum precession induced bearing loads will be one-third to one-tenth of those which would exist otherwise. If the bearing system will tolerate radial loads which are at least 60 times flywheel weight for short periods (up to 2 seconds each incident) for a total number of incidents equating to 0.5 percent of the system's operational life, the flywheel mounting will be independent of orientation restrictions. If, on the other hand, the flywheel bearing system will tolerate peak loads equal to 10 times the flywheel weight for up to 30 seconds per incident and a total number of incidents equating to 4 percent of the system's operational life, it can be used in any orientation in most low maneuver rate aircraft such as bombers and cargo aircraft. In addition, it will be satisfactory for application to all aircraft for utility functions such as landing gear.

For the B-1 landing gear application, the MPP installation envelope dictated that the flywheel axis be oriented so that it was subject to full roll rates (see Figure 6). However, the B-1 was a low maneuver rate aircraft so it was felt that the bearing system must be capable of handling loads equal to 10 times the flywheel weight (i.e., 82 lb) and, further, that it would be a design objective to achieve a load capability equal to 60 times the flywheel weight (i.e., 492 lb) for short periods of time.

Several types of bearings were studied as follows:

- 1) Rolling element bearings (roller and ball) - pressure jet and mist lubricated.
- 2) Precision hydrodynamic journal bearings - pressure lubricated.
- 3) Hydrostatic bearings - pressure lubricated.

It shortly became apparent that all bearings were in some kind of a load/speed squeeze. In the rolling element bearing, it was a problem of the high-speed stealing load carrying capacity from the bearing. Whereas, in the journal bearing, high speed had the opposite effect and increased load capacity. However, in the journal bearing, the wide load range of the application, which does not significantly impact the ball bearing, caused all kinds of problems in the form of high losses and/or instability. It became apparent, then, that the solution to this conflict lay in some kind of combination of two bearings in such a way that the strengths of one offset the weaknesses of the other.

This led to the selection of the hybrid bearing arrangement. An early version of such a bearing arrangement is shown in Figure 25. It consisted of a journal bearing in series with a double row ball bearing. The ball bearing was at the low speed end of the series such that its absolute speed was to be approximately 50,000 rpm. This speed was equivalent to a DN value of  $1.25 \times 10^6$  and was well down towards the lower end of the ultra high speed range. At this speed, ball centrifugal loads were felt to be much less of a problem than at 88,235 rpm ( $1.75 \times 10^6$  DN) since centrifugal loads decrease as the square of the rpm.

The journal bearing was at the high-speed end of the series with its journal surface turning at 88,235 rpm. However, this fact had negligible impact since a journal bearing is little affected by centrifugal forces. On the other hand, the fact that the differential velocity had been reduced to 38,235 rpm did much to improve loss performance, since journal bearing losses tend to decrease as the square of the decrease in (differential) speed.

General Discussion. In a rolling element bearing, the power lost to friction is a function of lubricant viscosity rotational speed, and radius of rolling element pitch circle. In the fluid journal bearing, either hydrodynamic or hydrostatic, the friction losses are essentially linear functions of lubricant viscosity, fluid film thickness, rotational speed, and shaft diameter. The rolling element bearing, either ball or roller, has less start-up and low-speed friction than the journal bearing (by nearly two orders of magnitude), but as speed increases, the friction losses in the rolling element bearing eventually become greater than those of the fluid bearing of the same load carrying capacity.

In a strictly hydrodynamic journal bearing, the oil is usually self-contained within the bearing cavity, and the fluid pressure which supports the loaded shaft is generated solely by the speed of the shaft and the viscosity of the lubricant (see Figure 31.) Thus, at no speed or under low amplitude oscillatory rotational motion, there is no supporting fluid pressure under the shaft and, depending upon the shaft load and film strength of the



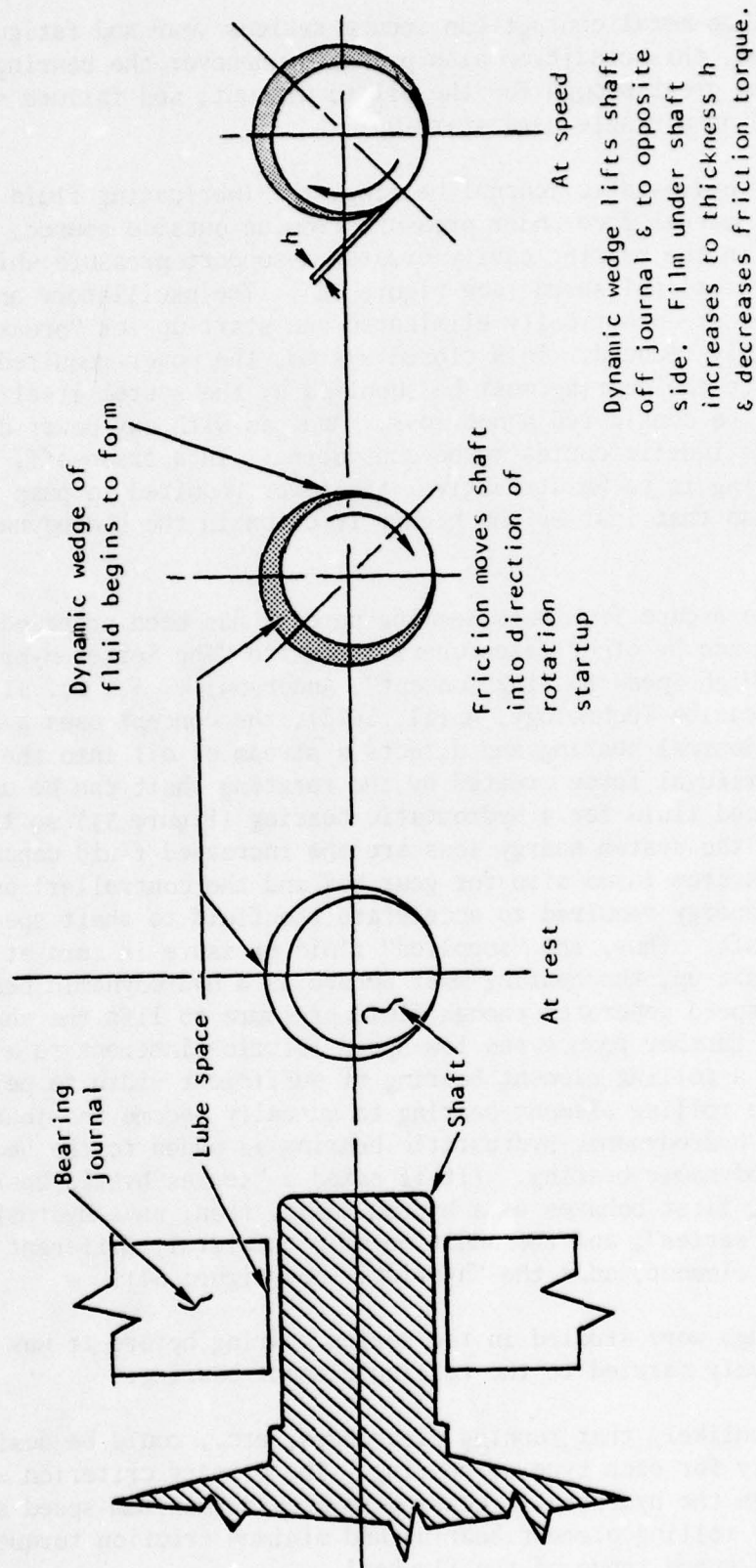


Figure 31. Typical Hydrodynamic Bearing

lubricant, metal-to-metal contact can induce serious wear and fatigue problems. Indeed, this condition also prevails whenever the bearing remains unused for a time great enough for the oil to dry out, and failure sequences can be initiated on a single hard start-up.

In a purely hydrostatic journal bearing, the lubricating fluid is supplied to the journal face under pressure from an outside source, while restricted flow in the bearing cavity creates a support pressure which is independent of rotational speed (see Figure 32). The oscillatory and start-up problems are practically eliminated and start-up (or "break-out") friction is greatly reduced. In a closed system, the power required to deliver the oil to the bearing must be supplied by the system itself and must, therefore, be considered a net loss. And, as with any power delivery system, there are inefficiencies to be considered. In a trade-off, if the hydrostatic bearing is to be attractive, the power required to pump the oil must be lower than that lost by the higher friction in the hydrodynamic type of bearing.

One possible escape from this seeming paradox has been proposed. Supported by tests made by other researchers (refer to "The Series-Hybrid Bearing - A New High Speed Bearing Concept", Anderson, W. J., et. al, ASME Journal of Lubrication Technology, April, 1972), the concept uses a hollow shaft under the journal bearing and directs a stream of oil into the hollow space. The centrifugal force created by the rotating shaft can be used to provide pressurized fluid for a hydrostatic bearing (Figure 33) so that the chief factors in the system energy loss are the increased fluid capacity of the lubrication system (used also for gear box and the controller) and the small amount of energy required to accelerate the fluid to shaft speed once it enters the shaft. Thus, the "supplied" fluid pressure is zero at zero speed, and on start-up, the bearing must behave as a hydrodynamic bearing until the shaft speed generates enough fluid pressure to lift the shaft off the journal. To further reduce the low-speed friction inherent to a hydrodynamic bearing, a rolling element bearing of sufficient width to permit the inner ring of the rolling element bearing to actually become the journal component of the hydrodynamic-hydrostatic bearing is added to the bearing set outside the hydrodynamic bearing. (It is named a "series-hybrid bearing" - the fluid bearing first behaves as a hydrodynamic, then, as a hydrostatic bearing for the "series", and the addition of a completely different type of bearing, rolling element, adds the "hybrid"; see Figure 34).

Several things were studied in the series bearing before it was felt it could be effectively married to the rolling element bearing:

- 1) It was unlikely that running clearances, etc., could be designed optimally for each type of bearing. The primary criterion would be to design the hydrostatic bearing to provide maximum speed sharing with the rolling element bearing and minimum friction torque in the 70%-100% speed range of the flywheel.

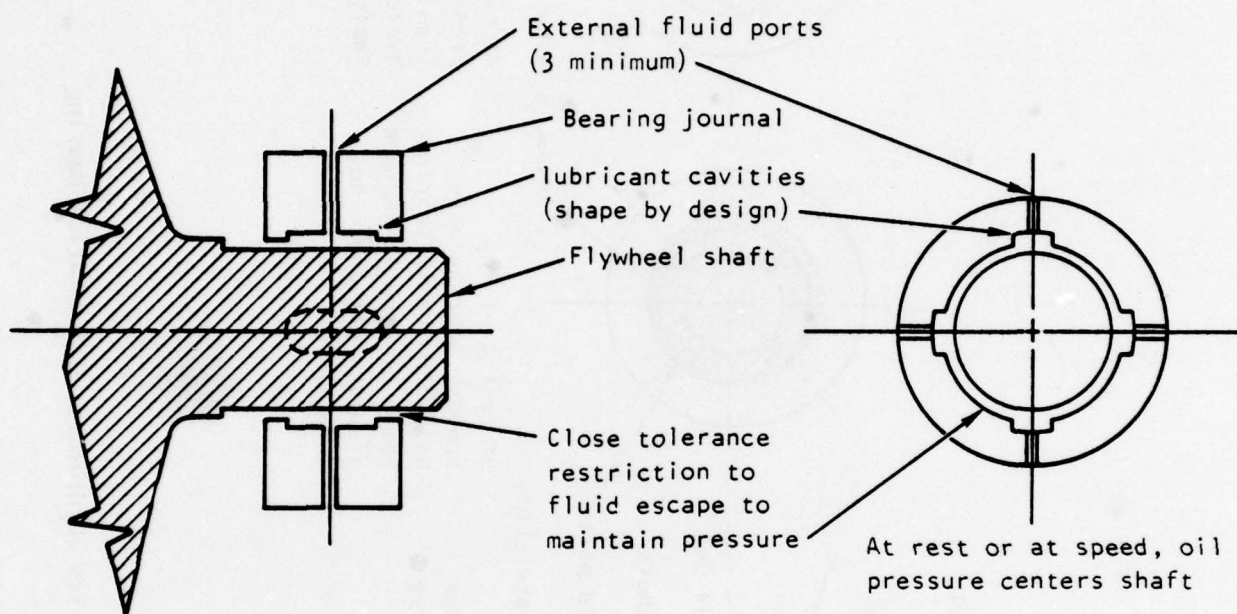


Figure 32. Typical Hydrostatic Bearing



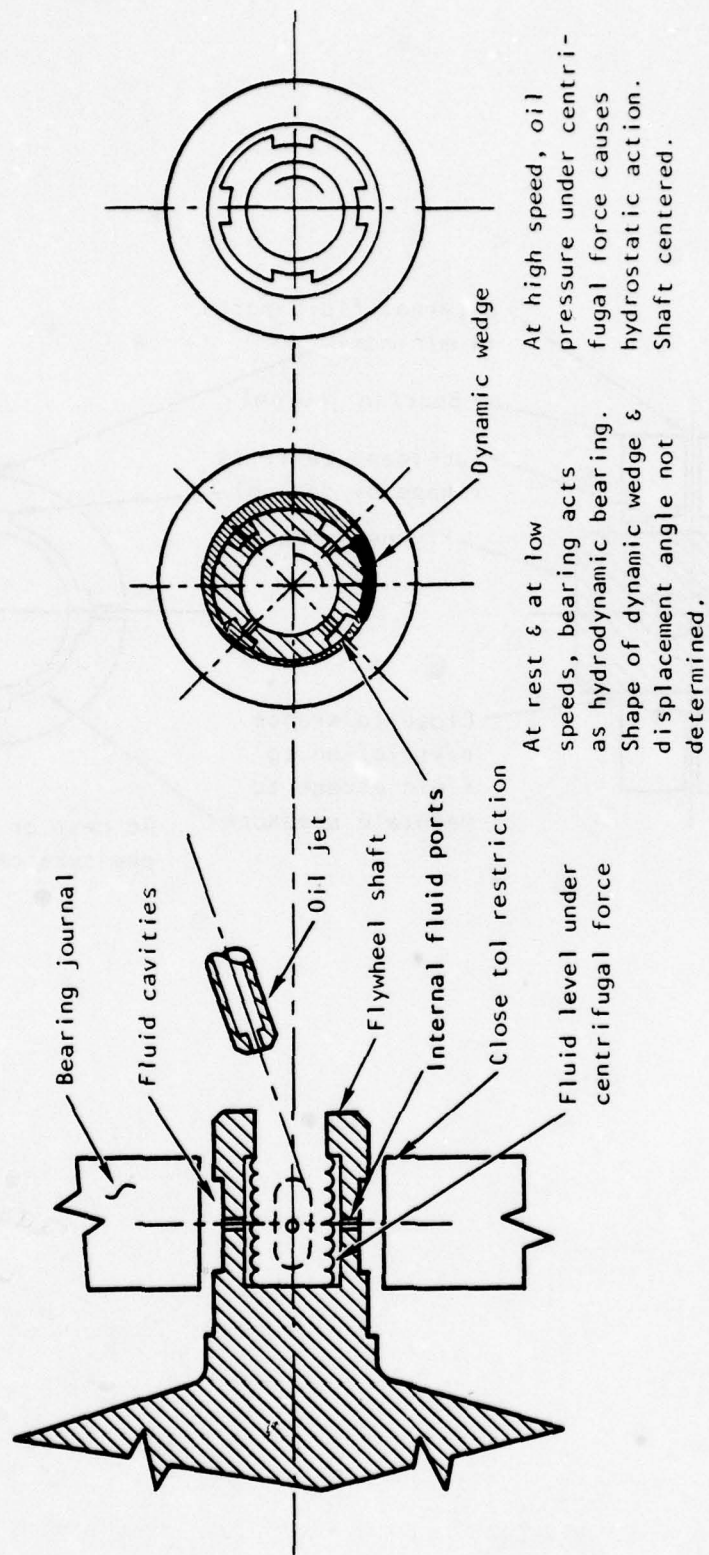


Figure 33. Proposed Series (Hydrodynamic-Hydrostatic) Bearing

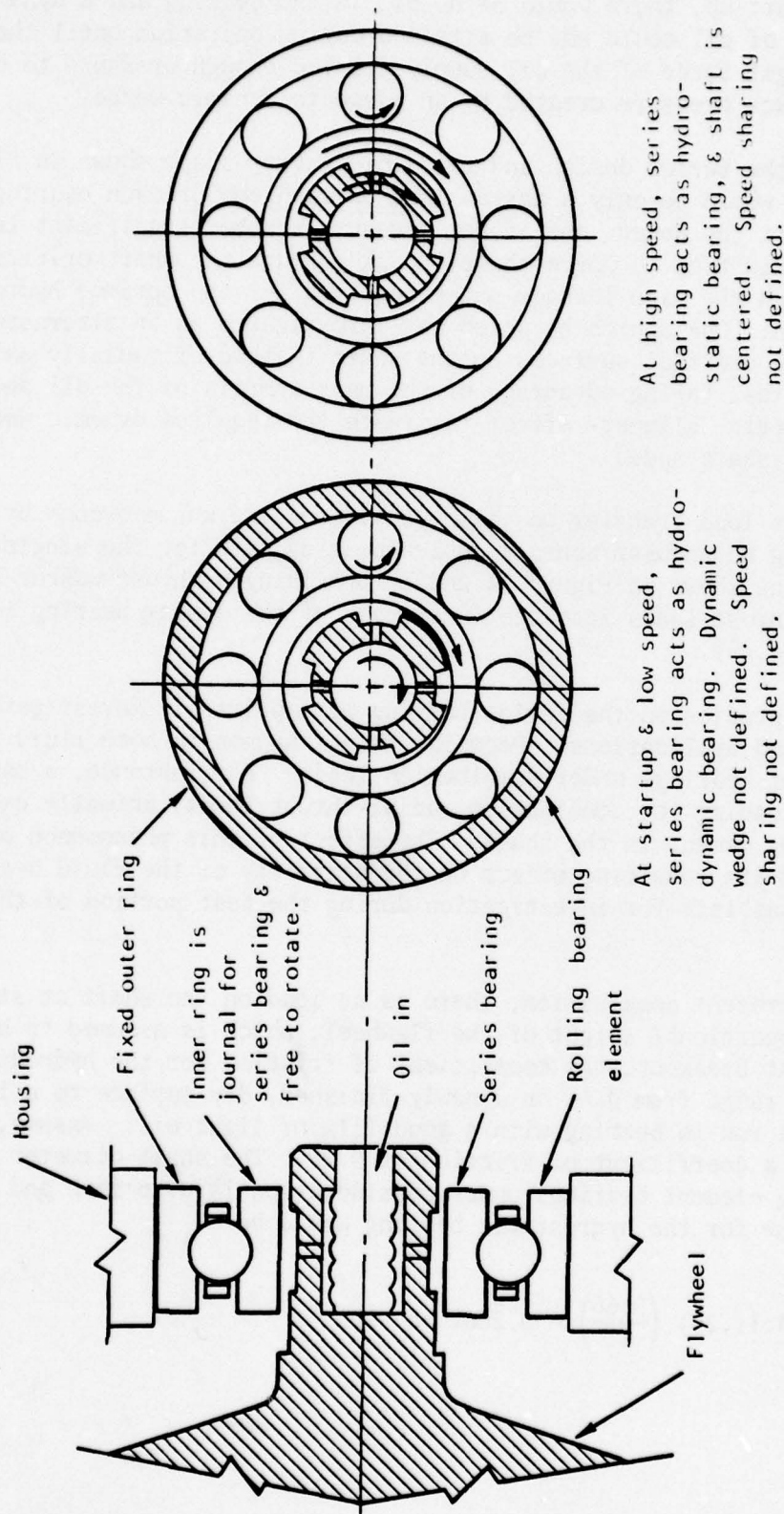


Figure 34. Proposed Series - Hybrid Bearing

- 2) At start-up, there would be no oil in the bearing and a dynamic wedge of oil could not be attained during operation until the centrifugal force of the oil supply created enough pressure to overcome the back pressure created by an adequate dynamic wedge.
- 3) With the series design and the fluid cavity shape shown in Figure 34, there would be only a narrow land on each end of each bearing to support the wedge, and if the pressure reached significant levels, it would tend to force the oil back through the shaft orifice or through the side leakage paths required for the optimum hydrostatic design. One approach, which was investigated as an alternate design, was to use flat surfaces on the shaft instead of radially uniform cavities, taking advantage of the mass inertia of the oil and the geometric "slipper" effect to create the required dynamic wedge at a lower shaft speed.
- 4) Thrust load transfer was also considered and was overcome by substituting an angular contact duplex bearing pair for the single ball bearing shown in Figure 34 and by providing a thrust washer to react the thrust loads into the inner race of the duplex bearing (see Figure 25).

Previous studies on the series bearing were primarily investigations on pure thrust load applications. Peculiar things happen to both fluid and rolling element bearings under combination loads. For instance, a ball bearing under moment loading (or combination radial-thrust loads) actually exerts a reverse bending moment in the shaft. The effect of this phenomenon on a free inner race and its resulting effect on the stability of the fluid bearing is a factor which was left for investigation during the test portion of this program.

For the present application, there is no load on the shaft at start-up except the proportional weight of the flywheel, which is assumed to be 4.1 pounds. At breakout, the coefficient of friction for the hydrodynamic bearing could range from 0.66 on a newly-finished, dry surface to a low 0.10 on a well run-in bearing with a good film of light oil. Assume, for this example, a coefficient of friction of 0.20. The shaft diameter of one of the rolling element bearings under consideration is 0.66 inch and the breakout torque for the hydrostatic bearing would be

$$T = 4.1(.20) \left( \frac{0.66}{2} \right) = 0.2662 \text{ in.-lb}$$



If the break-out torque of the rolling element bearing is less than this value, the friction torque will cause the rolling element bearing to start turning first and the shaft inner ring hydrodynamic bearing will not start to function until the friction torque of the rolling element bearing becomes greater than the breakout force of the hydrodynamic bearing. If, on the other hand, the breakout friction torque on the rolling element is high, due to preload or other design requirements, the hydrodynamic bearing properties become immediately apparent. However, exactly what happens at incipient hydrodynamic action and, later, at the transition of hydrodynamic to hydrostatic action must be carefully analyzed and tested.

Design Approach. Since the primary objective of the program was to reduce the flywheel and ancillary equipment parasitic losses, the first requirement of design and test procedure was to establish a baseline against which all other designs and test data could be compared. This was initially done for the rolling element bearing, then for the series bearing, and finally for the series-hybrid combination.

Baseline Design. The conventional approach to supporting high-speed rotors is to use rolling element bearings, the technology for which has been well investigated and developed. There are three methods of mounting the flywheel so that both radial and thrust loads can be accepted:

- 1) Single-row angular contact ball bearings on either end of the shaft - one of the bearings must be spring-loaded to position the bearing, accommodate manufacturing and running tolerances, and to provide the proper bearing preload. This method is widely used for supporting high-speed spindles and electric motor rotors.
- 2) Double-row (opposed) angular contact ball bearings on either end of the shaft - one of these pairs must be allowed to float without axial restraint to accommodate mounting and running tolerances. These bearings must be carefully designed and controlled to provide proper preload. This method is occasionally used for heavily loaded high-speed spindles. A more common variation of this method is to have a double-row pair at one end of the shaft with a single-row ball or roller bearing at the other.
- 3) Single-row cylindrical roller bearings at either end of the shaft with a single ball bearing at one end to accept thrust loads from either direction. This arrangement has gained universal acceptance for use in high-speed turbines, such as aircraft jet engines.

Fluid Bearing Design. The series bearing concept has not been widely tested and reported test data extant deal primarily with thrust bearings rather than with radial bearings. As pointed out previously, it was felt there might be some instability problems in the transitional phase which must be investigated and resolved before the final hybrid configuration was determined. A restriction in design freedom here was the necessity for fitting either the optimized fluid bearing to an un-optimized rolling element design, or vice-versa.

Series-Hybrid Design. From analytical investigations and the subsequent testing planned, it was felt trade-offs might be decided upon which would take a long step toward reaching the goal of minimum total power losses. For the final test phase in this program, it was recognized that it might be impossible to make the best decision on relative sizes, bearing designs, materials, etc due solely to long procurement lead times for special rolling element bearings. However, it was also felt that once analytical predictions were made to match actual test results, interpolative predictions of optimum designs should be possible.

Detail Design. The technologies of rolling element bearings, hydrodynamics, and hydrostatic bearings are significantly different in many aspects and do not readily yield to parametric analysis in combinations of types. Each type was investigated for a particular application and the interrelationships investigated.

Weight. The flywheel weight of 8.2 pounds was assumed to be equally distributed, 4.10 pounds per bearing. Since this is not a rotating load, its effect on the total load is  $4.10 \cos \phi_H$  where  $\phi_H$  is the angle between vertical dead center and the angle of maximum centrifugal force load.

Centrifugal Force Loads. Centrifugal force loads are created by several means:

- 1) Flywheel imbalance
- 2) Shaft deflection
- 3) Bearing and journal manufacturing errors
- 4) Bearing and journal radial clearance
- 5) Ball bearing deflection under radial load

The total centrifugal force is shown by:

$$P_{CF} = (2.842)(10)^{-5} WRN^2$$

where:

$P_{CF}$  = total centrifugal force (lb)

$W$  = weight of flywheel = 8.2 lb

$R$  = distance from geometric centerline to mass centerline

$N$  = rotational speed (rpm)

Assuming that bearings are equidistant from the transverse centerline of the flywheel, the bearing load,  $F_{RC}$ , becomes

$$F_{RC} = 1.165(10)^{-4} RN^2 \pm 4.1 \cos \phi_H$$

For the sake of notational consistence, let

$$R = e_T = e_1 + e_2 + e_3 + e_4 + e_5$$

where

$e_T$  = total eccentricity

$e_1$  = manufactured imbalance of flywheel

$e_2$  = radial runout of ball bearing

$e_3$  = shaft deflection

$e_4$  = radial clearance for fluid film bearing

$e_5$  = radial deflection of ball bearing

The total radial load per bearing, then becomes

$$F_{RC} = 1.165(10)^{-4} e_T N^2 \pm 4.1 \cos \phi_H$$

Figure 35 displays the eccentricities graphically.



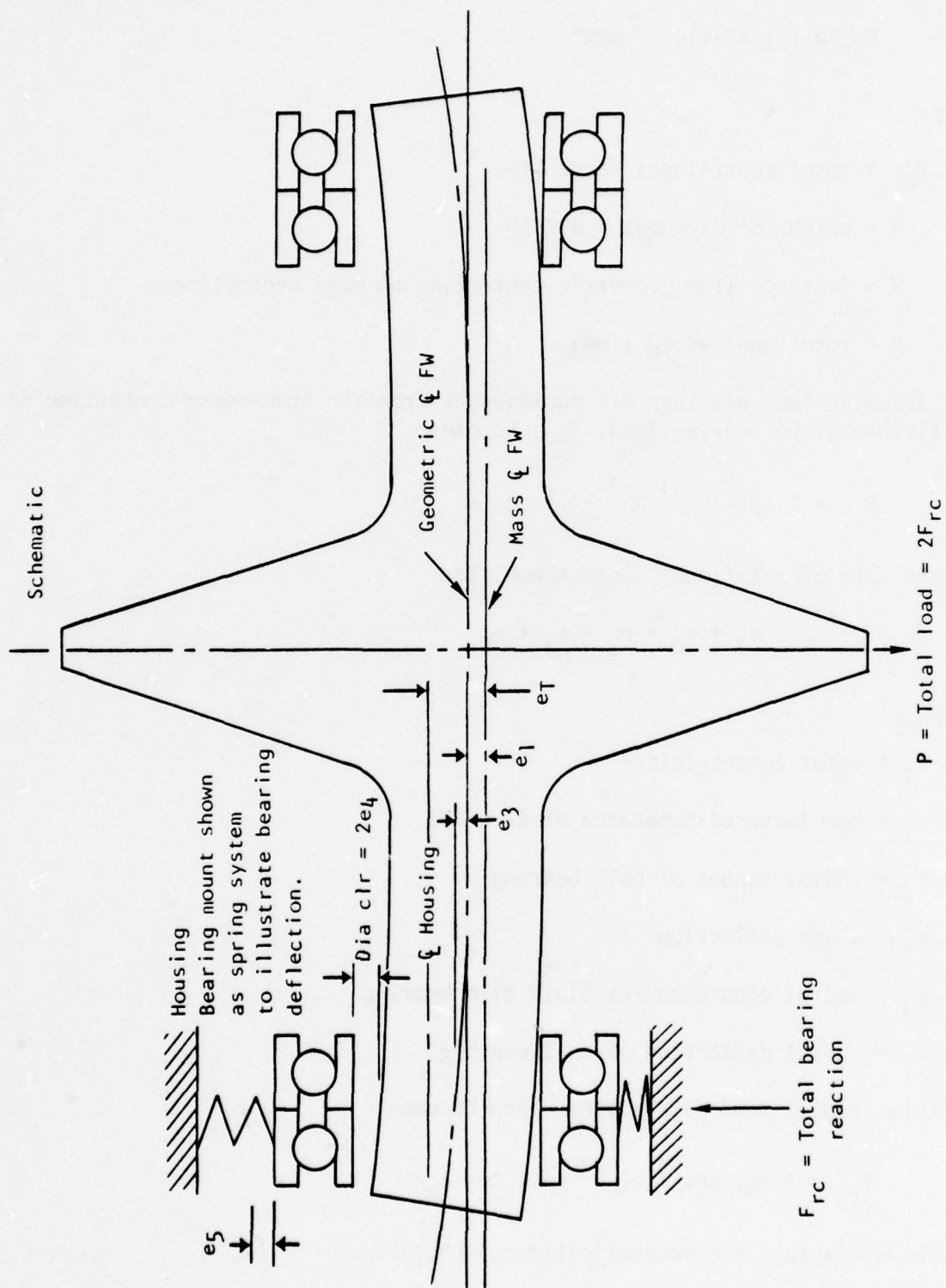


Figure 35. Flywheel Centrifugal Forces (Ball Bearing Radial Runout Omitted)

Flywheel Imbalance. The flywheel was balanced to  $5(10)^{-6}$  inches displacement using the actual shaft surfaces as a balancing reference surface. As this also compensates for shaft out-of-roundness, the value  $e$  becomes 0.000005 and

$$\begin{aligned} F_{rc_1} &= 1.165(10)^{-4} (.000005) N^2 \pm 4.1 \cos \phi_H \\ &= 5.825(10)^{-10} N^2 \pm 4.1 \cos \phi_H \end{aligned}$$

Bearing Radial Runout. The ball bearings selected were ABEC-7 with a maximum total radial runout of 0.0001 inch for the inner ring and 0.0002 inch for the outer ring. Since the inner ring is turning and the outer ring is fixed, the outer ring tolerance can, for the moment, be ignored, and the bearing eccentricity is one half the total radial runout, or  $e_2 = .00005$ . If the inner ring were fixed to the shaft (hard mount), the bearing load would become:

$$\begin{aligned} F_{rc_2} &= 1.165(10)^{-4} (.000005 + .00005) N^2 \pm 4.1 \cos \phi_H \\ &= 6.408(10)^{-9} N^2 \pm 4.1 \cos \phi_H \end{aligned}$$

Since, on this application, there is radial clearance for a fluid film bearing and the ball bearing inner race will be turning at a lower speed than the shaft, the radial eccentricity of the ball bearing becomes a perturbation rather than a steady-state load and must be considered dynamically. For preliminary investigation, this value was ignored.

Shaft Deflection. The shaft design is illustrated in Figure 36. If the entire flywheel is considered to be a simple beam supported on each end, the total deflection would be

$$e_3 = y_1 + y_2 + y_3$$

where

$y_1$  = deflection of small end of shaft

$y_2$  = deflection of large end of shaft

$y_3$  = deflection in flywheel, which can be ignored

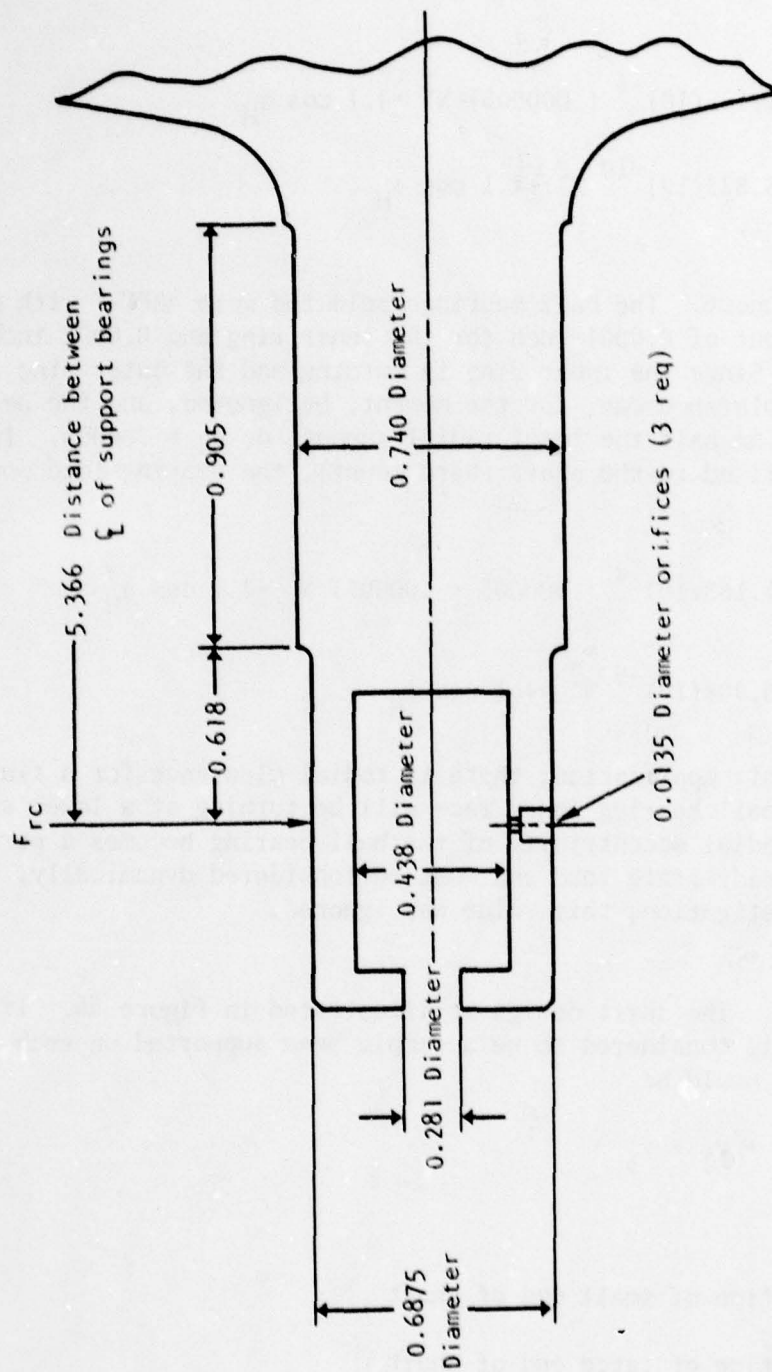


Figure 36. Flywheel Shaft Detail



$$y_1 = \frac{PL_1^3}{48EI_1}$$

where

$$P = \text{load from flywheel} = 2 F_{rc}$$

$$E = \text{elastic modulus of flywheel material} = 29(10)^6$$

$$I_1 = \text{moment of inertia}$$

$$D_o = \text{outer diameter of shaft} (0.6875)$$

$$D_i = \text{inner diameter of shaft} (0.438)$$

$$\begin{aligned} I_1 &= 0.0491 (D_o^4 - D_i^4) = 0.0491 [(0.6875)^4 - (0.4375)^4] \\ &= 0.009162 \text{ in.}^4 \end{aligned}$$

Similarly, for  $y_2$  and a solid shaft,

$$I_2 = 0.049 (0.740)^4 = 0.01472 \text{ in.}^4$$

$$y_2 = \frac{PL_2^3}{48EI_2}$$

$$e_3 = y_1 + y_2 = \frac{(0.618)^3 F_{rc}(2)}{48(29)(10)^6(0.009162)} + \frac{(0.905)^3 F_{rc}(2)}{48(29)(10)^6(0.01472)}$$

$$e_3 = 5.701(10)^{-8} F_{rc} + 7.235(10)^{-8} F_{rc}$$

$$e_3 = 1.094(10)^{-7} F_{rc}$$

For a bearing with radial clearance (ignoring the bearing runout) and at maximum load,

$$\begin{aligned}
 F_{rc} &= 1.165(10)^{-4} N^2 \left[ (10)^{-9} + e_3 \right] + 4.1 \\
 &= 1.165(10)^{-4} (10)^{-5} N^2 + 1.165(10)^{-4} (1.094)(10)^{-7} F_{rc} N^2 + 4.1 \\
 &= 1.165(10)^{-9} N^2 + 1.274(10)^{-11} F_{rc} N^2 + 4.1 \\
 F_{rc} - 1.274(10)^{-11} F_{rc} N^2 &= 1.165(10)^{-9} N^2 + 4.1 \\
 F_{rc} \left[ 1 - 1.274(10)^{-11} N^2 \right] &= 1.165(10)^{-9} N^2 + 4.1 \\
 F_{rc} &= \frac{1.165(10)^{-9} N^2 + 4.1}{1.274(10)^{-11} N^2}
 \end{aligned}$$

The shaft stresses in bending are

$$S_t = \frac{Mc}{I}$$

where

$M$  = moment load =  $F_{rc} L$

$c$  = distance to extreme fiber

$$= \frac{D}{2}$$

For the small end of the shaft,

$$S_{t_1} = \frac{F_{rc} L_1 D_1}{2I_1} = \frac{F_{rc} (0.618) (0.6875)}{2(0.009162)} = 23.18 F_{rc}$$

For the large end of the shaft,

$$S_{t_2} = \frac{F_{rc} (L_1 + L_2) D_2}{2I_2} = \frac{F_{rc} (0.618 + 0.905) (0.740)}{2(0.01472)} = 38.28 F_{rc}$$

Thus, if notch effect can be controlled, the stresses at the shaft-flywheel junction are critical. Another important consideration is the slope of the shaft, since it determines the clearance at each end of the fluid bearing. Let  $\phi$  = angle of slope (in radians)

$$\begin{aligned} \phi_H &= \frac{PL}{16EI} = \frac{2F_{rc} L_1}{16EI_1} + \frac{2F_{rc} (L_1 + L_2)}{16EI_2} \\ &= \frac{2F_{rc} (0.618)}{16(29)(10)^6(0.009162)} + \frac{2F_{rc} (0.618 + 0.905)}{16(29)(10)^6(0.01472)} \end{aligned}$$

$$\phi_H = 2.907(10)^{-7} F_{rc} + 4.460(10)^{-7} F_{rc} = 7.367(10)^{-7} F_{rc}$$

The total effective length of the duplex bearing plus a 0.3125 spacer in between is

$$l_e = 2(0.5518) + 0.3125 - 2(0.012) = 0.992 \text{ in.}$$

The total angle of permissible slope is

$$\phi_m = \frac{2e_4}{0.992} = 2.016 e_4 \text{ radians}$$

Beyond this, a counteracting couple will be introduced to the ball bearings, and the fluid film support characteristics will be drastically reduced.

Bearing Radial Clearance. The effect on load of the radial clearance between the journal and the inner race of the ball bearing required for proper operation of the fluid film bearing can be computed as in the preceding. Primarily, two conditions must be considered.



First, the dynamic forces of rotation tend to center the journal in the bearing. As the speed of rotation increases, the dynamic wedge of fluid becomes thicker and will, if the load permits, eventually approach the value of the radial clearance, centering the journal, depending on bearing design.

The second consideration, however, will to a great extent determine the failure mode of the ball bearings if adequate oil is not provided. While the ball bearing might continue to operate for a while without lubrication, the fluid film bearing without oil cannot form a compensating dynamic wedge; therefore, the full effect of radial clearance is felt, and the load on the bearings increases rapidly. This can become catastrophic. The effect on bearing load is:

$$F_{rc} = 1.165(10)^{-4} N^2 \left[ 5(10)^{-6} + e_3 + e_4 \right] + 4.1 \cos \phi_H$$

Ball Bearing Radial Deflection. The 17 to 25 mm bore bearings mounted in duplex have essentially linear radial deflection under preloaded mounting conditions. The effect on load can be determined as in the preceding:

$$F_{rc} = 1.165(10)^{-4} N^2 \left[ 5(10)^{-6} + e_3 + e_4 + e_5 \right] + 4.1 \cos \phi_H$$

Summary of Centrifugal Forces. If the effect of ball bearing radial runout is ignored; only the initial unbalance of the flywheel is actually a known load. The rest become functions of other design and operating factors. However, in order to approximate maximum loads which can occur if the oil supply fails, certain assumptions were made. The ball bearings initially selected were the duplex Fafnir 2MM9103. This bearing set, with a 40-pound preload, has a radial deflection rate of approximately  $5(10)^{-7}$  inch per pound of radial load. Therefore,

$$F_{rc} = 1.165(10)^{-4} N^2 \left[ 5(10)^{-6} + e_3 + e_4 + e_5 \right] + 4.1 \cos \phi_H, \text{ with}$$

$$e_3 = 1.094(10)^{-7} F_{rc} \text{ and, at max load,}$$

$$\phi_H = 90^\circ \text{ \& \; } \cos \phi_H = 1.000$$

$$F_{rc} = 1.165(10)^{-4} N^2 \left[ 5(10)^{-6} + 1.094(10)^{-7} F_{rc} + e_4 \right. \\ \left. + 5(10)^{-7} F_{rc} \right] + 4.1$$

$$F_{rc} = 1.165(10)^{-4} N^2 \left[ 5(10)^{-6} + e_4 \right] + 1.275(10)^{-11} F_{rc} N^2 \\ + 5.825(10)^{-11} F_{rc} N^2 + 4.1$$

$$F_{rc} - 7.100(10)^{-11} F_{rc} N^2 = 1.165(10)^{-4} N^2 \left[ 5(10)^{-6} + e_4 \right] + 4.1$$

$$F_{rc} = \frac{1.165(10)^{-4} N^2 \left[ 5(10)^{-6} + e_4 \right] + 4.1}{1 - 7.100(10)^{-11} N^2}$$

Thus, the load  $F_{rc}$  reaches infinity when the expression  $1 - 7.100(10)^{-11} N^2 = 0$  and

$$N = \left( \frac{1}{7.100(10)^{-11}} \right)^{1/2} = 118,678 \text{ rpm.}$$

The shaft is marginally safe at full load and full speed.

Using this equation, the load can be computed at various radial clearances and speeds:

|                   |  |
|-------------------|--|
| $\underline{e_4}$ | $\underline{F_{rc}}$                                       |
| 0.0005            | $\frac{5.883(10)^{-8} N^2 + 4.1}{1 - 7.100(10)^{-11} N^2}$ |

| $\underline{e_4}$ | $\underline{F_{rc}}$                                 |
|-------------------|--|
| 0.00075           | $\frac{8.796(10)^{-8}N^2+4.1}{1-7.100(10)^{-11}N^2}$ |
| 0.0010            | $\frac{1.171(10)^{-7}N^2+4.1}{1-7.100(10)^{-11}N^2}$ |
| 0.00125           | $\frac{1.462(10)^{-7}N^2+4.1}{1-7.100(10)^{-11}N^2}$ |
| 0.00150           | $\frac{1.753(10)^{-7}N^2+4.1}{1-7.100(10)^{-11}N^2}$ |
| 0.00175           | $\frac{2.045(10)^{-7}N^2+4.1}{1-7.100(10)^{-11}N^2}$ |
| 0.00200           | $\frac{2.336(10)^{-7}N^2+4.1}{1-7.100(10)^{-11}N^2}$ |
| 0.00250           | $\frac{2.918(10)^{-7}N^2+4.1}{1-7.100(10)^{-11}N^2}$ |
| 0.00300           | $\frac{3.501(10)^{-7}N^2+4.1}{1-7.100(10)^{-11}N^2}$ |



The loads and stresses are plotted graphically in Figures 37 and 38. For emphasis, Figures 37 and 38 show the zero radial clearance values. This must also include bearing radial runout.

$$\begin{aligned}
 F_{rc} &= 1.165(10)^{-5} N^2 [e_1 + e_2 + e_3 + e_5] + 4.1 \\
 &= 1.165(10)^{-5} N^2 \left[ 5(10)^{-6} + 5(10)^{-5} + 1.094(10)^{-7} F_{rc} \right. \\
 &\quad \left. + 5(10)^{-7} F_{rc} \right] + 4.1 \\
 &= 6.408(10)^{-10} N^2 + 7.100(10)^{-11} F_{rc} N^2 + 4.1 \\
 F_{rc} - 7.100(10)^{-11} F_{rc} N^2 &= 6.408(10)^{-10} N^2 + 4.1 \\
 F_{rc} &= \frac{6.408(10)^{-10} N^2 + 4.1}{1 - 7.100(10)^{-11} N^2}
 \end{aligned}$$

It must be emphasized that Figures 37 and 38 do not represent normal operating conditions but are possible if the oil supply is stopped. This comparison shows that at 0.001 clearance, if the shaft is free to rattle around inside the bearing because there is no oil and, thus, no centering action, the load in the bearings will increase by a factor of 100. This accentuates the extreme importance of journal bearing design and performance.

Flywheel Precessing Loads. Two types of precession loads are imposed on the flywheel support bearings:

1. Manufacturing tolerance loads.
2. Vehicle maneuvering loads.

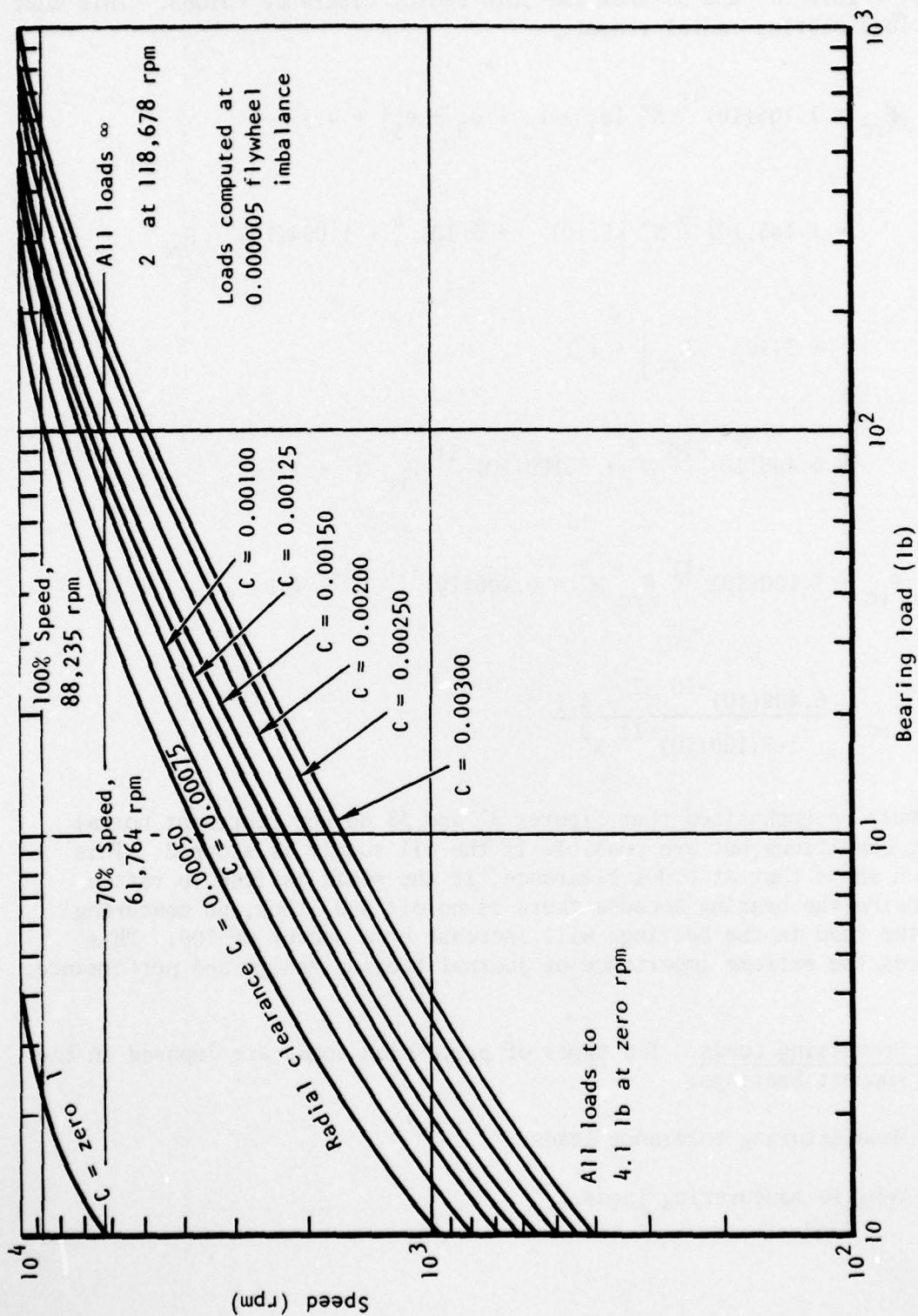


Figure 37. Bearing Loads Versus Radial Clearance and No Oil  
(Duplex 9103W0 Bearings, 40-pound Preload)

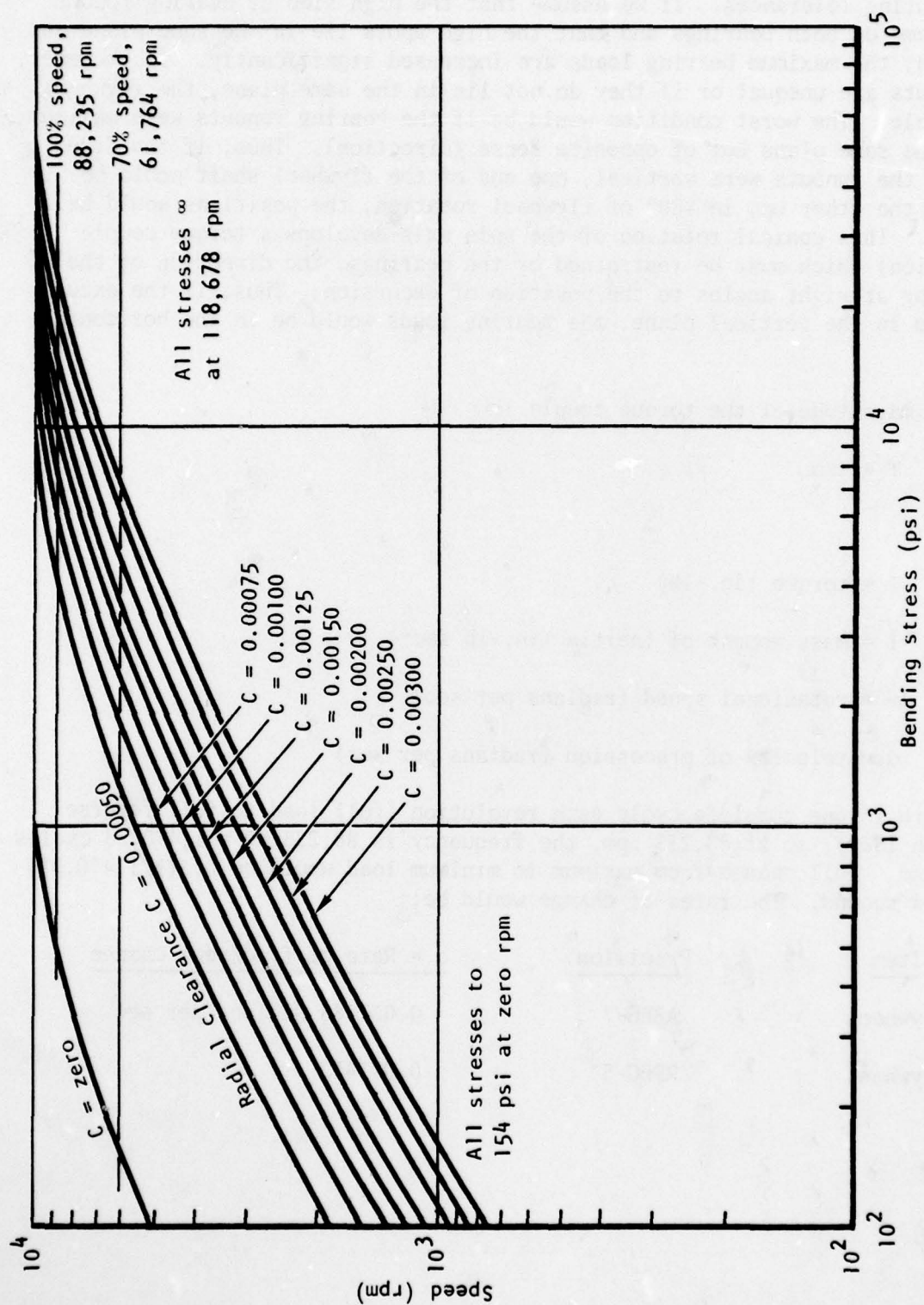


Figure 38. Shaft Bending Stresses Versus Radial Clearance and No Oil  
(Duplex 9103W0 Bearings, 40-pound Preload)



Manufacturing Tolerances. If we assume that the high side of bearing runout is the same on both bearings and that the high spots lie in the same plane and direction, the maximum bearing loads are increased significantly. If, however, the runouts are unequal or if they do not lie in the same plane, the flywheel will wobble. The worst condition would be if the bearing runouts were maximum and in the same plane but of opposite sense (direction). Thus, if the directions of the runouts were vertical, one end of the flywheel shaft would be down and the other up; in 180° of flywheel rotation, the positions would be reversed. This conical rotation of the spin axis develops a torque couple (precession) which must be restrained by the bearings, the direction of the load being at right angles to the position of excursion. Thus, if the excursion were in the vertical plane, the bearing loads would be in the horizontal plane.

The magnitude of the torque couple is

$$T = I\omega\alpha$$

where

$T$  = torque (in.-lb)

$I$  = mass moment of inertia (in.-lb sec<sup>2</sup>)

$\omega$  = rotational speed (radians per sec)

$\alpha$  = velocity of precession (radians per sec)

There is one complete cycle each revolution (full load to full reverse load each 180°), so at 88,235 rpm, the frequency is  $88,235/60 = 1,470.58$  cycles per second. Full change from maximum to minimum load would be  $0.5(1/1,470.58) = 0.00034$  second. The rates of change would be:

| <u>Item</u> | <u>Precision</u> | <u><math>\alpha</math> = Rate of (rad/sec) change</u> |
|-------------|------------------|---|
| Flywheel    | ABEC-7           | 0.051588 Radians per sec                              |
| Flywheel    | RBEC-5           | 0.077412  |

The computed torque ( $T = I\omega\alpha$ ) becomes

| <u>Item</u> | <u>Precision</u> | <u>I</u> | <u><math>\omega</math></u> | <u><math>\alpha</math></u> | <u>T (lb)</u> |
|-------------|------------------|----------|----------------------------|----------------------------|---------------|
| Flywheel    | ABEC-7           | 0.0513   | 9,240                      | 0.0516                     | 24.459        |
| Flywheel    | RBEC-5           | 0.0513   | 9,240                      | 0.0774                     | 36.688        |

The wobble, then, can become very significant if the rolling element bearing is required to take the full speed of rotation and the bearing inner races are  $180^\circ$  out of phase. If by using Precision 9 bearings, the vibration amplitude would be reduced by at least 50%, and if a journal fluid bearing can be designed to accept a large share of the rotational speed, the vibrational frequency can be reduced until the condition can be tolerated. This condition highlights a major procedure in conventional ultra-high-speed rotating machinery; i.e., the flywheel unbalance and the bearing eccentricity are mounted so as to cancel out the alignment error. This problem was considered carefully in final design.

Vehicle Maneuvering Loads. Two types of maneuvering loads affect the flywheel bearings; i.e., gyroscopic moments in the flywheel, which are introduced by vehicle directional changes and gravity loads (centrifugal force external to the flywheel), which are introduced during the execution of those changes in direction. Since the gyroscopic precessional loads are coupled and the g-force loads are unidirectional, the loads on the bearing are not in the same plane and, to some extent, can be additive on one end of the flywheel and subtractive on the other. For instance, if the rotational centerline of the flywheel were parallel to the vehicle fore-and-aft centerline and a "pull-up" maneuver were executed, the entire mass of the flywheel would exert a g-load downward on the flywheel bearings due to centrifugal force on the flywheel, while the flywheel itself would exert a gyroscopic moment in the horizontal plane (opposite in direction on either end of the flywheel). Thus, the actual load on the bearings would be a vector quantity downward and angled to the right or left on either end of the flywheel shaft.

Since the mechanical power package is some distance from the centerline of the B-1, roll maneuvers introduce a centrifugal force and, to a lesser extent, so do yaw maneuvers. However, even the greatest centrifugal force resulting from maneuvering is relatively small. For example, the greatest angular velocity about the vehicle centerline is the  $75^\circ$  per second roll rate, with acceleration-deceleration rates of twice that figure ( $150^\circ$  per  $\text{sec}^2$ ).

The distance from the vehicle centerline to the MPP is approximately 80 inches, and the angular rate of rotation is  $(75)(60)/360 = 12.5$  rpm. From the equation shown on page 71,

$$\begin{aligned} P_{cf} &= 2.842(10)^{-5} WRN^2 \\ &= 2.842(10)^{-5} (8.2)(80)(12.5)^2 \\ &= 2.91 \text{ lb} \end{aligned}$$

Depending entirely upon the orientation of the flywheel shaft centerline relative to the vehicle centerline, this reaction could range from 50% load applied equally and radially to each bearing, to 100% load applied axially (thrust) to a single bearing. In view of the much higher loads borne by the bearings from imbalance and manufacturing tolerances, these centrifugal forces have little significance.

Precession Loads. The vibrational problems discussed in the preceding paragraphs assumed rigid supports. However, they are unchanged in frequency but will show some increased amplitude of response when the spring rate of the actual flywheel housing and mounting system is considered. During maneuvering loads, the approach to solution is the same as has been outlined except that the effect of shaft and bearing deflection must be accounted for during the acceleration period leading to steady-state precession.

The effects of precession loads are illustrated in Figure 39. Compared to the effects of centrifugal force loading (Figure 37), one significant difference became immediately apparent. During centrifugal force loading, the force is always in the axial plane containing both the flywheel geometric centerline and the mass center of the flywheel and, if weight is disregarded, the bearings and the deflected shaft see the centrifugal force loads as a rotating load, always in the same direction relative to the plane described in the preceding and always of the same magnitude as long as the flywheel stays at the same speed. Thus, it was recognized that, if the flywheel were brought up to speed before a flight and allowed to remain at full speed during the flight, centrifugal forces would contribute only one shaft flex fatigue cycle per flight. Except for creep phenomena and possible crack propagation under constant stress, the flywheel shaft would practically never fail due to fatigue. Even when the flywheel was used as an energy source during flight, the contribution to fatigue cycles would be minimal. In this application, the flywheel was designed for use in the 100% to 70% speed range. Since flywheel shaft stresses and bearing loads are a function of the square of the speed, the shaft stresses would reduce to 49% of full load stress with never a stress reversal. It would take several such stress reductions to contribute the equivalent fatigue effect of a single full stress reversal (100% plus to 100% minus load in the same flywheel plane).



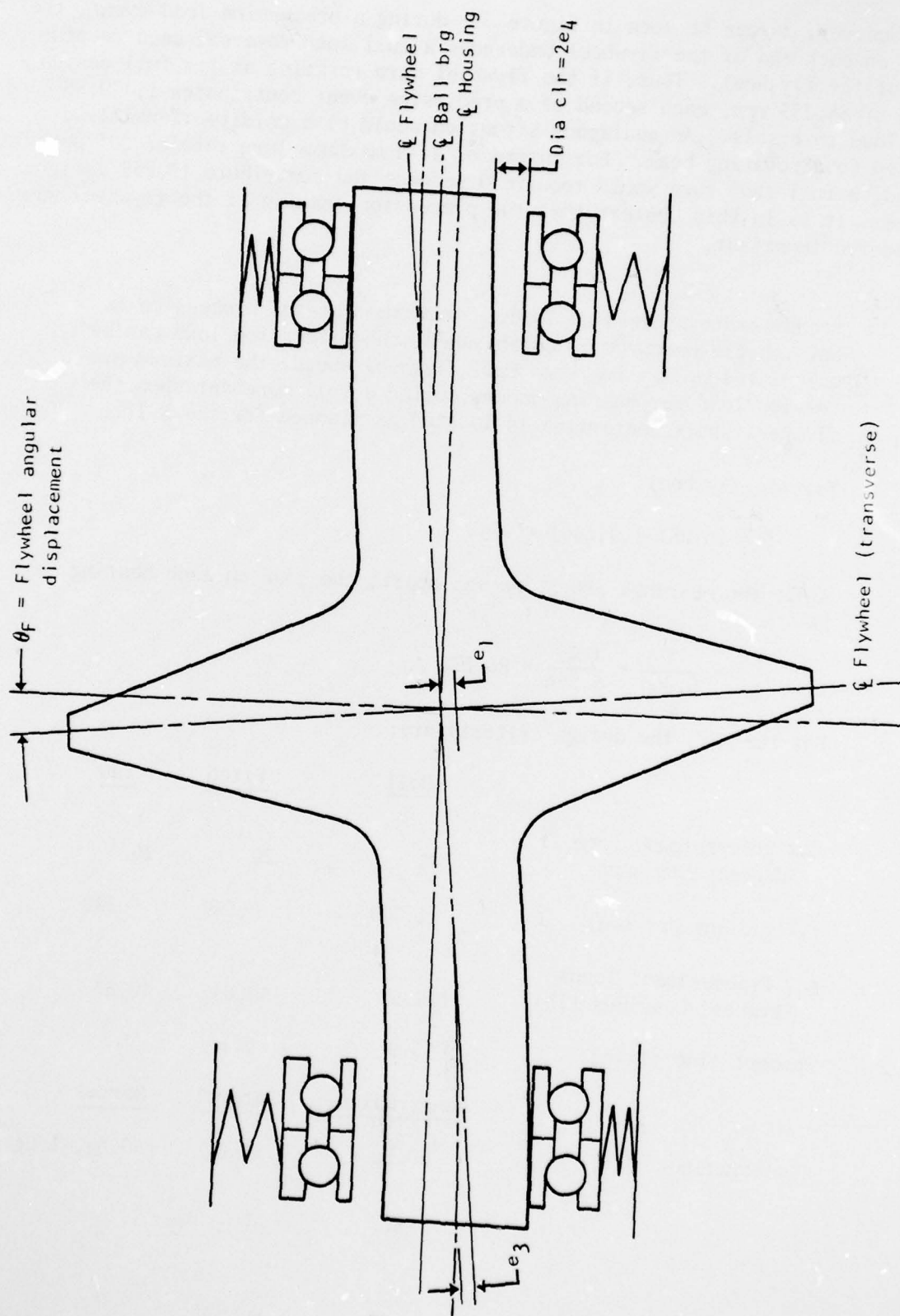


Figure 39. Precession Load Effects

AD-A073 297

ROCKWELL INTERNATIONAL EL SEGUNDO CA LOS ANGELES DIV  
MECHANICAL POWER SYSTEM FOR AIRCRAFT INTERMITTENT UTILITY FUNCT--ETC(U)  
APR 79 C W HELSLEY

F/G 1/3

F33615-75-C-2011

UNCLASSIFIED

RI/LAD-NA-79-64

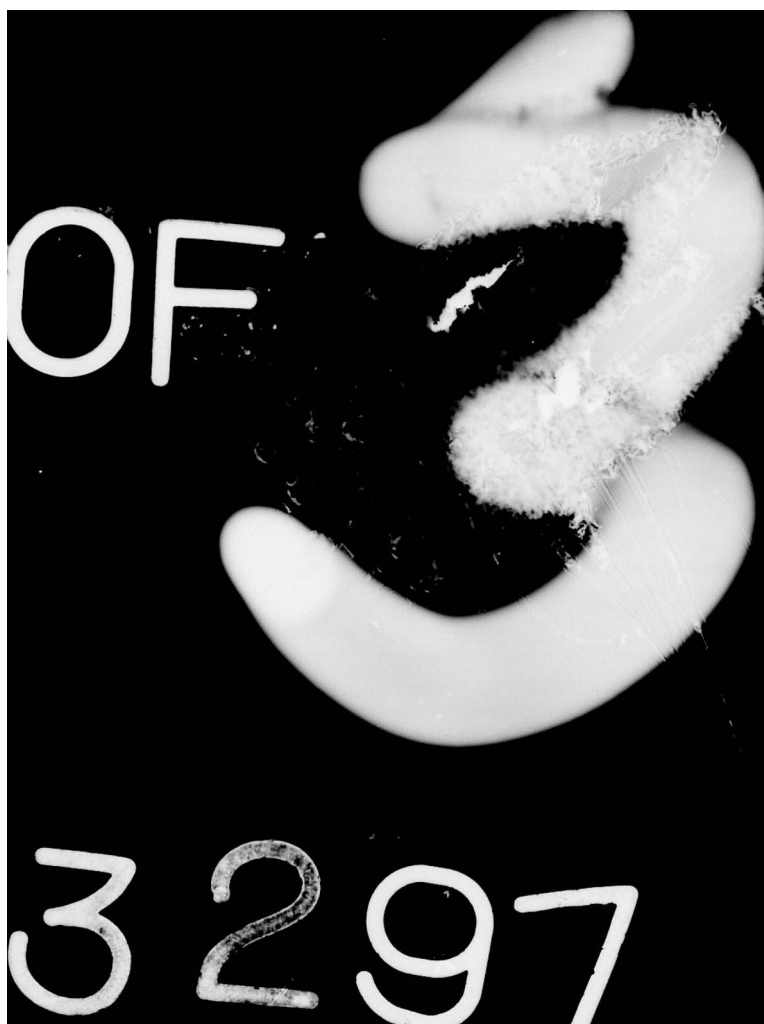
AFAPL-TR-79-2028

NL

2 OF 3

AD  
A073297







However, as can be seen in Figure 39, during a precession load event, the shaft on each end of the flywheel undergoes a full load reversal each revolution of the flywheel. Thus, if the flywheel were rotating at its full design speed of 88,235 rpm, each second of a precession event contributes 1,470.58 full load reversals. An analogous situation would be a unidirectional load applied to a rotating beam. For instance, at a maximum turn rate of 20° per second, a full 180° turn would require 9 seconds and contribute 13,235 fatigue cycles. It is in this context that the precession loading of the flywheel was considered important.

- 1) Steady-state precession loads - Once the rate of precession in any vehicle maneuver is established, the precession load can be calculated by  $T = I\omega\alpha$ . At full flywheel speed, the maximum precession load per bearing occurs during a roll maneuver when the flywheel shaft centerline is located as planned for the B-1.

For the flywheel:

$$T = (0.0515)(9,240) = 474\alpha$$

Since the bearings are 5.366 in. apart, the load on each bearing is

$$F_{pf} = \frac{T}{5.366} = \frac{474\alpha}{5.366} = 88.33\alpha$$

For the MPP, the design criteria are:

|   | <u>Roll</u>         | <u>Pitch</u>   | <u>Yaw</u>        |
|---|---------------------|----------------|-------------------|
| Max precessional rate<br>(degrees per sec)            | 75                  | 20             | 20                |
| ( $\alpha$ )(radians per sec)                         | 1.309               | 0.349          | 0.349             |
| $F_{pf}$ Precessional loads<br>Flywheel bearings (lb) | 115.62              | 30.83          | 30.83             |
| Percent time (life)                                   | 3.9                 | 0.1            | 0.1               |
|   | <u>Longitudinal</u> | <u>Lateral</u> | <u>Normal</u>     |
| Accelerations   | $\pm 0.5g$          | $\pm 1.0g$     | $\pm 3.0g, -1.0g$ |

As indicated in the preceding, the maximum induced load is 115.62 pounds per bearing. However, this does not include the perturbations introduced by imbalance, shaft deflection, and bearing deflection. From Figure 39, observe that the radial clearance does not enter into steady-state precession loads, but bearing radial runout would. The weight of the flywheel would also enter into the calculations as before. The bearing load and, therefore, shaft stresses become

$$\begin{aligned} F_{rp} &= 115.62 + 1.165(10)^{-4} N^2 [\pm e_1 \pm e_2 \pm e_3 \pm e_5] \pm 4.1 \cos \theta_H \\ &= 115.62 + 1.165(10)^{-4} N^2 \\ &\quad [\pm 5(10)^{-6} \pm 5(10)^{-5} + 1.384(10)^{-7} F_{rp} + 5(10)^{-7} F_{rp}] \pm 4.1 \cos \theta_H. \end{aligned}$$

at full flywheel speed, the maximum load

$$\begin{aligned} F_{rp_{\max}} &= 115.62 + 4.1 + 49.89 + 0.579 F_{rp} \\ F_{rp} - 0.579 F_{rp} &= 169.59 \\ F_{rp_{\max}} &= \frac{169.59}{1 - 0.579} = 402.83 \text{ lb} \end{aligned}$$

The minimum load is

$$\begin{aligned} -F_{rp_{\min}} &= -115.62 + 1.165(10)^{-4} N^2 [\pm e_1 \pm e_2 - e_3 - e_5] + 4.1 \cos \theta_H \\ &= -115.62 + 1.165(10)^{-4} N^2 \\ &\quad [+5(10)^{-6} + 5(10)^{-5} - 1.384(10)^{-7} F_{rp} - 5(10)^{-7} F_{rp}] + 4.1 \\ &= -115.62 + 49.89 - 0.579 F_{rp} + 4.1 \\ -F_{rp_{\min}} &= \frac{-60.71}{1 - 0.579} = -156.08 \text{ lb} \end{aligned}$$

If the flywheel had been positioned so that the roll maneuver precession load was zero, the maximum yaw and pitch rate would be only 20° per second and the precession load would be 30.83 pounds. Then

$$\begin{aligned} F_{rp_{\max}} &= 30.83 + 49.89 + 0.579 F_{rp} + 4.1 \\ &= \frac{84.82}{1 - 0.579} = 201.47 \text{ lb} \end{aligned}$$

$$-F_{rp_{min}} = -30.83 + 49.89 - 0.579 F_{rp} + 4.1$$

$$-F_{rp_{min}} = \frac{23.16}{1 - .579} = + 55.01 \text{ lb}$$

Thus, at the extreme condition postulated with no oil, the yaw rate precession load is not great enough to overcome the load from centrifugal force and these would not be stress reversal but stress reduction in the shaft.

As calculated previously, the shaft stress in bending is

$$S_t = 57.45 F_r$$

and the stresses become

$$\begin{aligned} \text{max roll rate } S_t &= + 15,086 \text{ psi} \\ S_{t_{max}} &- 5,845 \text{ psi} \\ S_{t_{min}} & \\ \text{max yaw rate } S_t &= + 7,545 \text{ psi} \\ S_{t_{max}} &= + 2,060 \text{ psi} \\ S_{t_{min}} & \end{aligned}$$

Thus, the stresses during precession events will not become great enough to induce rapid fatigue, but the amplitude with no oil was carefully considered a major factor for its effect on the ball bearings.

- 2) Precession loads during acceleration - The angular rate of acceleration allowed by vehicle design in leading into any maneuver is twice the design rate of angular change. Thus, the loads on the flywheel bearings from precession would be twice as great.

During a roll maneuver:

$$F'_{rp_{max}} = 217.8 + 49.89 + .579 F'_{rp} + 4.1$$

$$F'_{rp_{max}} = \frac{271.79}{1 - .579} = +645.58 \text{ lb}$$

$$-F'_{rp_{min}} = -217.8 + 49.89 - .579 F'_{rp} + 4.1$$

$$-F'_{rp_{min}} = \frac{-163.81}{1 - .579} = -389.10 \text{ lb}$$



$$S_{t_{\max}} = +24,176 \text{ psi}$$

$$S_{t_{\min}} = -14,571 \text{ psi}$$

During a yaw or pitch maneuver,

$$\begin{aligned} F'_{rp_{\max}} &= 58.04 + 49.89 + 0.579 F'_{rp} + 4.1 \\ &= \frac{112.03}{1-0.579} = +266.10 \text{ lb} \end{aligned}$$

$$\begin{aligned} F'_{rp_{\min}} &= -58.04 + 49.89 + 4.1 + 0.579 F'_{rp} \\ &= \frac{-4.05}{1-0.579} = -9.62 \text{ lb} \end{aligned}$$

$$S_{t_{\max}} = +9.965 \text{ psi}$$

$$S_{t_{\min}} = -360.27 \text{ psi}$$

- 3) Summary - As mentioned, the load levels described above could be reached only if the oil supply failed during or just before the maneuver began. Although radial clearance does not enter the calculations, a hard mounted bearing would not be subjected to the same loads since the flywheel could be balanced with the bearings in place, negating the significant influence of the bearing radial runout. However, the calculations did emphasize the necessity of maintaining an oil supply and a full film in the fluid film bearing to achieve the maximum damping of the load perturbations.

Steady-State Bearing Loads. When the vehicle is not maneuvering, there are no precession loads and the bearing loads are essentially the same as the maneuvering loads for any shaft orientation in which the precession loads are zero. Of course, during maneuvering, there are small "g" loads due to the centrifugal forces imposed on the entire flywheel, but these loads can be ignored in the computations. All the loads are summarized in Table 3.

TABLE 3. MPP FLYWHEEL BEARING LOAD SUMMARY (LB) AT 88,235 RPM

| Load Condition<br>Shaft & Direction | Steady State |           |             | Roll      |              |               | Pitch     |           |              | Yaw       |           |             |
|-------------------------------------|--------------|-----------|-------------|-----------|--------------|---------------|-----------|-----------|--------------|-----------|-----------|-------------|
|                                     | Long         | Tran      | Vert        | Long      | Tran         | Vert          | Long      | Tran      | Vert         | Long      | Tran      | Vert        |
| ABEC-7 Radial Thrust                | 60.3<br>0    | 60.3<br>0 | 60.0<br>8.2 | 60.3<br>0 | 130.1<br>4.1 | 130.1<br>12.3 | 69.2<br>0 | 60.3<br>0 | 69.4<br>16.4 | 71.7<br>0 | 71.7<br>0 | 69.4<br>8.2 |
| RBEC-5 Radial Thrust                | 82.7<br>0    | 82.7<br>0 | 82.9<br>8.2 | 82.7<br>0 | 145.8<br>4.1 | 145.8<br>12.3 | 90.9<br>0 | 82.7<br>0 | 90.1<br>16.4 | 91.6<br>0 | 91.6<br>0 | 90.1<br>8.2 |
| ABEC-9 Radial Thrust                | 37.9<br>0    | 37.9<br>0 | 37.5<br>8.2 | 37.9<br>0 | 117.9<br>4.1 | 118.7<br>12.3 | 50.4<br>0 | 37.9<br>0 | 50.2<br>16.4 | 53.3<br>0 | 53.3<br>0 | 50.2<br>8.2 |
| Percent of time                     | 95.9         |           |             | 3.9       |              |               | 0.1       |           |              | 0.1       |           |             |

Bearing Life Loads. When rolling element bearings are subjected to varying loads for different periods of time, an equivalent load can be calculated which will have the same influence on bearing life as the varying loads. These mean loads are:

- 1) ABEC-7 ball bearings - flywheel shaft:

$$\text{Long: } P = \left[ 0.959(60.3)^3 + 0.039(60.3)^3 + 0.001(69.2)^3 + 0.001(71.7)^3 \right]^{1/3} = 60.3$$

$$\text{Trans: } P = \left[ 0.959(60.3)^3 + 0.039(130.1)^3 + 0.001(60.3)^3 + 0.001(71.7)^3 \right]^{1/3} = 66.7$$

$$\text{Vert: } P = \left[ 0.959(60.0)^3 + 0.039(130.1)^3 + 0.001(69.4)^3 + 0.001(69.4)^3 \right]^{1/3} = 66.5$$

- 2) ABEC-5 ball bearings - flywheel shaft:

$$\text{Long: } P = \left[ 0.959(82.7)^3 + 0.039(82.7)^3 + 0.001(90.9)^3 + 0.001(91.6)^3 \right]^{1/3} = 82.7$$



$$\begin{aligned} \text{Tran: } P &= \left[ 0.959(82.7)^3 + 0.039(145.8)^3 + 0.001(82.7)^3 \right. \\ &\quad \left. + 0.001(91.6)^3 \right]^{1/3} = 87.5 \end{aligned}$$

$$\begin{aligned} \text{Vert: } P &= \left[ 0.959(82.9)^3 + 0.039(145.8)^3 + 0.001(90.1)^3 \right. \\ &\quad \left. + 0.001(90.1)^3 \right]^{1/3} = 87.4 \end{aligned}$$

3) ABEC-9 ball bearings - flywheel shaft:

$$\begin{aligned} \text{Long: } P &= \left[ 0.959(37.9)^3 + 0.039(37.9)^3 + 0.001(50.4)^3 \right. \\ &\quad \left. + 0.001(53.3)^3 \right]^{1/3} = 37.9 \end{aligned}$$

$$\begin{aligned} \text{Tran: } P &= \left[ 0.959(37.9)^3 + 0.039(117.9)^3 + 0.001(37.9)^3 \right. \\ &\quad \left. + 0.001(53.3)^3 \right]^{1/3} = 48.8 \end{aligned}$$

$$\begin{aligned} \text{Vert: } P &= \left[ 0.959(37.5)^3 + 0.039(118.7)^3 + 0.001(50.2)^3 \right. \\ &\quad \left. + 0.001(50.2)^3 \right]^{1/3} = 48.8 \end{aligned}$$

From the above calculations, it is apparent that maneuvering loads and shaft orientation had little effect on mean load.

Normal Operating Loads. During normal operating conditions of the hybrid bearing, adequate oil will be supplied to both the journal and rolling element bearings. With a fluid film supporting the flywheel shaft, the journal bearing initially behaves as described previously (Figure 31), and the loads applied to the journal bearing vertical plane are the steady flywheel weight and the rotating load from flywheel imbalance:

$$F_r = 4.1 + 1.165(10)^{-9} N^2 \cos \omega$$

where the angle " $\omega$ " is the angle of rotation of a plane through the flywheel geometric center and the mass center, away from bottom dead center. Thus, when the angle " $\omega$ " is between  $90^\circ$  and  $270^\circ$ , the effect of the rotating load is negative and tends to lift the journal in the bearing. At some speed, the minimum load becomes zero and,

$$\begin{aligned} F_r = 0 &= 4.1 + 1.165(10)^{-9} N^2 \cos 180^\circ \\ &= 4.1 - 1.165(10)^{-9} N^2 \end{aligned}$$

$$N_o = \left[ \frac{4.1}{1.165(10)^{-9}} \right]^{1/2} = 59,324 \text{ rpm}$$

Above that speed, the load becomes negative for some period on each revolution of the flywheel, reaching a minimum negative load at the rated flywheel speed of 88,235 rpm of

$$\begin{aligned} F_r &= 4.1 + 1.165(10)^{-9} (88235)^2 \cos 180^\circ \\ &= 4.1 - 9.070 \\ &= -4.970 \text{ lb} \end{aligned}$$

This negative shift on each revolution indicates that it is possible for the flywheel to start orbiting with possibly catastrophic effects if the journal bearing remained purely hydrodynamic. It is necessary, therefore, to achieve positive hydrostatic conversion before the critical speed is achieved. The loads are illustrated graphically in Figure 40. Note that the load goes negative when  $\omega = 116.87^\circ$  and stays negative for  $126.26^\circ$  (or 35% of the time) on each revolution of the flywheel.

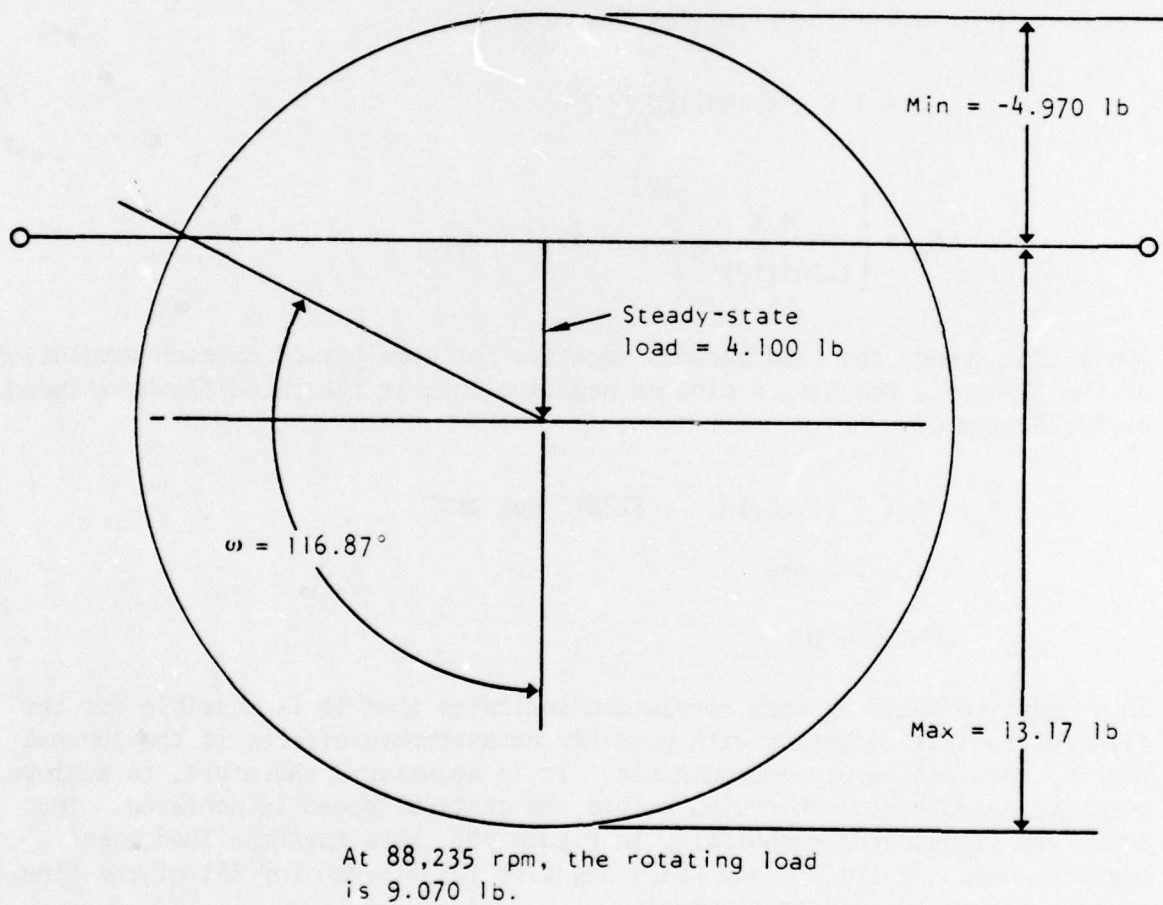
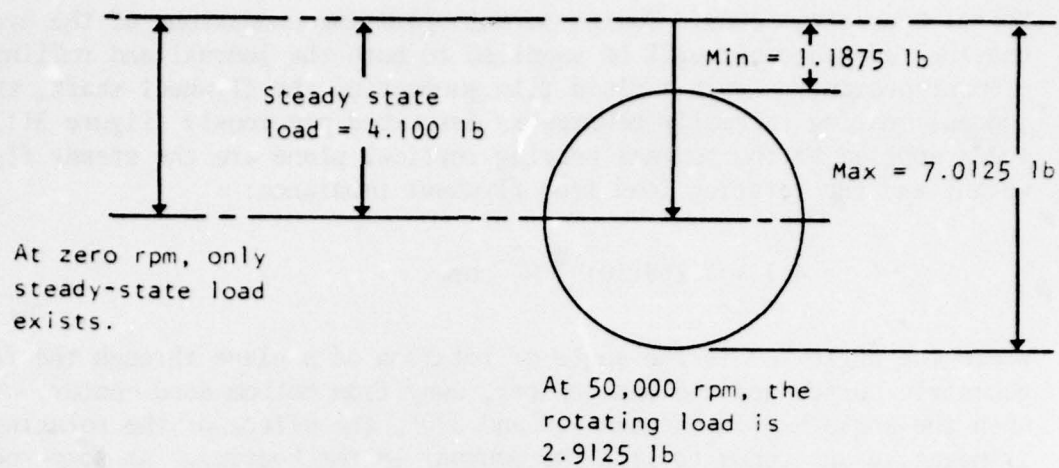


Figure 40. Rotating Load Diagram



- 1) Effects of cyclic loading on bearing life - The general methods of determining an equivalent mean load for use in calculating the life of a rolling element bearing are described in Reference 2. Where the load varies in a series of known steps, the equivalent load can be expressed as:

$$F_M = \left( \frac{F_1^3 N_1 + F_2^3 N_2 + F_3^3 N_3 + \dots + F_n^3 N_n}{N_1 + N_2 + N_3 + \dots + N_n} \right)^{1/3}$$

For vibratory loading, an integral form of the equation is:

$$F_M = \frac{1}{N} \int p^3 dN^{1/3}$$

In this case, the load "F" consists of steady-state load "F<sub>1</sub>", rotational-load "F<sub>2</sub>", and the total load as above:

$$F = F_1 + F_2 = 4.1 + 1.165(10)^{-9} N^2 \cos \omega$$

Then,

$$F_M = \left[ \frac{1}{\pi} \int_0^\pi (F_1 + F_2 \cos \omega)^3 d(\omega) \right]^{1/3}$$

Expanded and integrated,

$$F_M = \left[ F_1^3 \left( 1 + \frac{3}{2} \frac{F_2^2}{F_1^2} \right) \right]^{1/3}$$

or

$$F_M = \left[ (4.1)^3 \left( 1 + \frac{3(13.17)^2}{2(4.1)^2} \right) \right]^{1/3} = 10.433 \text{ lb}$$

This is the mathematical basis for the methods given in Reference 2, and is well-treated in the report, Reference 3.

Reference 2. SKF Engineering Data Manual

Reference 3. Lewis, P., and Malanoski, S., "Rotor-Bearing Dynamics Technology, Part IV: Ball Bearing Design Data," AFAPL-TR-65-45, May 1965

The mean load determined here is the load from the flywheel. As applied to the ball bearing in the hybrid configuration, it must be considered that, while the cyclic loading is applied at flywheel speeds, the ball bearing is rotating at a lesser speed and the cyclic load may be applied more than once per bearing revolution. Since ball bearing life is dependent upon the number of times the load is applied, the flywheel speed must be used in life calculations instead of the bearing speed.

- 2) Conclusions - It is evident from this discussion of loads that the flywheel must be balanced as finely as possible. For instance, the flywheel can be balanced so that the rotating load never causes the applied load to go negative, the hybrid bearing could function as a combination ball bearing and hydrodynamic bearing without consideration of the hydrostatic stage. This would occur if:

$$F_r = 0 = 4.1 + 1.165(10)^{-4} e_1 N^2 \cos \omega$$

let

$$N = 88,235$$

$$\omega = 180^\circ$$

$$e_1 = \frac{4.1}{1.165(10)^{-4} (88235)^2} = 0.00000452 \text{ inch}$$

This is, for all practical purposes, the limit of the present state-of-the-art and the level to which the test flywheel was balanced (0.000005).

Note that this level of flywheel balance would yield a minimum vertical load of zero, a maximum vertical load of 8.2 lb, and a mean vertical load of 7.843 lb. Depending on speed sharing factors and pre-loads finally selected, ball bearing life can be increased still further. In addition, if fluid damping coefficients can be maintained at a high enough level, the manufacturing precision required of the ball bearing may be reduced with considerable cost savings.

Ball Bearing Design. The characteristics of the duplex ball bearings which were considered are:

- 1) Bearing stiffness (or its inverse, the radial and axial deflection rates in inches per pound of load)
- 2) Bearing capacity and life
- 3) Bearing friction and power loss
- 4) High-speed effects on bearing life, stiffness and power loss

Although several bearings were investigated, three bearings of different size and configuration were considered representative of the size range required for this application. These bearings were all of the extra-precision type. They are described in Fafnir Bearing Co. catalog 68 and are numbered (in Fafnir terminology) 2MM 9305, 2MM 9104, and 2MM 9103. Further, two types of each bearings were considered; i.e., type W0, which has the inner ring counter-bored for assembly and the separator designed to ride on the lands of the outer ring, and type W1, which has the outer ring counterbored with the separator designed to ride on the outer ring land but only on a single side. Refer to Table 4 for bearing characteristics.

- 1) Ball bearing stiffness - The stiffness of a bearing is simply its rate of dimensional change under an applied load. As in any spring, the rate of deflection is usually expressed in pounds of load required to deflect the bearing 1 inch. The inverse of this dimension is the rate of deflection in inches of deflection per pound of load, which is of use in these calculations since, under radial load, radial deflection can increase the orbiting eccentricity of the flywheel under certain conditions. Unlike a helical spring, however, bearing deflection is an exponential function of load for pure thrust or radial loads, but becomes an involved combination of the two rates when both radial and axial loads are applied. A computer program for calculating ball bearing stiffness is contained in Part II of Reference 3. However, ball speed variation is also related to stiffness (BSV) and, unfortunately, this is not accounted for in the computer program. Figure 41 graphically displays part of what happens inside a ball bearing under various loading conditions. Figure 41a shows the ball paths on the raceways during the application of a pure radial load. At relatively low speeds (below 500,000 DN), the retainer speed is controlled by the speed of the most heavily loaded ball on the inner race which has the highest compressive stress. When the ball lifts off the inner race, its own speed tends to be controlled by the outer race, but the centrifugal forces are light and the skidding of the ball against both the raceway and the retainer pocket is minimal.



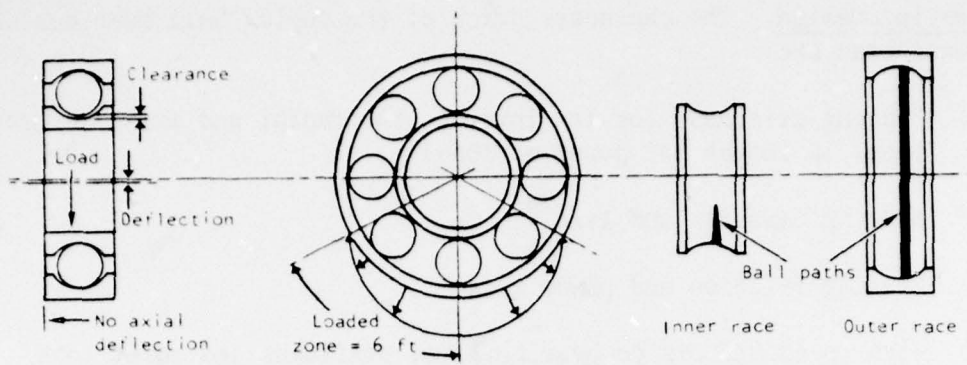


Figure 41a. Bearing with Pure Radial Load

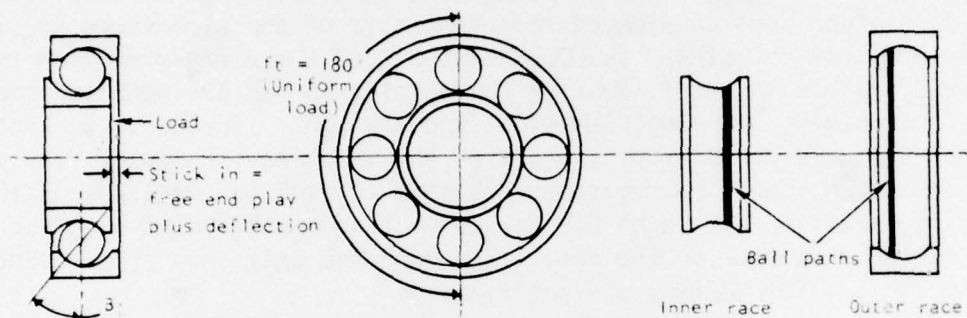


Figure 41b. Bearing with Pure Thrust Load

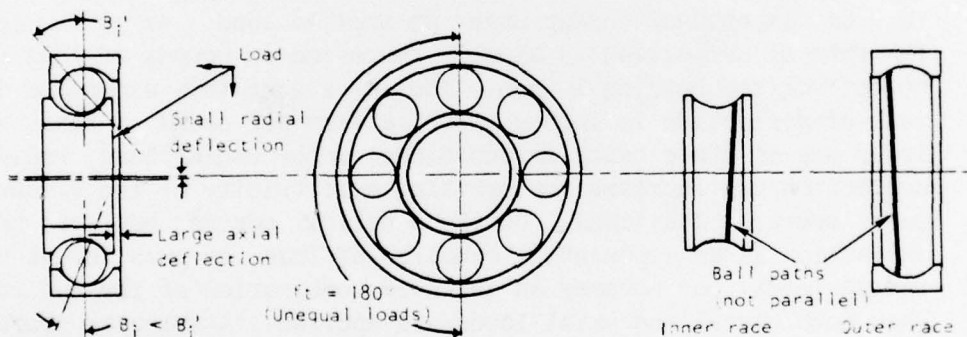


Figure 41c. Bearing with Heavy Thrust Load and Light Radial Load

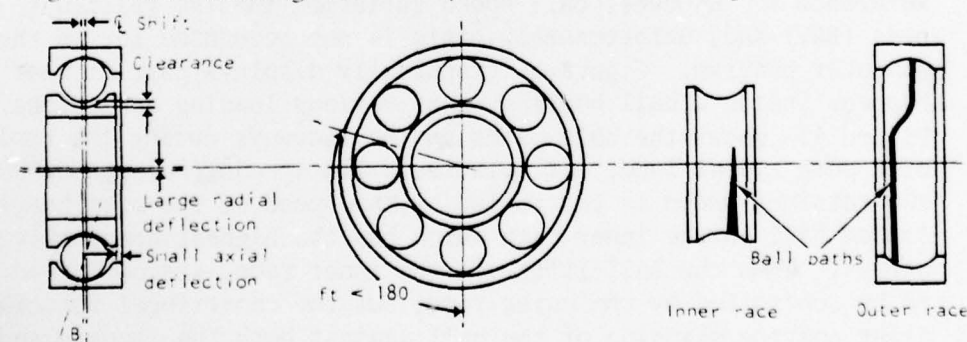


Figure 41d. Bearing with Light Thrust Load and Heavy Radial Load

Figure 41. Ball Path Characteristics Under Load

TABLE 4. BEARING CHARACTERISTICS

| Item                                  | Bearing No.  |              |                |
|---------------------------------------|--------------|--------------|----------------|
|                                       | 9103         | 9104         | 9305           |
| Bore dia                              | 17MM(0.6693) | 20MM(0.7874) | 25MM(0.9843)   |
| Outside dia                           | 35MM(1.3780) | 42MM(1.6535) | 42MM(1.6535)   |
| Mean dia                              | 26MM(1.0237) | 31MM(1.2205) | 33.5MM(1.3189) |
| Width (duplex brg)                    | 20MM(0.7874) | 24MM(0.9949) | 18MM(0.7087)   |
| Ball size                             | 0.21875"     | 0.250"       | 0.1875"        |
| No. balls                             | 10           | 11           | 17             |
| Contact angle ( $B_0$ )               |              |              |                |
| WI                                    | 12°          | 12°          | 12°            |
| WO                                    | 18°          | 18°          | 18°            |
| Ball/race conformity (f) <sup>a</sup> |              |              |                |
| Inner ( $f_i$ )                       | 52           | 52           | 52             |
| Outer ( $f_o$ )                       | 53           | 53           | 53             |

<sup>a</sup>Conformity, or the race curvature in the axial plane, is expressed as a decimal fraction of ball diameter. Thus, the conformity can never be as small as 0.50 (or equal to ball radius) since any load would result in sufficient ball-race deflection to cause the radial clearance between the ball and race to be less than zero, and the ball would be wedged into the race. There would be no room for a fluid film, and the resultant skidding would be unacceptable. "Normal" conformity varies from manufacturer to manufacturer according to bearing type, but the values generally regarded as an acceptable minimum are  $f_i$  (inner race) = 0.516 and  $f_o$  (outer race) = 0.530.

Moreover, at speeds above 500,000 DN, the centrifugal forces become great enough to cause the maximum contact stress to occur at the outer race, which, in turn, controls both ball and retainer speed, and the skidding occurs between the ball and inner race when the unloaded ball reenters the loaded zone.

Figure 41b illustrates a pure axial or thrust load condition. In this condition, the load on each ball is the same, and there is virtually no ball speed variation.

Figure 41c illustrates the effects of a combination radial and thrust load where the thrust load is dominant sufficiently to keep all balls in contact with both inner and outer races. In any angular contact ball bearing, an increase in thrust load tends to increase the contact angle and any radial load tends to decrease the contact angle.

Thus, under a combined load, each ball in the bearing has a different contact angle, but as long as all the balls remain in contact with both races, the angular change is essentially uniform as the bearing rotates, but the ball paths in the races are not parallel. Each ball also has a different normal load across it, with the most heavily loaded ball on the bottom having the lowest contact angle, and the most lightly loaded ball on top having the highest contact angle. Under normal operating conditions at speeds below 500,000 DN, the angular divergence of the ball paths is very small and the usual clearance between the ball and ball pocket in the retainer allows the retainer to run smoothly with little or no wobble. Ball speed is a function of the contact angle, and there is less than 1% ball speed variation. Higher speeds tend to decrease the outer race contact angle and increase the contact angle on the inner race so that the angular divergence of the ball paths is somewhat greater. The retainer can still be made to operate smoothly by enlarging the ball pockets in the retainer slightly.

As shown in Figure 41d, when the radial load becomes great enough to cause the top ball to lift off, there is no longer any control to force the free ball to maintain an angle of contact. The ball immediately tries to shift to the center of the outer race, and its speed is controlled by the outer race. The angular velocity of the ball about its own center can be expressed:

$$N_B = \frac{D_M N_i}{2d} \left[ 1 - \left( \frac{d}{D_M} \right)^2 \cos^2 \phi_1 \right] \text{ (inner race control)}$$

where

$D_M$  = ball pitch circle dia

$d$  = ball dia

$N_i$  = inner race speed

Using the 9305 bearing as an example,

$$\begin{aligned} N_B &= \frac{1.3189 N_i}{2(0.1875)} \left[ 1 - \left( \frac{0.1875}{1.3189} \right)^2 \cos^2 20^\circ \right] \\ &= 3.4543 N_i \end{aligned}$$



When the ball lifts off and its speed becomes controlled by the outer race, the speed ratio is

$$\begin{aligned} \phi &= \frac{D_M + d}{D_M - d \cos \beta} = \frac{1.3189 + 0.1875}{1.3189 - 0.1875 \cos 20^\circ} \\ &= \frac{1.5064}{1.1427} = 1.3183 \end{aligned}$$

The ball therefore tries to increase its own rotating speed by 31.83%, introducing unacceptable skidding. In addition, the ball instantaneously precesses its centerline of rotation by the full amount of the original contact angle and shifts its center in the retainer by the full amount of the axial deflection. Unless the retainer ball pockets provide adequate clearance, the side loads on the retainer can become high enough to cause immediate failure of the retainer. A good discussion of this problem is presented in the paper "Ball Speed Variation in Ball Bearings and Its Effect on Cage Design," by Thomas Barish (ASLE preprint 68AM 6C-2). Ball lift-off may be prevented by providing adequate preload to the bearings so that the maximum expected radial load from precession is less than the load required to achieve liftoff.

The combination of radial and thrust loads at incipient liftoff can be calculated (Figure 41c):

$$\phi' = 180^\circ = \cos^{-1} \frac{\sqrt{1 - (\sin \beta_o' + h')^2} - \cos \beta_o'}{k'}$$

where

$\beta_o'$  = mounted initial contact angle before load application

$$h' = \frac{h}{Bd}$$

$h$  = axial deflection from preload

$$B = f_i + f_o - 1$$

$d$  = ball diameter

$$k' = \frac{k}{Bd}$$

$k$  = radial deflection from radial load

This equation was solved by numerical integration for the three candidate bearings, for both  $12^\circ$  and  $18^\circ$  angles of initial unmounted contact. The stiffness characteristics of the bearings are illustrated in Figure 42. Generally speaking, the stiffness of a bearing increases with the number of balls, but decreases as the contact angle increases. This is apparent in the curves of Figure 42. In these computations, a load sharing factor of  $(i)^{0.7}$  was allowed where  $i$  = number of rows. Thus, when the number of rows,  $i$ , = 2, the two rows will not share the load equally due to manufacturing tolerances. (Radial runouts and ball diameter variations are to be considered, and the factor  $(i)^{0.7}$  is determined from test).

Let the capacity of a single-row bearing equal  $C$ . Then, for:

$$2 \text{ rows, } C_2 = C(2)^{0.7} = 1.625C$$

$$3 \text{ rows, } C_3 = C(3)^{0.7} = 2.158C$$

$$4 \text{ rows, } C_4 = C(4)^{0.7} = 2.639C$$

$$5 \text{ rows, } C_5 = C(5)^{0.7} = 3.085C$$

Therefore, adding extra rows of bearings to increase load-carrying capacity rapidly reaches a point of no return and, if extra capacity is required, it is better to use larger but fewer bearings. (Actually, while this factor is conservative due to the ultraprecision bearing tolerances, higher anticipated speeds obviate the use of a less conservative factor).

The maximum anticipated radial loads occur during the acceleration period of precession. If the flywheel shaft is oriented to permit maximum roll-rate precession, the loads become:

$$\begin{aligned} F_{rp} &= 2(115.62) + 4.1 + 1.165(10)^{-9}(88,239)^2 \\ &= 244.41 \text{ lb} \end{aligned}$$

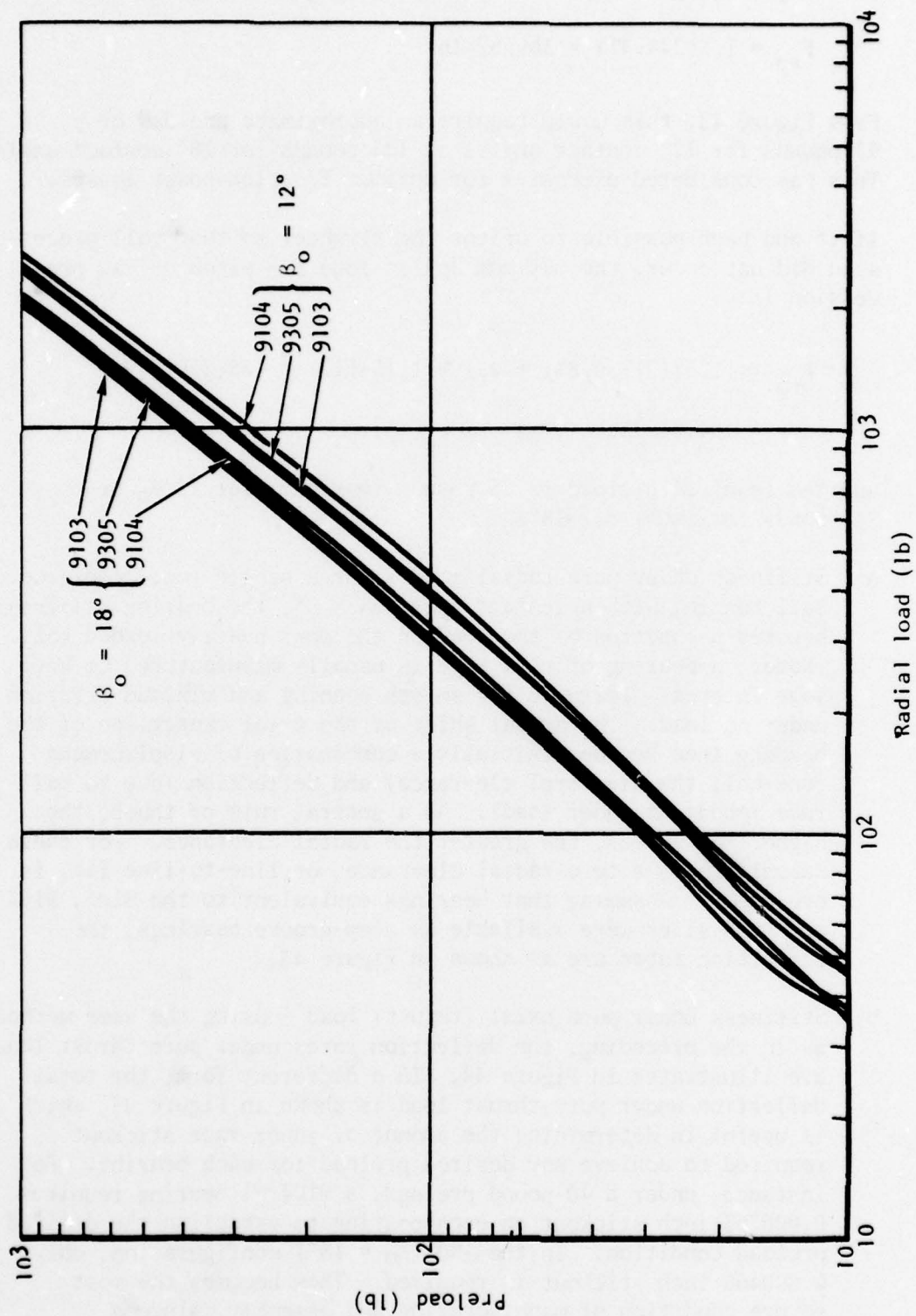


Figure 42. Bearing Deflection - Radial Load at Ball Liftoff Versus Preload in Duplex Sets (load-sharing =  $(i)^{0.7}$ )



Allowing a design factor of 1.5, the bearing should withstand

$$F_{rp} = 1.5(244.41) = 366.62 \text{ lb}$$

From Figure 42, this would require an approximate preload of 92 pounds for  $12^\circ$  contact angles or 128 pounds for  $18^\circ$  contact angles. This was considered excessive for optimum friction-power losses.

If it had been possible to orient the flywheel so that roll precession did not occur, the maximum design load for pitch or yaw precession is:

$$\begin{aligned} F_{rp} &= (1.5)(2)(30.83) + 4.1 + 1.154(10)^{-9} (88,239)^2 \\ &= 104.51 \text{ lb} \end{aligned}$$

and the required preload is 25 pounds (maximum) for  $12^\circ \beta_0$  or 34 pounds (maximum) for  $18^\circ \beta_0$ .

- a) Stiffness under pure radial load - For a single-row, deep-groove ball bearing with a contact angle  $\beta_0 = 0^\circ$ , the bearing stiffness becomes a function of the load on the most heavily loaded ball. (Note: a bearing of this type is usually manufactured to have some internal clearance for smooth running and minimum friction under no load. The actual shift of the axial centerline of the bearing then becomes initially a combination of displacement (one-half the diametral clearance) and deflection (due to ball-race imbedment under load). As a general rule of thumb, the higher the speeds, the greater the radial clearance. For these calculations, a zero radial clearance, or line-to-line fit, is presumed.) Assuming that bearings equivalent to the 9103, 9104 and 9105 sizes were available as deep-groove bearings, the deflection rates are as shown in Figure 43.
- b) Stiffness under pure axial (thrust) load - Using the same methods as in the preceding, the deflection rates under pure thrust load are illustrated in Figure 44. In a different form, the total deflection under pure thrust load is shown in Figure 45, which is useful in determining the amount of inner race stickout required to achieve any desired preload for each bearing. For instance, under a 40-pound preload, a 9104-WI bearing requires 0.000763 inch stickout on each bearing to establish the desired preload condition. In the -WO ( $\beta_0 = 18^\circ$ ) configuration, only 0.000466 inch stickout is required. This becomes the most severe condition of manufacturing and assembly, since a

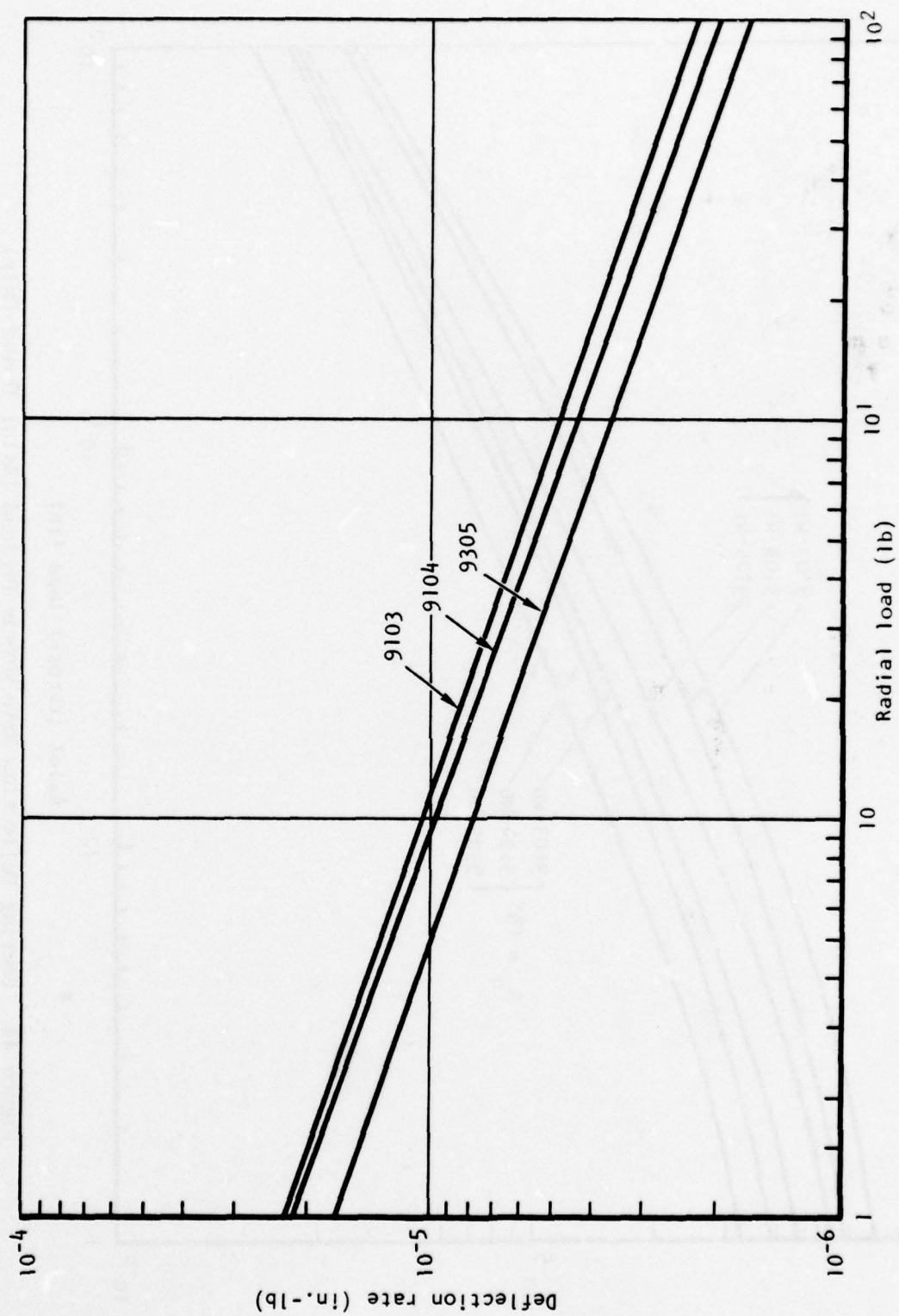


Figure 43. Bearing Deflection Rate Versus Radial Load Only  
 $(\beta_0 = 0^\circ)$  (Duplex Bearing)

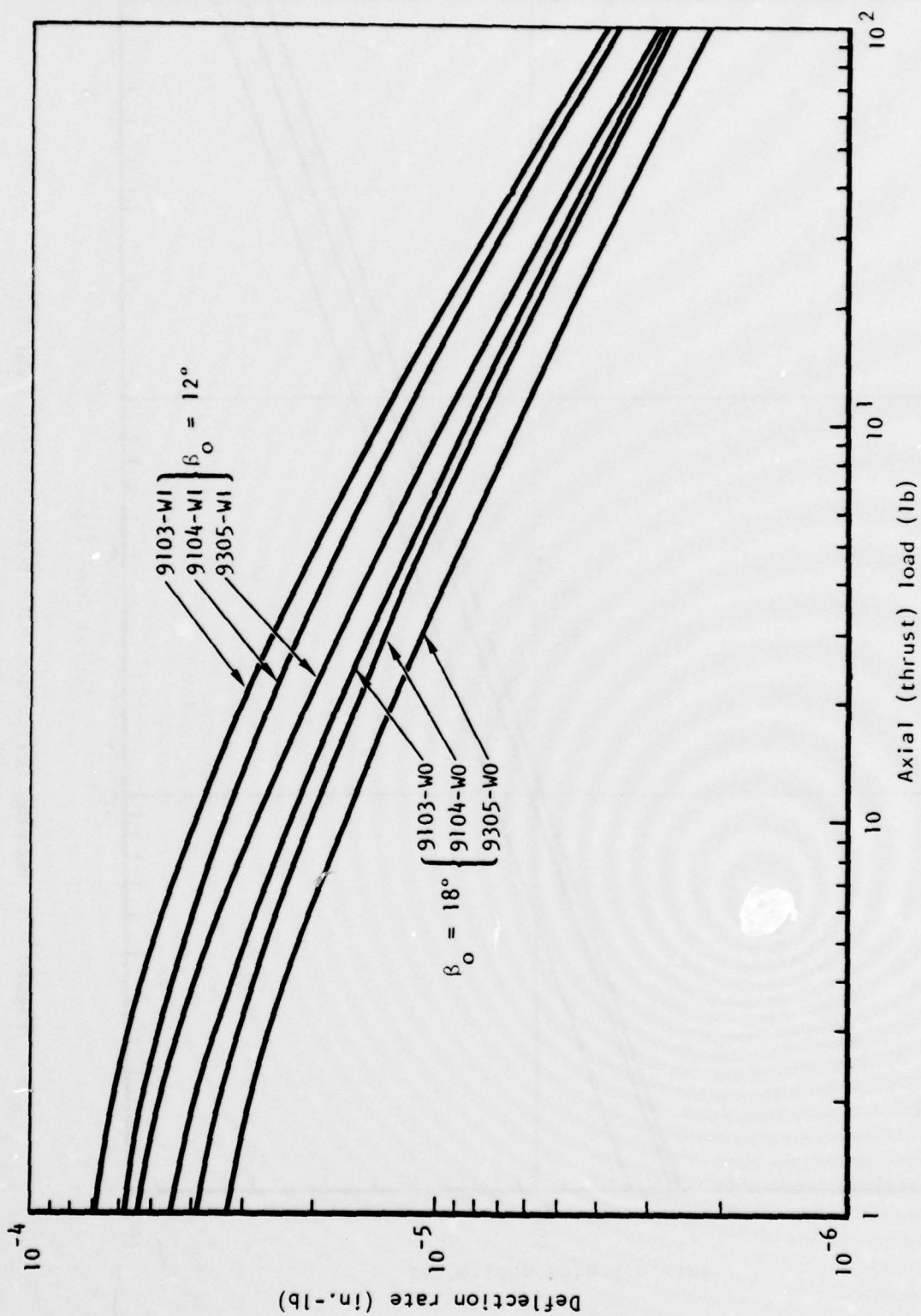


Figure 44. Bearing Deflection Rate Versus Preload (Axial Thrust Only)



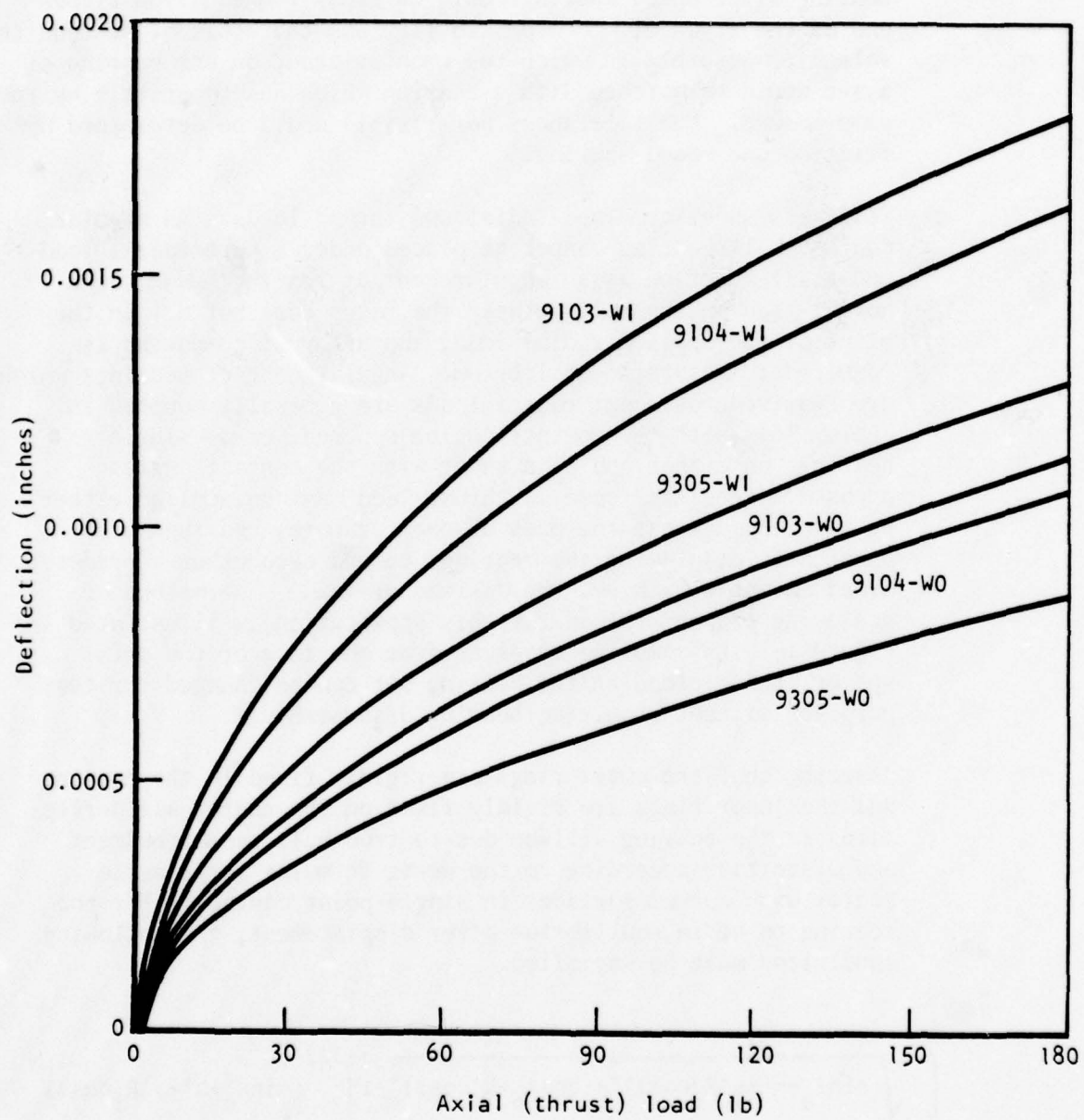


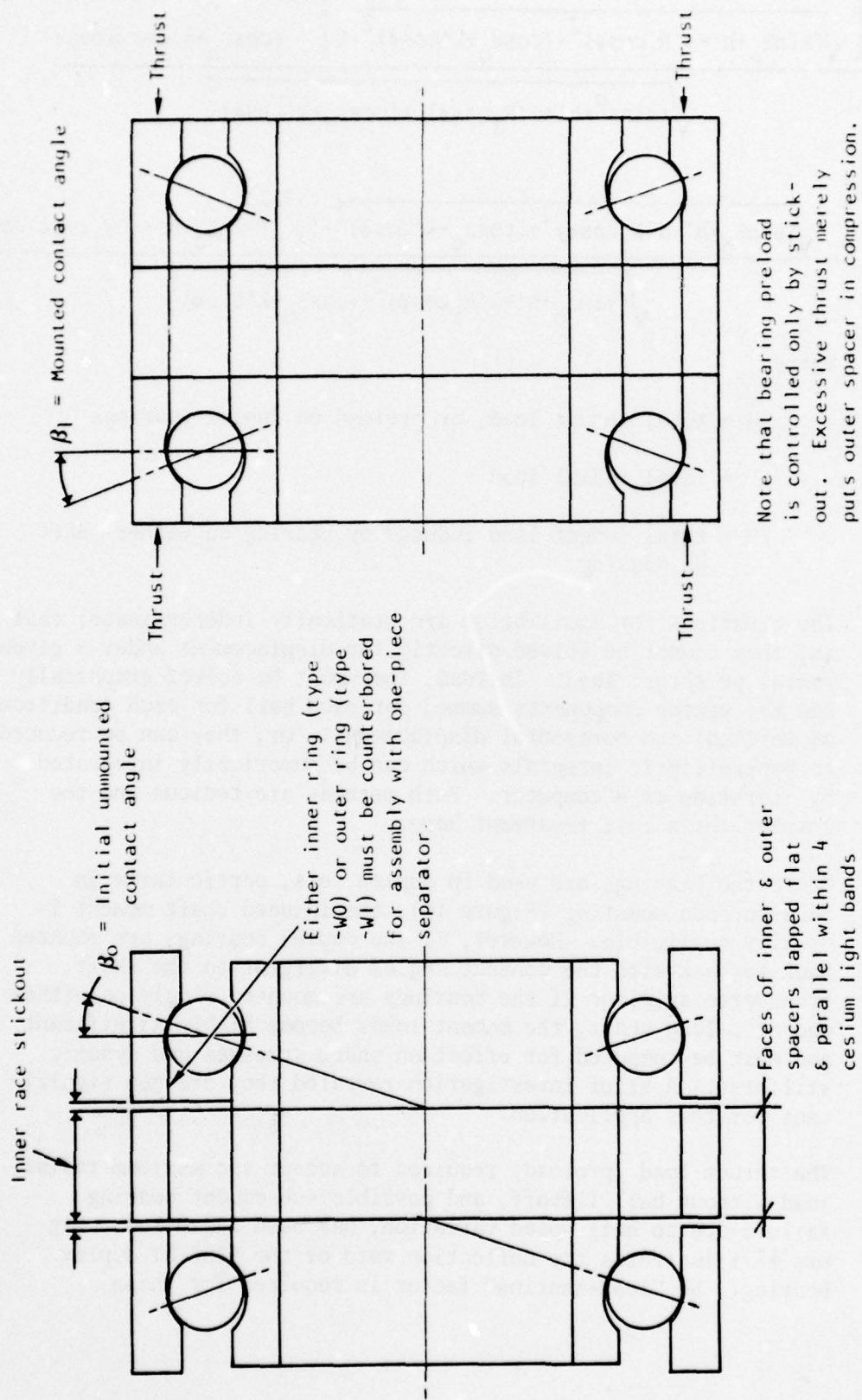
Figure 45. Bearing Deflection Under Pure Thrust Load Only

0.0001-inch error in stickout per bearing can mean a variation of +11.0, -9.5 pounds on the 9104-WI bearing and +16, -13.5 pounds on the 9104-WO; the higher the preload, the greater the deviation. This is not acceptable for the requirements of a series hybrid bearing since speed sharing could be grossly unequal on either end of the flywheel. One possibility was that this might require selective assembly in which too much stickout on one bearing of a set would be matched with a bearing which has too little by the same amount. The tolerances permissible would be determined by friction and speed sharing.

- c) Stiffness under combined radial and thrust loads - An angular contact ball bearing cannot be placed under a pure radial load and still function as an angular contact bearing because the normal load on the ball between the races does not act in the plane of the applied radial load, and a thrust component is required to maintain equilibrium. Angular contact bearings which are required to accept radial loads are generally mounted in duplex sets with the contact angles opposed, or as single bearings on either end of a shaft with the contact angles opposed. In either case, a thrust load must be applied either by a spring against the back of one (or both) bearings or by physically displacing the bearings toward each other a predetermined amount to achieve the desired preload. The method of achieving proper preload for this application is illustrated in Figure 46. By removing material from one face of the outer spacer, the preload on the bearing set can be changed for test purposes without requiring bearing disassembly.

Assuming that the outer rings are rigidly fixed in the housing and the inner rings are rigidly fixed on the shaft, all deflections in the bearing will be due to true ball race imbedment and distortion according to the Hertz formulae for elastic bodies with curved surfaces in single-point contact. For the bearing to be in equilibrium after displacement, the following conditions must be satisfied.

$$H = Kd^2 \frac{\left[ \sqrt{(\sin \beta_o + h' + a' R_1 \cos \phi)^2 + (\cos \beta_o + k' \cos \phi)^2} - 1 \right]^{3/2} (\sin \beta_o + h' + a' R_1 \cos \phi)}{\sqrt{(\sin \beta_o + h' + a' R_1 \cos \phi)^2 + (\cos \beta_o + k' \cos \phi)^2}}$$



Unmounted

Mounted

Figure 46. Typical Duplex Bearing Arrangement (Face-to-Face Mounting)



$$\Sigma V = Kd^2 \Sigma \frac{\left[ \sqrt{(\sin \beta_o + h' + \alpha' R_1 \cos \phi)^2 + (\cos \beta_o + k' \cos \phi)^2} - 1 \right]^{3/2} (\cos \beta_o + k' \cos \phi) \cos \phi}{\sqrt{(\sin \beta_o + h' + \alpha' R_1 \cos \phi)^2 + (\cos \beta_o + k' \cos \phi)^2}}$$

$$\Sigma M = \frac{EKd^2}{2} \Sigma \frac{\left[ \sqrt{(\sin \beta_o + h' + \alpha' R_1 \cos \phi)^2 + (\cos \beta_o + k' \cos \phi)^2} - 1 \right]^{3/2} (\sin \beta_o + h' + \alpha' R_1 \cos \phi) \cos \phi}{\sqrt{(\sin \beta_o + h' + \alpha' R_1 \cos \phi)^2 + (\cos \beta_o + k' \cos \phi)^2}}$$

where

$\Sigma H$  = total thrust load, or preload on duplex bearings

$\Sigma V$  = total radial load

$\Sigma M$  = total moment load induced by bearing on either shaft or housing

The equations for equilibrium are statically indeterminate; that is, they cannot be solved directly for displacement under a given radial or thrust load. Instead, they must be solved graphically and the vector components summed for each ball for each condition of vertical and horizontal displacement. Or, they can be reduced to hyperelliptic integrals which can be numerically integrated by iteration on a computer. Both methods are tedious and too complex for a full treatment here.

Where the bearings are used in duplex sets, particularly in face-to-face mounting (Figure 46), the induced shaft moment is usually negligible. However, if the duplex bearings are mounted back-to-back with the contact angles divergent to the shaft transverse axis, or if the bearings are mounted singly on either end of a long shaft, the moment loads become highly significant and must be computed for effect on shaft stresses and dynamic stiffness. A brief investigation revealed they are not significant for this application.

The thrust load (preload) required to accept the maximum radial load without ball liftoff, and possible subsequent bearing failure due to ball speed variation, has been discussed. Figure 47 illustrates the deflection rate of the 9103-WI duplex bearing. No "load-sharing" factor is required for these

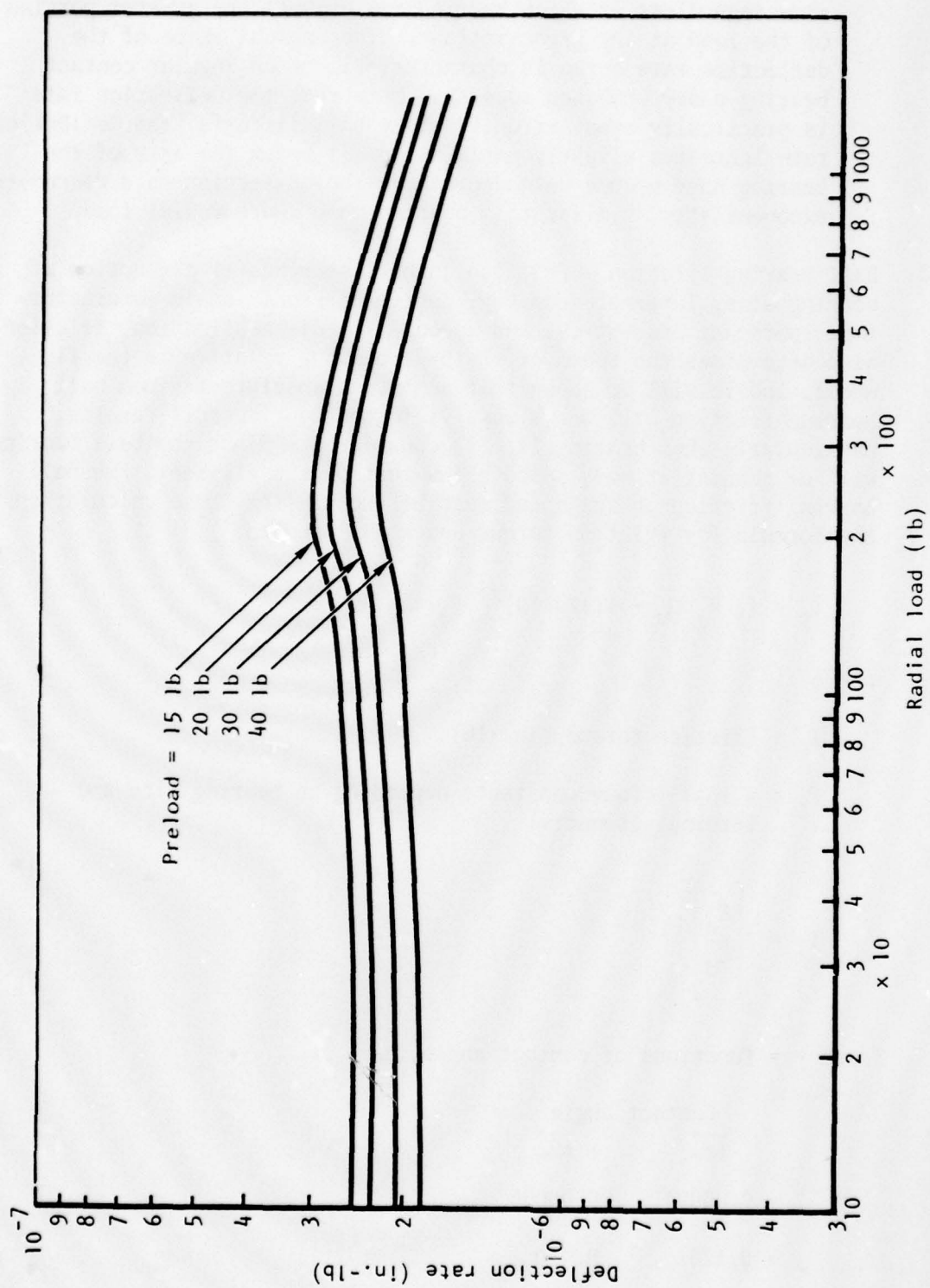


Figure 47. Deflection Rate Versus Radial Load, 9103-W1, Duplex Bearing

calculations since total deflection will be approximately the same regardless of which bearing row assumes the greater portion of the load at any given instant. The unusual shape of the deflection rate curve is characteristic of an angular contact bearing under combined loading. Note that the deflection rate is practically constant until after ball liftoff. The deflection rate increases slightly until all balls below the axis of the bearing have become unloaded; then, the deflection rate decreases exponentially, similar to a bearing under pure radial load.

- 2) Ball bearing friction - Friction in ball bearings is a function of bearing size, internal geometry, degree of precision in manufacturing, lubricant properties, and speed. In this application, friction also determines the speed of the ball bearing relative to the flywheel, and it will be shown that achieving absolute minimum ball bearing friction will not always yield the best overall results, particularly when bearing life is considered. Since the ball bearing will be running at some speed below that of the flywheel, the ball bearing friction at any speed must be known. For these calculations, the formula for friction torque which was used is:

$$T_F = f_1 P_{\beta} D_M + 1.420(10)^{-5} f_o (v N)^{2/3} D_M^3$$

where

$T_F$  = friction torque (in.-lb)

$f_1$  = a load-torque constant, depending on bearing size and internal geometry:

$$f_1 = z \left[ \frac{P_o}{C_o} \right]^y$$

$z$  and  $y$  = functions of contact angle,  $\beta_o$

| Contact angle |            |
|---------------|------------|
| <u>12°</u>    | <u>18°</u> |
| $z = 0.00094$ | $0.00096$  |
| $y = 0.426$   | $0.430$    |



$P_o$  = static equivalent load

$$= X_o F_r + Y_o F_a$$

$F_r$  = static radial load (wt)

$F_a$  = static thrust load (preload)

$X_o$  = load factor = 1.0 for low contact angle duplex brg

$Y_o$  = load factor = 0.84 for low contact angle duplex brg

$$P_o = (1.0)(4.1) + 0.84 (F_a)$$

$$C_o = \frac{8543 \text{ nd}^2 i \cos \beta_o}{f_s^3}$$

For  $f_i = f_o = 0.55$  = conformity of ball-race curvature:

$\beta_o$  = unmounted contact angle

$$= 12^\circ \text{ or } 18^\circ$$

$n$  = No. of balls per row

$d$  = ball dia

$f_s$  = load/stress factor based on race curvature and contact angle (for this bearing, use  $f_s = 1.29$ )

For  $\beta_o = 12^\circ$ ,

$$C_o = \frac{8543 \text{ nd}^2 (2) \cos 12^\circ}{(1.29)^3} = 7,605 \text{ nd}^2$$

For  $\beta_o = 18^\circ$ ,

$$C_o = \frac{8543 \text{ nd}^2 (2) \cos 18^\circ}{(1.29)^3} = 7,592.5 \text{ nd}^2$$

$$P_{\beta} = 0.9 F_a \cot \beta_o - 0.1 F_{rm}$$

$F_{rm}$  = mean radial load

$$= \left[ P_W^3 \left( 1 + \frac{3}{2} - \frac{P_S^2}{P_W^2} \right) \right]^{1/3}$$

where

$P_W$  = steady load on bearing due to weight = 4.1 lb

$P_S$  = sinusoidal load on bearing due to flywheel imbalance.  
Assume flywheel eccentricity = 0.000010,

$$P_S = 1.165(10)^{-9} N^2$$

where

$N$  = bearing speed of rotation

$$\begin{aligned} F_{rm} &= \left[ (4.1)^3 \left( 1 + \frac{3[1.165(10)^{-9} N^2]^2}{2(4.1)^2} \right) \right]^{1/3} \\ &= 4.1 \left[ 1 + 1.211(10)^{-19} N^4 \right]^{1/3} \end{aligned}$$

Then, for  $\beta_o = 12^\circ$ ,

$$P_{\beta} = 4.234 F_a - 0.41 \left[ 1 + 1.211(10)^{-19} N^4 \right]^{1/3}$$

and for  $\beta_o = 18^\circ$ ,

$$P_{\beta} = 2.77 F_a - 0.41 \left[ 1 + 1.211(10)^{-19} N^4 \right]^{1/3}$$

$D_M$  = pitch circle dia. Assume mean bearing dia (Table 4)

$f_o$  = viscous torque factor

= 2.0 for duplex bearings with mist lubrication

$\mu$  = lubricant kinematic viscosity in centistokes

= 3.8 cs for Santotrac 30 at 190° F

$N$  = rotating speed of bearing inner ring

Substituting these values into the basic equation:

For  $\beta_o = 12^\circ$ ,

$$\begin{aligned} T_{F(12)} &= 0.00094 \left[ \frac{4.1 + 0.84 F_a}{7605.0 n d^2} \right]^{0.462} \\ &\quad \left\{ 4.234 F_a - 0.41 \left[ 1 + 1.211(10)^{-19} N^4 \right]^{1/3} \right\} (D_M) \\ &\quad + 1.42(10)^{-5} (2) (3.8)^{2/3} N^{2/3} D_M^3 \\ T_{F(12)} &= 1.514(10)^{-5} \left[ \frac{4.1 + 0.84 F_a}{n d^2} \right]^{0.462} \\ &\quad \left\{ 4.234 F_a - 0.41 \left[ 1 + 1.211(10)^{-19} N^4 \right]^{2/3} \right\} (D_M) \\ &\quad + 6.916(10)^{-5} N^{2/3} D_M^3 \end{aligned}$$



For  $\beta_0 = 18^\circ$ ,

$$T_{F(18)} = 0.00096 \left[ \frac{4.1 + 0.84 F_a}{7392.5 n d^2} \right]^{0.43}$$

$$\left\{ 2.77 F_a - 0.41 \left[ 1 + 1.211(10)^{-19} N^4 \right]^{1/3} \right\} (D_M)$$

$$+ 1.42(10)^{-5} (2) (3.8)^{2/3} N^{2/3} D_M^3$$

$$T_{F(18)} = 2.083(10)^{-5} \left[ \frac{4.1 + 0.84 F_a}{n d^2} \right]^{0.43}$$

$$\left\{ 2.77 F_a - 0.41 \left[ 1 + 1.211(10)^{-19} N^4 \right]^{1/3} \right\} (D_M)$$

$$+ 6.916(10)^{-5} N^{2/3} D_M^3$$

Using the values given in Table 4, the friction torque for the three candidate bearings is plotted in Figures 48 and 49.

$$\text{Horsepower loss} = H_F = \frac{T_F N}{63025} = 1.5867(10)^{-5} T_F N.$$

The horsepower loss curves for the three candidate bearings are plotted in Figures 50 and 51.

The total heat loss per duplex set

$$q = 42.44 H_F \text{ (BTU/min).}$$

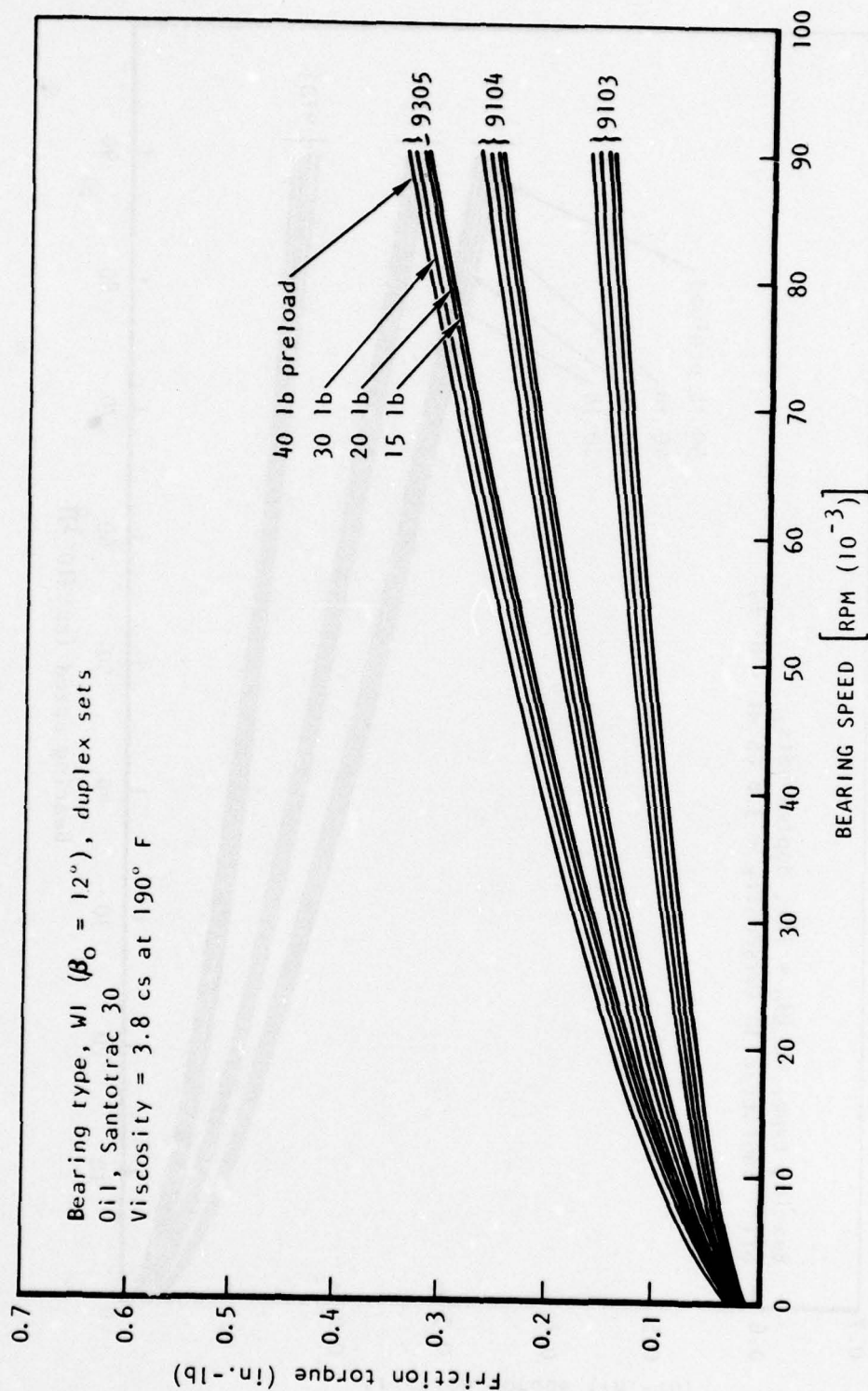


Figure 48. Bearing Friction Torque Versus Speed and Preload at Mean Radial Load

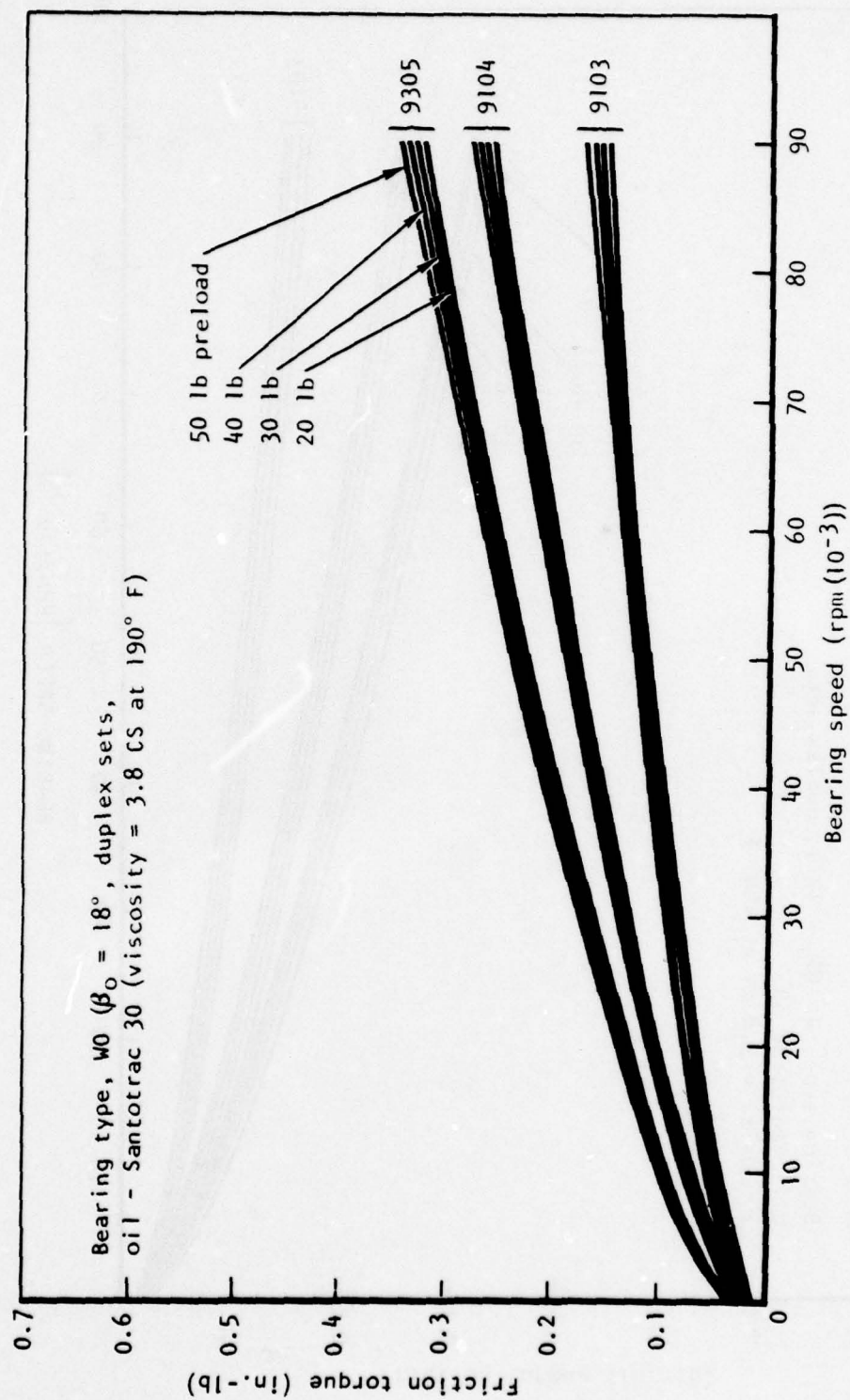


Figure 49. Bearing Friction Torque Versus Speed and Preload at Mean Radial Load



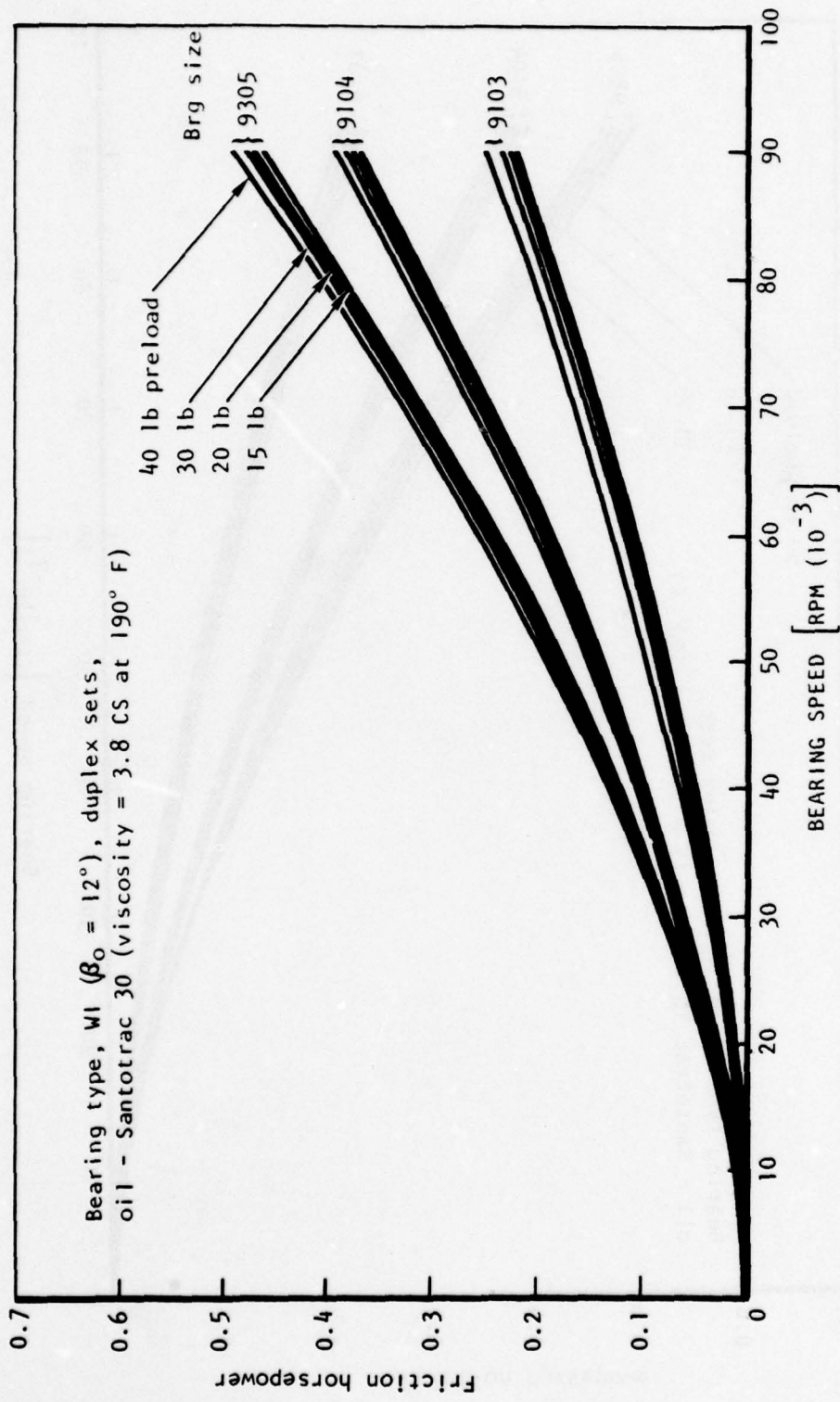


Figure 50. Bearing Friction Power Loss Versus Speed and Preload at Mean Radial Load

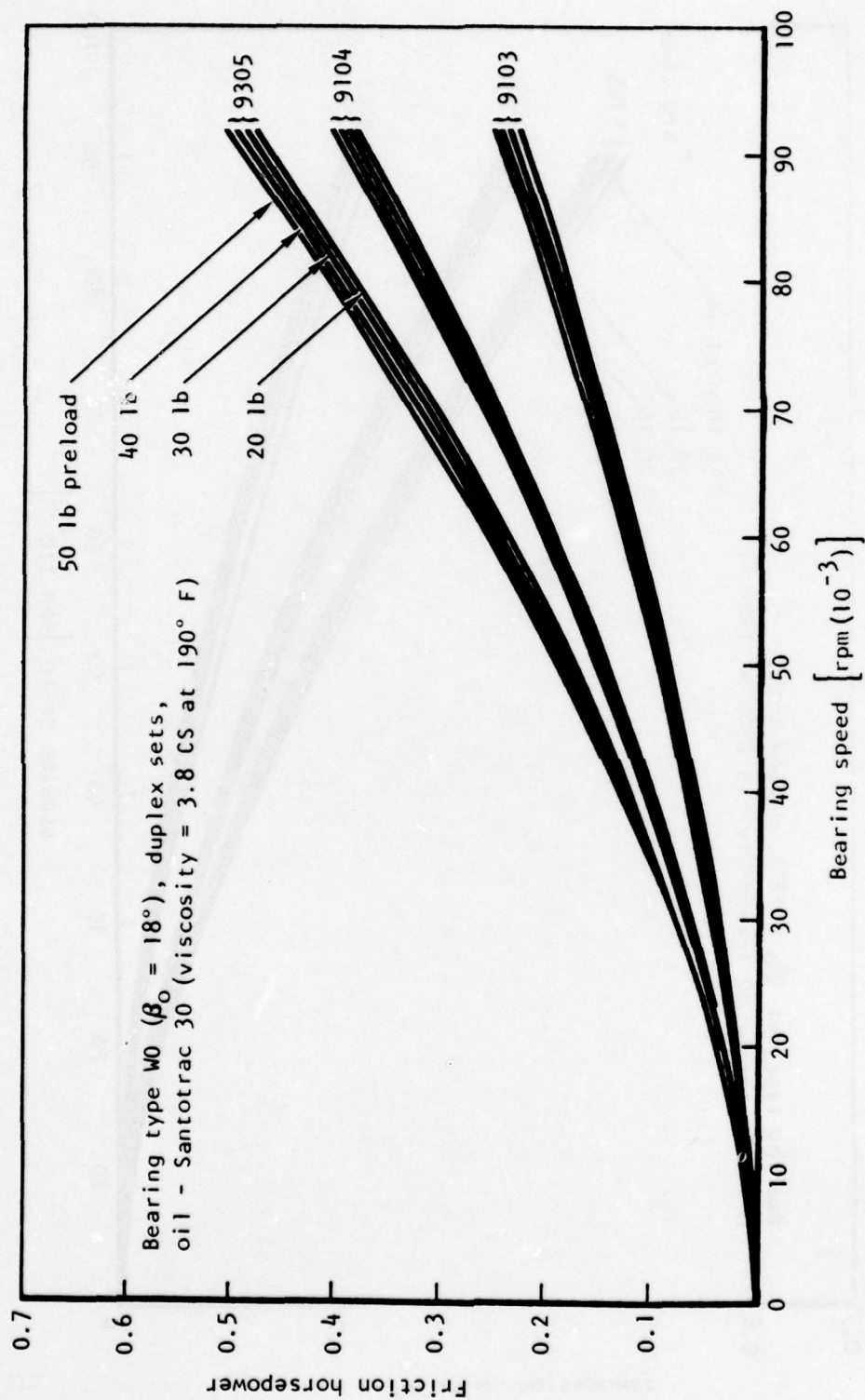


Figure 51. Bearing Friction Power Loss Versus Speed and Preload at Mean Radial load

The specific heat of Santotrac 30 at 200° F is 0.509 BTU/lb/min/°F. The density of the oil at 200° F is 0.853 g/cc or 6.89 lb/gal, or 0.1451 gal/lb. Then

$$C = \frac{0.509}{0.1451} \text{ BTU/gal/min/°F}$$

$$= 3.507 \text{ BTU/gal/min/°F}$$

Normally, a 25° C (45° F) temperature rise across a high-speed bearing is considered acceptable. If this value is used for these preliminary calculations,

$$C' = 25(3.507) = 87.68 \text{ BTU/gal/min}$$

and the total oil flow,  $Q'$ , required is

$$Q' = \frac{42.44H_F}{87.68} = 0.4841 H_F \text{ gal/min}$$

This is plotted in Figure 52 for the type WO bearings (there is little difference from the type WI since the friction horsepower losses are similar). For good lubrication, this type of bearing needs only an oil mist, say 10 drops of oil per second for each row, or approximately 40cc per minute (0.011 gallon). This quantity of oil would not cool the bearings above 15,000 rpm; therefore, additional means of cooling were provided in the form of cooling oil circulating loops in the flywheel housing around the outside diameter of the bearing.

- 3) Ball bearing capacity and life - Generally, the conventional approach to calculating the load-carrying capacity and life ratings as established by the AFBMA and ISO were used; exceptions and additional considerations are noted in the following.
  - a) Basic life and load formulas - The basic dynamic capacity of a rolling element bearing is defined as that radial load which a bearing will carry, with a 90% probability of survival, for 1 million revolutions of the inner race at constant speed, with the outer ring fixed. In other words, the basic dynamic capacity,  $C$ , is the load at which no more than 10% of the bearings will fail. From this has evolved the commonly used term " $L_{10}$ " life dating. Theories and formulas for the determination



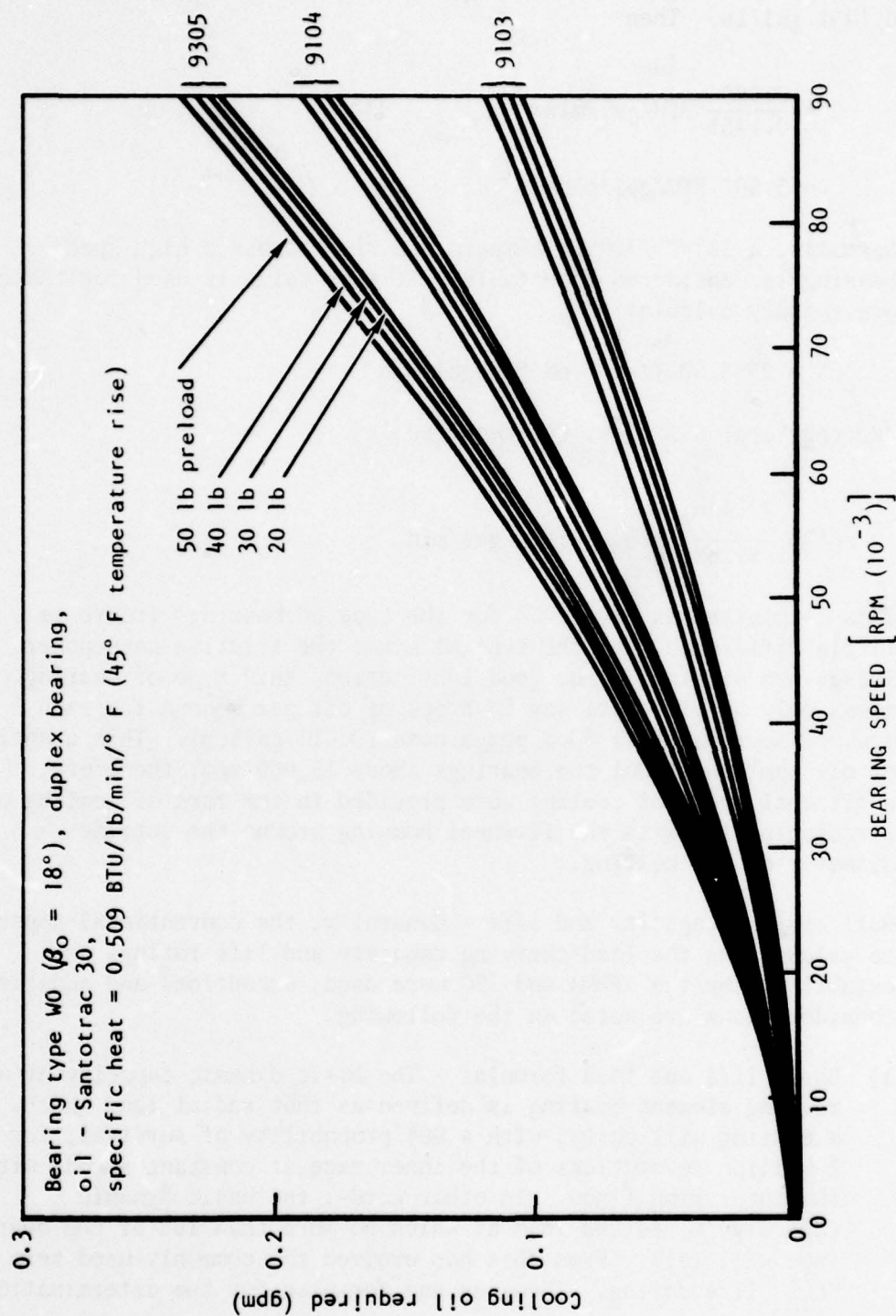


Figure 52. Cooling Oil Required Versus Speed and Preload

of bearing capacity and reliability have been developed from extensive experiment and research. The formula for ball bearings used in this study is:

$$C = f_c (i \cos \beta_o)^{0.7} n^{2/3} d^{1.8}$$

where

$f_c$  = a factor dependent upon bearing geometry and material

$i$  = No. of rows of balls

$\beta_o$  = initial unmounted contact angle

$n$  = No. of balls per row

$d$  = ball diameter

Referring to Table 4 and obtaining the  $f_c$  values from Reference 2, the basic dynamic capacities of the candidate bearings are:

| <u>Brg</u><br><u>Size</u> | <u>Brg type</u>          |                          |
|---------------------------|--------------------------|--------------------------|
|                           | <u>WI</u><br><u>(lb)</u> | <u>WO</u><br><u>(lb)</u> |
| 9103                      | 2,186                    | 2,147                    |
| 9104                      | 2,969                    | 2,911                    |
| 9305                      | 2,320                    | 2,280                    |

A 90% survival life for 1 million revolutions is equivalent to 500 hours of life at 33-1/3 rpm, the speed at which most manufacturers rate their bearings in their catalogs. The relationship of life to load has been found by experiment to vary (for ball bearings) as:

$$L_{10} = \left( \frac{C}{P} \right)^{1/3} \text{ in millions of revolutions}$$

where

$P$  = equivalent radial load of combined radial and thrust loads applied (Use  $P_3$  formula for friction)

$$P = 0.9 F_a \cot \beta - 0.1 F_a$$

The life formula converts to hours of life:

$$L_{10} = \frac{(10)^6}{60 \times N} \left( \frac{C}{P} \right)^3 \text{ hr}$$

where  $N$  = rpm

The apparent life for the candidate bearings were calculated (Figures 53, 54, and 55). In a single-row, deep-groove bearing, thrust loads do not seriously effect bearing life until the thrust/radial load ratio exceeds a certain value. (The extension of the loaded zone on the inner race as a function of inner race diameter is described in Reference 4.) In the case at hand, however, the normal operating loads are such that the radial load could almost be ignored and the bearing treated as if it were under thrust load only.

In low-contact angle bearings where the thrust load greatly exceeds the radial load, even a slight change in thrust load or contact angle becomes significant. Under pure thrust load only, the normal load on each ball is equal:

$$P_o = \frac{T}{n \sin \beta_1}$$

where

$T$  = total thrust load

$n$  = number of balls

$\beta_1$  = operating contact angle

If we neglect the effects of mounting and load on the contact angle and assume that  $\beta_1 = \beta_0$  (the initial unmounted contact angle), the effects on life of preload, contact angle, and speed are quickly apparent. The effect of speed on bearing life is, of course, inversely linear, to the point where centrifugal forces on the balls begin to be significant. That is, up to a point, doubling the speed cuts the apparent life in half. Doubling the load, however, has an exponential effect on life, and the life would be reduced by a factor of eight. If the thrust load and the speed remained unchanged, an increase in

- Reference 4. Palmgren, A., "Ball and Roller Bearing Engineering, Third Edition," SKF Industries, 1959



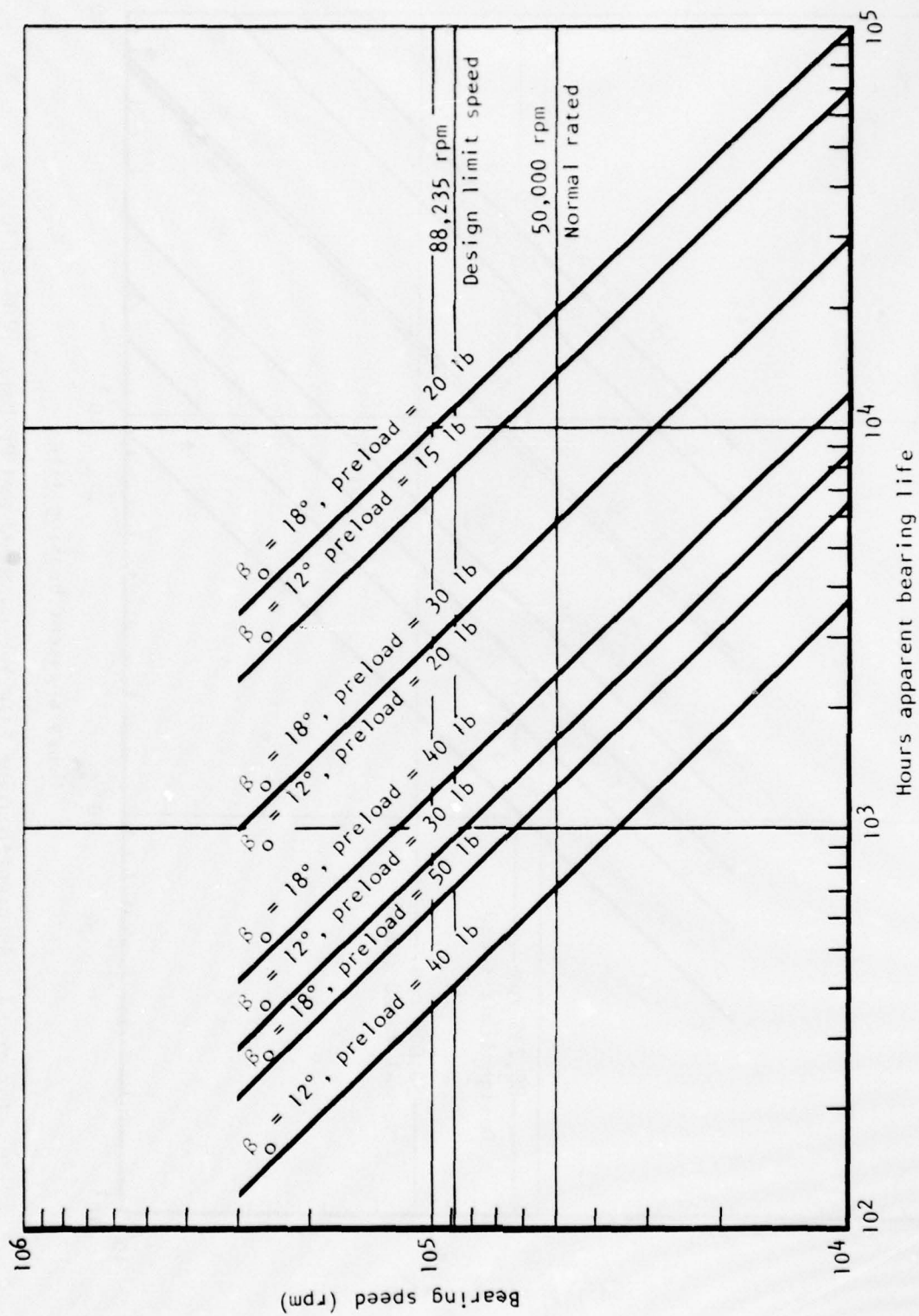


Figure 53. Apparent Bearing Life Versus Speed and Preload, 9103 Duplex

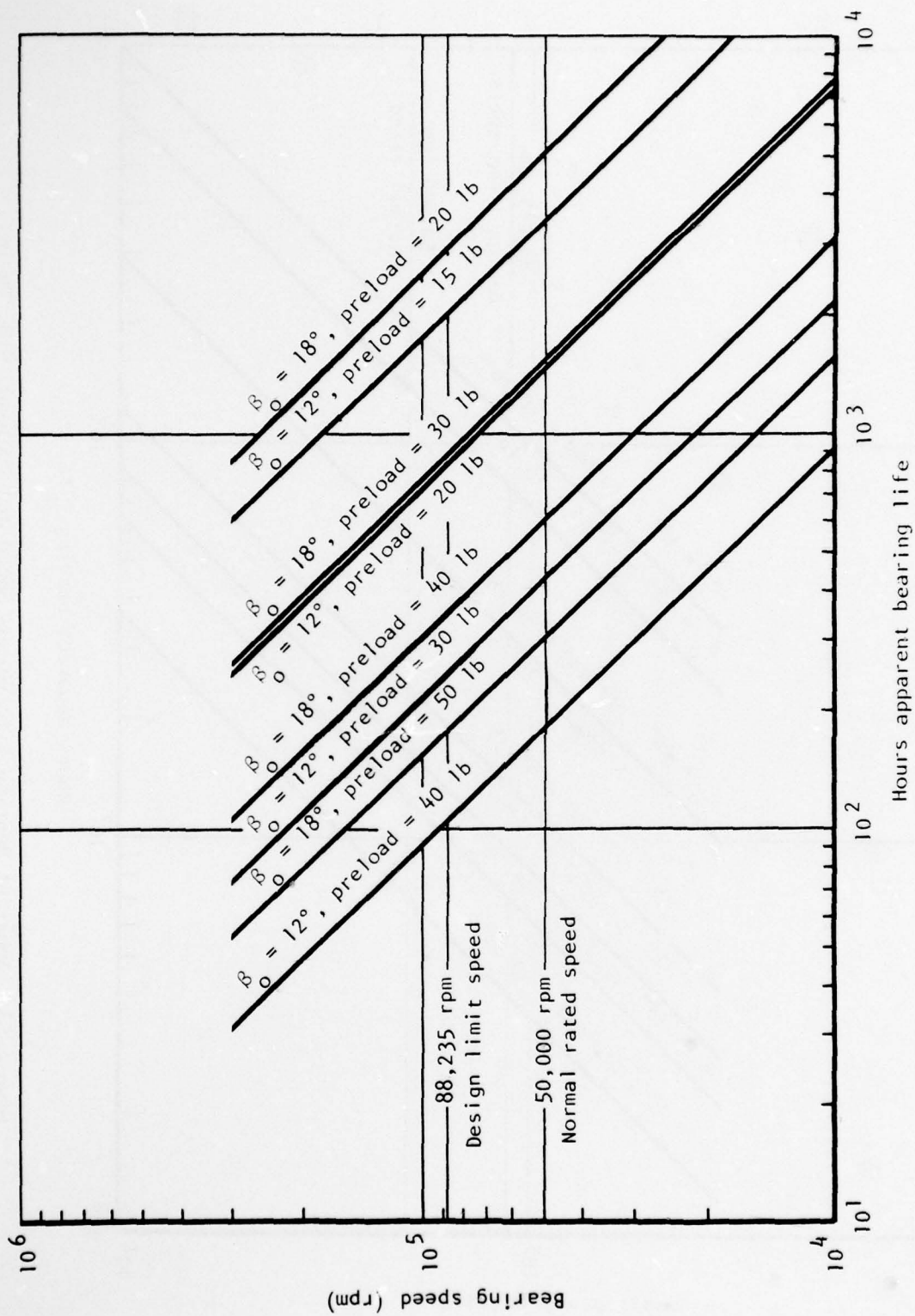


Figure 51. Apparent Bearing Life Versus Speed and Preload, 9104 Duplex

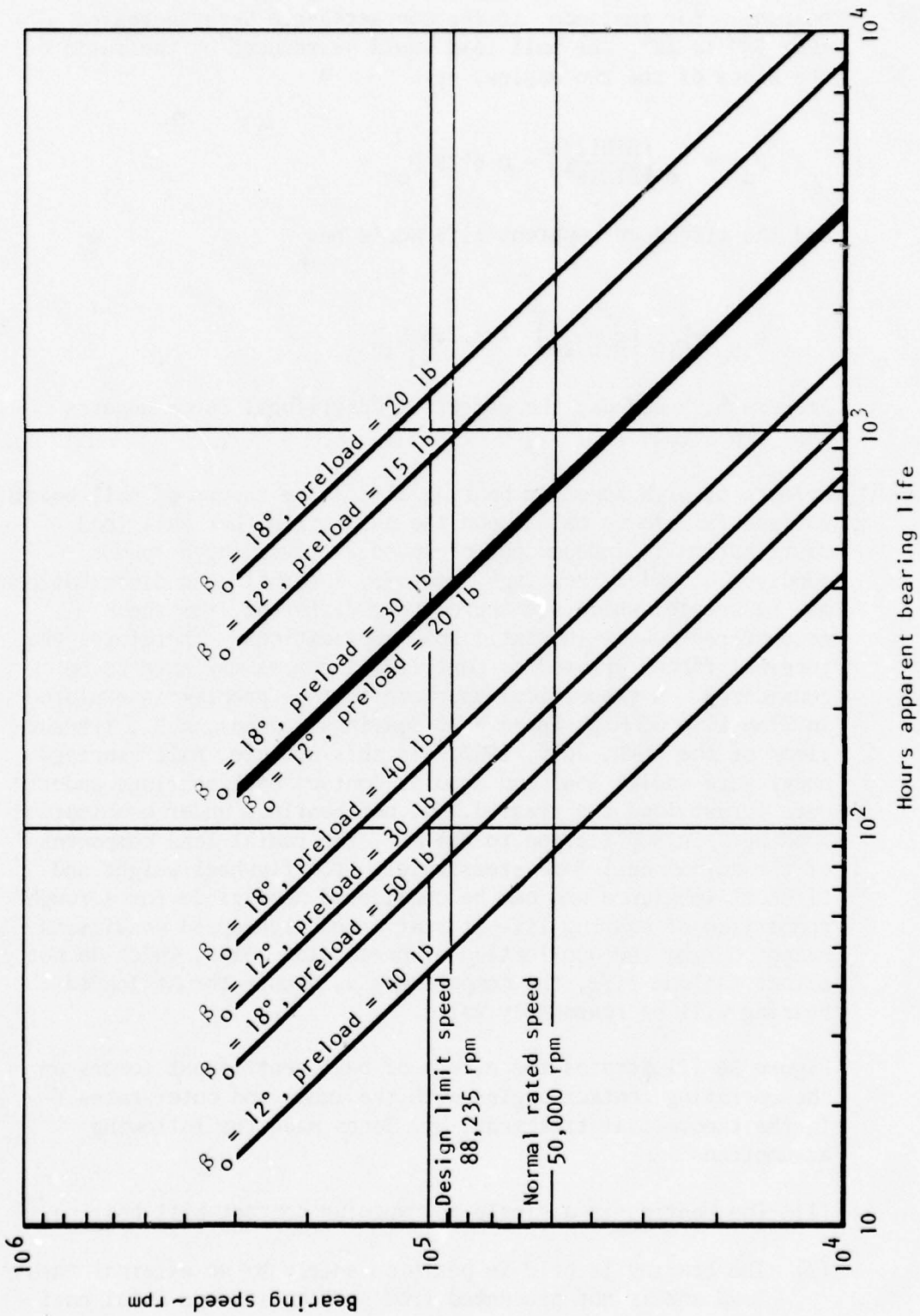


Figure 55. Apparent Bearing Life Versus Speed and Preload, 9305 Duplex



contact angle would actually increase the apparent life of the bearing. For instance, if the contact angle were increased from  $12^\circ$  to  $18^\circ$ , the ball load would be reduced by the ratio of the sines of the two angles, or

$$P_o' = P_o \left( \frac{\sin 12^\circ}{\sin 18^\circ} \right) = 0.6728 P_o$$

and the effect on apparent life would be:

$$L_{10}' = L_{10} \left( \frac{1}{0.6728} \right)^3 = 3.283 L_{10}$$

At very high speeds, the effect of centrifugal force negates this improvement.

- b) Effects of high speed on bearing life - The theory of ball-bearing fatigue failure is based upon the assumption that ball load distribution is independent of speed. At very high speeds required of modern bearings, however, internal load distributions may be created which are appreciably different from those encountered solely in static load applications. Therefore, the internal forces created by centrifugal forces may have to be considered. A theoretical approach to this problem is explored in "The Life of High-Speed Ball Bearings", Jones, A.B., Transactions of the ASME, July, 1952. In this article, ball bearings under pure radial load and angular contact ball bearings under pure thrust load are treated, but not bearings under combination loading. In application to the MPP, the radial load component of the normal ball load stems solely from flywheel weight and flywheel imbalance and can be considered negligible for a rough comparison of bearing life at static and high-speed conditions. Except during the application of precession loads, which do not affect fatigue life, the comparisons as a pure thrust loaded bearing will be reasonably valid.

Figure 56 illustrates the effect of ball centrifugal forces on the operating contact angles with the inner and outer races. In the theoretical treatment, Mr. Jones made the following assumptions:

- (1) The bearing is a single-row angular contact ball bearing.
- (2) The bearing is held in position solely by an external thrust load and is not prevented from seeking its own axial position of equilibrium.

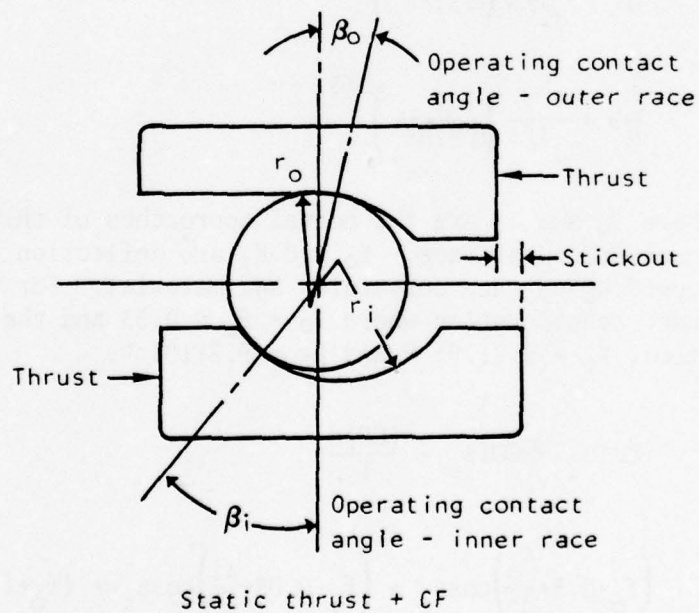
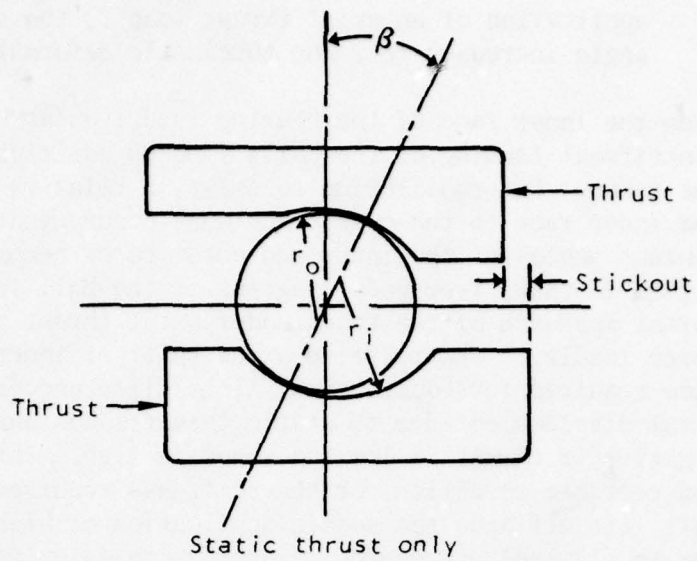


Figure 56. Ball Centrifugal Force Action

- (3) The initial mounted contact angle is  $\beta'$ . After the application of an axial thrust load  $T$ , the static contact angle increases to  $\beta$  due to elastic deformations.

When the inner race of the bearing is driven at high speed, the centrifugal loading of the balls imposes additional forces on the races. For equilibrium to exist, a relative axial shift of the inner race to the outer race must occur, and the operating contact angles of the inner and outer races become different. Figure 57 shows free-body diagrams of the ball loads and the normal approach of the races under axial thrust and centrifugal force loading. The relative axial shift of inner race to outer race required for equilibrium,  $X$ , is different from the normal axial displacement due to static thrust loads and may become negative if thrust is low and speed is high. This may be an unacceptable condition for the stiffness requirement to prevent ball lift-off upon the sudden application of high radial loads due to flywheel precession. In order to calculate the operating contact angles, ball loads, and axial shift, the following equations must be satisfied:

$$\frac{\delta_o}{d} = \frac{K_o}{d^{4/3}} \left( \frac{T}{n \sin \beta_o} \right)^{2/3} \quad (1)$$

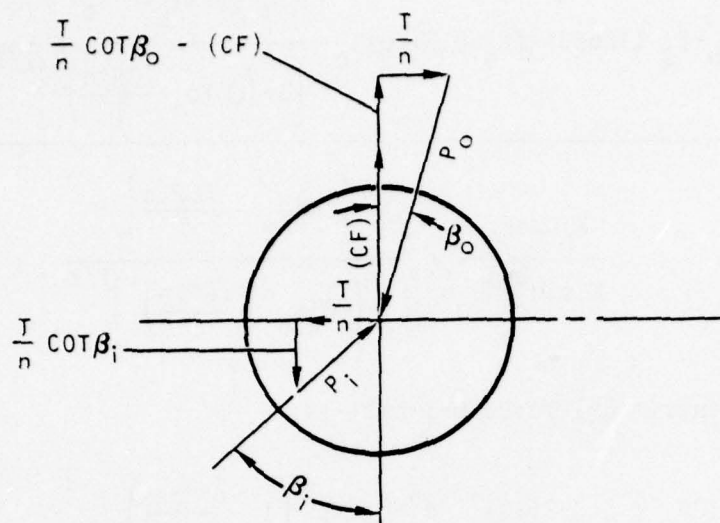
$$\frac{\delta_i}{d} = \frac{K_i}{d^{4/3}} \left( \frac{T}{n \sin \beta_i} \right)^{2/3} \quad (2)$$

where  $\delta_o$  and  $\delta_i$  are the normal approaches of the ball to the inner and outer race.  $K_o$  and  $K_i$  are deflection constants depending on race curvatures and material. For the bearings under consideration where  $f_o = f_L = 0.53$  and the material is steel,  $K_o = 9.2(10)^{-6}$  and  $K_i = 9.5(10)^{-6}$ .

$$\cot \beta_i = \cot \beta_o - \frac{(CF)n}{T} \quad (3)$$

$$\left( f_o - 0.5 + \frac{\delta_o}{d} \right) \cos \beta_o + \left( f_i - 0.05 + \frac{\delta_i}{d} \right) \cos \beta_i = (f_o + f_i - 1) \cos \beta' \quad (4)$$





Ball loads - schematic

Displaced center, inner race curvature, due to CF & thrust loads

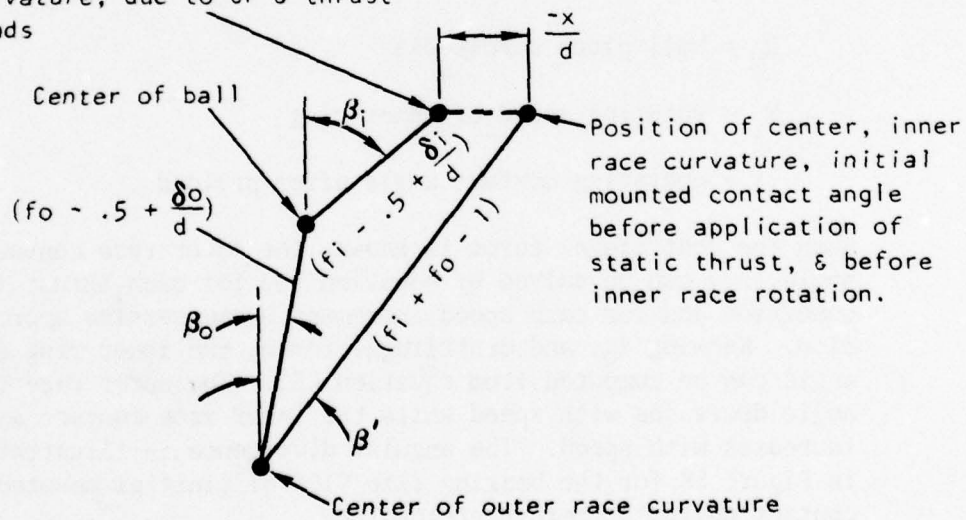


Figure 57. Normal Approach of Race Curvatures

Combining equations (3) and (4) with equations (1) and (2):

$$\frac{T}{nd^2} = \frac{1}{K_i^{3/2}} \left\{ \frac{(f_o + f_2 - 1) \cos \beta_o - (f_o - 0.5) \cos \beta_o - \frac{(f_i - 0.05) \left[ \cot \beta_o - \frac{(CF)n}{T} \right]}{\left[ 1 + \left( \cot \beta_o - \frac{(CF)n}{T} \right)^2 \right]^{1/2}}}{\frac{K_o \cos \beta_o}{K_i \sin^{2/3} \beta_o} + \frac{\left[ \cot \beta_o - \frac{(CF)n}{T} \right]}{\left[ 1 + \left( \cot \beta_o - \frac{(CF)n}{T} \right)^2 \right]^{1/2}}} \right\}^{3/2} \quad (5)$$

The centrifugal force per ball is:

$$(CF) = 5.257 (10)^{-7} d^3 D_m N_i^2 \left( 1 - \frac{d \cos \beta}{D_M} \right)^2$$

where

$d$  = ball dia

$D_M$  = ball pitch circle dia

$N_i$  = rotating speed of inner ring

$\beta$  = operating contact angle after preload

When the centrifugal force is known, the outer race contact angle,  $\beta_o$ , can be solved by equation (5) for each thrust load condition and for each speed increment by successive approximation. Knowing  $\beta_o$ , and centrifugal force, the inner ring contact angle can be computed from equation (3). The outer race contact angle decreases with speed while the inner race contact angle increases with speed. The angular divergence is illustrated in Figure 58 for the bearing size 9103-WI (initial mounted contact angle  $12^\circ$  before preloading).

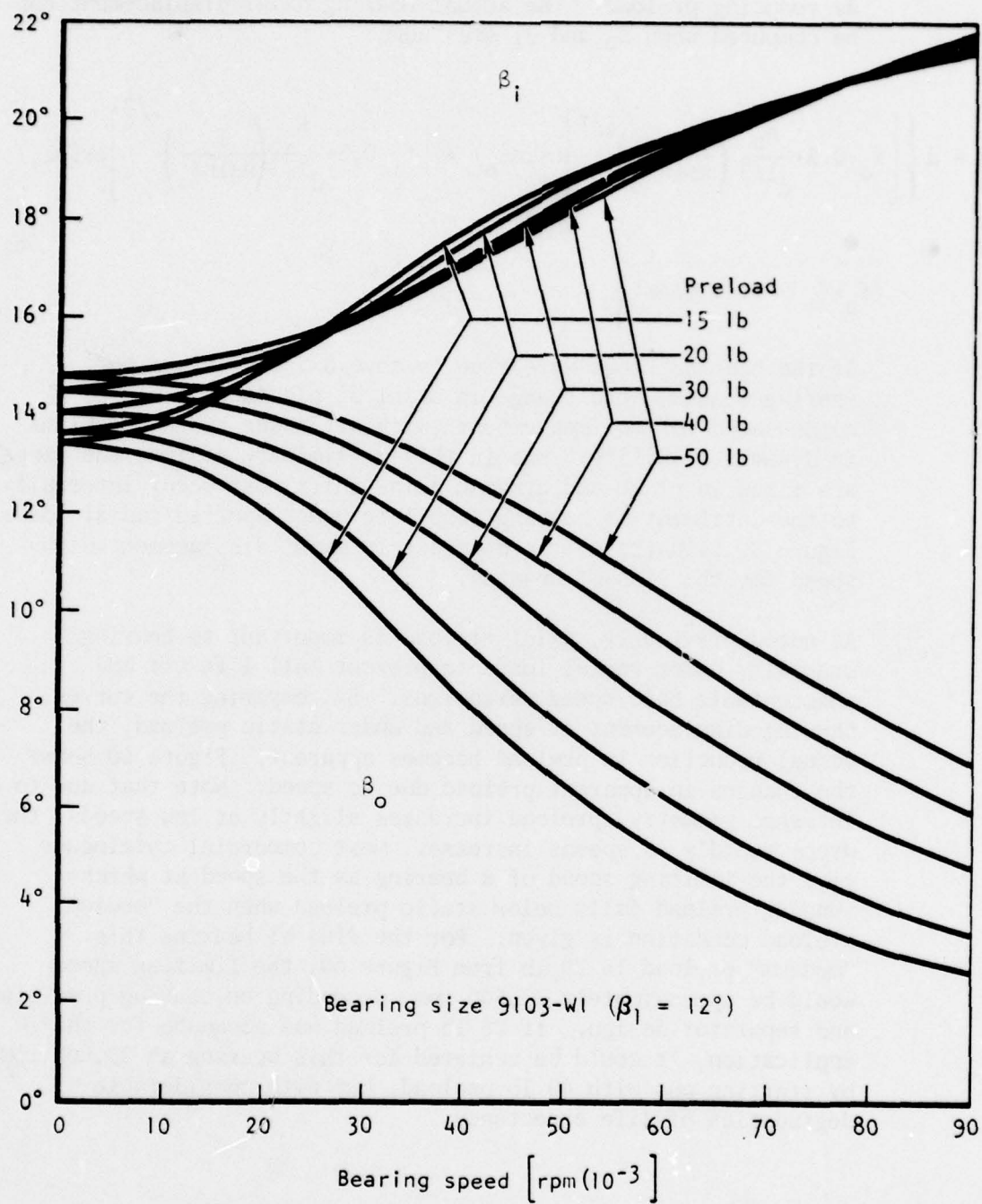


Figure 58. Contact Angle Change Due to Preload and Centrifugal Force



The axial deflections of the bearings under consideration were illustrated previously. However, under dynamic operating conditions, the axial shift reduces with speed with the same effect as reducing preload. The actual bearing axial displacement can be computed when  $\beta_o$  and  $\beta_i$  are known:

$$X = d \left\{ \left[ f_o^{-0.5} + \frac{K_o}{d^{1/3}} \left( \frac{T}{n \sin \beta_o} \right)^{2/3} \right] (\sin \beta_o) + \left[ f_i^{-0.5} + \frac{K_i}{d^{1/3}} \left( \frac{T}{n \sin \beta_i} \right)^{2/3} \right] (\sin \beta_i) - (f_o + f_i - 1.0) \sin \beta' \right\} \quad (6)$$

If the bearing rings were free to move axially in and out (spring-loaded), the change in axial displacement could be compensated for to some extent (with attendant spring problems in dynamic stability), but in this preliminary design, the rings are fixed in place and dynamic axial shift must occur internally to the detriment of bearing stability under applied radial loads. Figure 59 illustrates the decrease in axial displacement with speed for the 9103-WI bearing.

As noted previously, axial preload is important to bearing stability under radial loads to prevent ball lift-off and unacceptable ball speed variations. By comparing the curves showing displacement at speed and under static preload, the actual reduction in preload becomes apparent. Figure 60 shows the changes in apparent preload due to speed. Note that due to internal geometry, preload increases slightly at low speeds; then drops rapidly as speeds increase. Most commercial catalogues give the limiting speed of a bearing as the speed at which running preload falls below static preload when the "medium" preload condition is given. For the 9103 WI bearing this "medium" preload is 20 lb from Figure 60, the limiting speed would be approximately 22,500 rpm, depending on bearing precision and separator design. If 20 lb preload was adequate for the application, it could be achieved for this bearing at 90,000 rpm by starting out with 40 lb preload, but with considerable degradation of life expectancy.

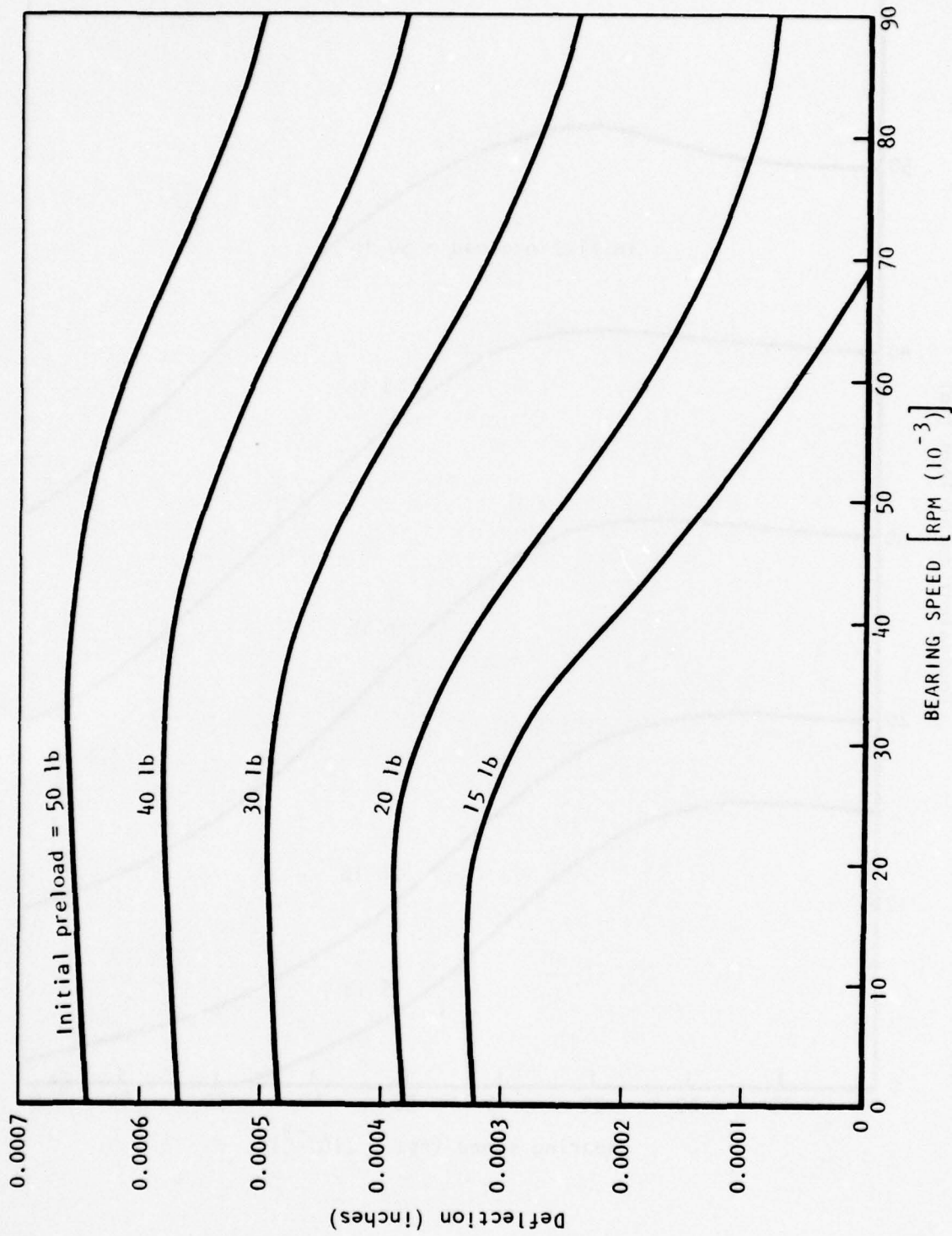


Figure 59. Axial Shift Due to Preload and Centrifugal Force at High Speeds, Bearing Size 9103-W1

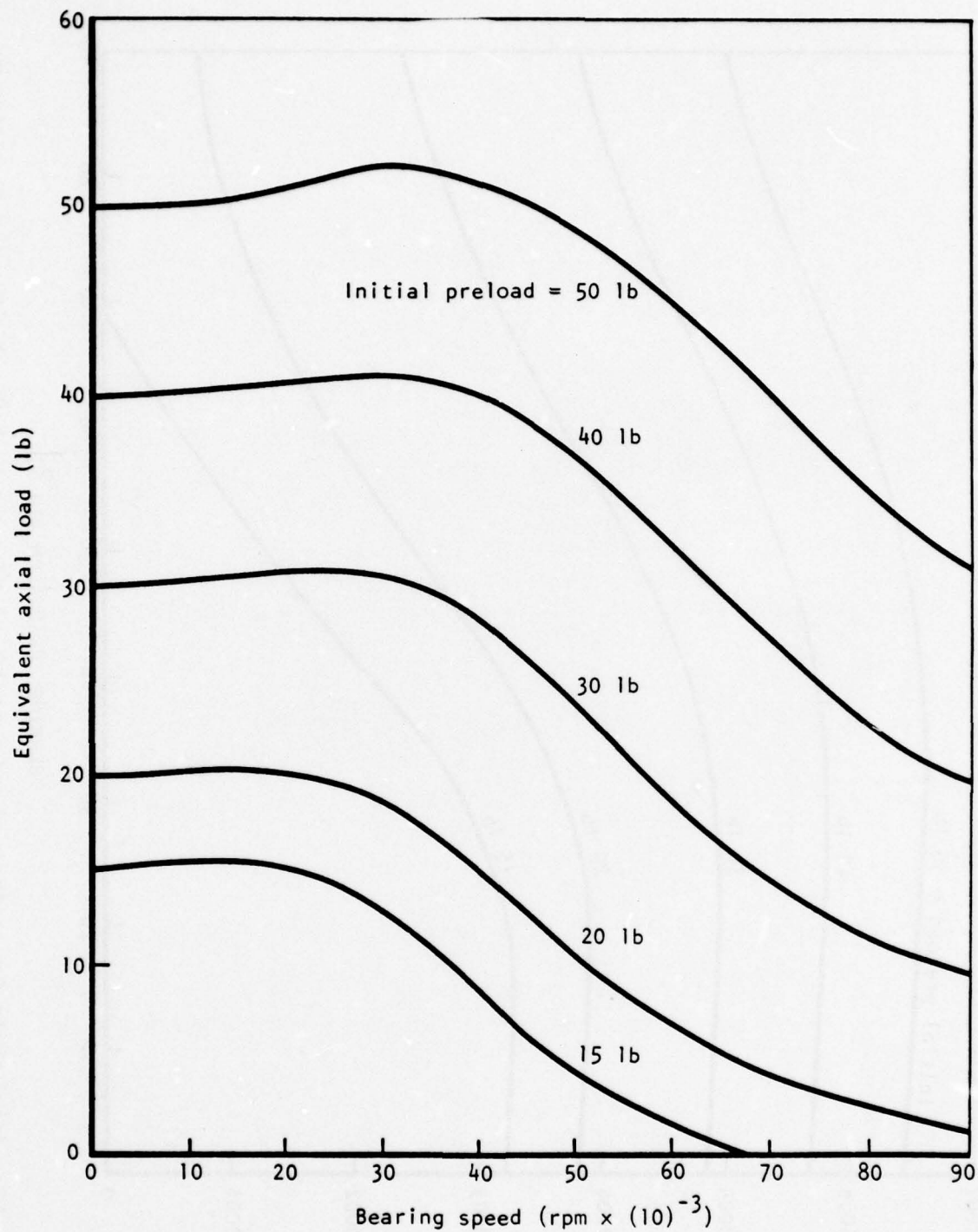


Figure 60. Apparent Decrease in Bearing Preload Due to Centrifugal Force at High Speeds, Bearing Size 9103-WI



Final Bearing Design. After all the analysis was completed, a final ball-bearing design was selected for test. This was a Marlin Rockwell Angular Contact Duplex Bearing No. D5-62688 meeting the specifications shown in Figure 61. This bearing is basically a 9305 (25 mm bore type) in which a special sleeve has been inserted to reduce the bore to 17 mm diameter. The sleeve was inserted to increase the load capacity of the bearing (i.e., the balls and races are large being equivalent to a 25 mm bore bearing) while achieving better speed division between the ball bearing and the hydrodynamic/hydrostatic journal bearing because the journal diameter is small.

The final dimensions of the flywheel stub shafts are as shown in Figure 56. These dimensions determine a number of interrelated performance characteristics which impact the bearing system as follows:

- 1) Distance between support bearings - a major determinant of the magnitude of the precession loads imposed on the bearing and the critical speed characteristics of the rotor system.
- 2) Stub shaft length to the center of the support bearing system and stub shaft diameters - a determinant of shaft deflection under dynamic conditions.
- 3) Journal bearing journal diameter - one of the elements which determines journal bearing clearance and thus hydrostatic/hydrodynamic bearing performance.
- 4) Hydrostatic swirl chamber diameters - a determinant of oil supply pressures at high rotating speed.
- 5) Hydrostatic swirl chamber orifices and porting - a determinant of hydrostatic bearing performance.

During various stages of the flywheels design, the nominal distance between support bearings varied from 5.700 in. to 5.125 in. but finally settled down at 5.566 in. Using this dimension plus the final stub shaft dimensions, the bearing characteristics and the housing spring rate characteristics, a final computerized critical speed analysis was run. The results of this critical speed analysis were quite different than those quoted earlier on page 50. The first critical was determined as lying in a range from 22,000 to 31,000 rpm. The quoting of a range (rather than a specific critical speed) resulted from variations introduced by the hydrostatic/hydrodynamic bearing when it operated at different oil "in" temperatures. The second critical moved outside the area of interest being in a range above 165,000 rpm. This meant that the flywheel would only have to accelerate through one critical speed and that the severity of that critical speed would be very much a function of the hydrostatic/hydrodynamic bearing's characteristics.

ALTERNATE SPECIFICATION A  
(Per -1 only)

Note: Omitted paragraphs are the same as shown in the basic Specification.

- 3.4 **Rings:** Material: S2100 steel per AMS 6444 (cleanliness per AMS 2301), vacuum induction melted, vacuum arc remelted individually forged rings or extruded rod or tube from rebar. H.T. to Rc-60 min. and stabilize in controlled atmosphere furnace at 450-475°F for 4 hours, Rc-58 min. after stabilization. Retained austenite shall not exceed 15% prior to stabilization. Raceway curvature shall be a true radius within .000020. Raceways to a surface roughness of 2AA (burnishing not permitted). Separator guide lands shall be concentric with raceway within .000050 T.I.R.
- 3.5 **Balls:** Material: S2100 steel per AMS 6444 (cleanliness per AMS 2301), vacuum induction melted, vacuum arc remelted, individually forged blanks or extruded tube from rebar. H.T. to Rc-60 min. Retained austenite shall not exceed 12%. Balls shall be spherical within .000010, and diametral deviation between balls shall not exceed .000020. Ball surface roughness 1AA.

ALTERNATE SPECIFICATION B  
(Per -3 only)

Note: Omitted paragraphs are the same as shown in the basic Specification.

- 2.1 **Intended Use:** This bearing is intended for use as a temporary, quickly available substitute for the -1 or -2 bearing to facilitate early testing. This bearing shall conform to the -1 configuration as nearly as possible with a minimum of re-work of an existing bearing.
- 2.6 **Life and Reliability:**  
Desired Life = 200 hours at 99.0% reliability.  
Basic Dynamic Capacity = 1500 lbs. min. ea. bearing row.  
AFPM Std L<sub>10</sub> Life = 500 hours min.

3.0 CONSTRUCTION DETAILS

- It is expected that this bearing will be made by reworking an existing bearing of ABEC-5, ABEC-7 or ABEC-9 precision. Anticipated rework includes:
- To achieve the higher ball/race conformity, new balls (Grade 20) of approximately 38 to 41 smaller diameter will be used, which, in turn, will increase the unmounted contact angle to a value higher than desired.
  - In order to reduce the mounted contact angle to under 15°, it may be necessary to increase the interference fit of the bearing on the sleeve.
  - A new separator may be required since most bearings of this type have inner land-riding separators.

3.1.1 Bearing Class ABEC-5 or better.

- 3.4 **Rings:** Material: SAE 52100, bearing quality (vacuum induction melted), H.T. Rc-60 min. Construction details shall agree with accepted industry standards for extra precision high speed spindle bearings.
- 3.5 **Balls:** Material: SAE 52100 bearing quality steel (vacuum induction melted), H.T. Rc-60 min. Balls shall be AFPM Grade 20 or better. Construction details shall agree with accepted industry standards for extra precision high speed spindle bearings.
- 3.6 **Separator:** Material: AMS 6381 (AISI 4140) aircraft quality steel, H.T. Rc-28 to 36. Silver plate .0010-.0020 all over per AMS-2410. Separator shall be outer land riding. It is preferred that the bearing assemble with some diametral interference and remain assembled during normal handling but this feature may be negated by the reduction in ball size and fit to be waived. Ball pockets shall be radially and axially true within .0010 true position. Ball clearance in pocket shall not exceed .006 before plating (one side face and the outside diameter shall establish the ball pocket centerline). Ball pocket surface roughness 63AA before plating. Critical dimensions apply before plating.

1.0 SCOPE

This document defines the requirements for a bearing. It takes precedence over all other Inc., (RU) Purchase Order.

2.0 REQUIREMENTS

- 2.1 **Intended Use:** This bearing is intended for a small, high speed flywheel. It will be in a clean air, 190°F.
- 2.2 **Environment:** Explosion-proof housing, clean air, 190°F.
- 2.3 **Lubrication:** "Santoprac 30" traction lubricant (viscosity=30 centistokes @ 70°F., 5.8 centistokes @ 190°F.).
- 2.4 **Mounting:** Shaft material, steel bar, ASTM-A5 aluminum bar, 2024T351, QQ-A-200/3.
- 2.5 **Loads and Speeds:** Plane of shaft horizontal.

Shaft: Horizontal  
Thrust Load: Preload plus 2g max. Intermittent in direction.

Radial Load:

Weight of Rotor = 4.1 lbs/avg assay  
Max Imbalance = (.000005 in. g displacement)  
Rotor Inertia = .0229 lb/in<sup>2</sup>/sec<sup>2</sup>  
Max Precession = 210 lbs for 4 sec  
Weighted Mean Load = 7.64 lbs.  
Max C Load = 5.0g design 20.0 g max. ultimate

2.6 Life and Reliability:

Desired Life = 500 hr @ 99.0% reliability  
Basic Dynamic Capacity = 1500 lbs min ea bearing  
AFPM std L<sub>10</sub> Life = 2000 hours min.  
(adjust life rating for material cond.)

3.0 CONSTRUCTION DETAILS

- 3.1 **Tolerances:** Unless otherwise specified.
- 3.1.1 Bearing Class ABEC-7, AFPM std., sect.
- 3.1.2 Drawing Tolerances: .0005-.01. .0005-.001.
- 3.2 **Break Sharp Edges:** .005-.015R, min fillet R=.
- 3.3 **Surface Roughness:** Per ANSI B46.1-1962. 32AA.
- 3.4 **Rings:** Material: M-50 tool steel, vacuum induction melted, individually forged rings or extruded rod or tube from rebar. H.T. to Rc-60 min. and stabilize in controlled atmosphere furnace at 450-475°F for 4 hours, Rc-58 min. after stabilization. Raceway curvature shall be a true radius within .000020. Raceways to a surface roughness of 2AA (burnishing not permitted). Separator guide lands shall be concentric with raceway within .000050 T.I.R.
- 3.5 **Balls:** Material: M-50 tool steel, vacuum induction melted, individually forged blanks or extruded tube from rebar. H.T. to Rc-60 min. and stabilize in controlled atmosphere furnace at 450-475°F for 4 hours, Rc-58 min. after stabilization. Retained austenite shall not exceed 12%. Balls shall be spherical within .000010, and diametral deviation between balls in the same LAA.
- 3.6 **Separator:** CERN 4340 steel, AMS-6429, except of extruded tube H.T. Rc-28/36. Silver plate .0010-.0020 all over per AMS-2410. Separator shall be outer land riding. It is preferred that the bearing assemble with some diametral interference and remain assembled during normal handling but this feature may be negated by the reduction in ball size and fit to be waived. Ball pockets shall be radially and axially true within .0010 true position. Ball clearance in pocket shall not exceed .006 before plating. (one side face and the outside diameter shall establish the ball pocket centerline). Ball pocket surface roughness 63AA before plating. Critical dimensions apply before plating. Separator weight .025 lbs.

4.0 INSPECTION

- 4.1 **Gaging Practices:** Per ANSI B3.4-71. Vendor Inc.
- 4.2 **Surface Defects:** Visible to the naked eye, such as scratches across the lay of normal machining must be removed prior to final inspection. If discovered after final inspection require R.I. and discovered but not corrected are subject to rework cause for rejection.
- 4.3 **Rings:** Shall be 100% magnetic particle inspection. Shall be nitral etch inspected prior to plating or cold forging or coloring not permitted. H.V. 4 hrs. at 550-600°F., max retained austenite 12%.
- 4.4 **Balls:** Shall be 100% fluorescent penetrant inspection. Shall be nitral etch inspected prior to plating or cold forging or coloring not permitted. H.V. 4 hrs. at 550-600°F., max retained austenite 12%.
- 4.5 **Separator:** Shall be 100% fluorescent particle inspection. Shall be nitral etch inspected prior to plating or cold forging or coloring not permitted. H.V. 4 hrs. at 550-600°F., max retained austenite 12%.
- 4.6 **Marking and Identification:** Both inner and outer process marking may be per AS-476, Cl. B. Inner runout of both inner and outer races shall be .0010 true position. Both inner and outer races shall be .0010 true position. Both inner and outer races shall be .0010 true position. Both inner and outer races shall be .0010 true position.
- 4.7 **Cleanliness:** All bearing parts shall be completely clean. All bearing parts shall be completely clean. All bearing parts shall be completely clean.
- 4.8 **Protective Finish:** After assembly, the complete bearing shall be protected with a protective finish.

5.0 PACKAGING, SHIPPING AND STORAGE

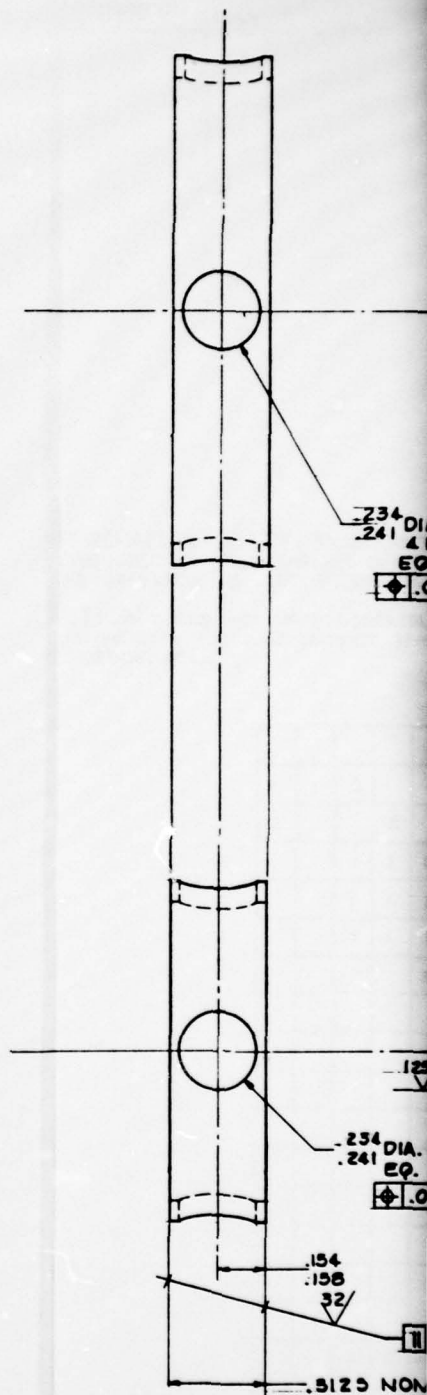
- 5.1 **Packaging:** After preservative treatment the bearing shall be packaged in a suitable plastic container and an outer box suitable for shipping. The shipping container shall protect the bearing from damage.
- 5.2 **Shipping:** The shipping container shall protect the bearing from damage.
- 5.3 **Storage:** Min storage 1114 by. in normal warehouse.

6.0 QUALITY ASSURANCE

Vendor shall submit a copy of vendors final inspection report of all deviations accepted per the above specifications.

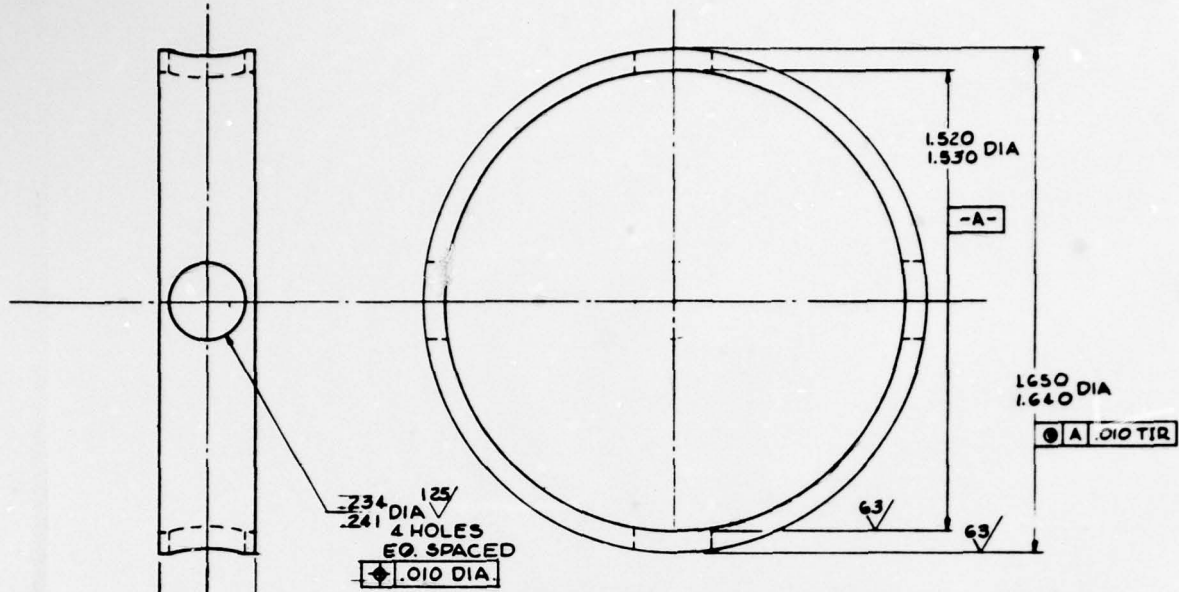
# **SPECIFICATION** (Per -1 only)

- 1.0 SCOPE:**  
This document defines the requirements for an extra-precision, high performance angular contact ball bearing. It takes precedence over all other sources of information except the Rockwell International, Inc., (RI) Purchase Order.
- 2.0 REQUIREMENTS:**
- 2.1 **Intended Use:** This bearing is intended for use as a mounted duplex bearing assembly used to support a small, high speed flywheel. It will be required to accept both radial and thrust loads.
  - 2.2 **Environment:** Explosion-proof housing, closed loop system. Pressure ambient (14 to 16 PSIA), normal clean air, 190°F.
  - 2.3 **Lubrication:** "Santotrac 30" traction lubricant, Monsanto Industrial Chemicals Co., St. Louis, MO. (viscosity 30 centistokes @ 70°F., 3.8 centistokes @ 190°F.) single oil jet for each bearing as shown.
  - 2.4 **Mounting:** Shaft material, steel bar, ASTM-A304, CR 4340H, H.T. 180/200,000 psi, housing material, aluminum bar, 2024T351, QQ-A-200/3.
  - 2.5 **Loads and Speeds:** Plane of shaft horizontal loads: (Per duplex set of bearings).
- Shaft:** Horizontal  
**Thrust Loads:** Preload plus 2g max. Intermittent either direction.
- |   |  |
|---|--|
| <b>Radial Loads:</b>                                      | <b>Speeds:</b>   |
| Weight of Rotor = 4.1 lbs/brg Assy                        | Normal rated mean 55,000 rpm   |
| Max Imbalance = .000005 in. cg displacement               | Normal rated min. 35,000 rpm   |
| Rotor Inertia = .0229 lb/in <sup>2</sup> sec <sup>2</sup> |  |
| Max Precession = 210 lbs for 4 sec                        | Design Limit 88,235 rpm  |
| Weighted Mean Load = 7.84 lbs.                            | Ultimate Limit 91,000 rpm  |
| Max G Load = 5.0g design 20.0 g max. ultimate             | Operation at limit speed for 5 min. or longer shall be cause for removal, disassembly and complete inspection. |
- 2.6 Life and Reliability:**  
Desired Life = 500 hr @ 99.99 reliability  
Basic Dynamic Capacity = 1500 lbs min as bearing row  
AFPM and L<sub>10</sub> Life = 2000 hours min.  
(adjust life rating for material cond.)
- 3.0 CONSTRUCTION DETAILS:**
- 3.1 **Tolerances:** Unless otherwise specified.
    - 3.1.1 Bearing Class ABC-7, AFPM std., sect. 4
    - 3.1.2 Drawing Tolerances, .XX=.01, .XXX=.001, angles = °2
  - 3.2 **Break Sharp Edges:** .005-.01SR, min fillet R=.020
  - 3.3 **Surface Roughness:** Per ANSI B46.1-1962. 32AA all over except as noted.
  - 3.4 **Rings:** Material, M-50 tool steel, vacuum induction melted, vacuum arc remelted, AMS-6490 (cleanliness per AMS-2301) individually forged rings or extruded rod or tube from re-forming bar. H.T. R-60 min. stabilize in controlled atmosphere furnace 4 hrs. at 550-600°F max, retained austenite 3%. Raceway curvature shall be a true radius within .000020. Raceways to a surface roughness of 2AA. (turnishing not permitted). Separator guide lands shall be concentric with raceway within .000050 T.I.R.
  - 3.5 **Balls:** Material: M-50 tool steel, vacuum induction melted, vacuum arc remelted, AMS-6490 (cleanliness per AMS-2301), made from individually forged blanks or extruded rod from re-forming bar (secondary cold forging or coining not permitted). H.T.R-60 min. stabilize in controlled atmosphere furnace 4 hrs. at 550-600°F max, retained austenite 3%. Balls shall be spherical within .000010 T.I.R., max diametral deviation between balls in the same bearing not to exceed .000020. Ball surface roughness 2AA.
  - 3.6 **Separator:** CDM 4340 steel, AMS-6429, except cleanliness per AMS-2301. Machine from re-formed bar or extruded tube M.T. R-28/36. Silver plate .0010-.0020 all over per AMS-2410. Separator to be outer land-riding. Inner Ring shall assemble with a min .001 diametral interference (snap) of counterbore. Slight (visible) brinelling marks are permitted on counterbore and inner ring raceway. Entire bearing shall remain assembled during normal handling and installation procedures. Ball pockets shall be radially and axially true within .0010 true position. Ball clearance in pocket shall not exceed .006 before plating. (one side face and the outside diameter shall establish the ball pocket centerline). Ball pocket surface roughness 63AA before plating. Critical dimensions apply before plating. Max separator weight .025 lbs.
- 4.0 INSPECTION**
- 4.1 **Guiding Practices:** Per ANSI B3.4-71. Vendor inspection procedure to be approved by Rockwell International, Inc.
  - 4.2 **Surface Defects:** Visible to the naked eye, such as dents, nicks, burrs, flashes, slivers, scabs or scratches across the lay of normal machining marks are not acceptable. These may be removed by usual machining methods prior to final inspection provided that detail tolerances are not exceeded. Defects discovered after final inspection require R.I. approval prior to taking corrective action. Defects discovered but not corrected are subject to review by RI except that burns discovered by Nitral etch are cause for rejection.
  - 4.3 **Ring:** Shall be 100% magnetic particle inspected per MIL-I-6849C, and raceways and separator guide lands shall be nitral etch inspected prior to plating or other application of protective finish.
  - 4.4 **Balls:** Shall be 100% fluorescent penetrant inspected and 100% nitral etch inspected.
  - 4.5 **Separator:** Shall be 100% fluorescent particle inspected prior to plating.
  - 4.6 **Corrosion:** Evidence of corrosion or etching is cause for rejection.
  - 4.7 **Marking and Identification:** Both inner and outer rings shall be identified per AS-478, method 3B (in-process marking may be per AS-478, Cl. B). Impression stamping is not permitted. The high side of radial runout of both inner and outer races shall be indicated by a red enamel dot .030-.040 dia. (in etched dimple) within 10° of true radial position. Sequential serialization begins with 0001 per bearing. Rockwell International and vendor markings shall appear as shown on face of drawing.
  - 4.8 **Cleanliness:** All bearing parts shall be completely degreased, chemically clean, and treated with finger print remover per MIL-C-15074C.
  - 4.9 **Protective Finish:** After assembly, the complete bearing shall be treated with preservative compound as per MIL-C-16113(2)GR.3.
- 5.0 PACKAGING, SHIPPING AND STORAGE**
- 5.1 **Packaging:** After preservative treatment the bearing shall be individually packaged in an air-tight re-sealable plastic container and an outer box suitable for flat storage. The outer box shall be capable of withstanding a 5g drop without bearing damage.
  - 5.2 **Shipping:** The shipping container shall protect the bearing(s) from a 20g shock load from any direction and be suitably marked for shipping fragile, precision items. Shipping temperatures -50-150°F.
  - 5.3 **Storage:** Min storage life 1yr. in normal warehouse environment, 0° to 130°F.
- 6.0 QUALITY ASSURANCE**  
Vendor shall submit a copy of vendors final inspection report including material certification and a record of all deviations accepted per the above specification with each bearing.

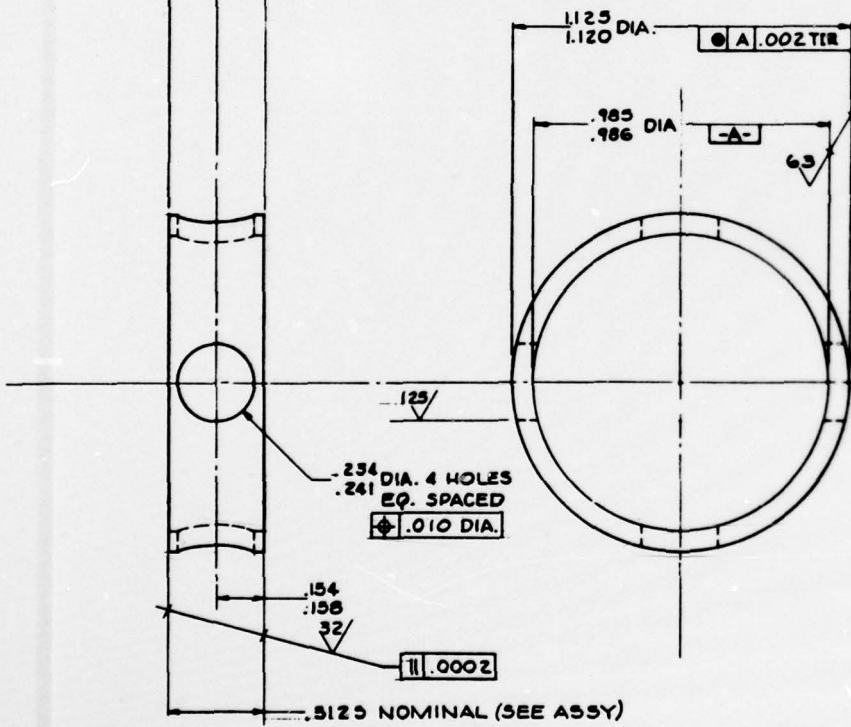


DETA





DETAIL-14



DETAIL-13

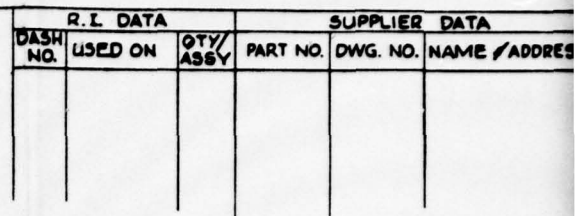
-A-

.9847  
.9845

2 REQ'D

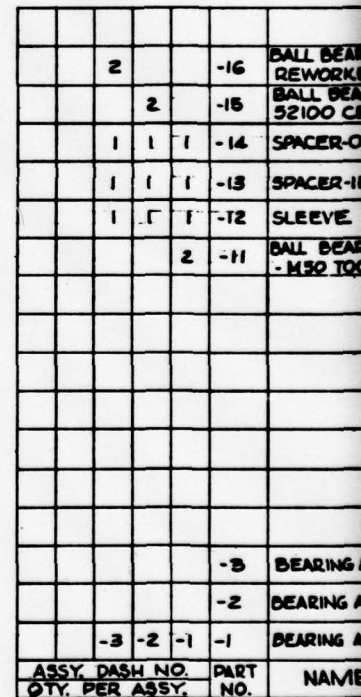
.620 R  
.600 R  
OIL JET  
IMPINGEMENT

16.37  
16.95 BRG. O.D.



INTERCHANGEABILITY: THIS ASSEMBLY IS A MATCH  
REQUIRED OF ASSEMBLIES ONLY. INTERCHANGEABLE  
ASSEMBLIES IS NOT REQUIRED.

**CAUTION: THIS BEARING ASSEMBLY SHALL NOT BE  
MAINTAINED BY THE AUTHORITY OF AND UNDER THE SUPERVISION  
OF PERSONNEL.**



|               |               |
|---------------|---------------|
| SCALE:<br>4/1 | DR. O.W. ROSS |
|               | DATE 12/10/76 |
|               | MODEL         |

BEARING ASSY  
SPECIFICATION

Figure 61. Flywheel Bearing Assy





Throughout the design phase, every effort was made to increase the diameter and shorten the length of the stub shaft to make it a stiffer cantilever beam. The deflection of the flywheel at speed is a function of support bearing spacing and stub shaft flexibility (the flywheel disc is considered infinitely stiff). As discussed earlier and illustrated in Figure 35, the displacement ( $e_3$ ) which results from stub shaft deflection is initiated by and directly additive to the initial flywheel imbalance displacement. The summed displacement which results and the associated loads increase by the square of the speed. Therefore, stiffening the stub shafts was considered extremely important. However, because the seal must be between the flywheel disc and the bearing to allow maintenance of a vacuum around the disk, any significant reduction of stub shaft length, below that shown in Figure 36, would start to encroach on minimum seal package lengths (ferro-fluid or carbon-face seal). Also any significant increase in shaft diameter would increase both seal and bearing losses accordingly. It was felt that, in the face of the imponderables surrounding hybrid-bearing and ferro-fluid seal performance, the dimensions shown in Figure 36 represented the best compromise.

Hydrodynamic Bearing Design. The journal bearing diameter was originally 0.6875 ( $\pm 0.0002$ ) inch. (See Figure 36.) This was later increased to 0.6885 ( $\pm 0.0002$ ) inch by silver plating. At this latter dimension, the diametral clearance between the journal surface and the bearing sleeve bore was 0.0015 ( $\pm 0.0003$ ) inch. This meant that the nominal radial clearance ( $c$ ), commonly used in journal-bearing calculations, was 0.00075 inch. A friction torque versus speed plot (Figure 62) and a friction horsepower versus speed plot (Figure 63) were prepared for this journal bearing showing the effects of various radial clearances ( $c$ ). The assumptions and formulae used in preparing these plots are as follows.

For hydrodynamic bearing friction power loss horsepower ( $HP_F$ ), if the shaft were perfectly smooth and running concentrically in a smooth journal, the fluid friction ( $F$ ) may be expressed as:

$$F = \frac{\mu \pi^2 R^2 L N}{15C}$$

where

$\mu$  = coefficient of viscosity (Reyns)

$R$  = shaft radius (inches)

$L$  = length of bearing (inches)

$C$  = radial clearance (inches)

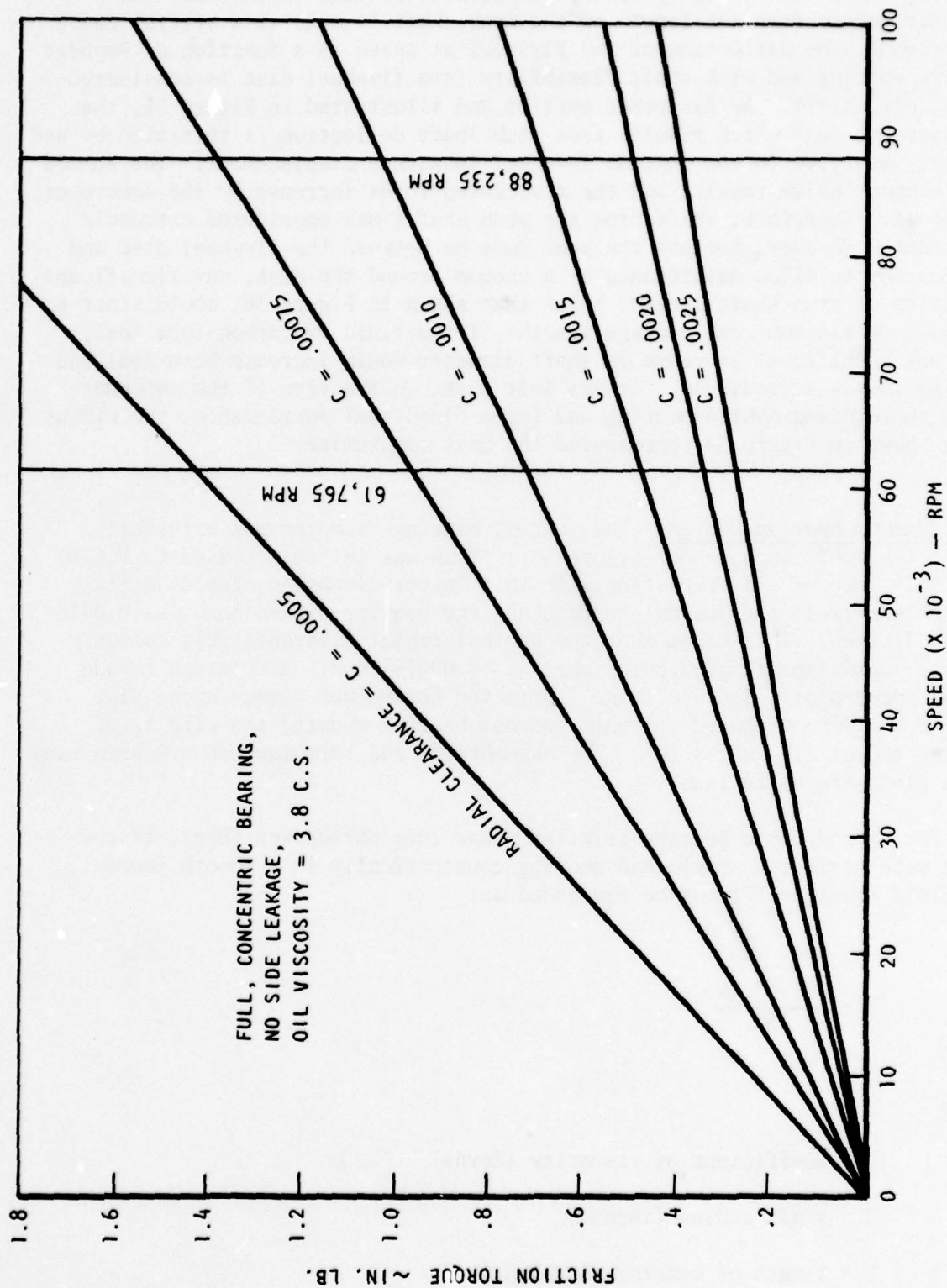


Figure 62. Friction Torque Versus Radial Clearance

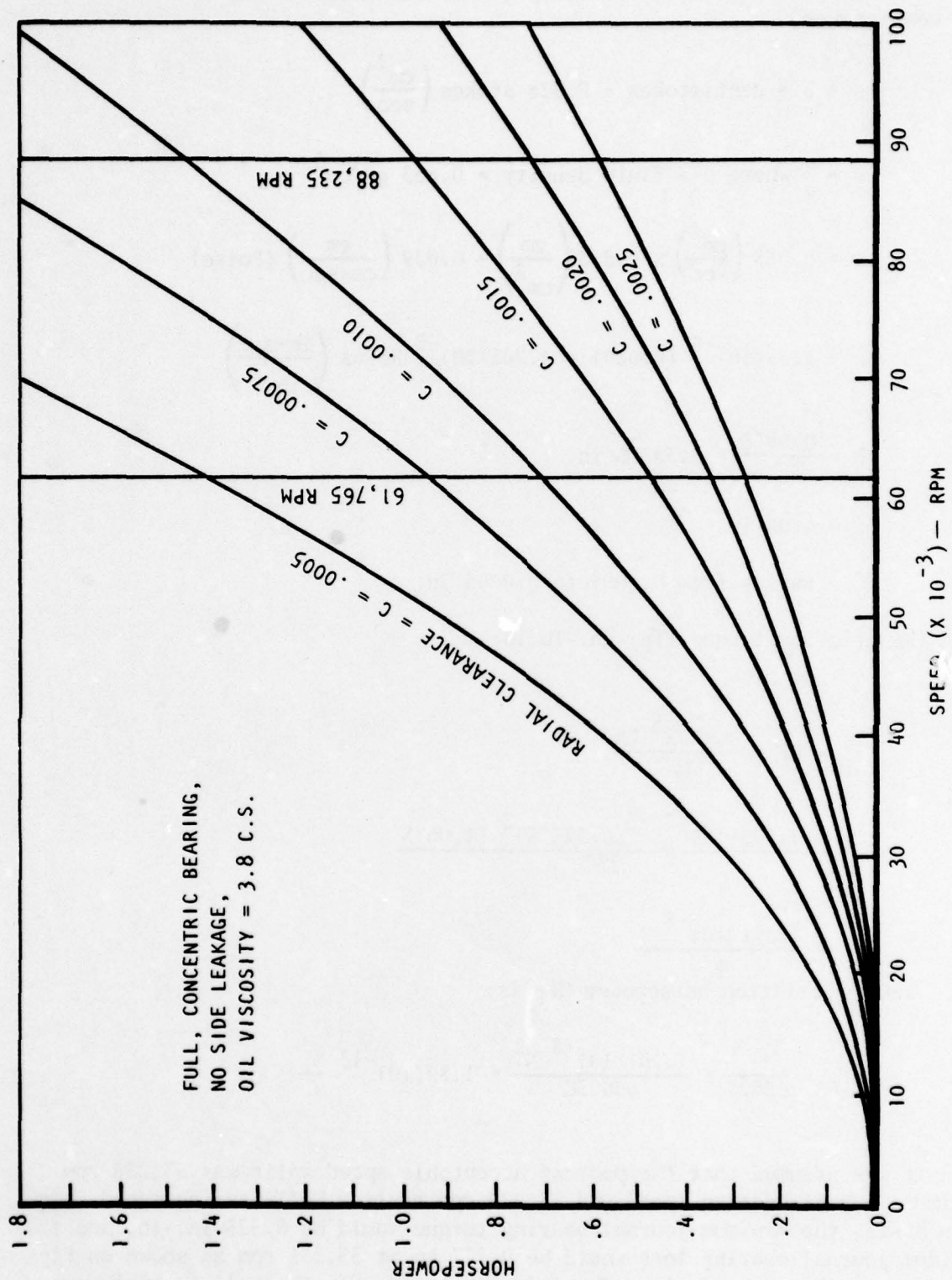


Figure 63. Friction Horsepower Versus Radial Clearance



The measured kinematic viscosity ( $\nu$ ) of Santotrac 30 oil is 3.8 centistokes.

$$\nu = 3.8 \text{ centistokes} = 0.038 \text{ stokes} \left( \frac{\text{cm}^2}{\text{sec}} \right)$$

$$\nu = \frac{\mu}{\rho} \text{ where } \rho = \text{fluid density} = 0.855 \text{ gm/cm}^3$$

$$\mu = 0.038 \left( \frac{\text{cm}^2}{\text{sec}} \right) \times 0.855 \left( \frac{\text{gm}}{\text{cm}^3} \right) = 0.029 \left( \frac{\text{gm}}{\text{cm-sec}} \right) \text{ (Poise)}$$

$$\mu = 1.45(10)^{-5} (0.029) = 4.205(10)^{-7} \text{ Reyns} \left( \frac{\text{lb-sec}}{\text{in.}^2} \right)$$

$$R = \frac{0.6875}{2} = 0.34375 \text{ in.}$$

$$L = 1.06 \text{ in.}$$

$$C \text{ varies from } 0.0005 \text{ to } 0.0005 \text{ in.}$$

The friction torque ( $T_F$ ) in.-lb is:

$$\begin{aligned} T_F = RF &= \frac{\mu \pi^2 R^3 LN}{15C} \\ &= \frac{4.205(10)^{-7} \pi^2 (0.34375)^3 (1.06)N}{15C} \\ &= \frac{1.191(10)^{-8} N}{C} \end{aligned}$$

And the friction horsepower  $HP_F$  is:

$$HP_F = \frac{T_F N}{63025} = \frac{1.191(10)^{-8} N^2}{63025C} = 1.89(10)^{-15} \frac{N^2}{C}$$

It was assumed that the poorest acceptable speed split was 33,235 rpm minimum journal-bearing speed and 55,000 rpm maximum ball-bearing speed. On this basis, the minimum journal-bearing torque would be 0.525 in.-lb, and the minimum journal-bearing loss would be 0.277 hp at 33,235 rpm as shown on Figures 62 and 63 respectively. The friction torque for the ball bearing, as

taken from Figure 48, is only 0.255 in.-lb, however, and shows that there is not a torque balance between the journal bearing and the ball bearing. To run in a speed split condition the torques of the ball and journal bearings must be equal. Moving down the  $C = 0.00075$  curve (Figure 62) and up the 40 lb preload 9305 bearing-type curve of Figure 48, it will be found that torque balance occurs at 0.294 in.-lb, which is equivalent to 70,000 rpm ball-bearing speed and 18,235 rpm journal-bearing speed. The situation could be improved by going to larger clearances. For example, using Figures 48 and 62, if the clearances are increased to 0.001, the speed split will be at 66,500 rpm ball-bearing speed and 21,735 rpm journal-bearing speed. The losses and other characteristics associated with these clearances and with three larger ones are:

| <u>Radial<br/>clearance<br/>(C)(in.)</u> | <u>Ball<br/>bearing<br/>speed (rpm)</u> | <u>Journal<br/>bearing<br/>speed (rpm)</u> | <u>Loss<br/>torque<br/>(T<sub>F</sub>)(in.-lb)</u> | <u>Loss<br/>power<br/>(H<sub>F</sub>)(hp)</u> |
|--|---|--|--|---|
| 0.00075                                  | 70,000                                  | 18,235                                     | 0.294  | 0.412   |
| .0010                                    | 66,500                                  | 21,735                                     | .284   | .398  |
| .0015                                    | 55,000                                  | 33,235                                     | .255   | .357  |
| .0020                                    | 44,500                                  | 43,735                                     | .222   | .311  |
| .0025                                    | 40,000                                  | 48,235                                     | .208   | .291  |

From the tabulation, it is apparent that losses decrease as the journal bearing share of the speed split becomes larger and that if bearing friction losses had been the only consideration, very large clearances would have been indicated.

However, there are other conditions that limit the clearance to not much over 0.0015. It will be noted that Figures 62 and 63 (journal-bearing torques and losses) were based on the assumption of a full concentric bearing operating with no side leakage. A hydrodynamic journal bearing operating concentrically is inherently unstable and is critically sensitive to destructive half frequency whirl. The only justification for the assumption of concentric operation was the further assumption that the hydrostatic features of the bearing would cause it to operate very nearly in this condition during high-speed operation.

A properly designed hydrostatic bearing is stable when operating concentrically, and with the light loads (4 to 8 lb) which will be encountered during most of its life, it should operate very nearly concentrically. However, if diametral clearance exceeds 0.003 ( $C = 0.0015$ ), the losses associated with pumping the large amounts of fluid necessary to maintain its effectivity as a hydrostatic bearing would become excessive. Therefore, clearances (C) greater than 0.0015 were not seriously considered.

Data from a bearing test on another program being conducted at Rockwell indicated that a similar set of bearings, to the ones being designed for this program, with a nominal clearance of  $C = 0.00125$  had a speed splitting characteristic directly opposite to that which would be predicted by computations. At 44,000 rpm, the journal bearing turned 34,500 rpm while the ball bearing turned at 9500 rpm. Some of this was undoubtedly due to the fact that the ball bearing may have been overlubricated (jet lubricated, rather than mist lubricated, in the interests of cooling), but some was also due to the journal bearing being more efficient than predicted.

In view of this data, plus a desire to avoid journal-bearing stability problems during initial testing, a design clearance of 0.0075 in. was used. It was felt that if excessive ball-bearing speeds were encountered, this clearance could be opened up until instabilities appeared much more easily than working in the other direction.

Hydrostatic Bearing Design. The significant shaft dimensions involved in hydrostatic bearing performance are shown in Figure 36. Other pertinent data are:

- 1) Bearing effective length ( $L$ ) = 1.06 in.
- 2) Radial clearance ( $C$ ) = 0.00075.

The effective fluid pressure which will be generated as a result of centrifugal force was determined for two conditions:

- 1) At inlet to orifice - This determined the pressure available to drive fluid through the orifice when the downstream pressure was low and the orifice was effectively metering.
- 2) At inner surface of ball bearing sleeve - This condition exists at the closest approach of the journal surface to the inner surface of the ball bearing sleeve in the load zone when the leakage out the end of the bearing is less than the flow rating of the orifice (i.e., the orifice is not metering), allowing the pressure generated at the bearing surface to exceed that at the inlet to the orifice.

The fluid pressure determination for condition 1 is as follows:

$$R_o = \text{outer radius of cavity}$$

$$= 0.438/2 = 0.219 \text{ in.}$$



$R_i$  = inner radius of cavity

$$= 0.281/2 = 0.141 \text{ in.}$$

$P_{CF}$  = centrifugally induced pressure (psi) at  $R_o$

$$= 2.840(10)^{-5} WRN^2$$

where

$W$  = weight of oil (lb)

$$= \pi \rho \ell (R_o^2 - R_i^2)$$

and

$\rho$  = oil density =  $0.03082 \text{ lb/in.}^2$  at  $200^\circ \text{ F}$

$\ell$  = length = unity

$$W = \pi (0.03082) (1) (R_o^2 - R_i^2) = 0.09682 (R_o^2 - R_i^2)$$

$R$  = mean effective radius (in.)

$$\cong 2/3 (R_o - R_i) + R_i$$

$N$  = speed (rpm)

Therefore

$$\begin{aligned} P_{CF} &= 2.840(10)^{-5} \left[ 0.09682 (R_o^2 - R_i^2) \right] \left[ 2/3 (R_o - R_i) + R_i \right] N^2 \\ &= 1.491(10)^{-8} N^2 \end{aligned}$$

For condition 2, everything is the same except  $R_o$  = outer R. of shaft  
 $= 0.688/2 = 0.344 \text{ in.}$  Therefore

$$P_{CF} = 7.481(10)^{-8} N^2$$

Data for the two conditions tabulate as follows:

| <u>Shaft<br/>speed (rpm)</u> | <u>PCF - effective pressure (psi)</u> |                                 |
|------------------------------|---------------------------------------|---------------------------------|
|                              | <u>Orifice<br/>metering</u>           | <u>Orifice not<br/>metering</u> |
| 88,235                       | 116.00                                | 582.42                          |
| 61,765                       | 56.84                                 | 285.39                          |
| * { 31,000                   | 14.31                                 | 71.89                           |
| 22,000                       | 7.21                                  | 36.21                           |

There are three metering orifices creating three pads whose effective projected area and maximum restoring force at 88,235 rpm was determined based on the following:

$R_o = 0.344 \text{ in.} = \text{projected width (chord of } 120^\circ \text{ segment) of projected area}$

$L = 1.06 \text{ in.} = \text{length of projected area}$

$A_p = 1.06 \times 0.344 = 0.365 \text{ in.}^2 \text{ projected area}$

$P_E = \text{average effective pressure in pad projected area}$

$$\cong 0.6 \times P_{CF} = 0.6 \times 582.42 = 349.45$$

from which maximum restoring force ( $F_R$ ) is

$$F_R = A_p \times P_E$$

$$= 0.365 \times 349.45 = 127.55 \text{ lb}$$

It will be noted that this restoring force was more than adequate to handle the 9.07-pound rotating load (Figure 40) (exceeded the rotating load by a factor of 14.06) and, with a slight assist (2.5 pounds) from the bearing acting hydrodynamically, could handle the maximum roll-induced precession load shown in Table 3. This indicated that the shaft should tend to run very close

\*Critical speed range

to centered in the journal bearings for most operating conditions and that the assumptions made, when computing the speed splitting losses, appear valid.

Flywheel Seal Design. The flywheel must operate in a nearly perfect vacuum. To illustrate the reason for this statement, if a flywheel of the size and speed used in this program were operated in an atmosphere air environment, the power needed to drive it would be nearly 23 hp (three times the power available for driving the whole MPP). There were two possible approaches to meeting this requirement. The first approach was to have the flywheel support bearings operating in the vacuum environment. This would have the dual advantage of:

- 1) Making it possible to move the bearings close to the flywheel (no space needed between the bearings and the flywheel disk for seals), thus moving the first critical speed above the flywheel operating speed because of the shortening and stiffening of the flywheel stub shafts.
- 2) Requiring only a single small diameter and, hence, low loss seal at the flywheel input.

However, the primary disadvantage was the pumping losses involved in trying to scavenge the lube and cooling oil required for the two bearings and simultaneously maintaining the required vacuum. Trying to pump approximately one-half gpm of oil at a 14 psi  $\Delta P$  with a 1/100 atmosphere inlet pressure would call for large lines, a large pump, and large losses. The second approach was to use two seals, one on each side next to the flywheel disk, thus allowing the bearings to operate at ambient pressure. This was the approach taken. It was implemented using ferro fluid seals because these offered the possibility of hermetically sealing the flywheel housing.

A typical ferro fluid seal is shown in Figure 64. The secret of the ferro fluid seal lies in the use of a ferro magnetic fluid in a magnetic field which has been focused (locally intensified) by a thread-shaped ridge in the flux path.

The ferro fluid itself can be nearly any liquid in which is suspended colloidal (100 angstroms) magnetic particles. Because the particles are so small, thermal molecular agitation (Brownian motion) keeps them from settling or coalescing, as iron filings typically do in a magnetic field. To further assist in keeping the particles in suspension, they are coated with a dispersing agent which keeps them from sticking together. The result is a homogeneous fluid that, unlike such magnetic fluids as those used in clutches, maintain their fluid characteristics under all conditions.



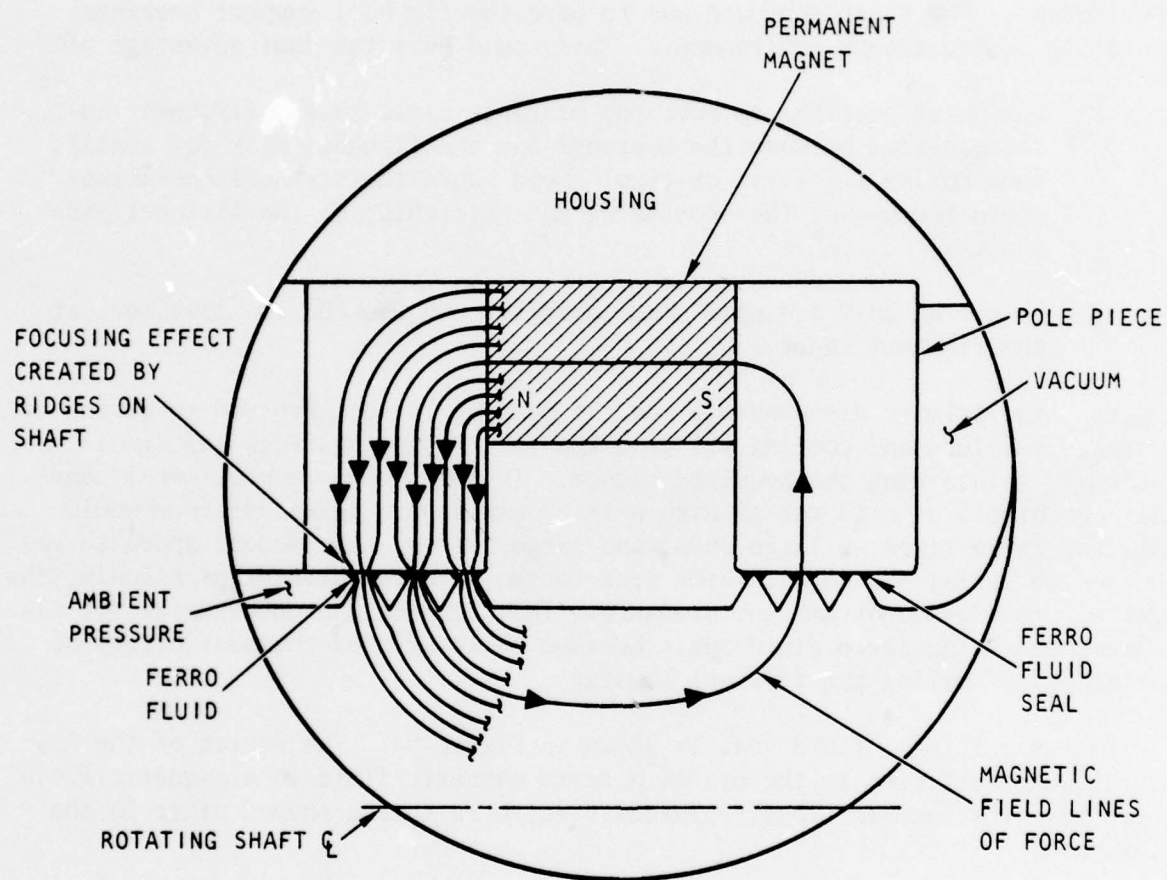


Figure 64. Ferro Fluid Seal

A diester such as MIL-L-7808 or a silicate ester such as M2V makes an excellent ferro fluid. When such a fluid is subjected to a focused magnetic field, the magnetic particles move closer together (i.e., the mean free path of the Brownian movement is reduced), but do not coalesce. In the process, the fluid is trapped (surface tension effects plus the laws governing colloidal suspensions ensure the trapping), and its internal pressure is increased. This causes a modest increase in viscosity, but the other properties of the fluid remain unchanged.

Figure 64 shows the magnetic flux path created by the magnets used in the sealing system and the thread-like ridges which focus the field. At the crest of each ridge, a small amount of ferro fluid is trapped to create a nearly permanent hermetic seal up to a specific differential pressure.

With the type of magnet used for this program (Alnico VIII), it was believed that differential pressures of 3 psi per ridge could be easily maintained. With exotic rare earth permanent magnets, such as samarium cobalt, differential pressures of 40 psi per ridge could be sustained. Figure 64 assumes an intermediate strength magnet, in that it uses six ridges at just over 3 psi differential pressure each to achieve the desired 20 psi total differential pressure. However, the final design of the ferro fluid seal differed from that shown, in that the ridges were increased to eight total and were switched from the shaft to the pole pieces. The switch of the ridges to the pole pieces was done in recognition of the fact that it was desirable to keep the stub shafts as stiff as possible without increasing the seal shear surface diameter. In this manner, the moment of inertia ( $I_1$ ) of the shaft was increased 25 percent with no increase in the critical shear velocities (17,100 fpm) which would occur in ferro-fluid-filled gap. The increase in the number of ridges was to allow the level of ferro fluidization to be decreased from 400 to 300 Gauss, reducing the ferro fluid effective viscosity and reducing the amount of shear-induced heating in each ridge.

It was recognized that an attempt to use a ferro fluid seal in this application involved considerable risk. However, it was felt that the payoff (i.e., a low-friction hermetic seal for a wide range of power system applications) was worth the possibility of failure. The success of the seal was critically dependent upon at least the following:

- 1) That a satisfactory traction fluid (for the controller) could be ferro-fluidized.
- 2) That adequate shaft centering was possible. The ferro fluid seal has a nominal 0.004 diametral clearance with respect to the shaft. This must cover diametral tolerance stackup, journal bearing slop, and shaft deflection. At high speed (hopefully, when the journal bearing was running centered), the shaft should never run more than 0.001 eccentric from the seal bore centerline.

- 3) That the shaft never touched the seal under any operating condition. If this happened, the ferro fluid would locally flash to a gas due to friction and the seal would be lost.
- 4) That the ferro fluid could tolerate the high surface speeds and high shear rates.

In recognition of the possibility of failure, the seal cavity in the flywheel was designed so that it could, with minimum modification, accept a conventional carbon face seal or a slinger-type seal. As discussed below, the first of the above criterion for success was met in a moderately satisfactory manner; however, the next two were not, and the last was never evaluated.

F-50 (General Electric) chlorinated silicone fluid, which has excellent wide temperature range capabilities ( $-70^{\circ}$  to  $+500^{\circ}$  F) and very good traction properties, proved to be non-ferro-fluidizable. M2V (Chevron) silicate ester fluid, which has nearly as good temperature range properties as F-50 ( $-65^{\circ}$  to  $+400^{\circ}$  F) and was thought to have adequate traction properties, proved to be the most ferro-fluidizable of all fluids seriously considered. Santotrac 30 (Monsanto) was the best traction fluid and was marginally adequate when ferro-fluidized but had an unsatisfactory temperature capability at the low-temperature end of the operational range ( $-25^{\circ}$  to  $300^{\circ}$  F). As discussed in later paragraphs, Santotrac 30 was the fluid eventually selected for the MPP and thus for the seal.

About the time the flywheel was ready for final assembly, test data became available from certain in-house Rockwell tests on a similar bearing seal combination. These data indicated that, even with very careful assembly, the tolerance stackup on this test rig, plus journal bearing slop and bending in the shaft, allowed the shaft to touch the seal at relatively low speeds (about 10,000 rpm); as expected, the seal failed. Up to that point, the seal had performed as predicted, holding a hermetic seal for 24 hours and then continuing to seal during initial low-speed runs.

Based on these test results, a quick change of direction was made, and the ferro fluid seal (D589-208) was replaced with a Sealol carbon face seal (753W-B0002CK-12) prior to the first flywheel tests.

#### Flywheel Lubrication Cooling and Assembly

The final flywheel design as released is shown in Figure 65. Every effort was made to provide adequate cooling in those areas where it was needed (i.e., the seals and the bearings). A lube oil "in" port was provided on each side of the flywheel disk for each bearing/seal grouping. The coolest oil (i.e., oil in) was first circulated around the outside diameter of the seal in the



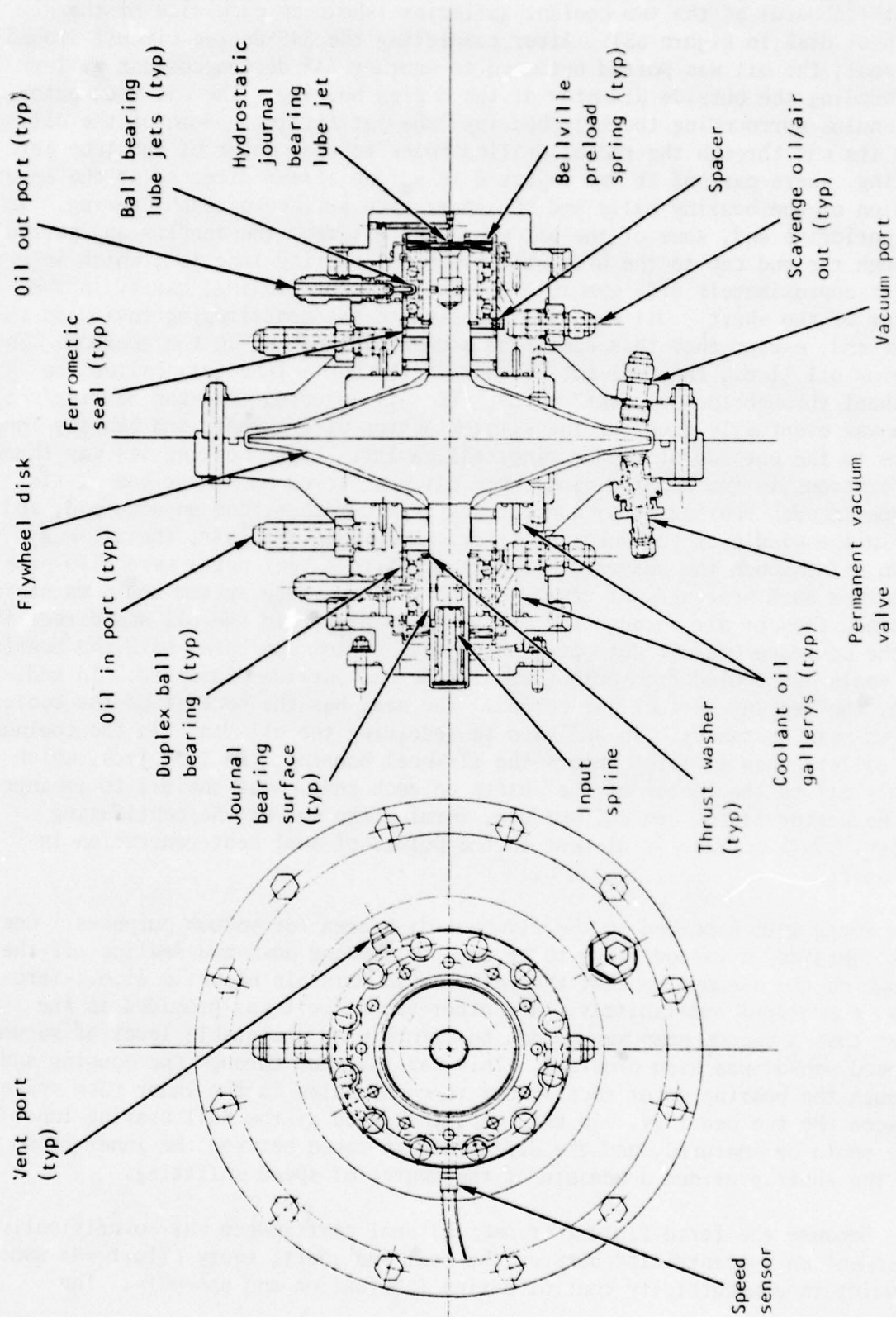


Figure 65. Flywheel Assembly

first (inboard) of the two coolant galleries (shown on each side of the flywheel disk in Figure 65). After completing the 345-degree circuit around the seal, the oil was ported outboard to another 345-degree coolant gallery surrounding the outside diameter of the duplex bearing. The oil then entered an annulus surrounding the ball bearing lube jet fitting. Some of the oil made its way through the radial drilled holes to the center of the lube jet fitting, where part of it was injected in a fine stream directed at the intersection of the bearing balls and the inner race surface of each bearing. In the antidrive end, some of the oil was drawn off from the annulus and ported through the end cap to the hydrostatic journal bearing lube jet, which injected oil at approximately 0.05 gpm into the hollow (centrifuging) cavity in the center of the shaft. Oil was also supplied to the centrifuging cavity on the drive end, except that this came from a coaxial lube jet in the gearbox. The surplus oil (i.e., that oil not discharged through a lube jet) exited the flywheel through the oil "out" ports. The oil injected into the bearing/seal area was eventually slung by the slinger action of the shaft and bearing inner races to the outside of the bearing seal cavity. After working its way through perforations in the bearing rings, the oil was picked up by any one of six (three in each bearing area) annular scavenge cavities, one on each end, and one in the middle of each bearing stack. Now mixed with air, the oil was drawn off through the scavenge oil/air out ports. Vent ports were also provided for each bearing/seal cavity so that the scavenge system could maintain a steady flow of air through the cavity to help entrain the oil and direct it to the scavenge oil/air out port. With this system approach, both the bearings and seals are cooled from both their inside and outside diameters. In addition, the bearing is lube jet cooled. The seal has the benefit of the coolest oil in both instances. In addition to receiving the oil "in" via the coolant oil gallery when it first enters the flywheel housing, the lube jets, which supply oil to the center of the shafts on each end, cause the oil to impinge on the center of the conical surface, forming the end of the centrifuging cavity. This surface is closest to the points of seal heat generation in the shaft.

Ports were provided in the flywheel disk area for vacuum purposes. One port contained a vacuum valve to be used in drawing down and sealing off the vacuum on the assumption that the seals could maintain hermetic (i.e., zero leak) conditions indefinitely. The other vacuum port was provided in the event that a vacuum pump was needed to maintain an acceptable level of vacuum. A speed sensor was also provided. This was inserted through the housing and through the bearing outer race spacer to count holes in the inner race spacer between the two bearings. In this way, the speed of the ball bearing inner race could be measured, and the difference in speed between the inner races and the shaft provided a measure of the degree of speed splitting.

Because the ferro fluid (Ferrometic) seal performance was so critically dependent on concentricity between the seal and shaft, every effort was made to maintain concentricity control during fabrication and assembly. The

flywheel housing halves were mated and indexed, and the bearing/seal bore was line bored as an assembly. It should also be noted (Figure 65) that step bores between the bearing and the seal were avoided. Between these two measures, supplemented by the fact that the flywheel shaft was machined on centers, plus the fact that the duplex bearing sleeve packet was procured as a mated assembly, the concentricity stackup was reduced to a practical minimum.

### MPP System Lubrication

The MPP cooling and lubrication system, as it was planned for test, is shown in Figure 66. The circuit shown is representative of the system which would be installed in an aircraft, except that the auxiliary lube pump and its relief valve would not be needed. It is also possible that, after testing, the jet pump could be deleted. The auxiliary lube pump was incorporated as an insurance policy. As previously stated, one of the major objectives in MPP development was to reduce losses. It was recognized that one of the significant contributors (about 0.25 hp) to overall system losses was the lube system. For this reason, the size of the pumps and, particularly, the lube pump was held to a minimum. The auxiliary lube pump acted as an insurance policy during the test program on several counts:

- 1) It provided a source of extra flow capacity to continue testing until corrective action could be taken, in the event the basic lube system proved to be undersized or the lube metering system proved to be oversized.
- 2) It provided an auxiliary source of pressure so that the system could be operated on a two-level basis until a single (minimum) pressure level, suitable to all components, could be found.
- 3) It provided an independently powered source of pressure and flow which could be used, if needed, during critical startup operations when the basic lube and scavenge system was just beginning to operate.

Figure 66 is self-explanatory except for the reservoir and jet pump. The reservoir is an all-attitude swirl can type which uses the relatively constant (70- to 100-percent rated) flow energy available during takeoff and landing to separate oil and air and to make solid oil available to the lube pump and the lube system in all flight attitudes. Coupled with proper baffling of the gearbox and controller, such a system was felt to guarantee air-free oil being supplied to the controller's critical ratio change control pistons in all attitudes of flight.

The jet pump was used in the flywheel scavenge system in recognition of the fact that, if two vented chambers are scavenged by a single scavenge pump



LUBE JET FLOWS BASED ON 27.5 CENTISTOKE FLUID AT 50 PSI  $\Delta P$   
 UNDERLINED, FLOWS AT 100% RATED SPEED  
 NONUNDERLINED FLOWS AT 70% RATED SPEED

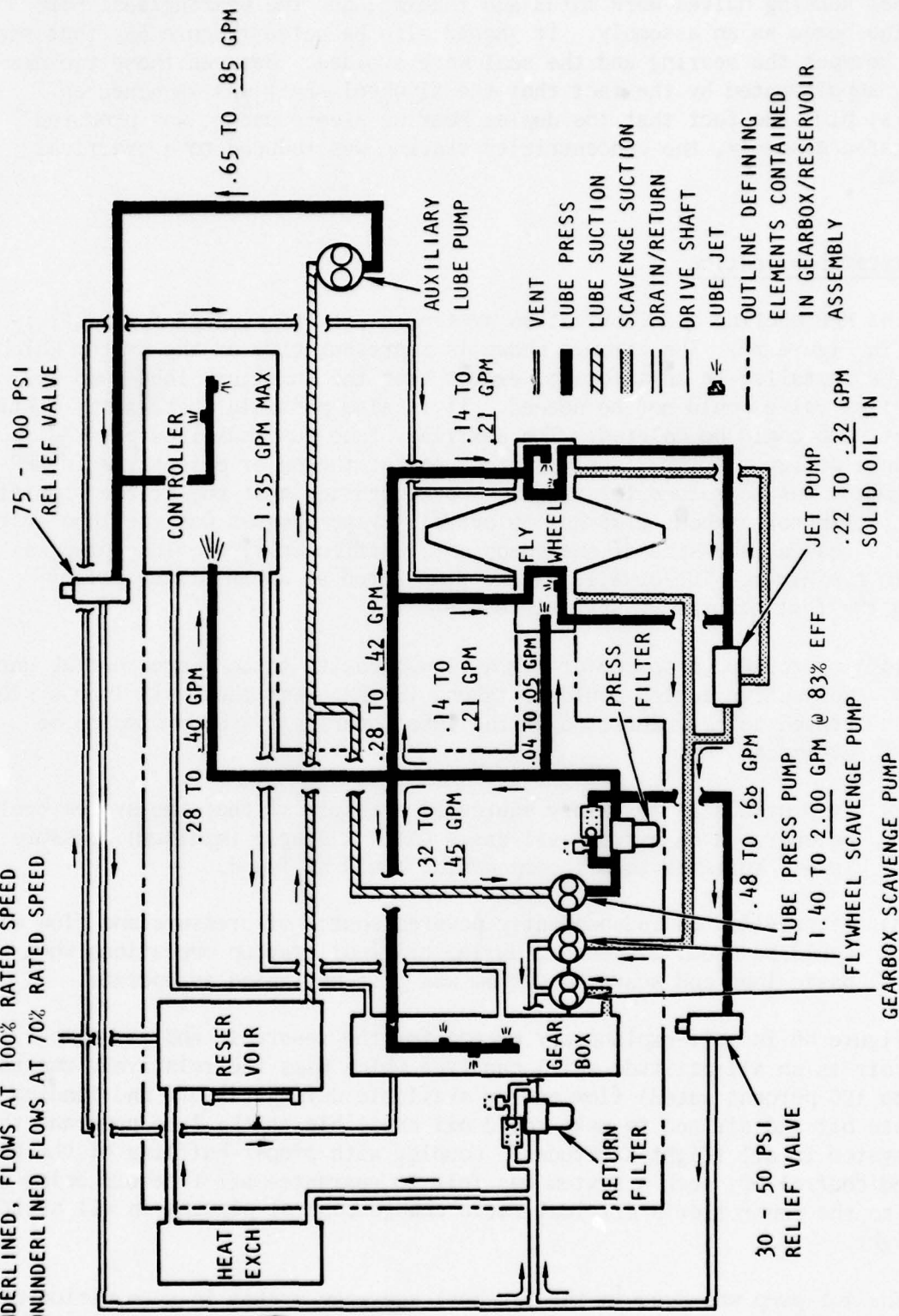


Figure 6 6. MPP Lubrication and Cooling System Schematic

and any one of three parameters (lube oil flow, vent line pressure drop, or scavenge line pressure drop) important to the scavenge function vary significantly between chambers, one branch will tend to flow air/oil mist and the other will tend to flood. This occurs because once an air/oil mist flow is established in one line, its pressure drop suddenly becomes so much lower than the semisolid-oil flow in the other line that the other line flow rate tends toward zero, and flooding of that chamber occurs. The solid-oil cooling flow returning from the flywheel bearing/seal cooling circuit provides the motive flow for the jet pump.

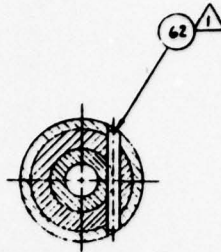
### Gearbox Design

An assembly drawing of the gearbox is shown in Figure 67. The gearbox provided mounting pads for the hydraulic motor, flywheel, and controller. The rated speeds and ratios between pads were as shown in Table 2. The gearbox also mounted a lube and scavenge pump stack, all of which were driven by a common shaft. The pump stack consisted of three pumping elements, all of the Gerotor type. The lube pump had a capacity of 2.0 gpm at 6,000 rpm and 83-percent efficiency. The scavenge pumps were sized to 1.5 times the lube pump capacity.

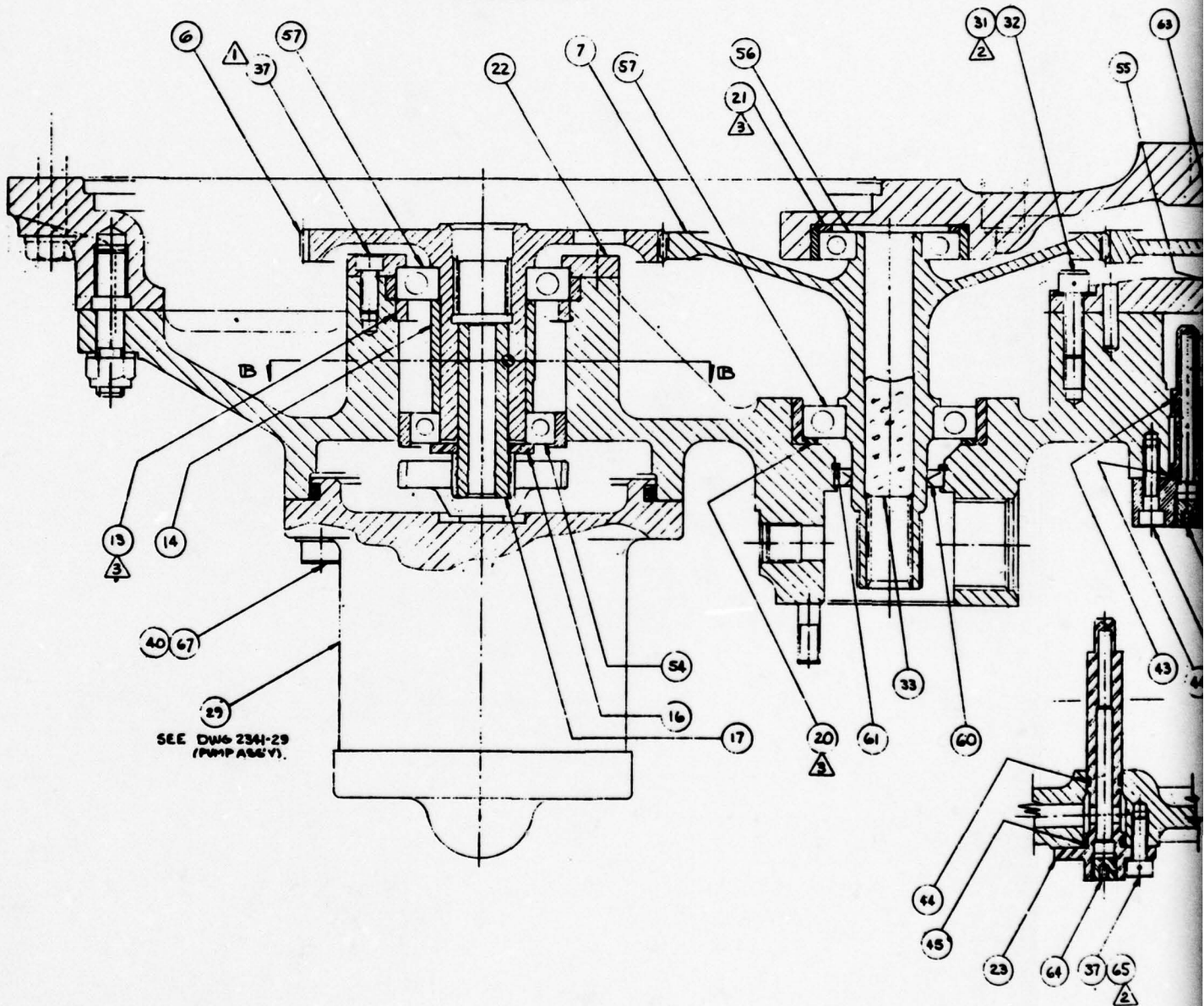
The gearbox layout was generally conventional except in the area of the high-speed (flywheel) pad. The high-speed (88,235 rpm) quill shaft had a small gear integrally machined in it and had no support bearings. The small integral gear became a sun gear in a planetary gear set and was supported by its three relatively large planet gears. These gears acted as support bearings, but gave the quill shaft a much greater tolerance to adapt to misalignment at the gearbox/flywheel interface than a conventional high-speed bearing system would have. The output end of the quill shaft was supported by the flywheel input spline, its shaft, and its bearing system. What appears to be a pressure-lubricated bearing next to the integral gear on the quill shaft in Figure 67 is actually a rather loose fitting damper device used to prevent any tendency for the quill shaft to operate unstably.

### Controller Design

As originally envisioned (reference NA-75-401B in Appendix A), the controller was to have been a relatively small unit (7-inch-diameter by 10-inch-long basic envelope) weighing 41.8 pounds. This small size was predicated on using a traction fluid (Santotrac 30) having a traction coefficient of 0.084. However, at the time the controller was in the design phase, it was decided to switch to Chevron M2V fluid because Santotrac 30 fluid would not meet the -65° F operational requirement. M2V has a traction coefficient (0.045) just slightly over one-half that of Santotrac 30. Since the controller is critically dependent upon the traction properties of the fluid it uses, the size



PART SECT (B) (B)





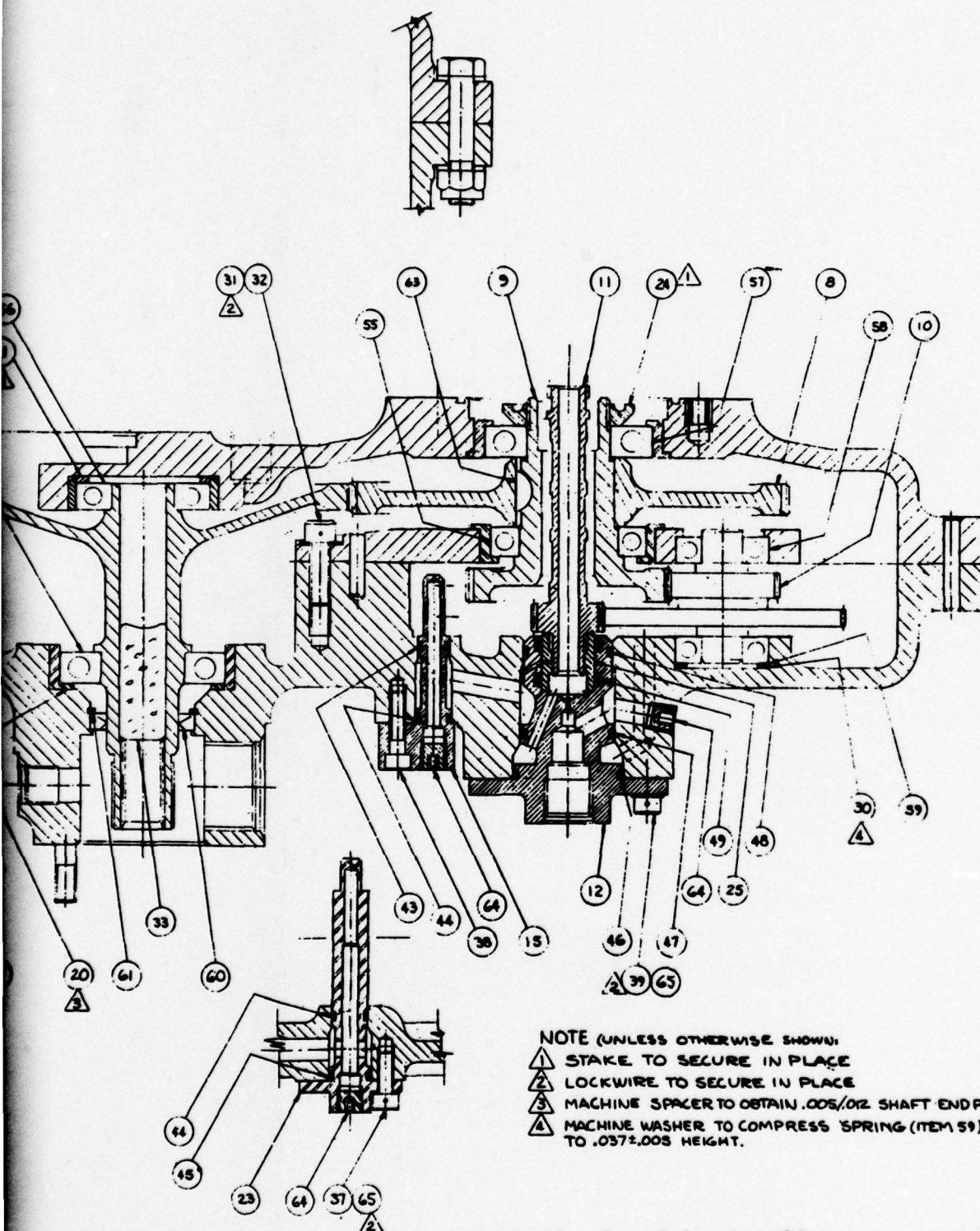


**Figure 67. Gear Drive Assembly**

and weight of the controller increased nearly one-third to 60 pounds and 9.75-inch diameter.

The controller assembly, as it was finally designed and built, is shown in Figure 68.

The basic purpose of the controller was to perform the same functions in an all-mechanical power train as those performed by a four-way valve in a hydraulic power distribution system. These functions were to:

- 1) Provide a controlled bidirectional output (i.e., up-down, extend-retract)
- 2) Provide a means for accelerating and decelerating (snubbing) an output-driven load in a smooth, controlled, shock-free manner

The controller (Figure 69) consisted of three basic elements:

- 1) An infinitely variable ratio change (traction) section
- 2) A bidirectional planetary gear set
- 3) An output control device

#### Infinitely Variable Ratio Change Section Functional Description

The infinitely variable ratio change section is shown in Figure 70. It is a roller-cone-type infinitely variable traction transmission in which ratios are changed by tilting rollers to change contact radii on input and output cones. To assist in understanding the functioning of the transmission, numerous function (load and motion) symbols have been added to Figure 70. An explanation of these symbols follows.

$F_{S1}$  &  $F_{S5}$  = roller tilt steering force

$R_{I1}$  &  $R_{I2}$  = input roller-cone contact radii at minimum and maximum output ratio positions, respectively

$R_{O1}$  &  $R_{O2}$  = output roller-cone contact radii at minimum and maximum output ratio positions, respectively

$F_{PL}$  = longitudinal preload force

$V_{IG_p}$  = rotational velocity of input cone

$V_R$  = rotational velocity of power-transmission rollers

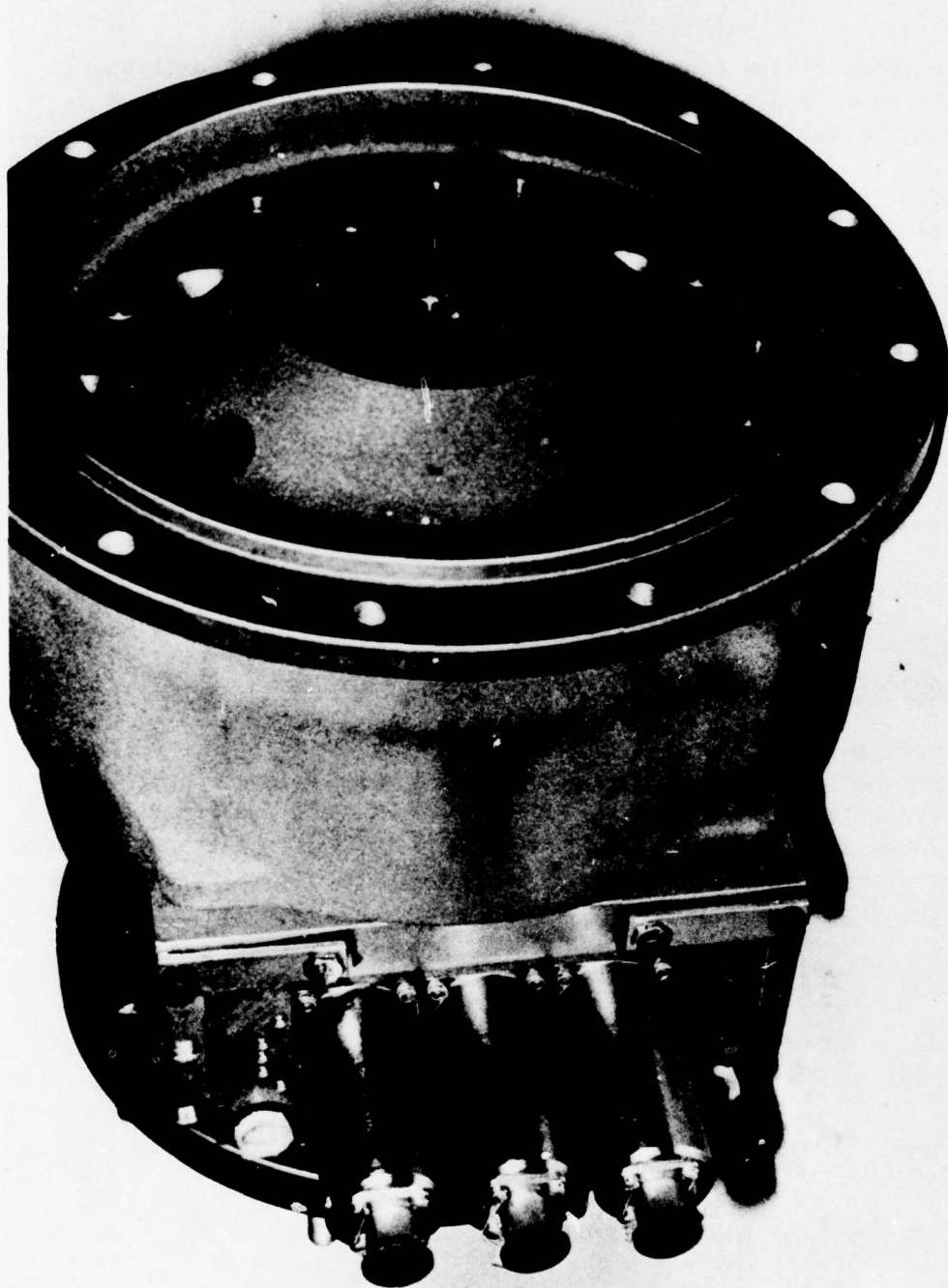


Figure 68. Controller Assembly



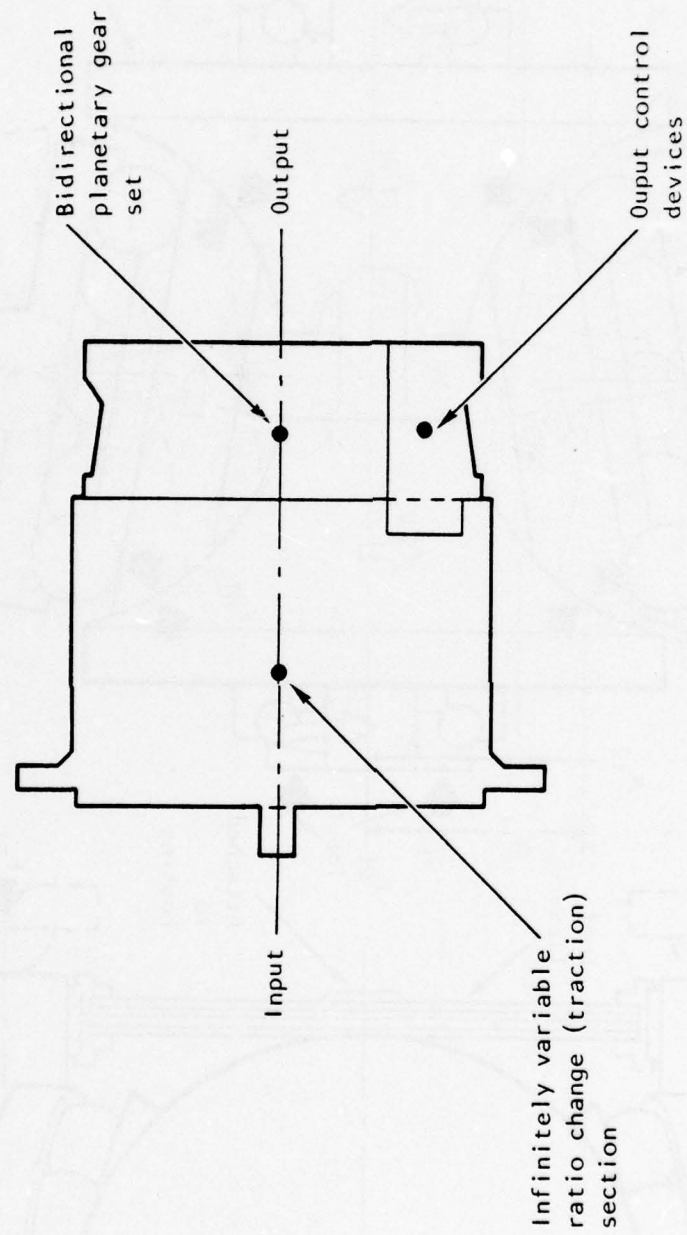


Figure 69. Controller



$V_{OC}$  = rotational velocity of output cone

$V_{RC}$  = rotational velocity of roller tilt about ratio change axis

$F_{PR}$  = radial preload force

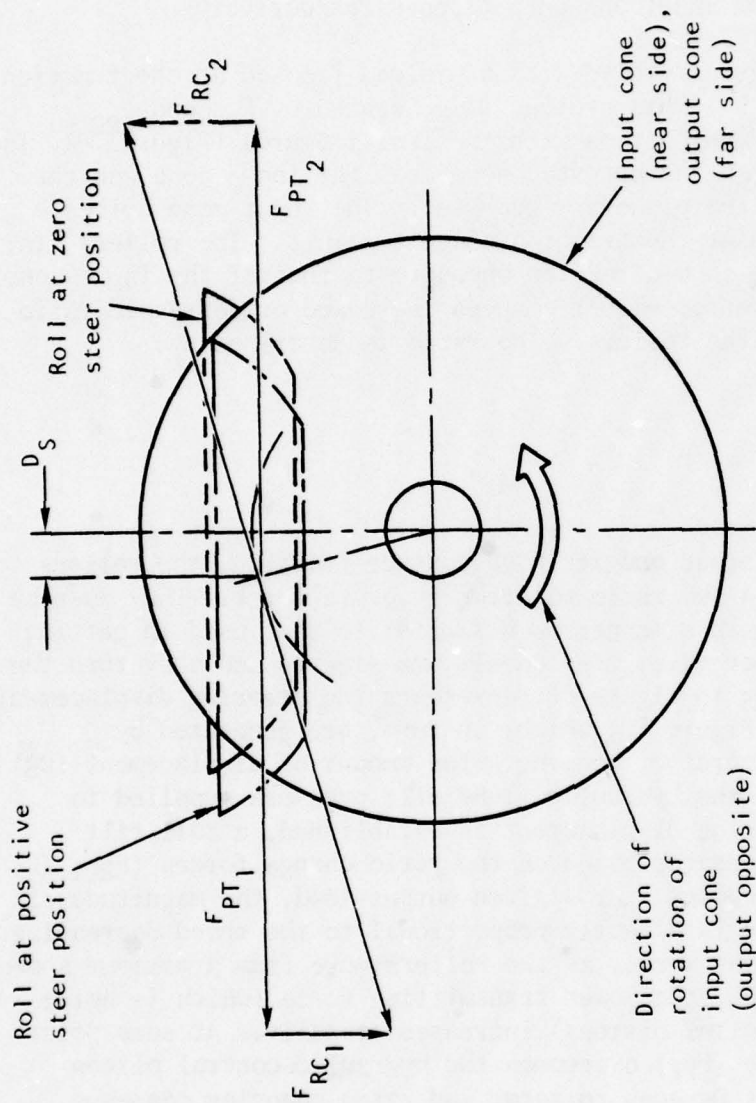
$FNT_i$  and  $FNT_o$  = normal force at traction contact point  
for input and output cones respectively

The traction section is assembled with a preload imposed at the traction contact points ( $FNT_i$  &  $FNT_o$ ). This preload is generated by  $F_{PL}$  and  $F_{PR}$  supplied by the housing in conjunction with the leaf flexures (Figure 70). The input shaft extending through the output cone drives the input cone and the larger of two sun gears in the planetary gear set. The input cone drives a pair of rollers by friction at the traction contact points. The rollers, in turn, drive the output cone in a direction opposite to that of the input cone. The output cone can be driven at either a speed increased or decreased ratio dependent upon the tilt of the rollers. The ratio is described by:

$$V_{OC} = V_{IC} \frac{RI}{RO}$$

Because of the high preload and its high contact friction, the rollers cannot be rotated ( $V_{RC}$ ) to a new ratio position by brute force. They must be steered to the new position in a manner much similar to that used in getting an automobile around a corner (i.e., the wheels are steered and they turn the auto). (See Figure 71.)  $D_S$  in Figure 71 represents the steering displacement generated by  $FS_1$  or  $FS_2$  in Figure 70, which, in turn, are generated by hydraulic pistons in the controller housing. The amount of displacement ( $D_S$ ) is directly proportional to the hydraulic (lube oil) pressure supplied to these pistons. Once a steering displacement is established, a roll tilt (ratio change) moment is generated based on the ratio change forces ( $F_{RC1}$  &  $F_{RC2}$ ) created by the displacement. At a given output load, the magnitude of the power transmitting force is directly proportional to the speed decreasing ratio thus achieved. In other words, as the rollers move from a maximum speed increasing ratio to a minimum, the power transmitting force (which is being reacted by the hydraulic control pistons) increases steadily. At some point, the power transmitting force ( $F_{PT}$ ) overcomes the hydraulic control piston force, steering displacement  $D_S$  goes to zero, and ratio changing ceases. Under some circumstances, power transmitting force can continue to increase even though ratio changing has ceased (a sharp increase in load on the load stroke curve, or the screw jack actuator hitting a stop after being snubbed to a low speed). In these circumstances, the continued increase of force will drive the hydraulic pistons to a negative steering condition and cause the rollers to steer to a maximum ratio condition. In this manner, the unit becomes inherently output load (torque) limiting.





$D_S$  = Steering displacement

$F_{RC1}$  &  $F_{RC2}$  = Ratio change force (roll tilt) for input contact (near side of roll) and output contact (far side of roll), respectively

$F_{PT1}$  &  $F_{PT2}$  = Power transmitting force for input and output contacts, respectively

Figure 71. Ratio Change Forces

The use of lube pressure-driven hydraulic pistons for roll steering control provides two further benefits in addition to torque limiting:

- 1) The acceleration and deceleration of the output load mass can be controlled by modulation of the lube pressure supplied to the hydraulic pistons.
- 2) The use of hydraulic pistons guarantees almost exact load-sharing between the rolls and markedly increases the roll life and transmission efficiency relative to attempting to accomplish the same objective mechanically.

It should be pointed out that, in the interests of clarity, certain liberties have been taken with the vector diagram of Figure 71.  $F_{PT2}$  is actually parallel to and points in the same direction as  $F_{PT1}$ . To be actually correct,  $F_{PT2}$  and  $F_{PT1}$  should be superimposed on top of one another. In addition,  $F_{RC1}$  and  $F_{RC2}$ , although displaced from each other by the width of the roller, would appear, in Figure 71, to start from the same origin point and be oppositely directed. The ratio change torque then is  $F_{RC1} + F_{RC2}/2$  times the diameter of the roller. The way the vector diagram is shown in Figure 71 assumes the viewer is looking at the subscript 1 vectors from the input end and the subscript 2 vectors from the output end.

#### Bidirectional Planetary Gear Set Functional Description

The basic function of the planetary gear set is to provide a bidirectional rotational output given a unidirectional rotational input.

With the infinitely variable traction section (IVTS) at maximum output ratio position, the first-stage planetary gear set (Figure 72) is so sized and proportioned that the first-stage cage (item I in Figure 72) is stationary. With the first-stage cage stationary, the second-stage cage (as well as all gearing) is also stationary. Under these conditions, either the lockup mechanism for gear retract (item J, Figure 72) or for gear extend (item K, Figure 72) may be easily engaged. The lockup mechanism is shown as a latching device in Figure 72 for clarity. In reality, it is a sliding spline-type component. The sequence of events for gear retraction, or extension, is to first lock-up the appropriate gear set elements at zero rotational velocity (there may be some creep due to heat-induced dimensional changes, but this will assist rather than hinder the lockup process) and steer the rolls to a reduced ratio position (i.e., minimum VOC in Figure 70.) The actual rate of change of roll ratio position will be governed by the inherent torque limiting of the hydraulic control pistons in relation to the output load experienced. As the roll ratio position is changed, sun gear (E) in the second stage begins to rotate. If lockup (J) is engaged for gear retract, the cage is, in effect, locked to sun gear (E) and everything, including output sun gear (G), rotates

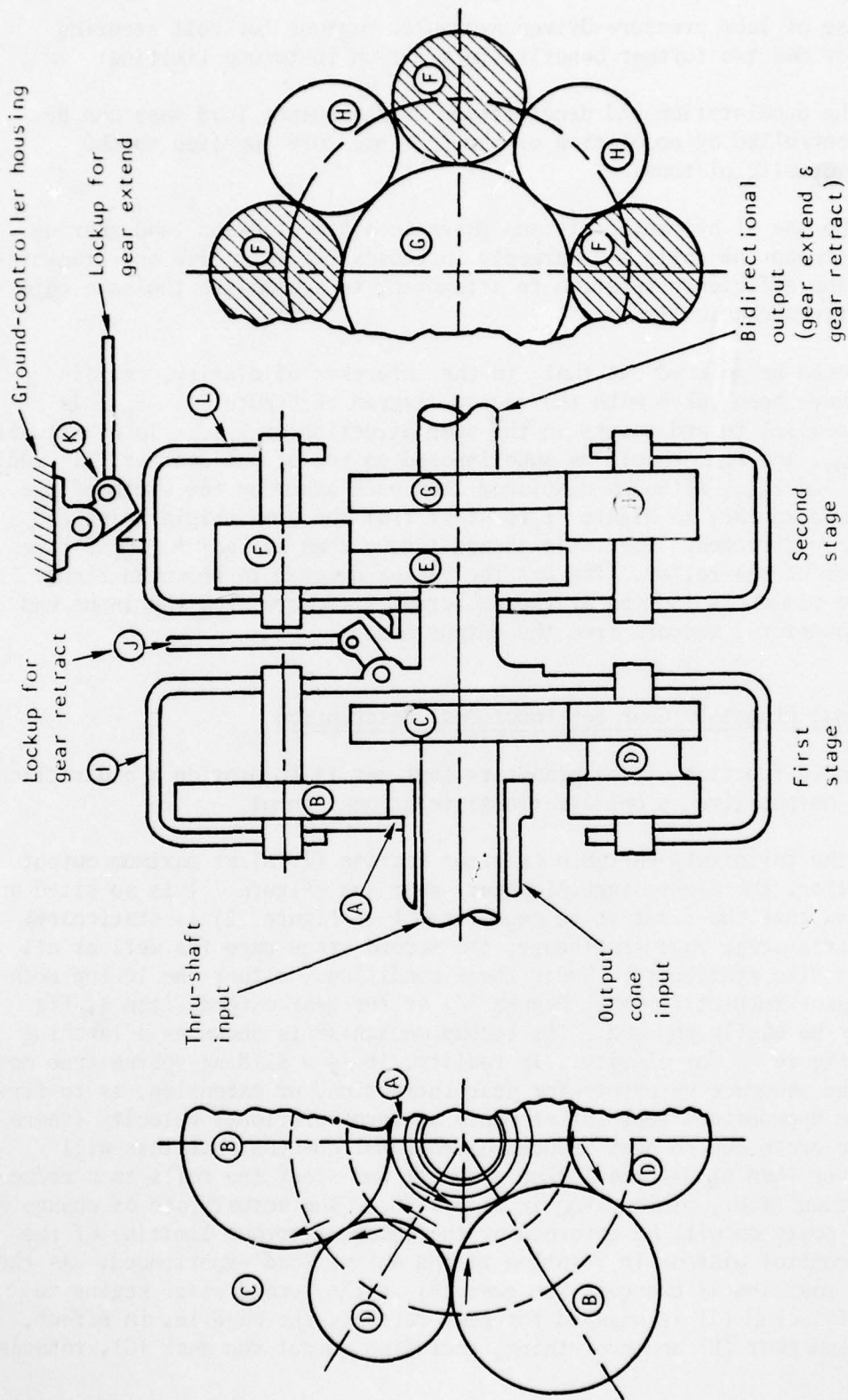


Figure 72. Bidirectional Planetary Gear Set



in the same direction and at the same speed as gear (E). If lockup (K) is engaged for gear extend, the second-stage cage (L) is prevented from rotating and sun gear (E) drives planet gears (F) in the opposite direction. Planet gears (F) have an offset mesh with planet gears (H) which causes these gears to be driven opposite to (F) but in the same direction as sun gear (E). Planet gears (H) mesh with output sun gear (G); therefore, rotational direction reverses once again and output sun gear (G) is caused to rotate opposite to input sun gear (E). With the second-stage cage (L) locked up to the housing, output rotation is opposite to that which occurs when both the first- and second-stage cages are locked together.

#### Output Control Device Functional Description

The output control device was purchased from Sterer Manufacturing Co. as their assembly part 59580. Essentially, this was a multifunctioned solenoid-operated hydraulic valve using lube oil pressure as the control medium. This control valve package is shown in Figure 68 mounted on the controller housing and can be identified by the three rather large uniform-sized solenoids projecting from the valve body in the left side of the photograph. These solenoids were much larger than would normally be necessary, but became as large as they were because they represented an attempt to procure low-cost commercially available solenoids which matched the B-1 electrical power system characteristics. The total control system schematic for the controller is shown in Figure 73. The various valves and functional elements contained in the Sterer control valve assembly are indicated by the phantom outline. The rest of the control elements are also indicated but are in the controller itself.

The basic function of the controller control system is to provide the control forces necessary to meet the controller output requirements. As indicated earlier, these requirements were to provide a bidirectional output when supplied with a unidirectional input and to provide a means for smoothly accelerating and decelerating an output load. Valves 1 and 2 working with cylinders A and B in Figure 73 provide the bidirectional control force. When deenergized, command valve 1 directs lube pressure to the retract (neutral) side of cylinder A. Command valve 2 operates in a similar manner except that it pressurizes cylinder B in the extend (but still neutral) direction. When valve 1 is energized, it directs pressure to cause cylinder A to extend. This action moves a shift fork in the controller to lock the first- and second-stage gearing together (see item J in Figure 72), giving gear retract (+) rotation. In order to ensure that the shift fork engagement could occur before first-stage rotation (other than a slow creep) occurred, a time-delay system was provided by shuttle valve 4 and sequence valve 5. The shuttle valve shuttles in an appropriate manner, depending upon whether the actuation flow is coming from valve 1 or 2, and directs the flow to the upper end of the spring loaded sequence valve 5. The preload of the spring and the effective



area of the end of the sequence valve spool is such that the valve spool will not move until 25 psi is reached. This guaranteed that no ratio changing action would occur, thus causing the first-stage gearing to rotate until the shift lock action was completed. The functioning of command valve 2 is identical to that of valve 1 except that pressure is directed to the net area side of the opposite shift fork actuation piston. This piston actuates the shift fork, which locks second-stage gearing to the controller housing and gives gear extend (-) rotation. (See item K in Figure 72.)

Once sequence valve 5 is open, flow proceeds through the 7,500 rpm limit valve 8 to the speed increasing side of both control pistons. Working against the return springs associated with each roller assembly, the pressure which builds up moves the roller assemblies to a speed-increasing position. The mechanics of ratio changing has been described earlier. However, the function of the roller cams shown at one end of each control piston in Figure 73 has not been described. These cams were inserted in the system to provide a position feedback, thus providing inherent system stability. As indicated in Figure 71 and related paragraphs, steering displacement ( $D_S$ ) is a function of the hydraulic (lube) pressure acting on the control pistons minus any tangential roll forces (power transmitting forces ( $F_{PT}$ )) which may exist. Once a given  $D_S$  is established, ratio changing will continue indefinitely at a rate proportional to that  $D_S$ . However, the control system under these circumstances is operating in an open-loop mode, and there is no intelligence which will tell the control system what  $D_S$  has actually been established. This leaves the control open to instability because the only feedback is the eventual buildup of power transmitting forces ( $F_{PT}$ ) resulting from output load stroke loads or inertia loads. Under these conditions, the control system could easily overshoot and go into cyclical unstable oscillation. The introduction of the roller cams, however, closes the control loop, in that it provides a pressure change feedback proportional to ratio change. As each roller tilts about the yoke centerline ( $V_{RC}$  in Figure 70), the cam roller displaces the control piston by an amount proportional to the actual change in roller ratio position. (See Figure 73.) This, in turn, displaces fluid in the control piston chambers. For a given ratio change, the fluid displacement will be "out" from one cam-roller-piston chamber and "in" for the other. The flow, thus created across the restrictor orifices (Figure 73) at the piston chamber inlets, creates a differential pressure across the ratio changing system which effectively damps oscillation and stabilizes the control system.

The torque control differential pressure valve 6 served the purpose of ensuring that the maximum output torque of the controller never exceeded limit torque (420 in.-lb). With a given control piston pressure, the torque output capabilities of the controller are extremely high at low speed (about three times those at high speed) before the torque limiting induced by  $F_{PT}$  takes effect. Therefore, valve 6 was required to modify control system pressure before the control system could meet specification requirements. Valve 6 is actuated by a cam directly linked to the roller yoke so that its cam rise is



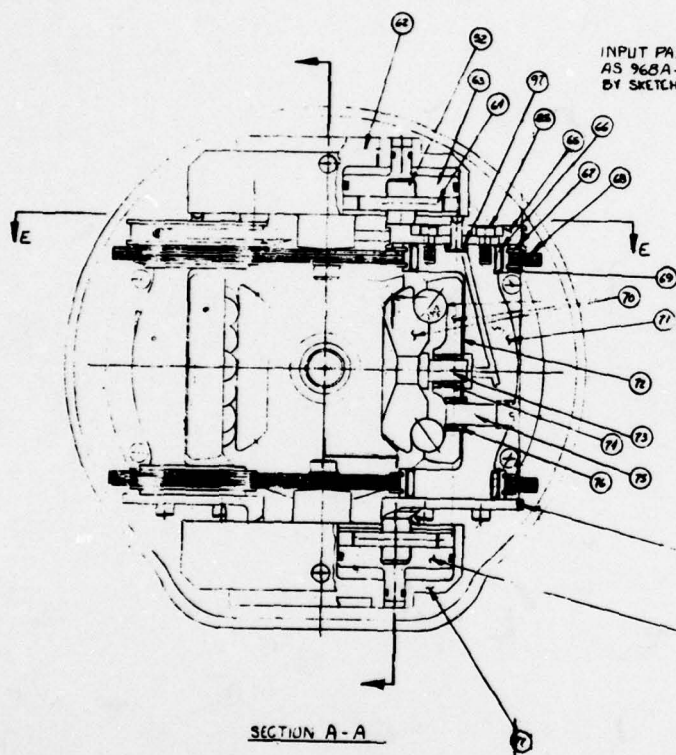
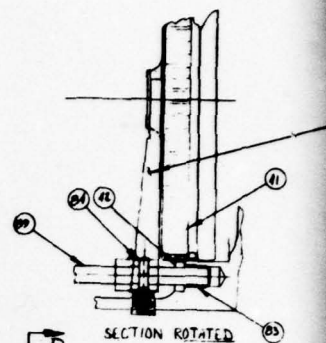
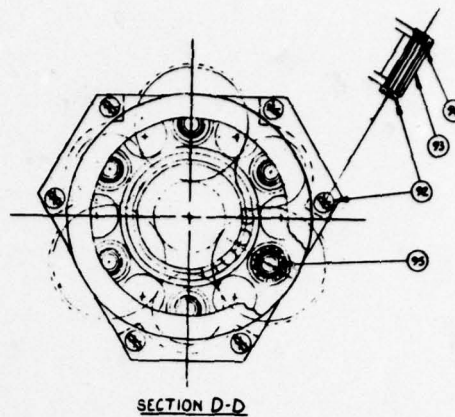
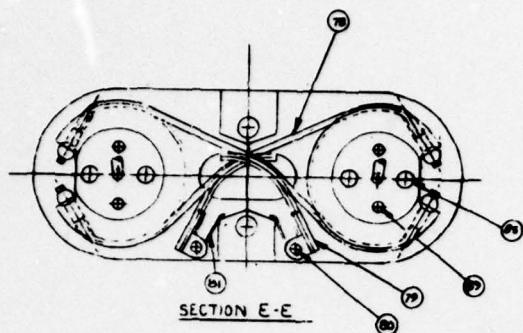
inversely proportional to ratio position. As seen in Figure 73, at zero speed the cam rise is a maximum and decreases as the output speed increases. The cam follower is part of a variable relief valve whose relief setting is varied by cam position. At zero speed, the relief setting is 50 psi, and at rated speed (7,500 rpm), it is 15 psi. The control piston pressure was related to ratio position such that  $F_{PT}$  would always be capable of returning the controller output to zero ratio position before 420 in.-lb output torque was exceeded.

In a similar manner, the 7,500 rpm limit valve 8 and zero limit valve 7 were mechanically connected to the ratio change roller yoke such that they sensed roller ratio position. They are spring-actuated, mechanically adjustable, sharp cutoff, spool-type slide valves which dump control pressure when a ratio position equal to 7,500 or zero rpm, respectively, is reached. Because there is very little slip in the traction elements of the controller, the speed settings and the repeatability of the speed settings resulting from valve adjustment can be very consistent.

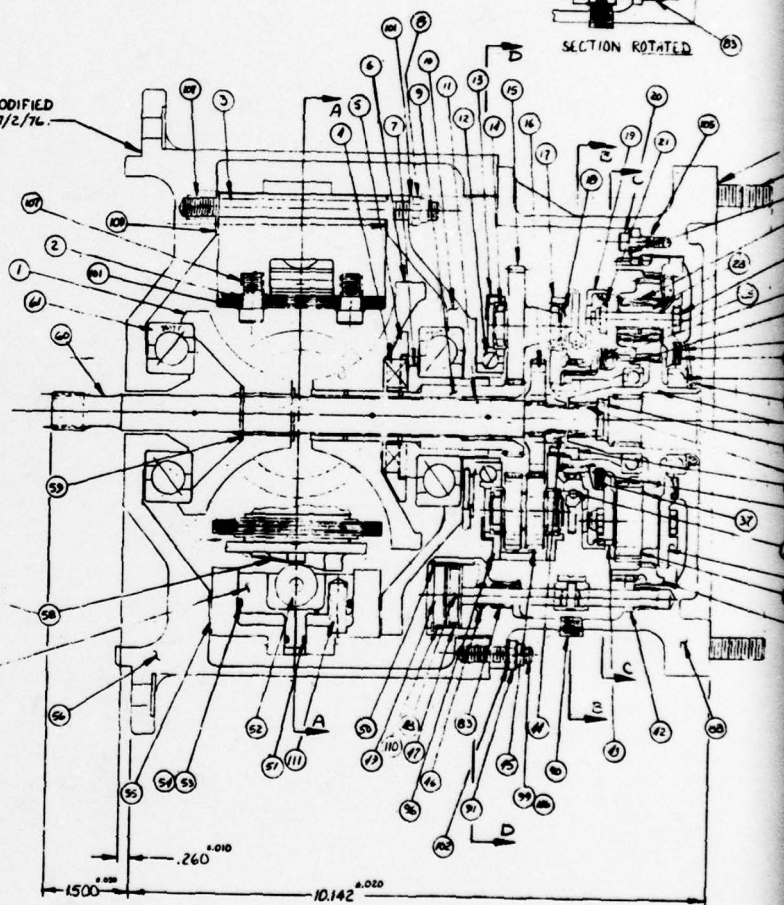
Deceleration command valve 3 was the third of three valves on the unit which was solenoid-controlled. The solenoid for this valve is energized by microswitches mounted on the landing gear linkage which are rigged to trip at a prescribed distance from the end of the gear extend or retract stroke. When energized, the valve opens and meters fluid across an orifice (0.052 inch) to the control piston chambers which tend to drive the rollers to the zero output ratio position. Because of the metering effect of the orifice, and because the control piston chamber will absorb a specific volume of fluid in going from maximum ratio (7,500 rpm) to minimum ratio (zero rpm) position, the reduction in output speed is essentially linear and occurs within a specific length of time within very narrow limits. It should be noted that, during most of the period when the deceleration command valve is open, it is metering fluid back to the sump via a 0.025-inch-diameter orifice in the 7,500 rpm limit valve return port and through 0.025-inch-diameter air-bleed holes in both control piston chambers. However, the 0.052-inch-diameter orifice in the deceleration command valve outlet will more than supply these leakages and will still be able to build up full supply system pressure in the control piston chambers. This pressure, aided by the control piston return spring forces and the power transmitting force, will overcome the full supply pressure ported by the 7,500 rpm limit valve to the other end of the control pistons and return the roller yokes to the zero output ratio position in a controlled manner.

### Controller Detail Design

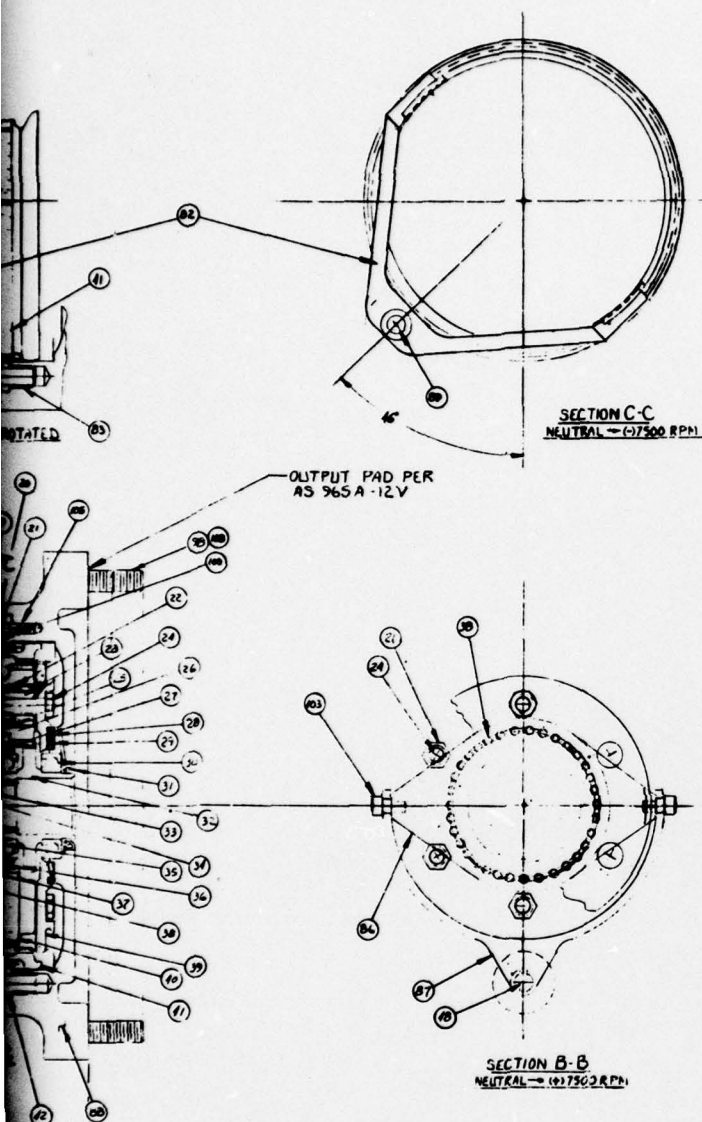
A cross section of the controller design as it finally evolved is shown in Figure 74. It can be seen that the design has the same general layout as that originally envisioned except that it is larger, turns at lower speeds,



INPUT PAD PER  
AS 968A-1 AS MODIFIED  
BY SKETCH DATED 7/2/76.







| ITEM | PART NO. | NAME          | DESCRIPTION          |
|------|----------|---------------|----------------------|
| 6    | 111      | COMP. SPRING  | LEE * LC 040 D-10    |
| 7    | 110      | O-RING        | 2-025                |
| 8    | 109      | DISC SPRING   | ROLEX * 91-00-3805   |
| 9    | 108      | HELICOID      | * 3591-SCN-750       |
| 10   | 107      | HELICOID      | * 3591-SCN-600       |
| 11   | 106      | HELICOID      | * 3591-SCN-350       |
| 12   | 105      | SHIM FLESH    | SPS * 2007-M-2-F-4-3 |
| 13   | 104      | DISC SPRING   | ROLEX * 91-00-3805   |
| 14   | 103      | DISC SPRING   | ROLEX * 91-00-3805   |
| 15   | 102      | DISC SPRING   | ROLEX * 91-00-3805   |
| 16   | 101      | RELATIVE SYND | 17-25 * 11-15        |

|    |    |          |                |                      |
|----|----|----------|----------------|----------------------|
| 1  | 98 | 1-76-036 | OUTPUT SYND    | SPS * 2007-M-2-F-4-3 |
| 2  | 97 | 0 RING   | 2-025          |                      |
| 3  | 96 | 1-76-040 | CHAM-FAST BOLT | SPS * 2007-M-2-F-4-3 |
| 4  | 95 | 1-76-041 | CHAM-FAST BOLT | SPS * 2007-M-2-F-4-3 |
| 5  | 94 | 1-76-042 | CHAM-FAST BOLT | SPS * 2007-M-2-F-4-3 |
| 6  | 93 | 1-76-043 | CHAM-FAST BOLT | SPS * 2007-M-2-F-4-3 |
| 7  | 92 | 1-76-044 | CHAM-FAST BOLT | SPS * 2007-M-2-F-4-3 |
| 8  | 91 | 1-76-045 | CHAM-FAST BOLT | SPS * 2007-M-2-F-4-3 |
| 9  | 90 | 1-76-046 | CHAM-FAST BOLT | SPS * 2007-M-2-F-4-3 |
| 10 | 89 | 1-76-047 | CHAM-FAST BOLT | SPS * 2007-M-2-F-4-3 |
| 11 | 88 | 1-76-048 | CHAM-FAST BOLT | SPS * 2007-M-2-F-4-3 |
| 12 | 87 | 1-76-049 | CHAM-FAST BOLT | SPS * 2007-M-2-F-4-3 |
| 13 | 86 | 1-76-050 | CHAM-FAST BOLT | SPS * 2007-M-2-F-4-3 |
| 14 | 85 | 1-76-051 | CHAM-FAST BOLT | SPS * 2007-M-2-F-4-3 |
| 15 | 84 | 1-76-052 | CHAM-FAST BOLT | SPS * 2007-M-2-F-4-3 |
| 16 | 83 | 1-76-053 | CHAM-FAST BOLT | SPS * 2007-M-2-F-4-3 |
| 17 | 82 | 1-76-054 | CHAM-FAST BOLT | SPS * 2007-M-2-F-4-3 |
| 18 | 81 | 1-76-055 | CHAM-FAST BOLT | SPS * 2007-M-2-F-4-3 |
| 19 | 80 | 1-76-056 | CHAM-FAST BOLT | SPS * 2007-M-2-F-4-3 |
| 20 | 79 | 1-76-057 | CHAM-FAST BOLT | SPS * 2007-M-2-F-4-3 |
| 21 | 78 | 1-76-058 | CHAM-FAST BOLT | SPS * 2007-M-2-F-4-3 |
| 22 | 77 | 1-76-059 | CHAM-FAST BOLT | SPS * 2007-M-2-F-4-3 |
| 23 | 76 | 1-76-060 | CHAM-FAST BOLT | SPS * 2007-M-2-F-4-3 |
| 24 | 75 | 1-76-061 | CHAM-FAST BOLT | SPS * 2007-M-2-F-4-3 |
| 25 | 74 | 1-76-062 | CHAM-FAST BOLT | SPS * 2007-M-2-F-4-3 |
| 26 | 73 | 1-76-063 | CHAM-FAST BOLT | SPS * 2007-M-2-F-4-3 |
| 27 | 72 | 1-76-064 | CHAM-FAST BOLT | SPS * 2007-M-2-F-4-3 |
| 28 | 71 | 1-76-065 | CHAM-FAST BOLT | SPS * 2007-M-2-F-4-3 |
| 29 | 70 | 1-76-066 | CHAM-FAST BOLT | SPS * 2007-M-2-F-4-3 |
| 30 | 69 | 1-76-067 | CHAM-FAST BOLT | SPS * 2007-M-2-F-4-3 |
| 31 | 68 | 1-76-068 | CHAM-FAST BOLT | SPS * 2007-M-2-F-4-3 |
| 32 | 67 | 1-76-069 | CHAM-FAST BOLT | SPS * 2007-M-2-F-4-3 |
| 33 | 66 | 1-76-070 | CHAM-FAST BOLT | SPS * 2007-M-2-F-4-3 |
| 34 | 65 | 1-76-071 | CHAM-FAST BOLT | SPS * 2007-M-2-F-4-3 |
| 35 | 64 | 1-76-072 | CHAM-FAST BOLT | SPS * 2007-M-2-F-4-3 |
| 36 | 63 | 1-76-073 | CHAM-FAST BOLT | SPS * 2007-M-2-F-4-3 |
| 37 | 62 | 1-76-074 | CHAM-FAST BOLT | SPS * 2007-M-2-F-4-3 |
| 38 | 61 | 1-76-075 | CHAM-FAST BOLT | SPS * 2007-M-2-F-4-3 |
| 39 | 60 | 1-76-076 | CHAM-FAST BOLT | SPS * 2007-M-2-F-4-3 |
| 40 | 59 | 1-76-077 | CHAM-FAST BOLT | SPS * 2007-M-2-F-4-3 |
| 41 | 58 | 1-76-078 | CHAM-FAST BOLT | SPS * 2007-M-2-F-4-3 |
| 42 | 57 | 1-76-079 | CHAM-FAST BOLT | SPS * 2007-M-2-F-4-3 |
| 43 | 56 | 1-76-080 | CHAM-FAST BOLT | SPS * 2007-M-2-F-4-3 |
| 44 | 55 | 1-76-081 | CHAM-FAST BOLT | SPS * 2007-M-2-F-4-3 |
| 45 | 54 | 1-76-082 | CHAM-FAST BOLT | SPS * 2007-M-2-F-4-3 |
| 46 | 53 | 1-76-083 | CHAM-FAST BOLT | SPS * 2007-M-2-F-4-3 |
| 47 | 52 | 1-76-084 | CHAM-FAST BOLT | SPS * 2007-M-2-F-4-3 |
| 48 | 51 | 1-76-085 | CHAM-FAST BOLT | SPS * 2007-M-2-F-4-3 |
| 49 | 50 | 1-76-086 | CHAM-FAST BOLT | SPS * 2007-M-2-F-4-3 |
| 50 | 49 | 1-76-087 | CHAM-FAST BOLT | SPS * 2007-M-2-F-4-3 |
| 51 | 48 | 1-76-088 | CHAM-FAST BOLT | SPS * 2007-M-2-F-4-3 |
| 52 | 47 | 1-76-089 | CHAM-FAST BOLT | SPS * 2007-M-2-F-4-3 |
| 53 | 46 | 1-76-090 | CHAM-FAST BOLT | SPS * 2007-M-2-F-4-3 |
| 54 | 45 | 1-76-091 | CHAM-FAST BOLT | SPS * 2007-M-2-F-4-3 |
| 55 | 44 | 1-76-092 | CHAM-FAST BOLT | SPS * 2007-M-2-F-4-3 |
| 56 | 43 | 1-76-093 | CHAM-FAST BOLT | SPS * 2007-M-2-F-4-3 |
| 57 | 42 | 1-76-094 | CHAM-FAST BOLT | SPS * 2007-M-2-F-4-3 |
| 58 | 41 | 1-76-095 | CHAM-FAST BOLT | SPS * 2007-M-2-F-4-3 |
| 59 | 40 | 1-76-096 | CHAM-FAST BOLT | SPS * 2007-M-2-F-4-3 |
| 60 | 39 | 1-76-097 | CHAM-FAST BOLT | SPS * 2007-M-2-F-4-3 |
| 61 | 38 | 1-76-098 | CHAM-FAST BOLT | SPS * 2007-M-2-F-4-3 |
| 62 | 37 | 1-76-099 | CHAM-FAST BOLT | SPS * 2007-M-2-F-4-3 |
| 63 | 36 | 1-76-100 | CHAM-FAST BOLT | SPS * 2007-M-2-F-4-3 |
| 64 | 35 | 1-76-101 | CHAM-FAST BOLT | SPS * 2007-M-2-F-4-3 |
| 65 | 34 | 1-76-102 | CHAM-FAST BOLT | SPS * 2007-M-2-F-4-3 |
| 66 | 33 | 1-76-103 | CHAM-FAST BOLT | SPS * 2007-M-2-F-4-3 |
| 67 | 32 | 1-76-104 | CHAM-FAST BOLT | SPS * 2007-M-2-F-4-3 |
| 68 | 31 | 1-76-105 | CHAM-FAST BOLT | SPS * 2007-M-2-F-4-3 |
| 69 | 30 | 1-76-106 | CHAM-FAST BOLT | SPS * 2007-M-2-F-4-3 |
| 70 | 29 | 1-76-107 | CHAM-FAST BOLT | SPS * 2007-M-2-F-4-3 |
| 71 | 28 | 1-76-108 | CHAM-FAST BOLT | SPS * 2007-M-2-F-4-3 |
| 72 | 27 | 1-76-109 | CHAM-FAST BOLT | SPS * 2007-M-2-F-4-3 |
| 73 | 26 | 1-76-110 | CHAM-FAST BOLT | SPS * 2007-M-2-F-4-3 |
| 74 | 25 | 1-76-111 | CHAM-FAST BOLT | SPS * 2007-M-2-F-4-3 |
| 75 | 24 | 1-76-112 | CHAM-FAST BOLT | SPS * 2007-M-2-F-4-3 |
| 76 | 23 | 1-76-113 | CHAM-FAST BOLT | SPS * 2007-M-2-F-4-3 |
| 77 | 22 | 1-76-114 | CHAM-FAST BOLT | SPS * 2007-M-2-F-4-3 |
| 78 | 21 | 1-76-115 | CHAM-FAST BOLT | SPS * 2007-M-2-F-4-3 |
| 79 | 20 | 1-76-116 | CHAM-FAST BOLT | SPS * 2007-M-2-F-4-3 |
| 80 | 19 | 1-76-117 | CHAM-FAST BOLT | SPS * 2007-M-2-F-4-3 |
| 81 | 18 | 1-76-118 | CHAM-FAST BOLT | SPS * 2007-M-2-F-4-3 |
| 82 | 17 | 1-76-119 | CHAM-FAST BOLT | SPS * 2007-M-2-F-4-3 |
| 83 | 16 | 1-76-120 | CHAM-FAST BOLT | SPS * 2007-M-2-F-4-3 |
| 84 | 15 | 1-76-121 | CHAM-FAST BOLT | SPS * 2007-M-2-F-4-3 |
| 85 | 14 | 1-76-122 | CHAM-FAST BOLT | SPS * 2007-M-2-F-4-3 |
| 86 | 13 | 1-76-123 | CHAM-FAST BOLT | SPS * 2007-M-2-F-4-3 |
| 87 | 12 | 1-76-124 | CHAM-FAST BOLT | SPS * 2007-M-2-F-4-3 |
| 88 | 11 | 1-76-125 | CHAM-FAST BOLT | SPS * 2007-M-2-F-4-3 |
| 89 | 10 | 1-76-126 | CHAM-FAST BOLT | SPS * 2007-M-2-F-4-3 |
| 90 | 9  | 1-76-127 | CHAM-FAST BOLT | SPS * 2007-M-2-F-4-3 |
| 91 | 8  | 1-76-128 | CHAM-FAST BOLT | SPS * 2007-M-2-F-4-3 |
| 92 | 7  | 1-76-129 | CHAM-FAST BOLT | SPS * 2007-M-2-F-4-3 |
| 93 | 6  | 1-76-130 | CHAM-FAST BOLT | SPS * 2007-M-2-F-4-3 |
| 94 | 5  | 1-76-131 | CHAM-FAST BOLT | SPS * 2007-M-2-F-4-3 |
| 95 | 4  | 1-76-132 | CHAM-FAST BOLT | SPS * 2007-M-2-F-4-3 |
| 96 | 3  | 1-76-133 | CHAM-FAST BOLT | SPS * 2007-M-2-F-4-3 |
| 97 | 2  | 1-76-134 | CHAM-FAST BOLT | SPS * 2007-M-2-F-4-3 |
| 98 | 1  | 1-76-135 | CHAM-FAST BOLT | SPS * 2007-M-2-F-4-3 |

TRACTION PROPULSION, INC.  
MASTER LAYOUT

NO. 1-76-2

Figure 74. Controller Assembly



and uses a roller cone rather than a roller toroid configuration in the traction section. The roller toroid configuration (Figure 22) was preferred at the time the MPP program started because it seemed to offer a smaller and lighter design. This was felt to be true because the roller toroid configuration reacts all its roller toroid squeezing loads (i.e., the loads required to achieve traction) through the rolls, toroids, and a single thrust bearing. The housing acts merely as a container, and the steering mechanism is fairly small and lightweight. In contrast, the roller cone configuration reacts large loads through the housing and must have heavy yokes, multileave flexures, and large hydraulic ratio control pistons.

At the time the contract was to be let for the design and fabrication of the controller, there had been no viable bids received for a roller-toroid-type configuration. Since a bid was received for the roller cone type and this type cone would meet contract requirements, the roller cone type was selected. Subsequently, it was found that the roller cone configuration had the following advantages:

- 1) Better traction footprint characteristics
- 2) Better load-sharing between rollers

The traction footprint (roll toroid contact point) characteristics in a traction transmission are the major determinant of transmission size and weight. The tractive effort which can be carried by each footprint is determined by three major factors:

- 1) Lubricant
- 2) Spin
- 3) Contact force

In a comparison between the two controller configurations, the fluid used in one could also be used in the other and, even though the fluid selected has a great impact on the load-carrying ability of a traction transmission, the effect is about equal on the two types; therefore, it does not enter into this comparison. In contrast, spin is a major consideration in comparing the two types. Spin is the phenomena very common in angular contact ball bearings where there is relative motion, or scrubbing action, between the two surfaces in the traction contact area. A uniform-diameter cylinder rolling on a flat plate represents a condition of pure rolling with zero spin. Needle bearings, cylindrical roller bearings, and most tapered roller bearings exhibit essentially pure rolling at their contact points. However, spherical rolling elements such as ball bearings, toroidal traction transmissions, etc, exhibit some degree of differential motion (or scrubbing) between their contact surfaces under nearly all operating conditions. The degree of spin

inherent in a design at its traction contact points is a major determinant of the actual traction coefficient (as opposed to theoretical) and of the magnitude of contact surface wear which will occur under a given set of operating conditions. The greater the spin, the lower the actual traction coefficient and the greater the surface wear. According to Reference 5, where roller toroid and roller cone transmission layouts having equal toroid radii are compared, the average spin encountered in the roller toroid type throughout the normal ratio range is five times that encountered in the roller cone type. This is a significant difference and greatly favors the roller cone configuration.

As discussed in Reference 5, the roller toroid configuration when meeting a given output horsepower develops high contact forces between the rolls and toroids, at both high speedup and high reduction ratios. Minimum contact force occurs at a 1:1 ratio. In the roller cone configuration, the contact force is high at high reduction ratios but drops off continuously as the ratio moves through 1:1 to maximum speedup. This more closely matches typical output demands and, as pointed out in Reference 5, says that a roller cone transmission, which has the same toroidal cavity as a roller toroid transmission, will be smaller in size but able to handle at least twice as much power throughout its speed range.

A computer tab run defining the controller design and performance is shown in Figure 75A, B & C. Notes have been added to aid in explaining the various entries. Particular note should be taken of the entry "input traction torque, all banks, ft-lb." This entry plus the entry "total loss, all banks, hp" show that, unlike the assumptions made at the beginning of the program and shown in Figure 21, losses do not decrease with decreasing output speed. With a regenerative layout, maximum losses occur at zero output speed. The regenerative layout was used because, when the drive size was increased to use M2V fluid, the roller and output thrust bearings were operating at high speed and high load simultaneously and, even for the relatively short periods this condition existed (i.e., only during gear operation), the bearings could not meet life requirements. By going to the regenerative layout, the bearings were heavily loaded only when they were at low speed (see entries "output disc speed, rpm" and "roller speed rpm" in Figure 75B & C. At high speed, they were essentially unloaded. Although this made sense and was necessary from the bearing design point of view, it meant that controller parasite losses were much higher than anticipated. Figure 21 estimates that the parasite losses would be 1.664 hp; however, the actual losses, as will be seen from subsequent test data, were in the 5 to 6 hp range. About 40 percent of this increase was due to the transmission size increase due to the switch to M2V fluid. The rest was due to the use of a regenerative layout.

Reference 5. Kraus, C.E., "Rolling Traction - Analysis and Design," Excelermatic, Inc.



TOROIDAL AUTOMOTIVE TRANSMISSION INPUT DATA (MODIFIED)\*

|   |                 |  |  |
|---|-----------------|--|--|
| RATED ENGINE HURSEPOWER                         | 100.00          | HP/USE   | *  |
| DELIVERED INPUT SPEED, MPH                      | 150.00          | SP/1   | *  |
| MAXIMUM ALLOWABLE AXLE THRUST, LBS (4)          | 12 IN. X 35.185 | THRUST = 420 IN-LB (REQ. MAX. OUTPUT LIMIT TORQUE) |  |
| MAX. GEAR M.P. (PERCENT OF HP/USE)              | 100.00          | MP/AX  | *  |
| MAX. ALLOWABLE TANGENTIAL FORCE                 | 600.            | TAN/AX   | *  |
| NUMBER OF IVU HANKS                             | 1.              | HANK OF ROLLS                                      |  |
| TOROID DIAMETER, INCHES                         | 4.5900          | DIUR   |  |
| TOROID CAVITY DIAMETER, INCHES                  | 3.4000          | DIACV  |  |
| INCLUDED ANGLE BETWEEN ROLLER CONTACTS, DEGREES | 100.0000        | ANCON  |  |
| ROLLER CONTACT RADIUS, INCHES                   | 1.3600          | RADCUN   |  |
| RAMPED CAM LEAD, INCHES-ONE SIDED CAM           | .4500           | LEAD   |  |
| CAM OPTION, 0=CAM=1 FOR INPUT, 2 FOR OUTPUT     | 2               | UTCAM  | OUTPUT CAM IS ADDED REQ.*  |
| DESIGN TRACTION FACTOR                          | .0100           | TRACFA   | *  |
| USABLE TRACTION BASE COEFFICIENT                | .4500           | TRACUN   | COEFF. OF TRACTION AT ZERO SPEED & ZERO ROLLING (THEORETICAL)                    |
| AXIAL PRELOAD FORCE, LBS                        | 500.            | PRELOD   |  |
| CONTROL PISTON DIAMETER, INCHES                 | 2.0000          | CPDIA  | ONE PISTON IN ACTUAL DESIGN IS SLIGHTLY LARGER                                   |
| NUMBER OF ROLLERS                               | 2.              | NRULL  |  |
| ROLLER CRUP, INCHES                             | .8000           | CRUP   | *  |
| OIL TEMP ENTERING CHANGE PUMP, DEG F            | 150.00          | TEMP   | HIGHER OIL TEMP THAN THIS WOULD FAVOR CONTROLLER EFFICIENCY                      |
| OIL PRESSURE INCREASE IN CONTROL VALVE, PSI     | 70.             | UPRV   | *  |
| COOLING OIL FLOW, OUTSIDE PUMP, GPM             | .80             | COUL   | FLOW REQ FOR CONE-ROLLER SECTION ONLY  |
| FLOW RATE THRU BEARING PUMPS, GPM               | .00             | COMPUT   | *  |
| EFFICIENCY OF OIL PUMP                          | .70             | EFFPMP   | *  |
| AGRATION FACTOR, OIL/AIR                        | .90             | AIRFAC   | *  |
| GEAR OPTION (1=SPLIT, 2=NONE, 3, 4, 5=REGEN)    | 5               | GEAR   | INVERSE REGENERATIVE GEARING (ADDED REQ)*  |
| PURER FACTOR (NORMAL=1, PROPELLER DUTY=2)       | 1               | PURFAC   | % OF TIME AT LISTED THRUST (1) (1) ACTIVITY CYCLE) APPLIES ONLY TO LIFE EQUATION |
| TRANSMISSION REDUCTION RATIO - INTO DRIVE       | 1.000           | REDU   |  |
| TRANSMISSION REDUCTION RATIO - OUT OF DRIVE     | 1.000           | REDU   |  |
| AXLE RATIO                                      | 1.000           | AAR  |  |
| WHEEL RADIUS                                    | .425            | RIS  | SETS UP PROGRAM SO LBS. THRUST IS THE SAME AS OUTPUT TORQUE                      |
| RING/SUN DIAMETER RATIO (4)                     | 1.000           | REDU   |  |
| INPUT GEARING REDUCTION RATIO                   | 1.000           | REDU   |  |
| OUTPUT GEARING REDUCTION RATIO                  | 1.000           | REDU   |  |

|                          |       |         |         |         |
|--------------------------|-------|---------|---------|---------|
| ANTI-FRICTION BRG.       | BRGCF | 100000. | OUTPUT  | MULLEN  |
| CONSTANT FLOW RATES FLOW | FLOW  | .0000   | 100000. | 100000. |
| O.M. OF BELLEVILLE       | ROM   | 2.6000  | 3.2500  | .0000   |
| I.M. OF BELLEVILLE       | IM    | 1.0000  | 1.1000  | 2.1000  |
| BELLEVILLE THICKNESS     | T     | .1250   | .1250   | 1.1000  |
| PIVOT DIA.               | PIV   | 2.0000  | 2.2500  | 1.6000  |
| RADIUS OF LAND           | MO    | 15.     | 15.     | 15.     |

DROPS OUT - INDICATING DESIGN IS BASED ON ANTI-FRICTION (AS OPPOSED TO HYDROSTATIC) GEARINGS

\* BASICALLY THIS IS AN AUTOMOTIVE TRANSMISSION DESIGN COMPUTER PROGRAM MODIFIED FOR USE IN DESIGNING THE CONTROLLER

\* INDICATES THIS ENTRY NOT APPLICABLE TO THE DESIGN OF THE CONTROLLER

Figure 75A. Controller Design Tab Run, Sheet 1



| TOROIDAL AUTOMOTIVE TRANSMISSION COMPUTED DATA                                 |          |          |          | OPERATION AT RATED OUTPUT TORQUE (9) |          |          |          | ZERO OUTPUT TORQUE |  |  |  |
|--|----------|----------|----------|--------------------------------------|----------|----------|----------|--------------------|--|--|--|
| OPERATING SPEED RANGE DURING LANDING GEAR OPERATION                            |          |          |          |                                      |          |          |          |                    |  |  |  |
| DELIVERED OUTPUT SPEED, RPM (2)  | -7499.83 | -6923.08 | -5304.62 | -3461.54                             | -2014.23 | -989.01  | .00      |                    |  |  |  |
| OUTPUT DISC SPEED, RPM (3)   | 4500.45  | 6000.00  | 10000.00 | 15000.00                             | 15000.00 | 21428.57 | 24000.00 |                    |  |  |  |
| INPUT DISC SPEED, RPM  | 3.33     | 2.50     | 1.50     | 1.00                                 | .80      | .70      | .63      |                    |  |  |  |
| DRIVE SPEED RATIO (RPM IN/RPM OUT) (4)   |          |          |          |                                      |          |          |          |                    |  |  |  |
| TRANSMISSION SPEED RATIO (RPM IN/RPM OUT) (5)                                  |          |          |          |                                      |          |          |          |                    |  |  |  |
| POWER TRANSMITTED BY DRIVE, PER CENT (6)                                       | -2.00    | -2.17    | -2.79    | -4.33                                | -7.43    | -15.17   | -30.00   |                    |  |  |  |
| POWER TRANSMITTED BY GLIDING, PER CENT (7)                                     | 23.08    | 33.33    | 71.43    | 166.67                               | 357.14   | 833.33   | 1500.00  |                    |  |  |  |
| POWER TRANSMITTED BY DRIVE, ALL BANKS, HP (8)                                  | 123.08   | 133.33   | 171.43   | 266.67                               | 457.14   | 933.33   | 1500.00  |                    |  |  |  |
| INPUT TRACTION TORQUE, ALL BANKS, FT-LBS                                       | 4.02     | 5.36     | 8.93     | 13.39                                | 16.74    | 54.83    | 100.00   |                    |  |  |  |
| POWER TRANSMITTED BY GLIDING, ALL BANKS, HP (9)                                | 61.19    | 61.19    | 61.19    | 61.19                                | 61.19    | 61.19    | 61.19    |                    |  |  |  |
| PUMP LOSS, ALL BANKS, HP   | .00      | .00      | .00      | .00                                  | .00      | .00      | .00      |                    |  |  |  |
| INPUT DISC TRACTION LOSS PER CONTACT, HP                                       | .07      | .06      | .27      | .39                                  | .40      | .39      | .39      |                    |  |  |  |
| OUTPUT DISC TRACTION LOSS PER CONTACT, HP                                      | .06      | .06      | .14      | .21                                  | .21      | .21      | .21      |                    |  |  |  |
| INPUT DISC BEARING LOSS, ALL BANKS, HP (10)                                    | .04      | .04      | .14      | .21                                  | .21      | .21      | .21      |                    |  |  |  |
| OUTPUT DISC BEARING LOSS, ALL BANKS, HP (11)                                   | .04      | .04      | .14      | .21                                  | .21      | .21      | .21      |                    |  |  |  |
| ROLLER DISC BEARING LOSS, ALL BANKS, HP (12)                                   | .10      | .14      | .25      | .38                                  | .46      | .36      | .36      |                    |  |  |  |
| TOTAL BEARING LOSS, ALL BANKS, HP (13)   | .18      | .29      | .56      | .96                                  | 1.09     | 1.26     | 1.26     |                    |  |  |  |
| GRADING LOSS, ALL BANKS, HP (14)   | .73      | .76      | .87      | .99                                  | 1.09     | 1.16     | 1.16     |                    |  |  |  |
| TOTAL LOSS, ALL BANKS, HP (15)   | 1.17     | 1.29     | 2.25     | 3.45                                 | 4.40     | 5.11     | 5.11     |                    |  |  |  |
| HYDROSTATIC PRESSURE (LIT), PSI  | .00      | .00      | .00      | .00                                  | .00      | .00      | .00      |                    |  |  |  |
| HYDROSTATIC PRESSURE (LIT), PSI  | .00      | .00      | .00      | .00                                  | .00      | .00      | .00      |                    |  |  |  |
| HYDROSTATIC PRESSURE IN ROLLER, PSI  | .00      | .00      | .00      | .00                                  | .00      | .00      | .00      |                    |  |  |  |
| OIL FLOW IN BEARINGS, ALL BANKS, GPM   | .00      | .00      | .00      | .00                                  | .00      | .00      | .00      |                    |  |  |  |
| TOTAL SHEAR HEAT, ALL BANKS, BTU/MIN   | 7.59     | 12.37    | 23.66    | 36.67                                | 46.39    | 53.49    | 53.49    |                    |  |  |  |
| DRIVE HEAT REJECTION, ALL BANKS, BTU/MIN                                       | 49.50    | 54.79    | 95.59    | 146.39                               | 186.65   | 216.09   | 216.09   |                    |  |  |  |
| OIL TEMPERATURE INTO SEAL RINGS, DEG F   | 150.00   | 150.00   | 150.00   | 150.00                               | 150.00   | 150.00   | 150.00   |                    |  |  |  |
| OIL TEMP EXITING DRIVE, DEG F  | 168.56   | 170.54   | 185.84   | 204.87                               | 219.99   | 231.33   | 231.33   |                    |  |  |  |
| OUTPUT HORSEPOWER DELIVERED, ALL BANKS   | 49.98    | 46.14    | 36.88    | 23.07                                | 13.46    | 6.59     | .00      |                    |  |  |  |
| OUTPUT TORQUE DELIVERED, ALL BANKS, FT-LBS                                     | 35.00    | 35.19    | 35.19    | 35.19                                | 35.19    | 35.19    | 35.19    |                    |  |  |  |
| WHEEL THRUST, LBS (OUTPUT TORQUE)  | 35.00    | 35.00    | 35.00    | 35.00                                | 35.00    | 35.00    | 35.00    |                    |  |  |  |
| USABLE INPUT HORSEPOWER (NO SLIP), HP  | 51.15    | 47.43    | 38.14    | 26.52                                | 17.86    | 11.71    | .30      |                    |  |  |  |
| DRIVE EFFICIENCY   | .962     | .966     | .946     | .936                                 | .931     | .928     | .900     |                    |  |  |  |
| TRANSMISSION EFFICIENCY  | .971     | .973     | .941     | .920                                 | .914     | .903     | .800     |                    |  |  |  |
| GEARING ACTUAL OVERALL EFFICIENCY PROBABLY 950                                 |          |          |          |                                      |          |          |          |                    |  |  |  |
| MILES PER HOUR   | -535.49  | -494.31  | -384.46  | -247.15                              | -144.17  | -70.64   | .00      |                    |  |  |  |
| MINUS SIGN INDICATES ROTATION IN REVERSE OF NORMAL                             |          |          |          |                                      |          |          |          |                    |  |  |  |
| NO SIGN INDICATES NORMAL (COUNTERROTATING) DIRECTION OF ROTATION               |          |          |          |                                      |          |          |          |                    |  |  |  |
| SEE FIGURE FOR DEFINITION OF DRIVE FIRST STAGE SECOND STAGE                    |          |          |          |                                      |          |          |          |                    |  |  |  |
| INCLUDES DRIVE FIRST STAGE ONLY  |          |          |          |                                      |          |          |          |                    |  |  |  |
| SHOULD BE INFINITY-COMPUTER PRINTS OUT .00                                     |          |          |          |                                      |          |          |          |                    |  |  |  |
| SHOWS INVERSE REGENERATIVE CHARACTERISTICS OF TRANSMISSION IN THAT             |          |          |          |                                      |          |          |          |                    |  |  |  |
| DIFFERENCE BETWEEN PERCENT POWER TRANSMITTED BY DRIVE AND                      |          |          |          |                                      |          |          |          |                    |  |  |  |
| WEARING IS ALWAYS 100% (IE OUTPUT OF TRANSMISSION)                             |          |          |          |                                      |          |          |          |                    |  |  |  |
| RECIRCULATED KANGES FROM 23.08% TO 833.33%                                     |          |          |          |                                      |          |          |          |                    |  |  |  |
| POWER RECIRCULATED AS A RESULT OF INVERSE REGENERATIVE LAYOUT                  |          |          |          |                                      |          |          |          |                    |  |  |  |
| GEAR RATIO (LIMIT) OUTPUT TORQUE 420 IN-LB PER SPEC. (IE. 35 FT-LB X 12 IN/FT) |          |          |          |                                      |          |          |          |                    |  |  |  |
| AS OUTPUT SPEED LOSSES INCREASE  |          |          |          |                                      |          |          |          |                    |  |  |  |
| HIGHEST ROTATIONAL SPEED BUT LOSSES ARE LESS BECAUSE OUTPUT LOAD IS ZERO AND   |          |          |          |                                      |          |          |          |                    |  |  |  |
| THUS LOSSES ARE ONLY THOSE ASSOCIATED WITH PRELOAD                             |          |          |          |                                      |          |          |          |                    |  |  |  |
| SHORT THINNESS AT COMPLETION   |          |          |          |                                      |          |          |          |                    |  |  |  |
| POWER OUTPUT COULD BE 44.6   |          |          |          |                                      |          |          |          |                    |  |  |  |
| HP KATL A F NO SLIP  |          |          |          |                                      |          |          |          |                    |  |  |  |

Figure 75B. Controller Design Tab Run, Sheet 2

# TOROIDAL AUTOMOTIVE TRANSMISSION COMPUTED DATA

|   |                   |          |          |          |          |          |          |
|---|-------------------|----------|----------|----------|----------|----------|----------|
| DELIVERED OUTPUT SPEED, MPH               | -7499.83          | -8223.08 | -5304.62 | -3461.54 | -2019.23 | -989.01  | .00      |
| MOLLIN SPEED, MPH                         | 7475.45           | 8613.54  | 11253.36 | 13042.04 | 15455.36 | 16486.77 | 17409.53 |
| ROLLER SPEED, FPS                         | 84.84             | 97.72    | 127.72   | 157.11   | 175.41   | 187.14   | 197.59   |
| CONTACT RADIUS(1), INCHES                 | .648              | .747     | .976     | 1.200    | 1.340    | 1.430    | 1.509    |
| CONTACT RADIUS(2), INCHES                 | 2.160             | 1.867    | 1.464    | 1.200    | 1.072    | 1.001    | .943     |
| CONTACT RADIUS(3), INCHES                 | 30.708            | 37.406   | 50.589   | 63.440   | 71.809   | 77.344   | 81.484   |
| TANGENTIAL FORCE(1), LBS                  | 17.743            | 26.154   | 41.977   | 56.449   | 65.538   | 71.466   | 74.351   |
| TANGENTIAL FORCE(2), LBS                  | 1324.541          | 1667.284 | 2253.513 | 2799.301 | 3184.573 | 3465.545 | 3746.887 |
| CONTACT FORCE, LBS-INPUT                  | 1324.541          | 1667.284 | 2253.513 | 2799.301 | 3184.573 | 3465.545 | 3746.887 |
| CONTACT FORCE, LBS-OUTPUT                 | .023              | .022     | .022     | .023     | .023     | .022     | .022     |
| TRACTION COEFFICIENT(1)                   | INPUT THEORETICAL | .031     | .034     | .029     | .029     | .029     | .029     |
| TRACTION COEFFICIENT(2)                   | OUTPUT ACTUAL     | .013     | .016     | .019     | .020     | .021     | .021     |
| USABLE TRACTION COEFFICIENT(1)            | THEORETICAL       | .023     | .028     | .030     | .028     | .027     | .025     |
| AXIAL FORCE(1), LBS                       | 657.              | 1377.    | 2842.    | 4283.    | 5269.    | 5767.    | 6244.    |
| AXIAL FORCE(2), LBS                       | 2641.             | 3227.    | 3971.    | 4283.    | 4424.    | 4494.    | 4540.    |
| ROLLER AXIAL FORCE, LBS                   | 1706.             | 2147.    | 2903.    | 3606.    | 4102.    | 4464.    | 4788.    |
| CONTROL PISTON FORCE, LBS                 | 48.               | 64.      | 93.      | 120.     | 137.     | 149.     | 161.     |
| EQUIVALENT DIAMETER OF ROLLING(1), INCHES | 15.               | 20.      | 29.      | 38.      | 44.      | 47.      | 49.      |
| EQUIVALENT DIAMETER OF ROLLING(2), INCHES | 1.794             | 2.046    | 2.613    | 3.145    | 3.465    | 3.665    | 3.841    |
| MAJOR CONTACT ELLIPSE DIAMETER(1), INCHES | 5.181             | 4.597    | 3.740    | 3.145    | 2.844    | 2.674    | 2.535    |
| MINOR CONTACT ELLIPSE DIAMETER(1), INCHES | .226              | .246     | .238     | .252     | .261     | .266     | .266     |
| MAJOR CONTACT ELLIPSE DIAMETER(2), INCHES | .036              | .041     | .055     | .066     | .073     | .078     | .084     |
| MINOR CONTACT ELLIPSE DIAMETER(2), INCHES | .070              | .070     | .084     | .086     | .086     | .086     | .086     |
| MEAN HERTZ PRESSURE(1), PSI               | 209631.           | 210460.  | 217754.  | 213798.  | 212820.  | 213356.  | 213356.  |
| MEAN HERTZ PRESSURE(2), PSI               | 130283.           | 149656.  | 182909.  | 213798.  | 235329.  | 249434.  | 264434.  |
| SYSTEM BID OF TRANSMISSION, MACLAURE      | 15388.71          | 12234.72 | 6092.50  | 3528.77  | 1897.54  | 1188.32  | 90938.87 |
| SYSTEM BID OF INDUSTRIAL DRIVE, SKF       | 3057.66           | 2782.44  | 2373.27  | 1598.01  | 674.73   | 337.93   | 20916.92 |
| SPIN(1)                                   | -2.79             | 1.65     | 4.25     | 4.27     | 3.80     | 3.39     | 1.64     |
| SPIN-IPS FACTOR-11                        | .1527             | .0657    | .2156    | .2149    | .1711    | .1707    | .0891    |
| ENERGY FACTOR(1)                          | .94               | .79      | 1.79     | 2.07     | 2.11     | 2.09     | .12      |
| INPUT DISC TRACTION LOSS PER CONTACT, MP  | .07               | .06      | .27      | .39      | .40      | .39      | .00      |
| SPIN(2)                                   | -1.68             | .52      | 2.69     | 4.27     | 4.86     | 5.06     | 2.78     |
| SPIN-IPS FACTOR-21                        | .0373             | .0281    | .1392    | .2149    | .2416    | .2496    | .1490    |
| ENERGY FACTOR(2)                          | .39               | .35      | 1.23     | 2.01     | 2.45     | 2.70     | .51      |
| OUTPUT DISC TRACTION LOSS PER CONTACT, MP | .06               | .06      | .14      | .41      | .71      | .96      | .00      |

⑤ MAX. CONTACT PRESSURE REQUIRED - SAYS 50 PSI MIN LUBE SUPPLY PRESS. O.K.  
 ⑥ REFERENCE VALUE OF ZERO OUTPUT LOAD 3-DEFINITION WHICH IS CONSIDERED THEORETICAL  
 WILL OPERATE UNIFORM FOR 57% OF ITS OPERATIONAL LIFE

NORMAL FORCE  
 TRACTION COEFFICIENTS  
 CHARACTERISTIC OF  
 M2 V FLUID  
 RELIEF VALVE CAM  
 CONTINUED TO THIS  
 DIFFERENTIAL PROCESS.  
 APPLIES TO ROLLER  
 DISC CONTACTS ONLY

Figure 75C. Controller Design Tab Run, Sheet 3

## Screwjack Design

The final design of the screwjack is shown in Figures 76 and 77. The screwjack was built around an existing available Saginaw ball screw (3000-0660-SGT). The dimensions of the major load-carrying elements of this ball screw were approximately two-thirds of those estimated at the beginning of the program. These comparative dimensions are:

|                       | <u>Projected<br/>design</u> | <u>Final<br/>design</u> |
|-----------------------|-----------------------------|-------------------------|
| Ball circle dia (in.) | 4.000                       | 3.000                   |
| Ball diameter (in.)   | 0.750                       | 0.500                   |
| Lead (in.)            | 1.000                       | 0.660                   |

This reduction was made possible by a much more refined duty cycle analysis.

The original design anticipated the use of a worm gear and an aluminum housing. The use of the worm gear created a relatively large "window" in the side of the housing at right angles to the tensile stress path created when the unit was subjected to 107,000-pound tensile loads during normal operation on the load stroke curve. This load could not be bridged over or around the window without an excessive buildup in the aluminum housing wall thickness in the immediate area. The situation could have been helped by substituting steel for aluminum; however, both the weight and, particularly, the cost would have been negatively impacted by such a move. It was therefore decided to use a new approach employing spur and bevel gears. This cut down the size of the window and solved the stress problem. Also, it had the additional advantage that it allowed the use of grease throughout the screwjack. The worm gear design required the use of oil at the worm gear mesh and required seals to separate the oil from the grease used elsewhere in the screwjack.

It can be seen in Figure 76 that the end of the housing from which the ball screw emerges has a steel ring around its diameter. The use of this arose from the fact that the retaining nut which backs up the main roller thrust bearing was eccentrically loaded with respect to its threads. The nut threads in their turn loaded the aluminum housing threads and caused a high eccentric loading with an associated turnover moment at the mouth of the screwjack housing, which was converted to an unacceptably high hoop stress at the outer surface of the housing in this area. This problem was overcome by shrinking on a high-strength steel band around the housing threads.

It can be seen in Figure 76 that the basic housing walls were very thick. This was because the housing was made of aluminum, with its relatively low strength and low modulus of elasticity. Aluminum was selected because of its castability and ease of machining. It was the only way to go to keep costs



AD-A073 297

ROCKWELL INTERNATIONAL EL SEGUNDO CA LOS ANGELES DIV  
MECHANICAL POWER SYSTEM FOR AIRCRAFT INTERMITTENT UTILITY FUNCT--ETC(U)

F/G 1/3

APR 79 C W HELSLEY

F33615-75-C-2011

UNCLASSIFIED

RI/LAD-NA-79-64

AFAPL-TR-79-2028

NL

3 OF 3  
AD  
A073297

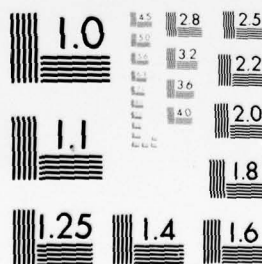


CLASSIFIED

3 OF 3

AD

A 073 297



MICROCOPY RESOLUTION TEST CHART  
NATIONAL BUREAU OF STANDARDS-1963-A

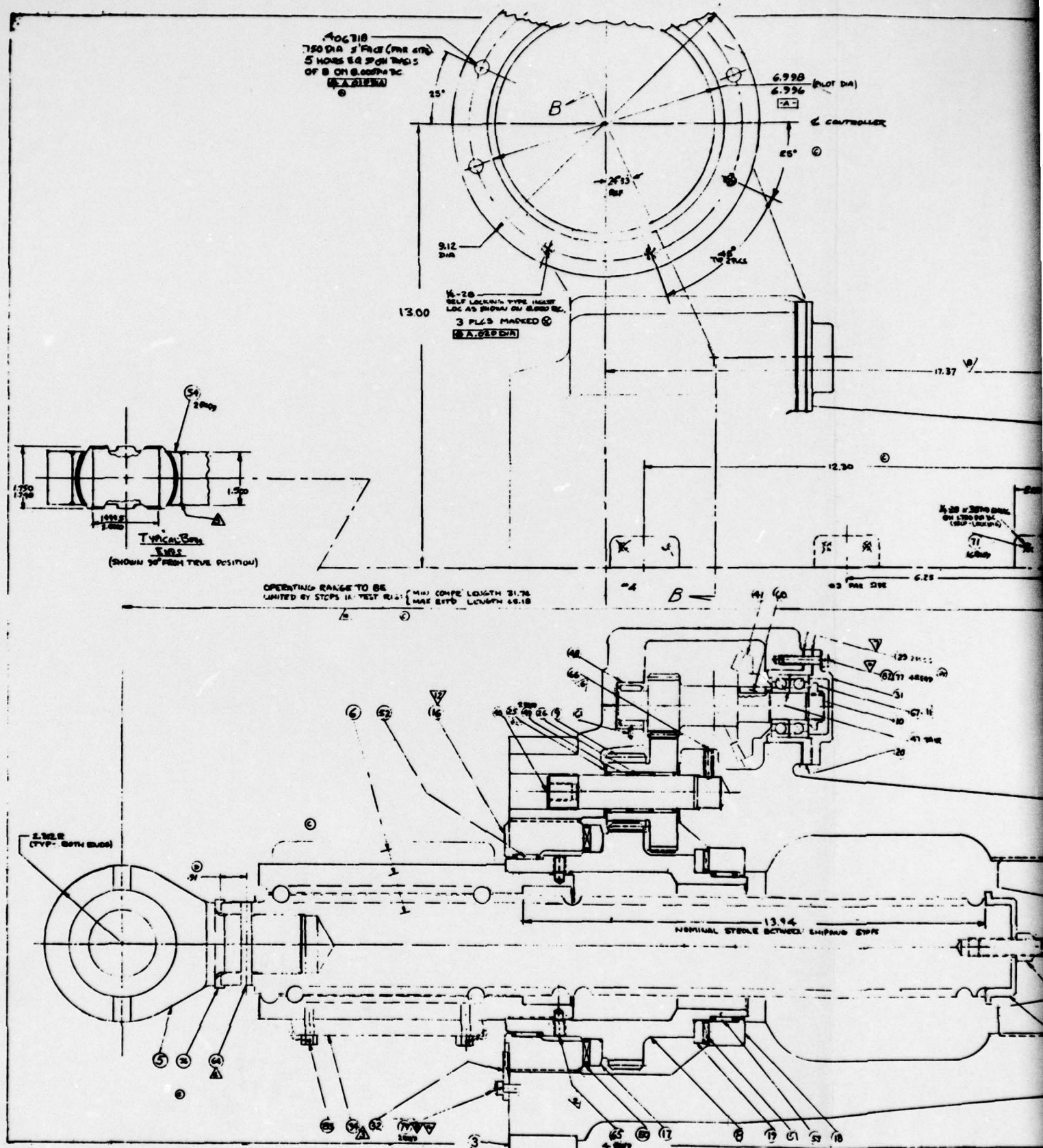
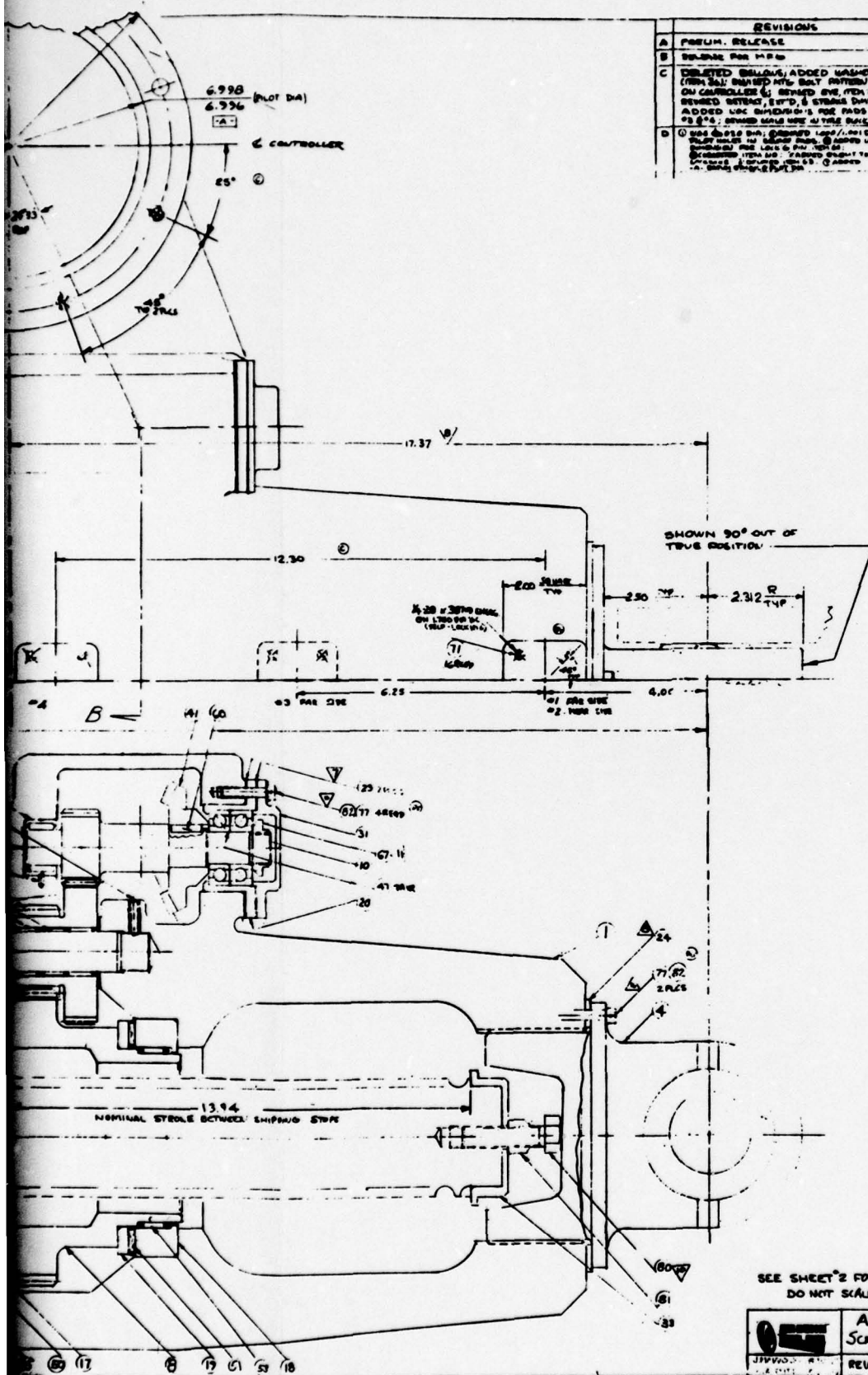



Figure 76. Screwjack Actuator Assembly, Sheet 1 183

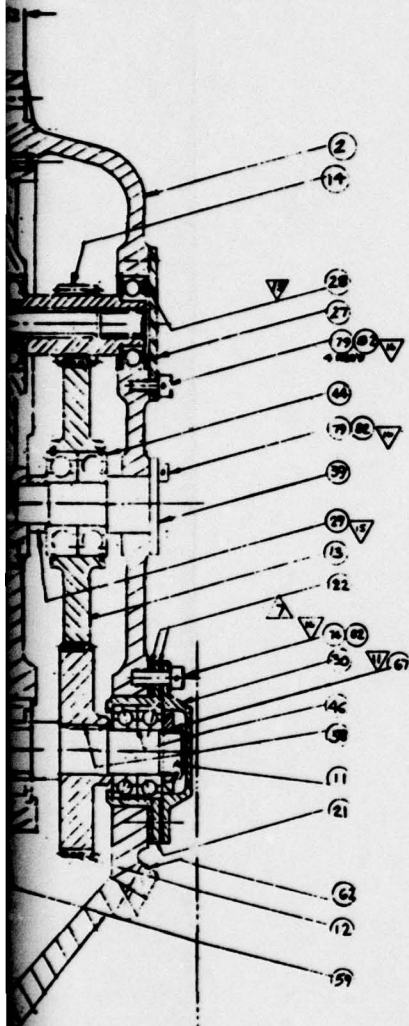




SEE SHEET 2 FOR NOTES  
DO NOT SCALE DRAW

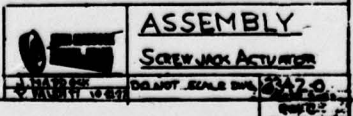
|   |                     |        |
|---|---------------------|--------|
|  | ASSEMBLY            |        |
|   | SCREW JACK ACTUATOR |        |
| JPM 1155-1  | REV D               | 2943-0 |





- 46 SECURE FASTENER WITH LOCKWIRE**
- 1** TRIM LENGTH OF SPACER **2** TO OBTAIN .003-.015 END PLAY
- 3** APPLY GRAS TUNG-OIL-13587 TO CONTACT SURFACES, BRILL SCREWS, STAYS AND SPACERS
- 4** TURN GEAR TO A QUOTE .003-.008 END TO END PLAY
- 5** AFTER TIGHTENING (6) TO ACHIEVE DESIRED PRESSURE PAUSE 10-15 SECS. TO 20 SECS. TO 30 SECS.
- 6** WITH STRESS ON MOUNTING SCREWING CLIP **7**
- 8** AFTER TIGHTENING STAY TO LOCK
- 9** ADJUST **10** TO ACHIEVE .3154 INTRACT LENGTH THERE **11** TO LOCK
- 12** TURN **13** TO ACHIEVE 17.57 DEG. ANG. POSITION OF EVE
- 14** STAY SHOT TO ACHIEVE CORRECT TIGHT CONTACTS AND STAYING CLIP ON
- 15** TURN BALL AND PIN 100% WITH NO END PLAY
- 16** BALL STAY 100% WITH NO END PLAY AND STAY 100% WITH NO END PLAY
- 17** AFTER TURNING 100% AND STAY 100% WITH NO END PLAY
- 18** PRESS FIT FOR CROSS-PIN IN
- 19** TURN **20** TO ACHIEVE 30% TURNING OF BALL AND THRU AROUND ON BALL SURFACES
- 21** AFTER TURNING 30% TURNING OF BALL AND THRU AROUND ON BALL SURFACES

NOTES:





down on this "one of a kind" item. However, in production quantities, the housing would be made of steel, and through the use of this material all basic housing walls would be reduced to at most one-third of their present thickness.

Figure 77 shows the "tower" gear train that connects the ball screw to the controller output. The controller pad is in the upper center of the figure. This gear train is grease lubricated, as is the ball screw, and reduces the controller output of 7,500 to 178 rpm at the ball nut. This ball nut speed is one-third greater than that shown in Table 2, and the reduction ratio is one-third less, being 42.15.

## TASK III - SYSTEM TESTS

### MECHANICAL POWER PACKAGE TEST PLAN

The MPP in its final form, as it was to be tested, is shown in Figure 78. The pertinent major supplier part numbers are also shown.

A system test plan was developed and is included in the appendix as Appendix B (Document No. TFD 77-639). This test plan called for a logical sequence of tests which gradually built up, building-block style, to full MPP system tests. Along the way, each component was to receive a detail component test using its predecessor in the building-block chain as a test rig. In addition, the flywheel was to have received additional development testing in a separate test rig. However, program funding did not allow this projected test program to be followed. Instead, testing was confined to certain very limited development and acceptance tests conducted by the supplier, a limited gearbox-controller test, and an attempt to operate the whole MPP as a unit. The tests which will be discussed are as follows:

- 1) Supplier controller tests
- 2) Hydraulic motor-gearbox-controller tests
- 3) MPP tests

#### Supplier Controller Tests

The following tests were conducted by the controller supplier, Traction Propulsion Inc (TPI), as part of the acceptance test requirement.

#### Controller Limit Stop Settings

The limit stop settings were made in the mechanical linkage which connects the roller (ratio position) with the 7,500 rpm limit stop valve and the zero stop valve. This mechanical linkage is shown in Figure 73 as a dotted line connecting the respective valves and rollers. As the roller assemblies approach a ratio position equivalent to  $\pm 7,500$  rpm output at rated (15,000 rpm) input speed, the 7,500 rpm limit stop valve reduces the pressure differential tending to drive the rollers to an ever increasing ratio position and continues to do so until ratio changing stops. The zero limit stop performs essentially the same function in the opposite direction except it tends to increase pressure differential to the modest degree necessary to balance the control piston return spring force and cause ratio changing to cease at the zero output ratio position.

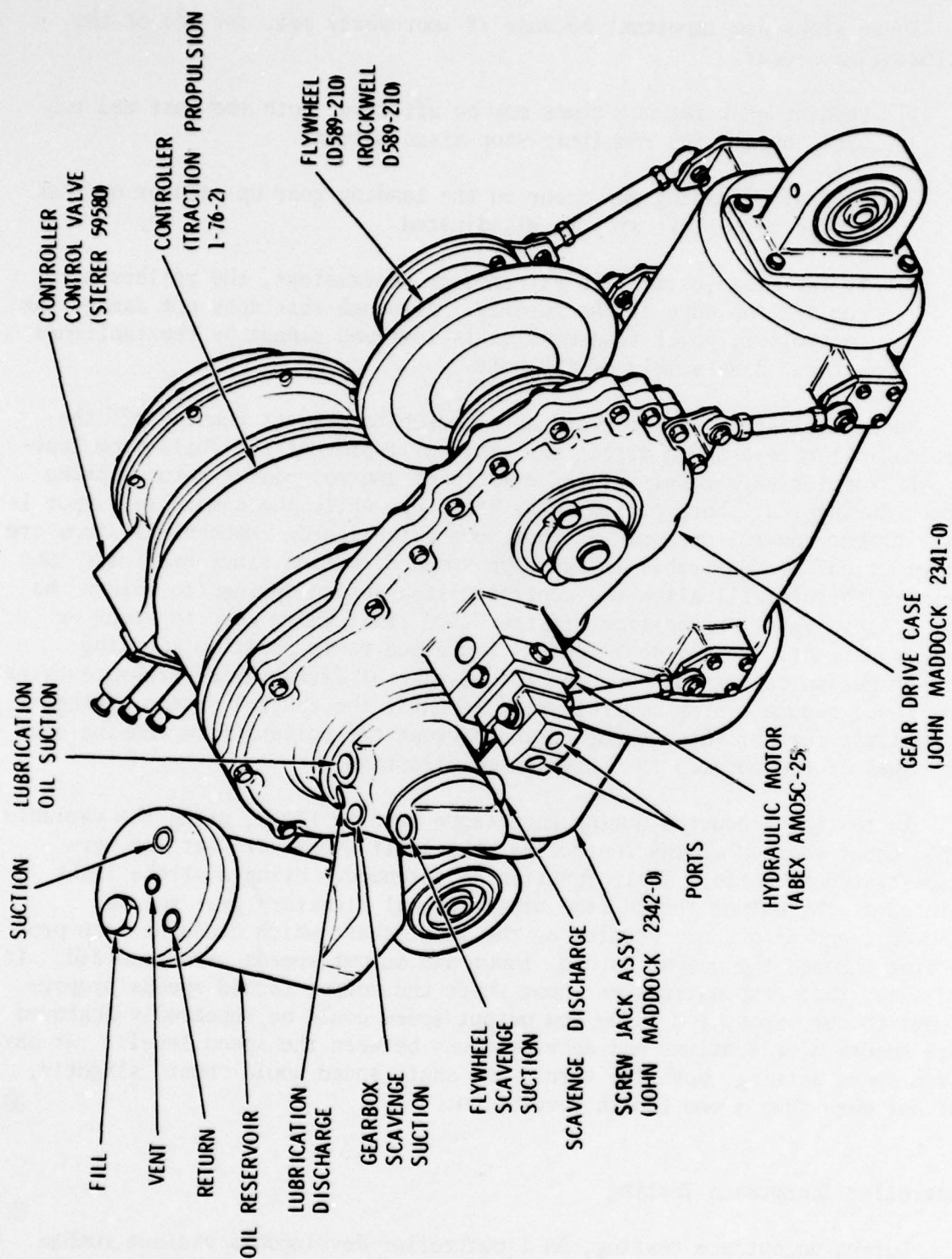


Figure 78. MPP Assembly for Test



These stops are important because if improperly set, any one of the following may occur:

- 1) Landing gear retract times may be affected, both too fast and too slow, by a 7,500 rpm limit stop misadjustment.
- 2) Excessive loading may occur on the landing gear up-stop or up-lock if the zero limit stop is misadjusted.
- 3) If the misadjustment is extreme, or nonexistent, the rollers may run off the edge of the toroids. Although this does not damage the controller, power transmission is lost and cannot be reestablished without disassembly of the unit.

Mechanical stops are provided as a backup to prevent running off the toroids in the zero-speed direction. This will prevent the rolls from leaving the toroids as a result of the effects of control piston return spring force, during that short period after start up, while the controller input is rotating but control pressure has not been established. Mechanical stops are not practical nor desirable in the high-speed direction since hydraulic lube pressure failure will allow the control piston return springs to return the unit to zero rpm. In addition, if the 7,500 limit valve were to stick or lose adjustment, the movement towards increased ratio position, working through mechanical linkage and the torque control differential pressure valve cam, would reduce system control pressure until the control piston springs could limit further ratio changing and prevent the rollers from running over the edges of the toroids in a high-speed direction.

In testing conducted during acceptance test by (TPI), using the variable ratio input section of the controller, the limit stops were set and were demonstrated to perform their function as intended. Using a strobe light pointed at the output toroid (the bidirectional planetary gear set was removed), and at a short section of the input shaft which could be seen projecting through the output toroid, input and output speeds were recorded. It was shown that combinations of input shaft and output toroid speeds proportional to zero speed and 7,500 rpm output speed could be repeatedly achieved with smooth accelerations and decelerations between the speed levels. At any given speed setting, both the toroid and shaft speed would "hunt" slightly, but not more than  $\pm$  one-fourth revolution.

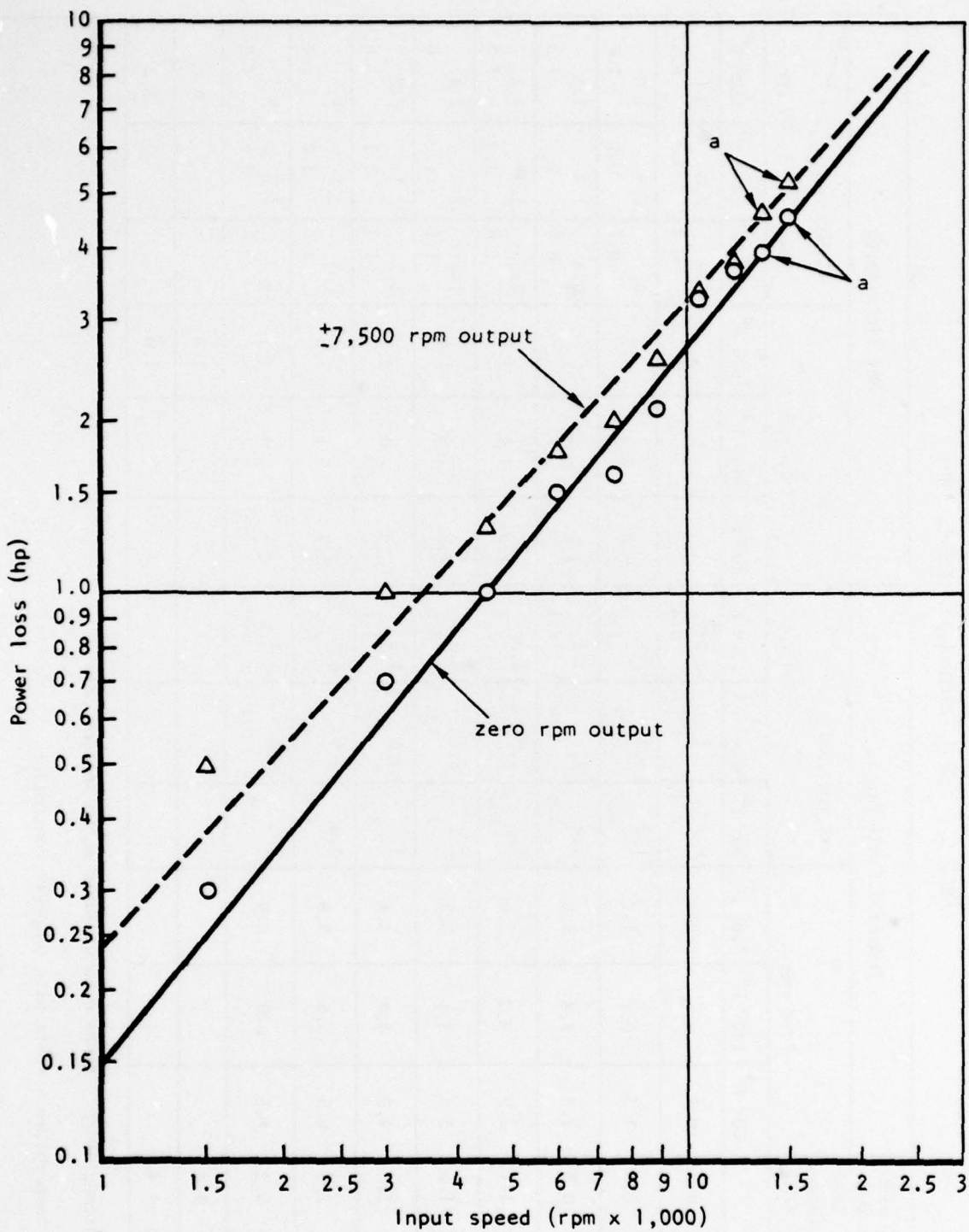
#### Controller Acceptance Testing

During acceptance testing, SN 1 controller developed a violent rumble between 12,000 and 13,000 rpm input speed. The rumble was violent enough to shake bolts off the test stand. However, even though unsuccessful at passing acceptance test, this unit did yield the first controller loss data. This data is shown in Table 5 and is plotted in Figure 79.

TABLE 5 . SN 1 CONTROLLER LOSSES (HP)

| Input Speed (rpm) | Basic Dyno Tare Losses (hp) | Measured (incl tare) |                     |                     |                    |                     |                     | Net (less tare)    |                     |                     |                    |                     |                     |
|-------------------|-----------------------------|----------------------|---------------------|---------------------|--------------------|---------------------|---------------------|--------------------|---------------------|---------------------|--------------------|---------------------|---------------------|
|                   |                             | Zero rpm             |                     |                     | +7,500 rpm         |                     |                     | Zero rpm           |                     |                     | +7,500 rpm         |                     |                     |
|                   |                             | 80° F <sup>a</sup>   | 140° F <sup>a</sup> | 180° F <sup>b</sup> | 80° F <sup>a</sup> | 140° F <sup>a</sup> | 180° F <sup>b</sup> | 80° F <sup>a</sup> | 140° F <sup>a</sup> | 180° F <sup>b</sup> | 80° F <sup>a</sup> | 140° F <sup>a</sup> | 180° F <sup>b</sup> |
|                   |                             |                      |                     |                     |                    |                     |                     |                    |                     |                     |                    |                     |                     |
| 1,500             | 0.3                         | 0.7                  | 0.6                 | 0.6                 | 0.7                | 1.1                 | 0.8                 | 0.4                | 0.3                 | 0.3                 | 0.4                | 0.8                 | 0.5                 |
| 3,000             | 0.5                         | 1.3                  | 0.9                 | 1.2                 | 1.2                | 1.4                 | 1.5                 | 0.8                | 0.4                 | 0.7                 | 0.7                | 0.9                 | 1.0                 |
| 4,500             | 0.8                         | 2.3                  | 1.5                 | 1.8                 | 1.6                | 2.1                 | 2.1                 | 1.5                | 0.7                 | 1.0                 | 0.8                | 1.3                 | 1.3                 |
| 6,000             | 1.1                         | 2.9                  | 2.2                 | 2.6                 | 2.1                | 2.5                 | 2.9                 | 1.8                | 1.1                 | 1.5                 | 1.0                | 1.4                 | 1.3                 |
| 7,500             | 1.6                         | 3.8                  | 3.1                 | 3.2                 | 2.7                | 3.2                 | 3.4                 | 2.2                | 1.5                 | 1.6                 | 1.1                | 1.6                 | 1.8                 |
| 9,000             | 2.0                         | 4.9                  | 4.0                 | 4.1                 | 3.2                | 4.1                 | 4.2                 | 2.9                | 2.0                 | 2.1                 | 1.2                | 2.1                 | 2.2                 |
| 10,500            | 2.5                         | 6.3                  | 5.6                 | 5.8                 | 4.8                | 5.9                 | 5.7                 | 3.8                | 3.1                 | 3.3                 | 2.3                | 2.5                 | 3.2                 |
| 12,000            | 3.2                         | 8.5                  | 0.9                 | 6.9                 | 5.5                | 6.0                 | 6.7                 | 5.2                | 5.7                 | 3.7                 | 2.5                | 2.8                 | 3.5                 |
| 13,500            | 3.8                         |                      |                     |                     |                    |                     |                     |                    |                     |                     |                    |                     |                     |
| 15,000            | 4.4                         |                      |                     |                     |                    |                     |                     |                    |                     |                     |                    |                     |                     |

<sup>a</sup>Oil "in" temperature - tests with variable ratio section only.<sup>b</sup>Oil "in" temperature - tests with complete controller<sup>c</sup>Extrapolated values from Figure 78



<sup>a</sup>Refer to Table 5

Figure 79. Controller Loss Characteristics



On its initial build up controller Unit 2 successfully passed its required acceptance tests. This included operating at 15,000 rpm input and zero rpm output which was a major point of interest since this was the operating condition which had caused trouble with Unit 1. On this basis, it was reported that Unit 2 was acceptable and was being shipped to Rockwell. During subsequent operation, however, the unit repeated the distinct low frequency rumble type of vibration experienced in Unit 1. This is shown as Run 1 in Table 6 .

At this point it was assumed that the problem was bearing instability and/or half frequency whirl in the bearing system that supported the output tordidal cone since this was where the distress was noted. (i.e., in the output tordidal cone thrust bearing or in the bushing associated with it); however, after 12 basic changes to the output thrust bearing cage (see Table 6) and/or the bushing system stabilizing this bearing, it was concluded that because none of the changes made any significant difference in the vibration (rumble) speed, the cause had to lie elsewhere. This was verified at the end of run 12 when it was noticed that the control system cam showed dents and beating marks which indicated that the ratio change rollers had been ratio changing in an uncontrolled and violent manner when they should have been maintaining a fixed ratio. This led to the addition of flow restrictors and the apparent successful test of run 13 (i.e., no vibration occurred and the test was only stopped due to the scoring of one of the "add on" bushings from previous tests); however, when the "add on" bushing was removed (along with the drag load it represented) ratio change vibration reappeared at the usual speed.

It then became quite certain that this vibration phenomena resulted from entrained air in the oil. Santotrac 30 does not deaerate well at 140° F (the temperature of the tests runs 1 through 14) and the deaeration system used with the test stand will not remove the entrained air at this temperature (the Santotrac oil was milky throughout the circuit). At 180° F the temperature of the initial successful test), the oil was clear. The tests were repeated at 180 F oil "in" and stable operation up to 15,000 rpm was achieved. The loss data from this test is tabulated in Table 7.

The losses in Table 7 , when added to the predicted losses of the fly-wheel and gearbox, totaled approximately 9.7 hp. This approached the 10.15 hp capability of the hydraulic motor at its 100 percent rating and 3,600 psi. This was the first of several indications that the hydraulic motor might be shy of power and torque to drive this particular assemblage of equipment.

Serial No. 2 unit was then shipped to Rockwell and testing was reinstituted on Serial No. 1 unit. These tests verified that, as long as the oil was free of entrained air, operation was stable. However, the tests also showed that some chemical or physical change was taking place in the oil which required

TABLE 6. MPP CONTROLLER CHANGES TO ELIMINATE RUMBLE

| Run No. | Thrust bearing identification | Bearing type         | Ball separator (cage)                                  |          | Journal bearing configuration   | Input power |            | Vibration speed (rpm)         | Remarks  |
|---------|-------------------------------|----------------------|--|----------|---|-------------|------------|-------------------------------|--|
|         |                               |                      | Configuration  | Material |   | Initial     | Final      |                               |  |
| 1       | MBC 7507P <sup>b</sup>        | Angular contact (AC) | Inner band riding cage (standard)                      | Bronze   | Sleeve-type bushing at output end, 0.004 dia. axial clearance, grooved shaft.<br><br>Added bushing guiding on center shaft under inboard end of toroidal cone | 5.5         | 1.7        | 10.5 × 11 × 10 <sup>5</sup>   | Ball retainer burned inner race at guide dia. It was run vibrating a long time.                  |
| 2       | MBC 7507P                     | AC                   | Ball pockets opened up 0.01" dia                       | Bronze   |   | 4.0         | 1.9        | Unchanged                     |  |
| 3       | MBC 7507P                     | AC                   | Lightened above cage by turning on a lathe             | Bronze   |   | 4.0         | 1.9        | Unchanged                     |  |
| 4       | MBC 7507P                     | AC                   | Closed cage guide dia clearance by filling with solder | Bronze   |   | 4.0         | 1.9        | Unchanged                     |  |
| 5       | MBC 7507P <sup>c</sup>        | AC                   | Standard but opened cage guide dia clearance by 0.040  | Bronze   |   | 5.1         | 1.5        | 12,000                        | Lowest loss (final), highest vibration (initial) speed except run 15                             |
| 6       | MBC 907R <sup>c</sup>         | Radial               | Standard   | Phenolic |   | 4.8         | 1.9        | 11,000                        | Violent vibration (initial)  |
| 7       | MBC 7507P <sup>c</sup>        | AC                   | New standard for phenolic cage configuration           | Phenolic |   | 4.1         | 5.1 × 2.9  | 9,000 × 9,500                 | Lowest vibration (initial) speed   |
| 8       | New MBC 7507P                 | AC                   | Standard   | Bronze   |   | 5.7         | 1.9        | 11,000                        | New baseline, check run for short time   |
| 9       | New MBC 7507P                 | AC                   | Standard   | Bronze   |   | 4.1         | 2.7        | 10.5 × 11.5 × 10 <sup>5</sup> | Additional bearing preload relative to previous runs from 0.2005 in. added shims                 |
| 10      | New MBC 7507P                 | AC                   | Standard   | Bronze   |   | 5.3<br>5.2  | 2.2<br>2.0 | 10,000<br>10,800              | Eliminated 0.005 in. shim used in run 9, total shimming now 0.008 in.                            |
| 11      | Same bearing as run 7         | AC                   | New standard for phenolic cage configuration           | Phenolic | Same as run 2 thru 9 except added stabilizing bush between stress liner & output 5  | 2.9         | 1.8<br>1.9 | 10,800<br>11,800              |  |
| 12      | Same bearing as run 7         | AC                   | New standard for phenolic cage configuration           | Phenolic |   | 2.5         | 1.9        | 11,200                        | Bushes driven between stress liner and outer housing to increase stiffness                       |
| 13      | Same bearing as run 7         | AC                   | New standard for phenolic cage configuration           | Phenolic |   | 5.4         | 5.2        | 15,500, no vibration          | 500 lbf in. 0.038 dia. flow certs in piston control lines. Test stopped, stabilizing bush froze. |
| 14      | Same bearing as run 7         | AC                   | Same as run 5  | Bronze   |   | 5.2         | 2.7        | 11,000                        | 500 lbf in. flow certs in, but stabilizing bush removed.   |

<sup>a</sup>All tests at 140° F.

<sup>b</sup>35 mm bore bearing (10-19/32 dia balls) 57.5 to 40 deg contact angle.

<sup>c</sup>Identical bearing parts except for replacement of cage.

<sup>d</sup>840,000 DN at max (15,000 rpm) input speed, 0.16,000 dn at rumble (11,000 rpm) input speed.

<sup>e</sup>Contact angle - 9 to 10 deg.

<sup>f</sup>Controller characteristics affecting bearing performance:

|                                    |                      |                |
|------------------------------------|----------------------|----------------|
| Zero controller output speed       | Input bearing        | 13,000 rpm max |
|                                    | Output toroidal cone | 24,000 rpm max |
|                                    | Ratio change roller  | 17,000 rpm max |
| 57,500 rpm controller output speed | Ratio change roller  | 7,500 rpm max  |
|                                    | Output toroidal cone | 4,500 rpm max  |

TABLE 7. CONTROLLER LOSSES (HP)

| Input speed (rpm) | Basic dyno tare losses (hp) | Measured (incl tare)       |                          | Net (less tare) |                          |
|-------------------|-----------------------------|----------------------------|--------------------------|-----------------|--------------------------|
|                   |                             | Zero rpm                   | +7,500 rpm<br>-7,500 rpm | Zero rpm        | +7,500 rpm<br>-7,500 rpm |
|                   |                             | Oil "in"<br>Temp: (180° F) | (180° F)                 | (180° F)        | (180° F)                 |
| 1,500             | 0.3                         | 0.7                        | 1.5<br>1.5               | 0.4             | 1.2<br>1.2               |
| 5,000             | 0.5                         | 1.0                        | 2.0<br>2.0               | 0.5             | 1.5<br>1.5               |
| 4,500             | 0.8                         | 1.7                        | 2.7<br>2.8               | 0.9             | 1.9<br>2.0               |
| 6,000             | 1.1                         | 2.5                        | 3.6<br>3.6               | 1.4             | 2.5<br>2.5               |
| 7,500             | 1.6                         | 3.5                        | 4.6<br>4.5               | 1.9             | 4.0<br>3.9               |
| 9,000             | 2.0                         | 4.5                        | 5.3<br>5.2               | 2.5             | 5.5<br>5.2               |
| 10,500            | 2.5                         | 6.1                        | 6.8<br>7.1               | 3.6             | 4.5<br>4.6               |
| 12,000            | 3.2                         | 7.2                        | 8.3<br>8.2               | 4.0             | 5.1<br>5.0               |
| 13,500            | 3.8                         | 9.2                        | 10.9<br>11.0             | 5.4             | 7.1<br>7.2               |
| 15,000            | 4.4                         | 11.0                       | 10.2<br>10.2             | 6.6             | 5.8<br>5.8               |



higher temperatures to get it air free. This is shown in Table 8 which records a mild tendency to rumble at 185° F. In addition, the table showed (test points 1 through 5 and 6 through 8) an unusual loss phenomena which had been repeated time after time. This was the fact that, after any disassembly and rebuild (whether old or new parts were used in the rebuild was inconsequential), the loss were initially high and then, after a shakedown run of several hours, would gradually drop by as much as 50 percent. This was not a wear-in phenomena but resulted from the various highly preloaded balls working their way from their "as assembled" position and rolling track to a minimum loss rolling track. This was attested to by the fact that, when the violent vibrational rumble occurred, the reduction in losses to minimum occurred almost instantaneously.

#### Hydraulic Motor - Gearbox - Controller Tests

In the original test plan, it had been planned that the building-block concept would be implemented by having at least two dummies (one for the screwjack and one for the controller) made of channel iron and incorporating sensing devices which would act as stand-ins for the actual equipment item until it was ready for test. This was to allow all testing (except some special flywheel testing) to be done at the site of the B-1 main landing-gear qualification test rig and to insure that the same instrumentation would be used at all times while the component was under test. The dummies had the additional advantage that they could incorporate in their framework special sensing devices (torque, speed, flow, and pressure) and any other special test equipment required for the adjacent item under test (i.e., the controller dummy would be equipped to measure gearbox output parameters and the screwjack dummy would measure controller output parameters). In the interest of cost reduction, and at a considerable increase in risk, this approach was abandoned and actual components were used in place of the dummies. This seriously impaired the ability to measure output parameters and tests could not be conducted until all components were available. Also, for this reason, a fit check became necessary before testing could proceed.

#### MPP Fit Check

All the components making up the MPP Assembly (i.e., the screwjack, controller, gearbox-reservoir, hydraulic motor, and flywheel) were assembled for fit check in the landing gear actuator qualification test fixture. The MPP as assembled is shown from the inboard side in Figure 80 and from the outboard side in Figure 81. Figure 80 shows the screwjack and its tower gear train housing along with the controller, the flywheel, and some of the outrigger support struts. Figure 81 shows the MPP from the opposite side and provides the best view of the reservoir and its sight glass, the gearbox lube-scavenge pump stack housing, and the hydraulic motor which powers the whole unit. Note that

TABLE 8. MPP CONTROLLER STABILITY TESTS SHEET 1 OF 3

| Test point | Input speed (rpm) | Measured (a) losses incl tare (hp) | Net (b) losses (hp) | Operating temperature |           | Remarks   |
|------------|-------------------|------------------------------------|---------------------|-----------------------|-----------|---|
|            |                   |                                    |                     | In (° F)              | Out (° F) |   |
| 1          | 4,500             | 2.8                                | 1.8                 | 70                    | -         | Initial startup losses (c)  |
| 2          | 4,500             | 2.1                                | 1.1                 | 140                   | -         | After 1 hr operating while attempting to heat up                  |
| 3          | 4,500             | 1.9                                | 0.9                 | 150                   | -         | After 2 hr operation  |
| 4          | 4,500             | 1.9                                | 0.9                 | 165                   | -         | After 3 hr operation  |
| 5          | 4,500             | 1.8                                | 0.8                 | 170                   | -         | After 4 hr operation, heating very slowly                         |
| 6          | 7,500             | 4.0                                | 2.3                 | 175                   | -         | After 5 hr operation, input speeded up to increase heating rate   |
| 7          | 7,500             | 3.5                                | 1.8                 | 180                   | -         | After 6 hr operation  |
| 8          | 7,500             | 3.4                                | 1.7                 | 185                   | 195       | After 7 hr operation, oil beginning to look free of air           |
| 9          | 13,500            | No reading                         |                     | 185                   | 195       | Mild vibration- backed down in speed and ran some more to heat up |
| 10         | 15,000            | 8.4                                | 3.8                 | 195                   | 205       | Air-free oil, controller operated smoothly                        |
| 11         | 15,000            | 10.2                               | 5.1                 | 195                   | 205       | Air-free oil, controller operated smoothly                        |

TABLE 8. MPP CONTROLLER STABILITY TESTS SHEET 2 OF 3

| Test point | Input speed (rpm) | Measured (a) losses incl tare (hp) | Net (b) losses (hp) | Operating temperature |           | Remarks  |
|------------|-------------------|------------------------------------|---------------------|-----------------------|-----------|--|
|            |                   |                                    |                     | In (° F)              | Out (° F) |  |
| 12         | 15,000            | 8.5                                | 5.2                 | 195                   | 205       | Air-free oil controller operated smoothly                                |
| 13         | 15,000            | 10.2                               | 5.1                 | 195                   | 205       | Air-free oil controller operated smoothly                                |
| 14         | 12,000            | 6.7                                | 5.0                 | 195                   | 205       | Air-free oil controller operated smoothly                                |
| 15         | 10,500            | 4.9                                | 1.8                 | 195                   | 205       | Air-free oil controller operated smoothly                                |
| 16         | 9,000             | 3.8                                | 1.5                 | 195                   | 205       | Air-free oil controller operated smoothly                                |
| 17         | 7,500             | 3.0                                | 1.3                 | 195                   | 205       | Air-free oil controller operated smoothly                                |
| 18         | 6,000             | 2.2                                | 0.9                 | 195                   | 205       | Air-free oil controller operated smoothly                                |
| 19         | 4,500             | 1.5                                | 0.5                 | 195                   | 205       | Operated smoothly  |
| 20         | 15,000            | 10.2                               | 5.1                 | 195                   | 205       | Moved up and down thru critical speeds smoothly - approx. 8 hr operation |



TABLE 8. MPP CONTROLLER STABILITY TESTS SHEET 3 OF 3

(a) Includes basic dynamometer tare losses which are as follows:

| <u>Input<br/>speed<br/>(rpm)</u> | <u>Tare<br/>losses<br/>(hp)</u> | <u>Input<br/>speed<br/>(rpm)</u> | <u>Tare<br/>losses<br/>(hp)</u> | <u>Input<br/>speed<br/>(rpm)</u> | <u>Tare losses<br/>(hp)</u> |
|----------------------------------|---------------------------------|----------------------------------|---------------------------------|----------------------------------|-----------------------------|
| 1,500                            | 0.5                             | 7,500                            | 1.7                             | 13,500                           | 4.6                         |
| 3,000                            | 0.8                             | 9,000                            | 2.3                             | 15,000                           | 5.1                         |
| 4,500                            | 1.0                             | 10,500                           | 3.1                             | 16,500                           | 6.6                         |
| 6,000                            | 1.3                             | 12,000                           | 3.7                             |                                  |                             |

(b) Controller losses as tested without output gearing.

(c) The losses in the controller, as initially assembled (or as reassembled after teardown), is always at least 25 percent greater than the losses which exist after a shakedown run of at least 1 hour.

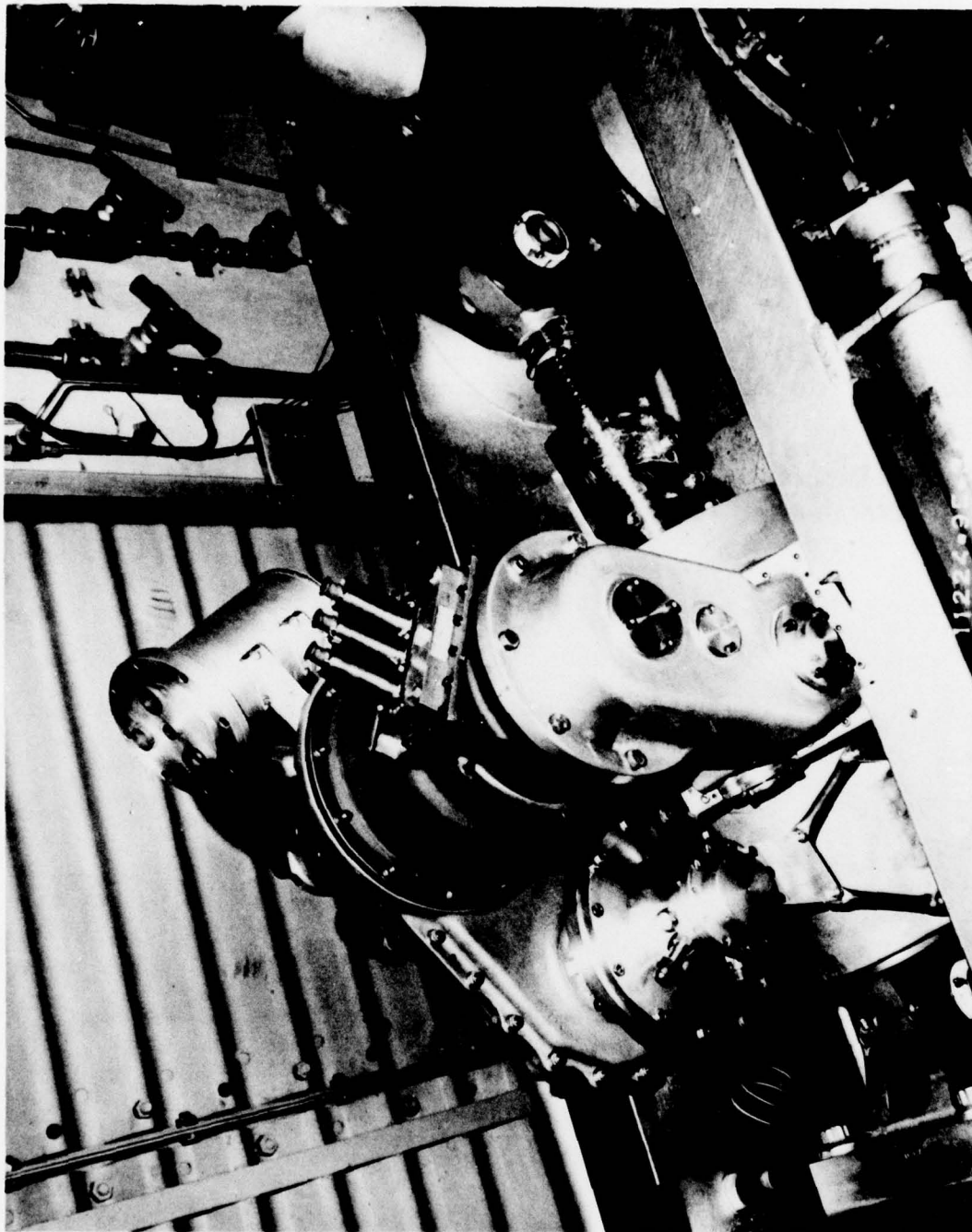


Figure 80. MPP Assembly Fit Check - Inboard View

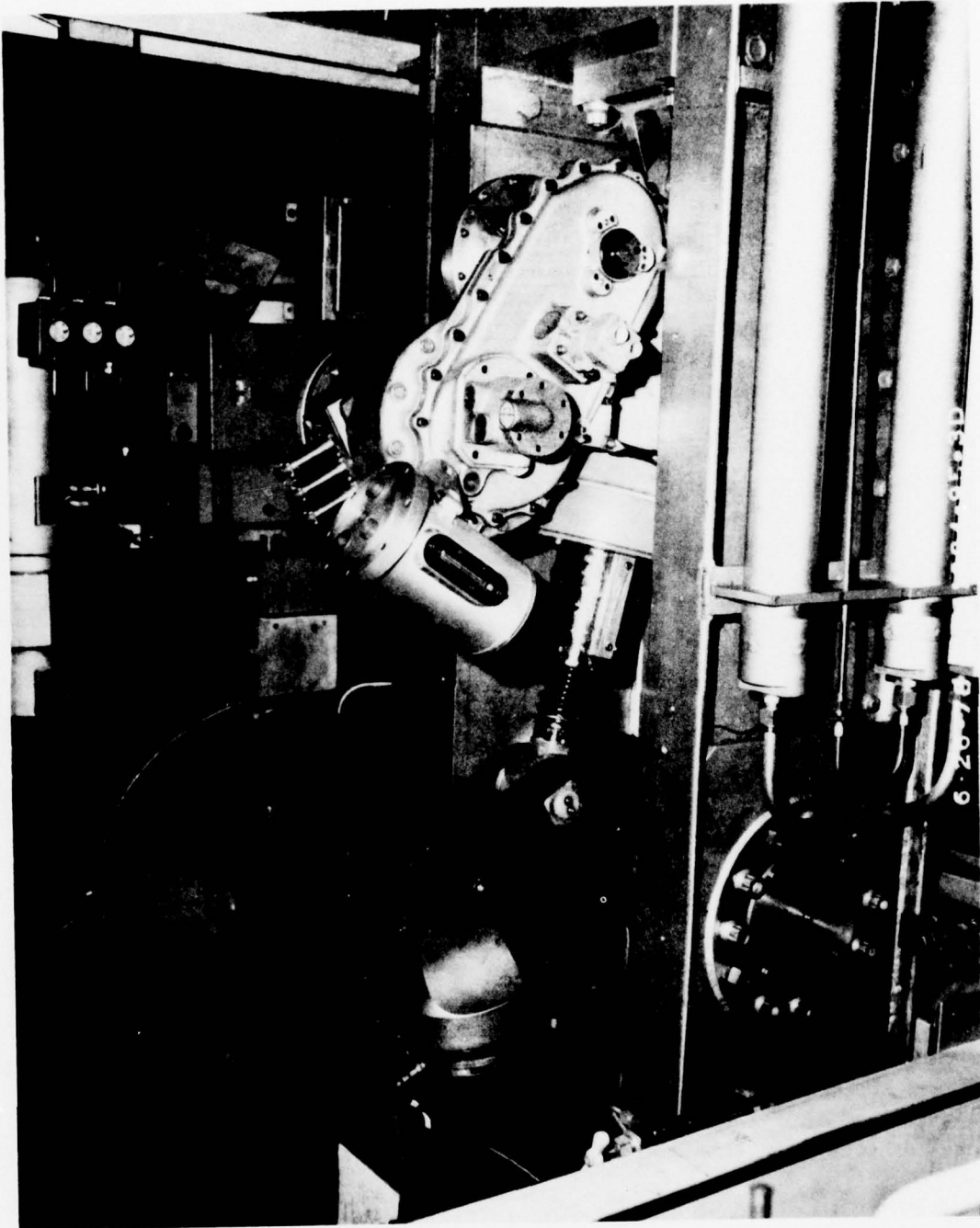


Figure 81. MPP Assembly Fit Check - Outboard View



the hydraulic motor is by far the smallest unit making up the MPP and is even smaller than the lube-scavenge pump stack. The fit check was accomplished with no major difficulties and all interfaces seemed to mate perfectly.

#### MPP Rework to Test Configuration

After fit check, the MPP was partially disassembled so that it could be reworked to its first test configuration. For this test, the flywheel was removed and a special cap placed over the flywheel pad on the gearbox to collect lube oil and redirect it to the flywheel scavenge pump inlet. The sun gear, which is an integral part of the flywheel input shaft, also had to be removed because, without the flywheel in place, its output end is unsupported and it would whip uncontrollably at high speed. The input gear in the screwjack tower gear train as well as its closeout cap was also removed and a torque/speed sensor unit was installed in its place. In effect, the controller output was disconnected from the screwjack and a means for measuring controller output characteristics (in terms of speed, torque, and snubbing) substituted so that controller performance could be verified before any attempts to run the screwjack into its stops were made. The first configuration consisted of operating the hydraulic motor, the gearbox-scavenge lube pump stack, the reservoir, and the controller as a unit. In this way, in addition to measuring controller output characteristics, problems involved with filling, lubrication, scavenging deaeration, and general test rig operation could be worked out before attempting to transfer high loads through the power train.

#### Operational Tests

Using the test configuration discussed above, certain operational tests were conducted. The first test consisted of accelerating the unit to and operating at 6,000 rpm (controller input speed). This was approximately 40 percent of rated speed and was selected as the initial speed to be used to heat the system up to 190° F. It will be recalled from earlier discussions that it is necessary to achieve 190° F before attempting to operate the controller to ensure proper deaeration of the fluid so that controller instability will not be encountered. The unit operated smoothly and quietly at 6,000 rpm; however, system heating was occurring at a very low rate and, as seen in a sight glass in the lube pressure line, there was considerable aeration in the oil being supplied to the controller. This was a disappointment because it had been hoped that the swirl-type reservoir used in the MPP would deaerate the oil more effectively than had been the case in tests at the controller suppliers.

In order to increase the heating rate, the input speed was raised to 7,000 rpm. The unit continued to run smoothly for several minutes and then there was a cyclical speed change followed by a self induced slow down. The

unit was shut down and while it was coasting to a stop, it was noted that the reservoir had suddenly been emptied. Since there were no external leaks, it was at first assumed that the missing oil might have leaked to the water side of the heat exchanger. This was checked, but no oil was found. The only remaining place then was the gearbox sump.

It was felt that oil could remain in the gearbox sump for any one of three reasons as follows:

- 1) Sheared shaft key to the scavenge pump
- 2) Blocked scavenge pump suction or return line
- 3) Excessive foaming in gearbox

In order to check out Reasons 1 and/or 3, the unit was gingerly started, after what was considered sufficient time to allow a majority of the foam to settle, and was run at a low speed. Although there was no sign of excessive friction or binding, the unit failed to re-establish scavenge flow (as evidenced by refilling the reservoir) and the lube pump continued to pump air (as evidenced by large air bubbles in the pressure line sight glass).

Based on this data suspicion focused on Reason 2 (line blockage). All pertinent lines were disconnected and checked, as were all filters, and no blockage was found. However, when the scavenge suction line at the bottom of the gearbox was disconnected, a large amount of solid oil drained out which solved the mystery of the location of the missing oil. This refocused attention on Reason 1 (failed scavenge pump).

The lube-scavenge pump stack was removed and disassembled. It was found to be in excellent shape with no sheared keys or other signs of internal damage. This information caused the finger to be repointed at Reason 3 (foaming). It is now believed that the increase in speed from 6,000 to 7,000 rpm was enough to upset the delicate balance of foam settling time versus foam generation rate to the point where the scavenge pump lost its prime and could not regain it. The apparent solutions are as follows:

- 1) Heat the unit and all the oil in the circuit to 190° F prior to starting any tests rather than depending on operation to heat the oil.
- 2) Determine if a foam suppressant has become available for Santotrac fluids and, if so, procure some.
- 3) Change fluid.

All three possibilities were being explored at the time the test program was terminated.



### Final Demonstration Test

In an effort to demonstrate operational functioning of the whole MPP, it was decided to conduct one last test with all components mounted in place. This test was to have been run at half-speed, i.e., below the speed where foam generation had been a problem, and well below the speed at which "rumble" in the controller had been encountered.

When conducting the initial operational tests, it had frequently (although not always) been necessary to give the hydraulic motor a manual torque boost during start up to overcome breakout friction. This was done by means of a wrench used on the shaft of the torque/speed sensor at the controller output. Since overcoming breakout friction had been an erratic problem without the flywheel mounted, it was felt that the additional drag resulting from the flywheel would amplify the problem.

It was believed that a large part of the starting torque problem might be the high initial loss phenomena, characteristic of the controller prior to run-in, shown in Table 8 and discussed on page 196. It was felt that, even though the unit, with the flywheel attached, might require several assisted starts, it would eventually start by itself. When this occurred, the torque/speed sensor could be removed and the output of the controller could be reconnected to the screwjack.

However, the actual tests led to a different conclusion. The first attempted start failed to achieve rotation even though the pressure was raised to 3,900 psi. The second attempted start was assisted by a drill motor applied to the torque/speed sensor's shaft. The unit accelerated easily to 16,000 RPM flywheel speed and, with the drill motor removed, ran with an unexpectedly low  $\Delta P$  (1,050 psi) at this speed. Two data traces from the tail end of the run are shown in Figures 82 and 83. Figure 82 shows the flywheel bearing inner race speed which, in this instance, is presumed to be equal to flywheel speed. The hash in the trace may be either unfiltered electrical hash in the instrumentation (this was the first shake-down run on the instrumentation), or it may indicate incipient differential speed in the journal bearing portion of the journal bearing. Figure 83 shows the input and output hydraulic pressures to the hydraulic motor, and shows that the differential pressure while running averages 1,050 psi.

The output of the controller was cycled several times between gear extend, stop, and gear retract and performed smoothly. The unit was then shut down and attempts to restart were made; none were successful. As soon as the drill motor was removed the unit slowed gradually to a stop. Although it could not be proven, it was felt that the phenomena experienced was due to some kind of "force fight" between the rollers in the controller at low speed. In the one successful test, the unit succeeded in achieving sufficient speed to get the rollers into a balanced, "non-fighting" position. In the other attempts the rollers, after the previous shutdown, had assumed two slightly different and more adverse ratio change positions which prevented further successful starts.



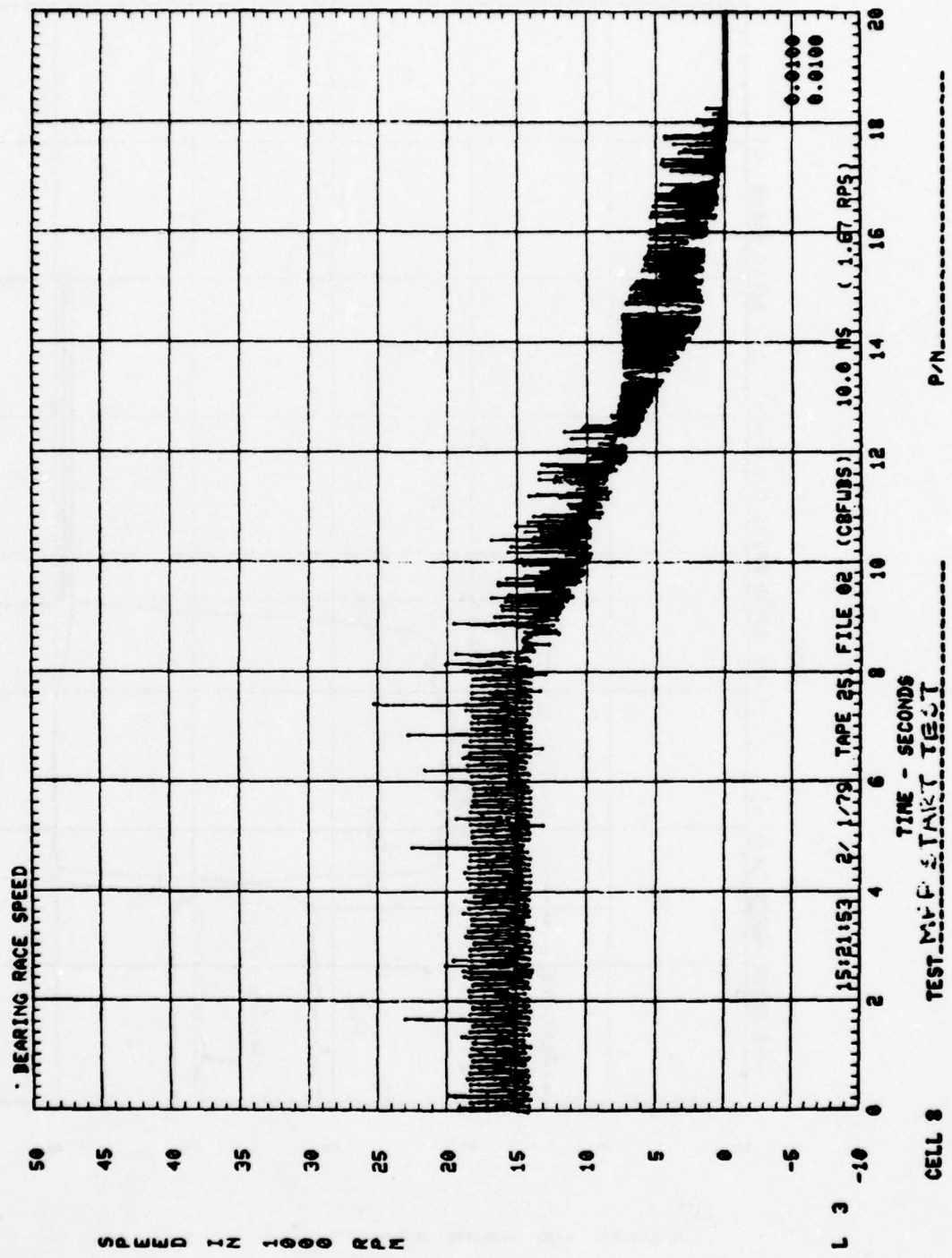


Figure 82. Bearing Race Speed

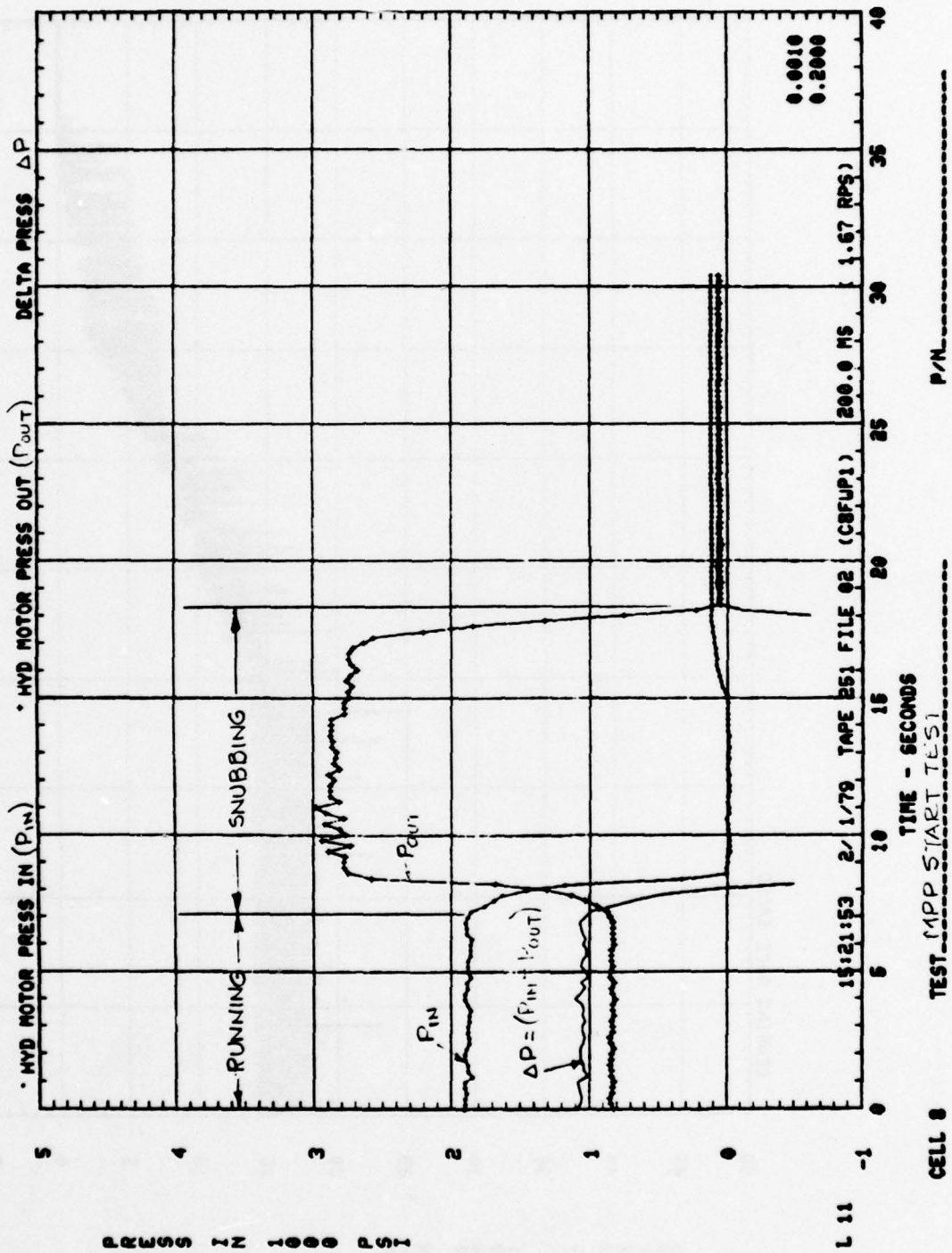


Figure 83. Hydraulic Motor Pressure

### SECTION III

#### CONCLUSIONS AND RECOMMENDATIONS

Although insufficient tests were run to draw any hard and fast conclusions, several general observations and recommendations can be made:

- 1) Both the flywheel and the controller need extensive testing as individual components before any attempt is made to integrate them into the MPP. They need this, not only to provide time for debugging, but so that their individual performance characteristics can be evaluated and documented to provide a basis for trouble shooting the MPP when it has arrived at the integrated testing phase. Time was allotted for these types of tests in the original test plan (see Appendix B), but it is now felt that more time and more allocations for redesign and/or rework than originally anticipated would be necessary.
- 2) The serious foaming problem encountered with Santotrac fluid was unexpected. If further tests were to be conducted on the MPP and its components, it might be well to conduct these tests with M2V fluid.
- 3) The flywheel design does not appear to be completely satisfactory. It is now apparent that a ferro fluid seal cannot be used inboard of the bearings in this type of application. The shaft deflections, incident to passing through critical speed and/or those resulting from dynamic unbalance or precessional loads, eat up the small clearance allowable between the shaft and the inner diameter of the seal. This could be avoided by heavying-up the shaft, but would defeat its purpose by increasing the differential surface speed between shaft and seal to an unacceptable value. Carbon face seals are a stopgap measure, but do not appear to be the ultimate solution.
- 4) The controller appears to be a rugged piece of equipment which is overdesigned for this application. The erratic start-up drag torque characteristics may be inherent to the unit, but their reduction to reasonable values probably involves only fine-tuning the ratio change system. From the very small amount of testing conducted, it appears that the controller will meet the output speed, load, acceleration, and deceleration requirements. However, even a smaller unit more properly sized to the load requirements will not meet the zero-output loss requirement as long as it must use the regenerative layout.



NA75-363B

SERIAL NO.

APPENDIX A  
SPECIFICATION  
POWER TRANSMISSION GEARBOX  
MECHANICAL POWER PACKAGE

*F. D. Halferty*  
F. D. HALFERTY  
ADVANCED DESIGN

*C. W. Helsley Jr*  
C. W. HELSLEY  
ENERGY SYSTEMS PROGRAM MANAGER

Rev. B: 12-14-77  
Rev. A: 11-26-75  
DATE 05-16-75  
NO. OF PAGES 13



Rockwell International

Los Angeles Division  
International Airport  
Los Angeles, California 90009  
(213) 670-9151

PRECEDING PAGE BLANK



## GEARBOX

A. GENERAL

This specification establishes the requirements for a power transmission gearbox, the central unit of a Mechanical Power Package (MPP) which will be developed and tested by the Los Angeles Aircraft Division of Rockwell International Corporation (RI) for the Air Force Systems Command, Aero Propulsion Lab, Wright Patterson Air Force Base, Dayton, Ohio, Contract F33615-75-C-2011.

The MPP, described schematically in Figure 1, is intended to replace the high horsepower (high delivery) hydraulic actuation systems of certain intermittent duty aircraft functions with a low horsepower, stored energy system to eliminate the high peak demands which tend to size an aircraft hydraulic system.

As shown in Figure 1, the gearbox will receive power from a pad-mounted hydraulic motor at moderate speed and utilize that power to accelerate and maintain a pad-mounted flywheel assembly at  $88,235 \pm 800$  RPM. This is the energy storage phase.

A third pad on the gearbox will mount a reversible, infinitely variable, mechanical transmission type controller. During the energy storage phase, the controller is programmed to zero output. During the energy utilization phase, energy is extracted from the flywheel by the controller via the gearbox. The controller is programmed to the direction of output rotation desired, and power is transferred through a reduction gear train to a ball screw actuator which provides linear motion to accomplish the aircraft actuation function.

After the actuation function is complete, the controller returns to zero output, and the flywheel is accelerated by the hydraulic motor to its peak energy storage RPM.

B. OPERATING REQUIREMENTS

1. The rated speed and directions of rotation of the various gearbox pads are shown in Figure 1. Maximum speed will not exceed 105% of the rated speed.
2. The maximum operating torques which will be encountered at the various gearbox pads are as shown in Table I.

C. ENVELOPE AND ARRANGEMENT

The arrangement of the gearbox and gearbox mounted components will be

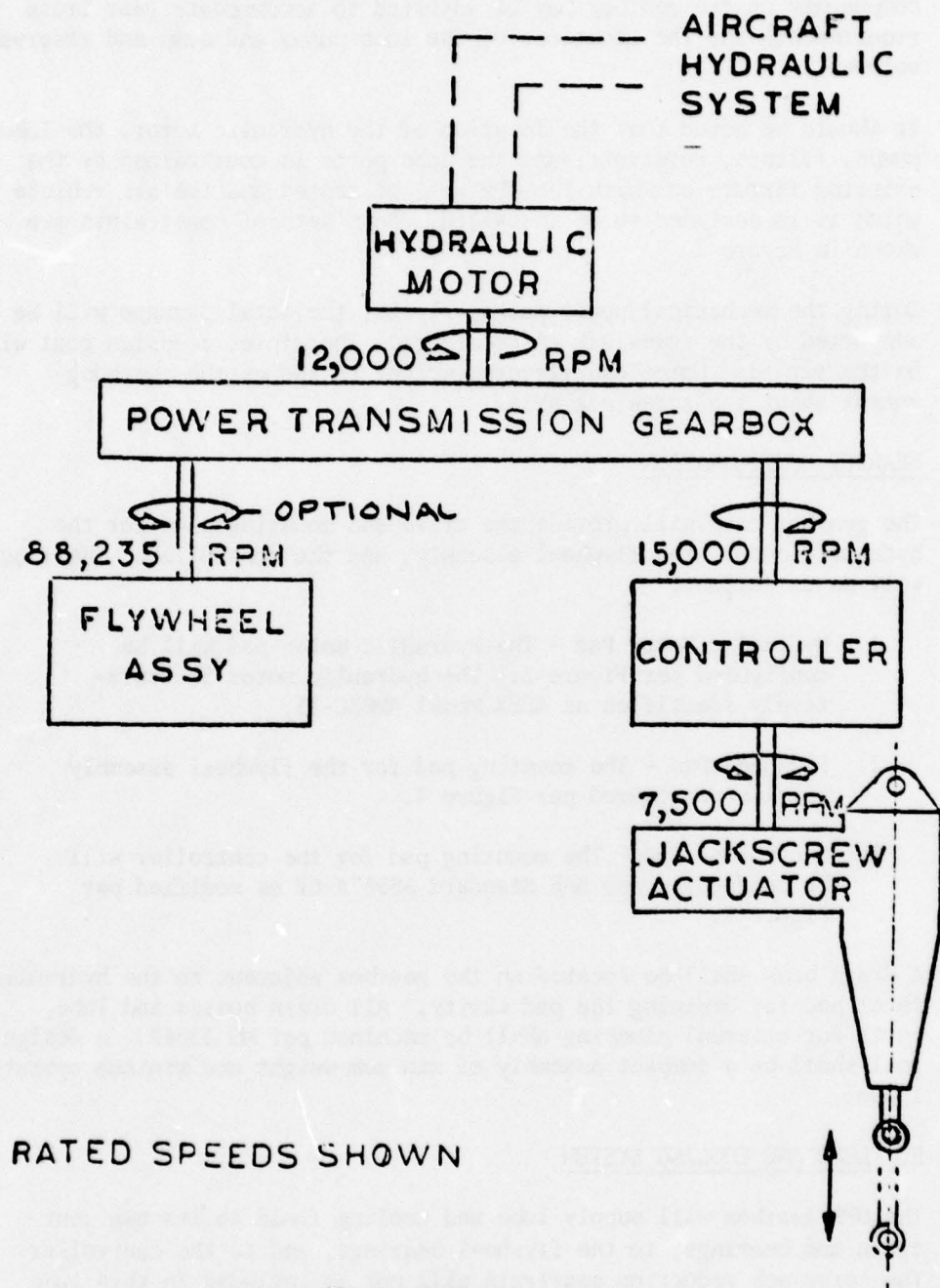


FIGURE 1  
SCHEMATIC - MECHANICAL  
POWER PACKAGE



essentially as described in Figure 2. Relative positioning of the major components on the gearbox may be adjusted to accommodate gear train requirements and the locations of the lube pumps and sump and reservoir volumes.

It should be noted that the location of the hydraulic motor, the lube pumps, filters, reservoir, and the lube ports is constrained by the existing fixture on which the MPP will be tested and the air vehicle in which it is designed to be installed. Both sets of constraints are shown in Figure 2.

During the mechanical power package tests, the total package will be supported by the screwjack end bearings. Therefore, a design goal will be the minimization of cantilevered weight to reduce the overhung moment about the screwjack axis.

#### D. GEARBOX CONFIGURATION

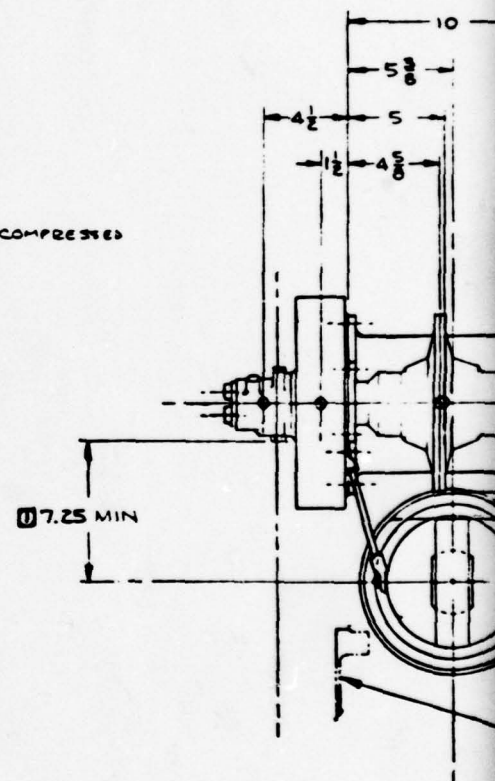
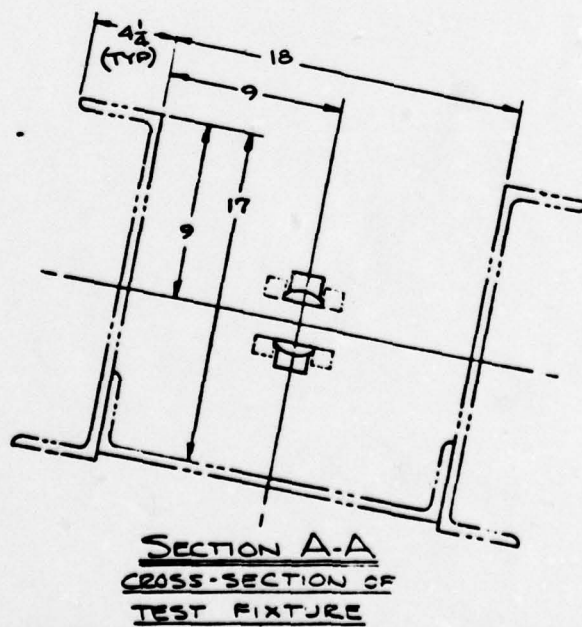
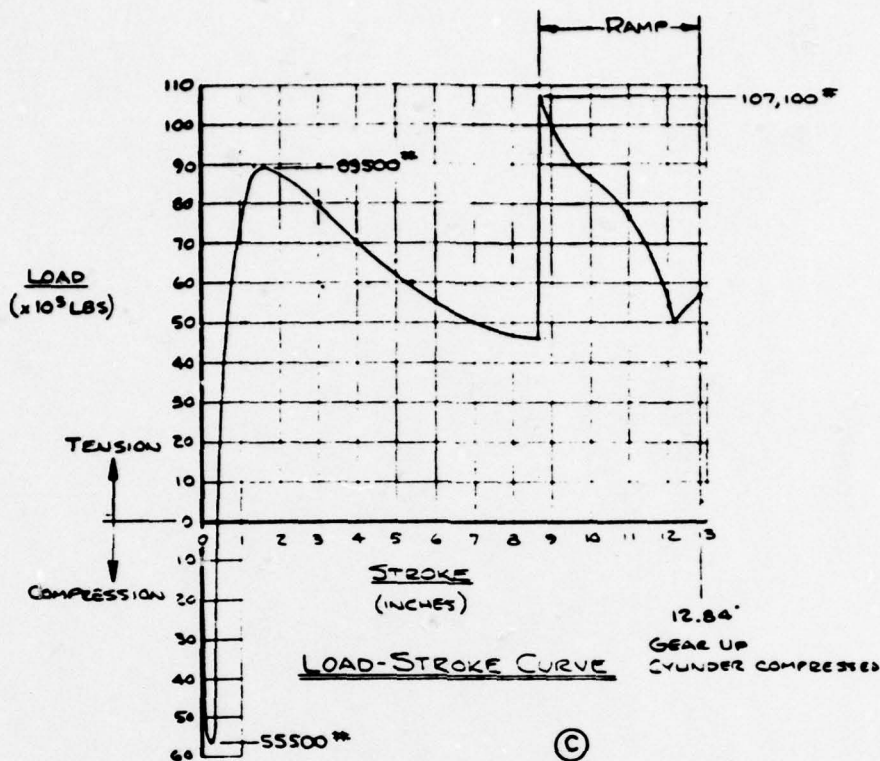
The gearbox case will provide the drive and mounting pads for the hydraulic motor, the flywheel assembly, and the controller. Interfaces will be as follows:

1. Hydraulic Motor Pad - The hydraulic motor pad will be configured per Figure 3. The hydraulic motor is tentatively identified as ABEX Model AM05C-25.
2. Flywheel Pad - The mounting pad for the flywheel assembly will be configured per Figure 4.
3. Controller Pad - The mounting pad for the controller will be configured per SAE Standard AS967A-6V as modified per Figure 5.

A drain boss shall be located on the gearbox adjacent to the hydraulic motor pad for draining the pad cavity. All drain bosses and lube ports for external plumbing shall be machined per MS 33649. A design goal shall be a compact assembly of minimum weight and minimum operating losses.

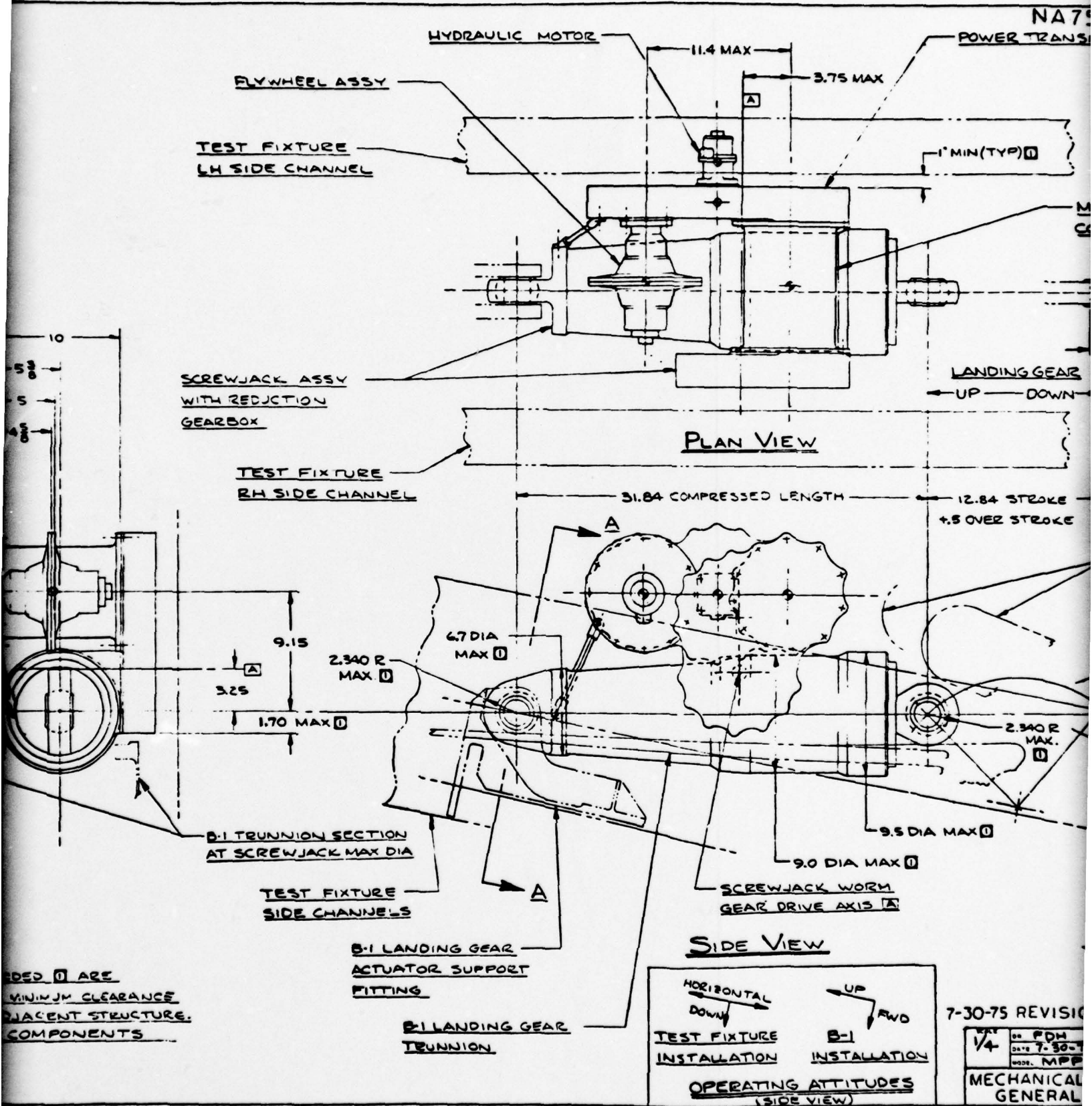
#### E. LUBE AND COOLING SYSTEM

The MPP gearbox will supply lube and cooling fluid to its own gear train and bearings, to the flywheel bearings, and to the controller. The screwjack reduction geartrain will not be included in this lube system. The fluid used for this application will be SANTOTRAC 30, Monsanto Industrial Chemicals, St. Louis, Mo.



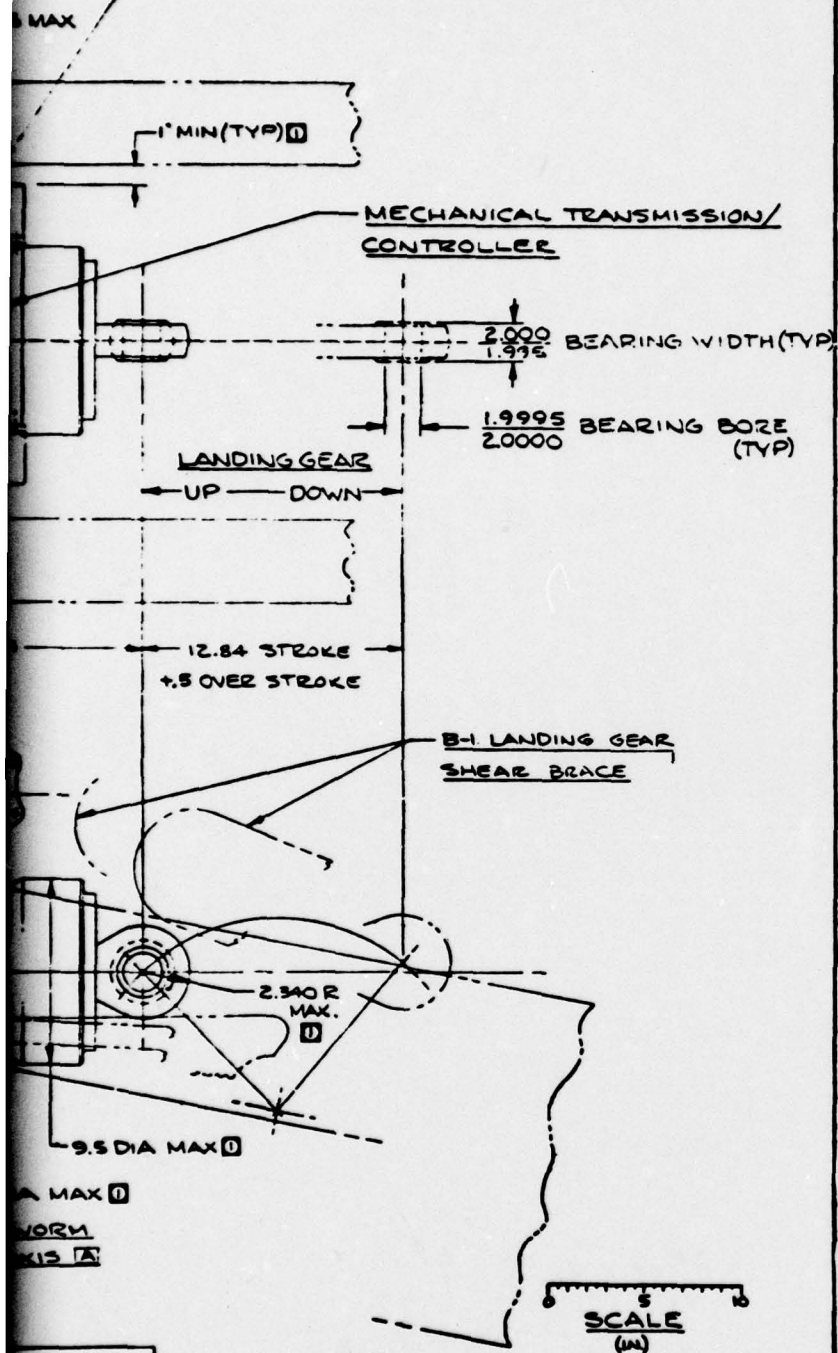
2. DIMENSIONAL LIMITS CODED 01 ARE  
REQUIRED TO MAINTAIN MINIMUM  
BETWEEN THE MPP & ADJACENT  
1. APPROXIMATE CGS OF COMPONENTS  
SHOWN

NOTES



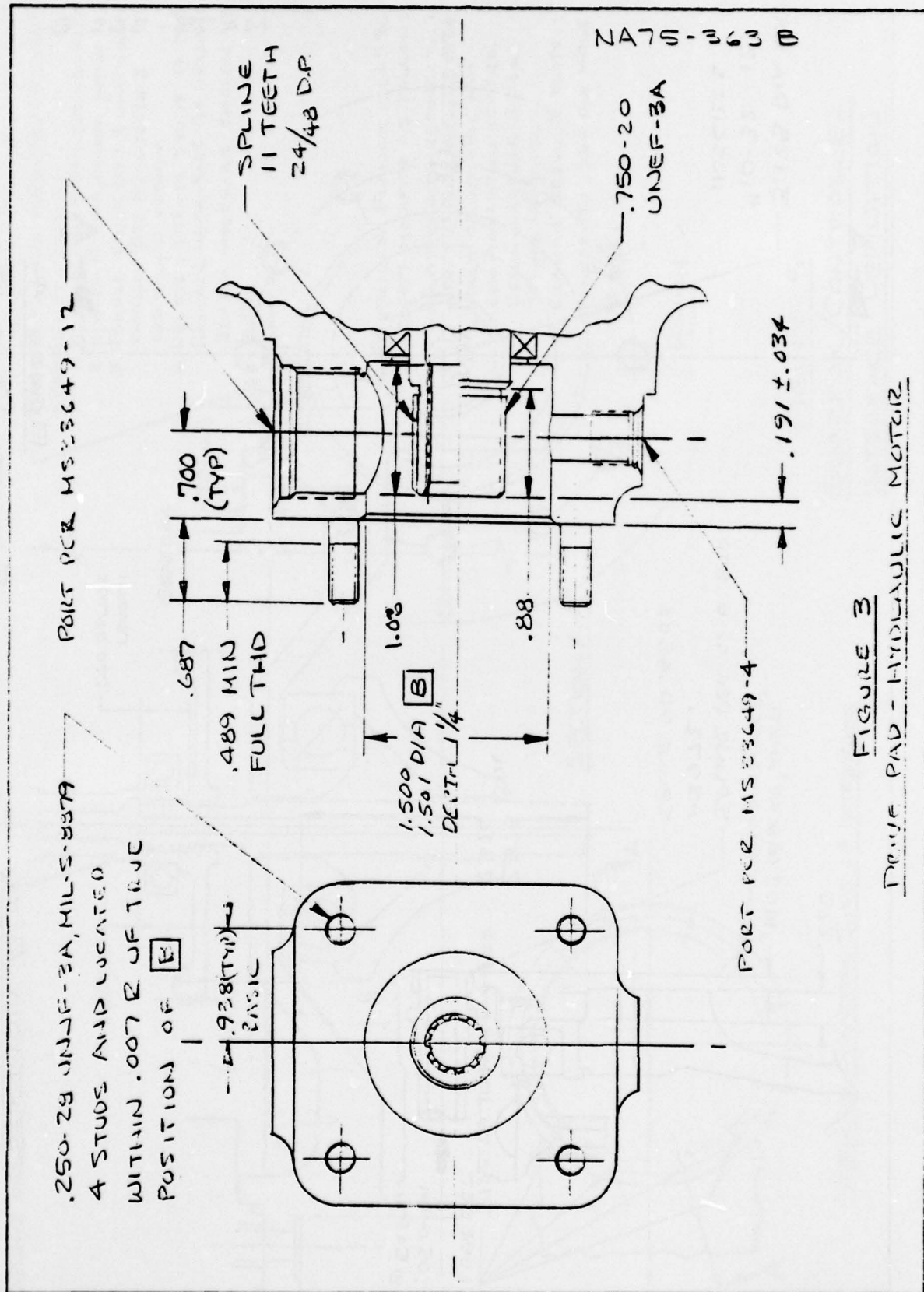


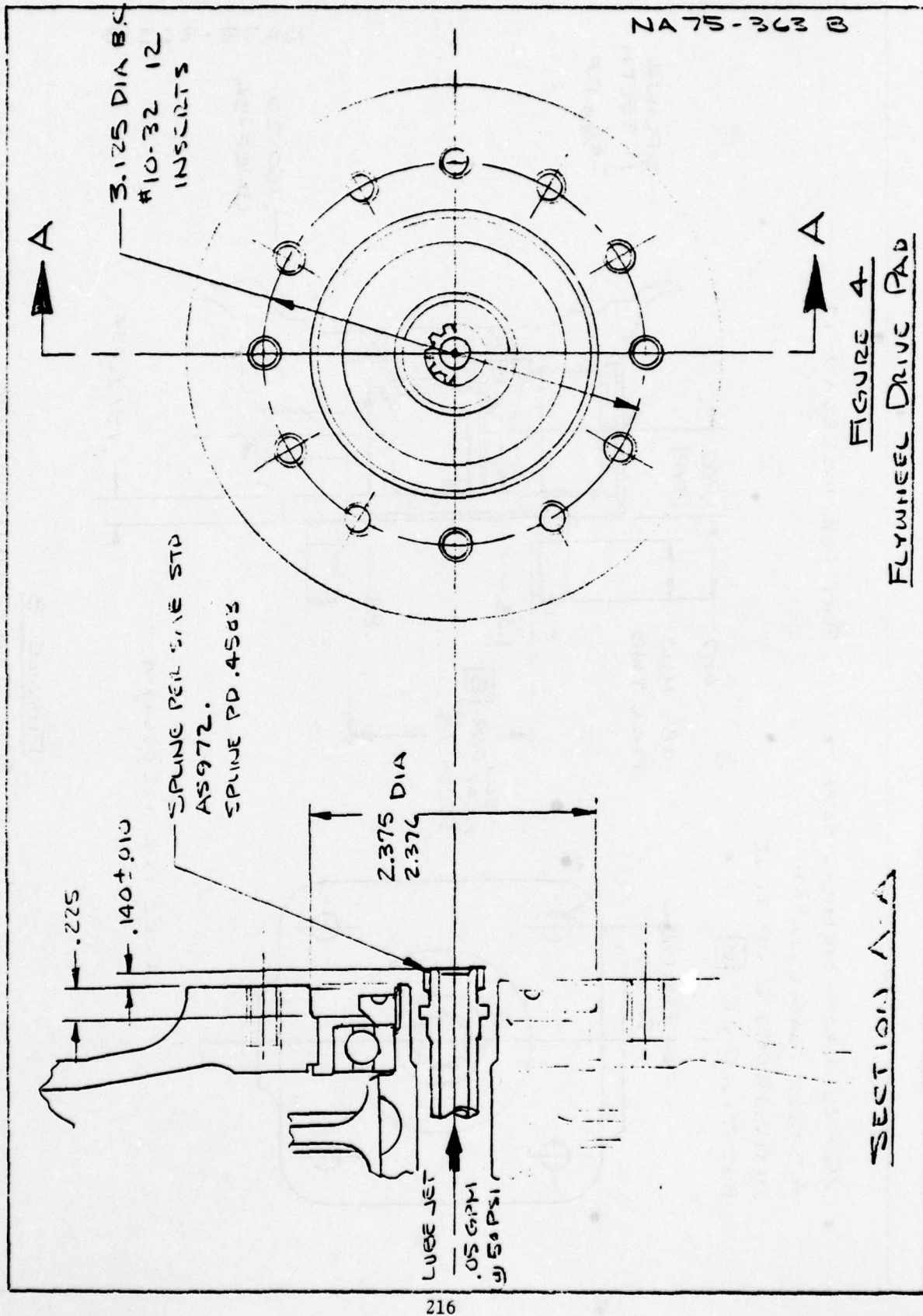
NA75-363B FIG. 2

POWER TRANSMISSION GEARBOX

7-30-75 REVISION B - REVISED &amp; REDRAWN

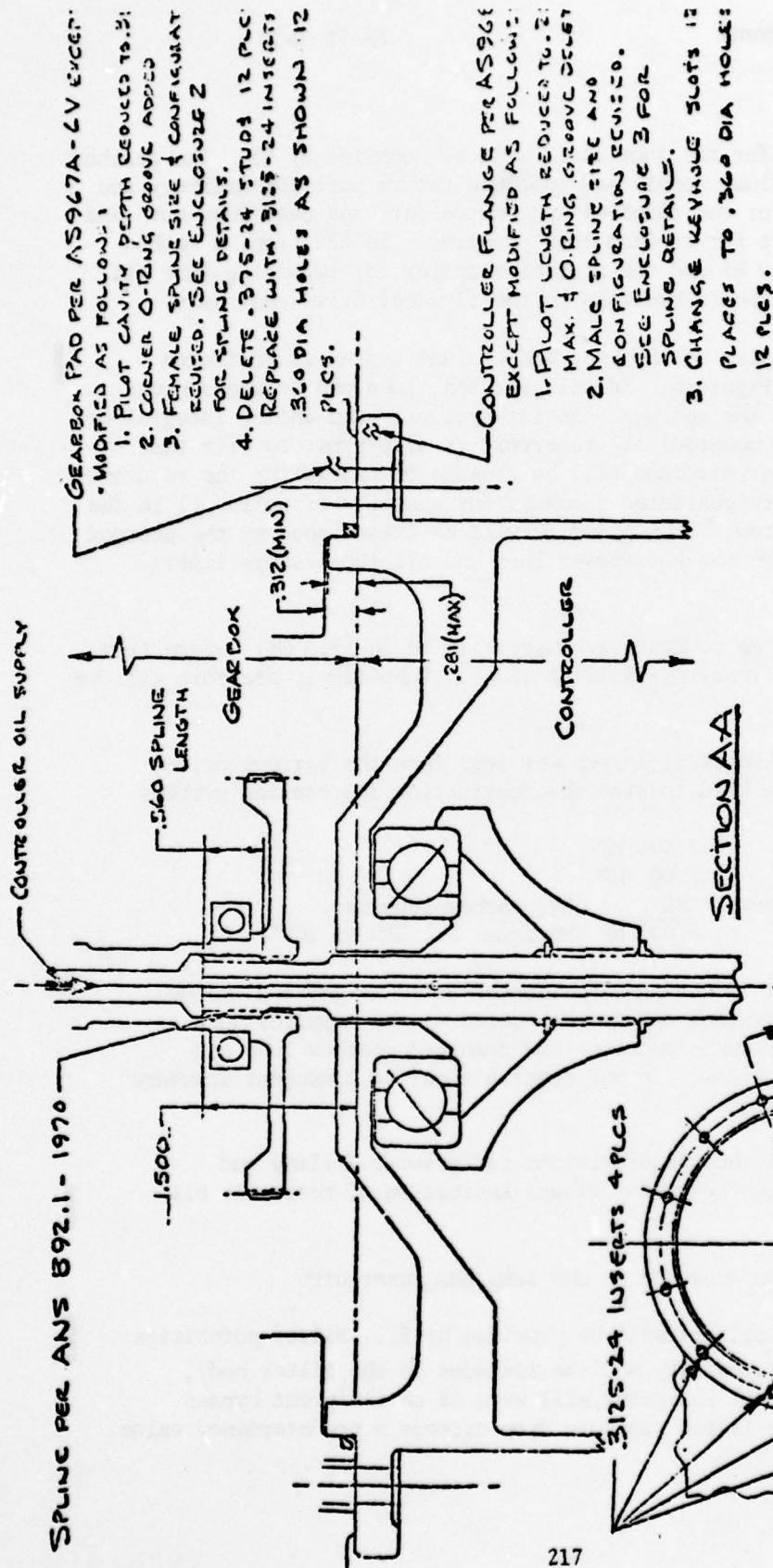
|  |              |   |                    |
|--|--------------|---|--------------------|
| REV<br>1/4                                       | BY<br>PDH    | Los Angeles Aircraft Division<br>Rockwell International | ADVANCED<br>DESIGN |
| DATE<br>7-30-75                                  | MODE.<br>MPP | INTERNATIONAL AIRPORT - LOS ANGELES, CALIFORNIA 90009   |                    |
| MECHANICAL POWER PACKAGE-<br>GENERAL ARRANGEMENT |              |   | D589-200           |







NA75-363B





The coolant loop for the lube fluid will be supplied by RI. The gearbox will provide one lube supply and one lube return port for delivery and return of fluid for the flywheel and controller, and one 'lube out' and one lube 'in' port for coolant loop plumbing. In addition, a method will be evolved by RI and the gearbox supplier for supplying lube oil to the flywheel inboard bearings on the flywheel drive gear axis.

One potential version of the lube and coolant system is portrayed schematically in Figure 6. In this version, lube and scavenge pumps are provided with the gearbox. An integral oil sump and an integral or separate (gearbox mounted) oil reservoir is also provided with the gearbox. The reservoir/sump will be capable of deaerating the return oil sufficiently to guarantee a consistent quantity of solid oil in the lube pressure system. Sump capacity will be established by the gearbox supplier based upon the horsepower loss and oil temperature limits given below.

Maximum oil out temp to heat exchanger will be 300°F. Oil return from heat exchanger to reservoir will be 180°F. Lube supply pressure will be 50 PSI MIN.

The following estimates of horsepower loss from the various driven components will be used to size the lubrication and cooling systems:

|                 |          |                              |
|-----------------|----------|------------------------------|
| Flywheel        | 2.000 HP |                              |
| Controller      | 2.00 HP  |                              |
| Adapter Gearbox | TBD      | (By gearbox supplier)        |
|                 | 6.00 HP  | (Maximum 5.1 GPM at 100°F T) |

In the interest of reduced gearbox losses (also weight and volume) other simplified systems may be considered by the supplier such as combined reservoir/sump functions and combined gearbox lube and scavenge pump functions. In any event a separate component scavenge pump will be required.

The reservoir will include provisions for gravity filling and suitably placed sight gage for visual indication of reservoir oil level.

Drain plugs will be provided on the sump and reservoir.

Lube and scavenge filters will be provided by RI. Filter porosities are TBD. Bypass capability will be included in the filter body, and a visual (popout) indicator will warn of an incipient bypass condition when the filter pressure drop exceeds a predetermined value.

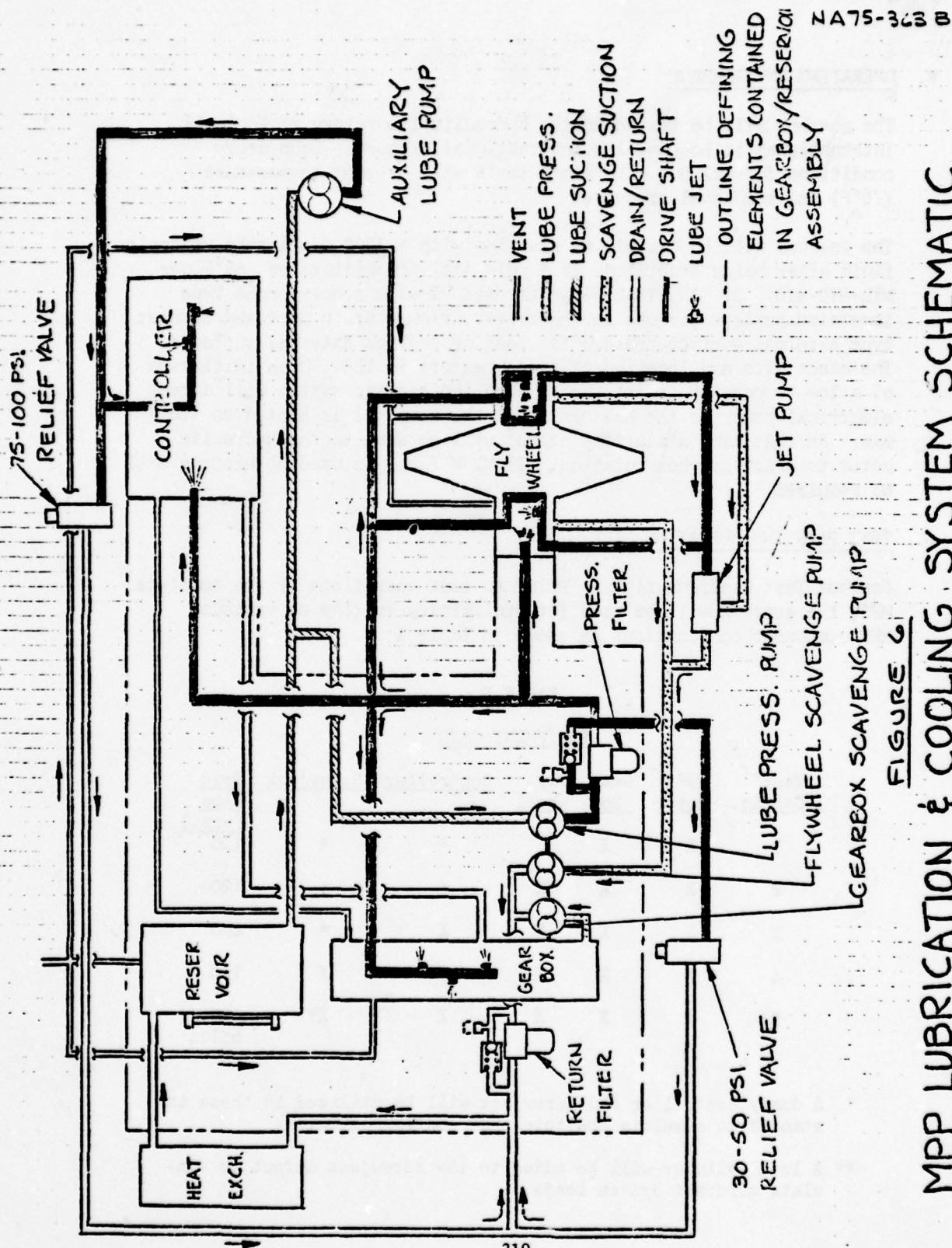


FIGURE 6

# MPP LUBRICATION & COOLING SYSTEM SCHEMATIC





#### F. OPERATING ENVIRONMENT

The gearbox will be tested in the hydraulic laboratory of Rockwell International at Los Angeles International Airport. Laboratory conditions for all but cold start tests will be room temperature (70°F) and sea level pressure.

The gearbox will be capable of starting with a 3000 centistoke viscosity fluid after being stabilized at a cold soak temperature of -65°F per MIL-STD-810. If SANTOTRAC fluid is used RI will supply probe type immersion heaters for use in the reservoir/sump drain port and blanket type external surface heaters for heating gearbox external surfaces. The exact size and location of these heaters is TBD. Upon initiation of a low temperature start the RI supplied heating system will direct electrical power to the heaters until the sump oil is heated to -20°F min. At that time a starting signal will be sent to the hydraulic motor to start gearbox rotation. If M2-V fluid is used no heating will be required.

#### G. TEST PLAN AND OPERATING LIFE

Gearbox Test Configurations - Prior to test operations of the complete MPP, the gearbox will be used for preliminary testing of various MPP component combinations as shown in Table I .

TABLE I  
EQUIPMENT USED

| <u>Test Config.</u> | <u>Hyd Motor</u> | <u>Gear Box</u> | <u>Fly-Wheel</u> | <u>Controller</u> | <u>Screwjack</u> | <u>Test Time (Hrs.)</u> |
|---------------------|------------------|-----------------|------------------|-------------------|------------------|-------------------------|
| 1                   | X                | X               |                  | *                 | *                | 120                     |
| 2                   | X                | X               | X                | *                 | *                | 120                     |
| 3                   | X                | X               | X                | X                 | *                | 200                     |
| 4                   | X                | X               | X                | X                 | X                | 100                     |
| 5                   | X                | X               | X                | X                 | X**              | <u>111.4</u><br>651.4   |

\* A dummy controller and screwjack will be utilized in these instances to simulate the total MPP configuration.

\*\* A load cylinder will be added to the screwjack output to simulate aircraft system loads.



#### H. INSTRUMENTATION REQUIREMENTS

1. An RPM sensor shall be installed adjacent to the controller drive gear to measure gearbox output speed.
2. Thermocouples shall be installed on the gearbox housing proximate to the flywheel drive gear bearings to monitor bearing temperatures.
3. Provisions shall be made for mounting accelerometers at three points on the gearbox adjacent to the flywheel mounting pad. Locations and configuration of the mounting provisions are TBD.

#### I. QUALITY ASSURANCE

1. Design of the gearbox shall adhere to good aircraft design practice.
2. Acceptance Tests - Each gearbox shall be tested prior to acceptance to demonstrate functional and physical integrity. These tests will include the following:

- a. Static Load Test (Conducted using supplier facilities)

- 1) With controller drive spline locked against rotation, apply 340 inch-pound to the hydraulic motor drive spline.
- 2) With the flywheel drive spline locked against rotation, apply 68 inch-pounds to the hydraulic motor drive spline.

- b. Load Test (Conducted using RI facilities)

With maximum torques per paragraph B applied to the controller drive, and no load on the flywheel drive, run the gearbox at rated RPM until the oil 'out' temperature stabilizes within  $\pm 1^\circ$  for at least 5 minutes. Oil 'in' temperature shall be  $170 \pm 10^\circ\text{F}$ .

- c. Overspeed Test (Conducted using RI facilities)

Accelerate the gearbox to 105% of rated speed and hold for 10 seconds.

3. The gearbox shall be designed for an operating life of 2,805.3 Hrs. which consists of 2,000 Hrs. at 100,000 RPM flywheel output speed, plus 0.2 Hr. at 105,000 RPM flywheel output speed plus 20,000 load cycles in which torque varies from normal running torque to maximum cycle torque (See Table II) in 15

TABLE II  
OPERATING TORQUES

| OPERATING<br>CONDITION           | TORQUE (IN-LB)                                    |                 |                   |
|----------------------------------|---|-----------------|-------------------|
|                                  | Hyd. Motor<br>Pad                                 | Flywheel<br>Pad | Controller<br>Pad |
| MAXIMUM LOAD<br>(DURING CYCLING) | +44.0   | +34.00          | -233.0            |
| RUNNING LOAD<br>(NO CYCLING)     | +19.0   | -1.47           | -7.3              |
| ACCELERATION LOAD<br>(STARTUP)   | +45.5   | -6.50           | -7.3              |
| DECELERATION LOAD<br>(SHUTDOWN)  | -6.8  | +2.38           | -7.3              |
|                                  | + = Torque Input to Pad<br>- = Drag Torque at Pad |                 |                   |





sec cycles (83.3 Hr.) plus 10,000 startup cycles in which torque varies, in a step input fashion from zero torque to acceleration torque and gradually returns to running torque (last 10% of cycle) in 54 sec. cycles (147.7 hours) plus 10,000 shutdown cycles in which torque varies gradually from running torque to zero torque in 207 sec. cycles (574.1 Hrs.).

4. The gearbox shall demonstrate at least 211.4 Hrs. of operating life consisting of 200 Hrs. of operation at 88,235 RPM flywheel output speed plus two one half minute dwells at 92,647 RPM over-speed, plus 2,000 load cycles in which torque varies from normal running torque to maximum cycle torque (See Table II) in 15 second cycles (8.4 Hrs.) plus 40 startup cycles in which torque varies, in step input fashion, from zero torque to acceleration torque and gradually returns to running torque (last 10% of cycle) in 54 sec. cycles (0.6 Hrs.) plus 40 shutdown cycles in which torque varies gradually from running torque to zero torque in 207 sec. cycles (2.3 Hrs.).

NA75-401 B

SERIAL NO.

SPECIFICATION --

MECHANICAL TRANSMISSION/CONTROLLER,

MECHANICAL POWER PACKAGE

*F. D. Halferty*

F. D. HALFERTY  
ADVANCED DESIGN

*C. W. Helsley Jr.*

C. W. HELSLEY  
PROGRAM MANAGER,  
ENERGY SYSTEMS

|              |          |
|--------------|----------|
| REV. B       | 11-3-77  |
| REV. A       | 12-18-75 |
| DATE         | 07-24-75 |
| NO. OF PAGES | 13       |



**Rockwell International**

Los Angeles Division  
International Airport  
Los Angeles, California 90009  
(213) 670-9151



#### A. GENERAL

This specification establishes the requirements for a mechanical transmission type controller, one component of a mechanical power Package (MPP) which will be developed and tested by the Los Angeles Aircraft Division of Rockwell International (RI) for the Air Force Systems Command, Aero Propulsion Laboratory, Wright - Patterson Air Force Base, Dayton, Ohio, under Contract F33615-75-C-2011.

The MPP, described schematically in Figure 1, is intended to replace the high horsepower (high delivery) hydraulic actuation systems of certain intermittent duty aircraft functions with a low horsepower, stored energy system to eliminate the high peak demands which tend to size an aircraft hydraulic system.

As shown in Figure 1, the gearbox will receive power from a pad-mounted hydraulic motor at moderate speed and utilize that power to accelerate and maintain a pad-mounted flywheel assembly at  $88,235 \pm 800$  RPM.

A third pad on the gearbox will mount the reversible, infinitely variable, mechanical transmission type controller which is the subject of this specification. During the energy storage phase the controller is to be programmed to zero output. During the energy utilization phase, energy is to be extracted from the flywheel by the controller via the gearbox. The controller is to be programmed to the direction of output rotation desired, and power is to be transferred through a reduction gear train to a jack screw actuator which provides linear motion to accomplish the aircraft actuation function.

After the actuation function is complete, the controller is to be returned to zero output, and the flywheel will be accelerated by the hydraulic motor to its peak energy storage RPM.

The direction of rotation of the various MPP components are shown on Figure 1. Rated speeds are shown on Figure 1.

Design of the controller shall adhere to good aircraft design practice. Weight shall not exceed 41.8 pounds.

#### B. OPERATING REQUIREMENTS

##### 1. Operating Modes



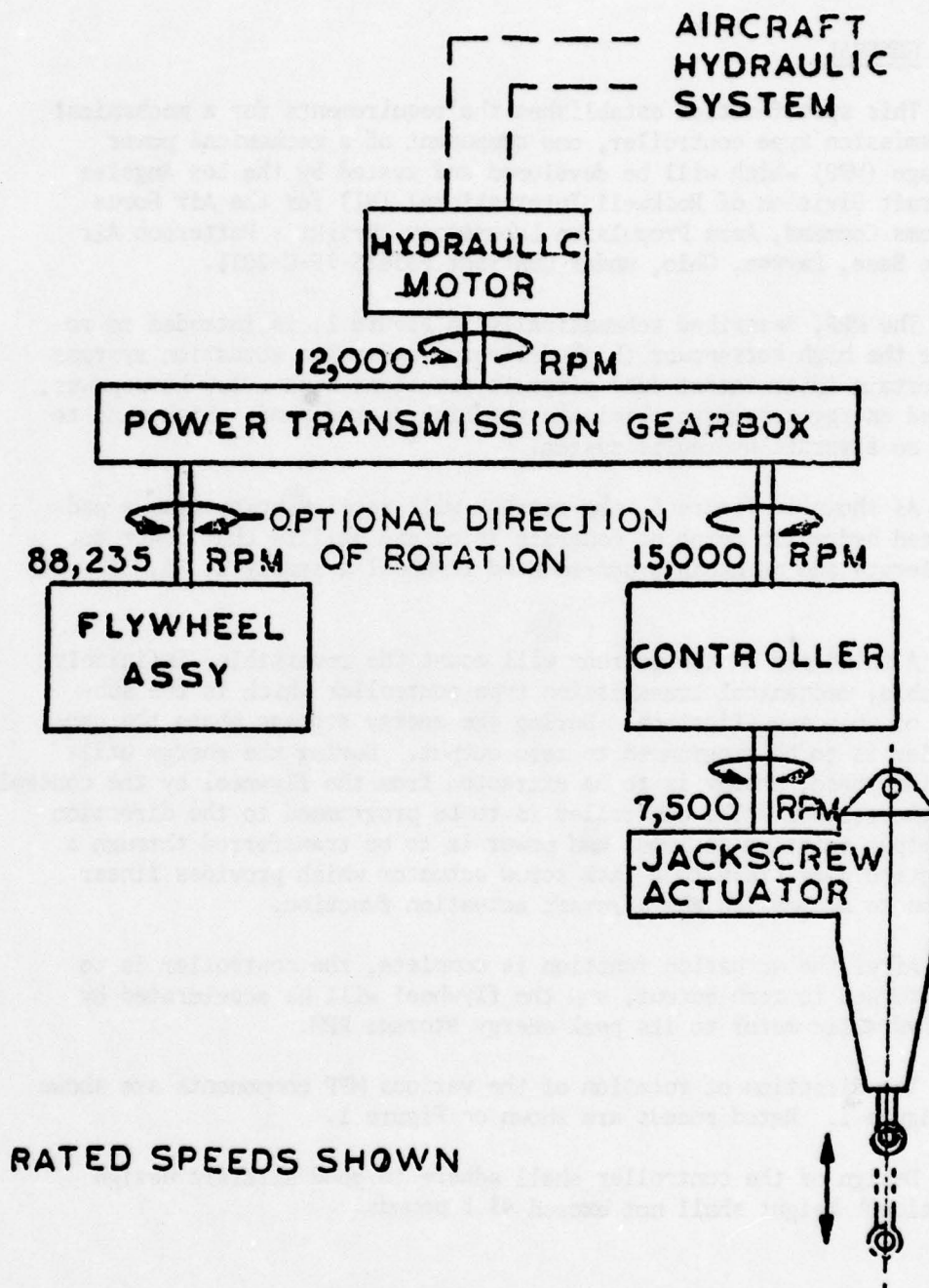


**FIGURE 1**  
**SCHEMATIC - MECHANICAL**  
**POWER PACKAGE**



When the signal to the controller is 'neutral' there must be no output other than the small biasing torque discussed in the next paragraph. When the signal is 'extend', the controller must accelerate the output shaft to 50 percent input speed clockwise. When the signal is 'retract', the controller must accelerate the output shaft to the same speed counterclockwise.

## 2. Torque Characteristics

Since the controller is sandwiched between two high-inertia devices (i.e. the flywheel and the landing gear) and is rigidly coupled to each, it must be capable of controlling its own internal torque to avoid "skidding." At all times, when the signal is 'extend' or 'retract', the unit must control its maximum output torque within a band of 395-425 inch-pound (in-lb) when accelerating the system up to speed, when decelerating the system to a stop, and when meeting peaks on the load-stroke curve. When the signal to the controller is 'neutral' and the system is in the retract position, the output torque shall be +5 to -25 in-lb biased to the retract position. When the system is in the extend position the biasing, if any, shall be reversed.

## 3. Torque-Speed Characteristics

As the controller extracts power from the flywheel and delivers it to the actuation system, the flywheel will be slowed to a minimum speed of 61,765 RPM (30 percent speed reduction). The controller must be capable of delivering up to +425 in-lb torque to the output at this speed, and up to 405 in-lb at rated input speed.

The controller shall provide snubbing on both the retract and extend cycles. Snubbing shall begin at a point  $10^{+2}_{-0}\%$  from the end of the retract stroke. The controller output speed shall be reduced linearly from 7500 RPM to 750 RPM max by the time the stroke is completed. A micro switch attached to the screw jack actuator will provide the signal to begin snubbing. Two additional micro switches on the screw jack actuator will provide signals to return the controller to neutral at the end of the retract and extend strokes.

## 4. Operating Life

The controller shall be designed for an opera-



ting life of 2,805.3 hrs. which consists of 2,000 hrs. at 15,000 RPM controller input speed, plus 0.2 hr. at 15,750 RPM controller input speed plus 20,000 load cycles in which torque varies from running load torque to maximum cycle torque (See Table I) in 15 sec cycles (83.3 hr.) plus 10,000 54 sec startup cycles and 10,000 207 sec shutdown cycles (721.8 hr.) in which the torque varies from zero to running load torque.

The controller shall demonstrate at least 211.4 hrs. of operating life (See items 4 and 5 Table II) consisting of 200 hrs. of operation at 15,000 RPM controller input speed plus two one-half minute dwells at 15,750 RPM overspeed, plus 2,000 load cycles in which torque varies from running load torque to maximum cycle torque (See Table I) in 15 sec cycles (8.4 hrs.) plus 40 startup and shutdown cycles (2.9 hrs.) in which torque varies from zero torque to maximum load torque and decays to running load torque during start-up and varies from running load torque to zero torque during shutdown.

TABLE I

OPERATING TORQUES

| <u>OPERATING CONDITION</u>       | <u>TORQUE (IN/LB)</u><br>(drag torque at<br>input pad) |
|----------------------------------|--|
| MAXIMUM LOAD<br>(during cycling) | -233.0   |
| RUNNING LOAD<br>(no cycling)     | -7.3   |
| ACCELERATION LOAD<br>(startup)   | -7.3   |
| DECELERATION LOAD<br>(shutdown)  | -7.3   |

5. Solenoid Electrical Power Supply

The control solenoid shall be operated by unfiltered





dc power resulting from full wave bridge rectification of nominal 230 volts RMS, single-phase line-to-neutral, 400 hz ac power.

RI will supply the bridge rectifier.

The input signal will be generated by switching the ac input to the bridge rectifier.

#### C. ENVELOPE AND ARRANGEMENT

The general arrangement of the MPP and the location of the controller within that arrangement is shown in Figure 2.

During testing the MPP will be supported by the screw jack end bearings. The controller will be mounted on the screw jack housing and will support the gearbox, flywheel and hydraulic motor. An adjustable support will be added between the screw jack housing and the gearbox near the flywheel pad as shown in Figure 2. Weights of the components supported by the controller are as follows:

|                 |         |
|-----------------|---------|
| Flywheel        | 17 lbs. |
| Gearbox         | 20 lbs. |
| Hydraulic Motor | 2 lbs.  |

The CG locations of the above components are noted on Figure 2.

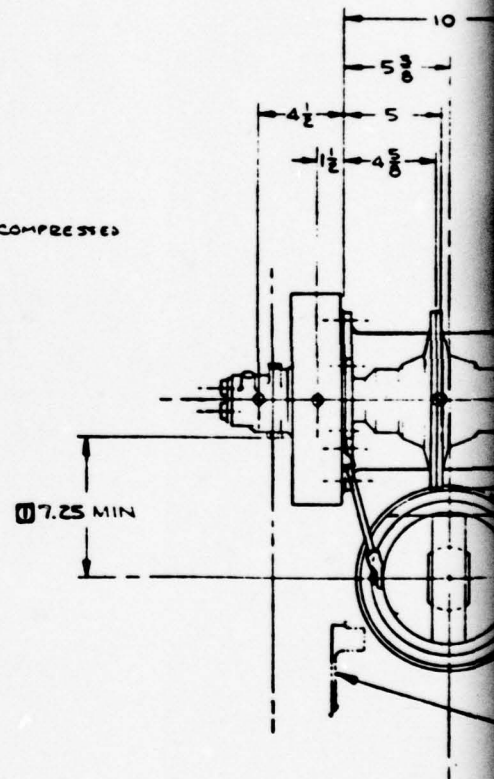
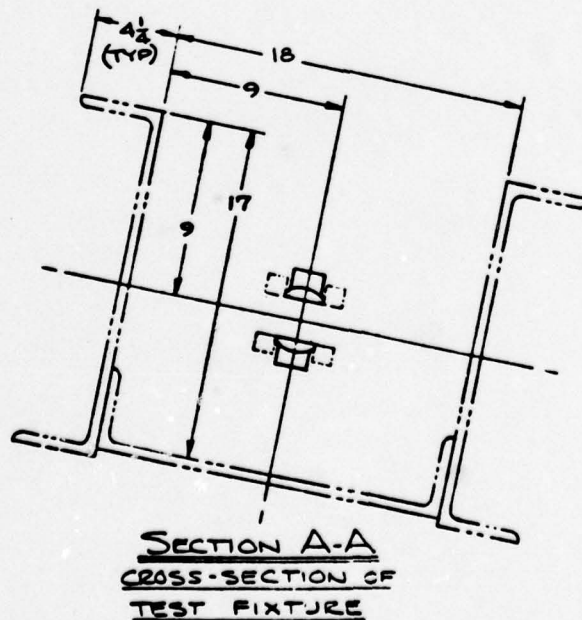
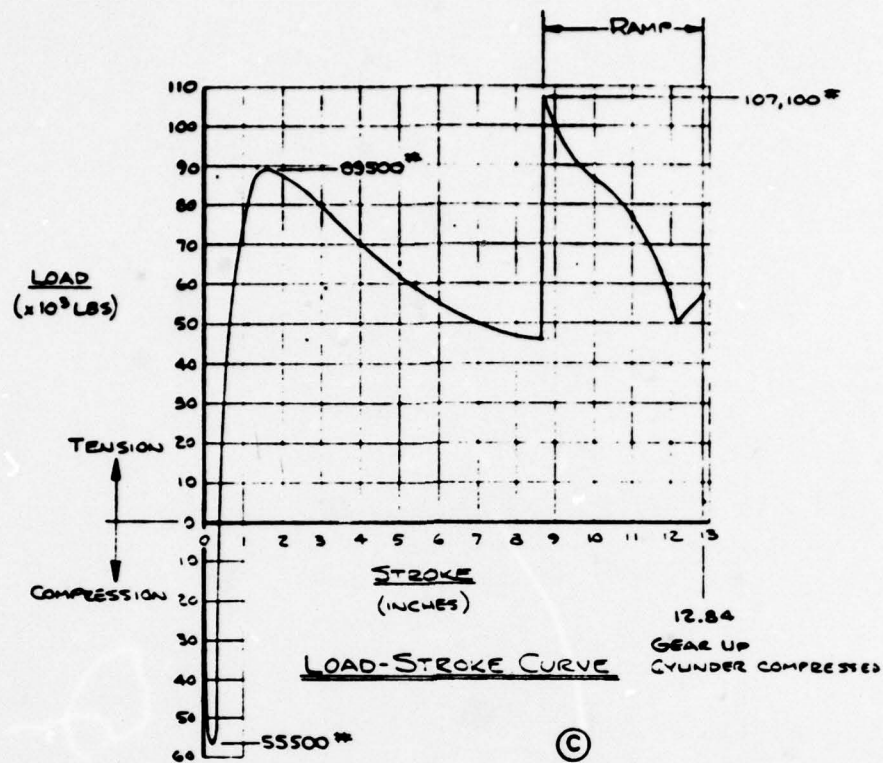
The controller shall be capable of supporting the above units when subjected to the vibration, acoustic noise, shock and acceleration environments of aircraft zones 2F and 3F as defined in B-1 prime item development specification CP621L2006B.

#### D. CONTROLLER CONFIGURATION

The controller envelope is described by a 7 in. diameter 10 in. long cylinder. The 7 in. diameter may be exceeded in local areas (TBD) to provide for signal input device housing, lube ports, etc. The 10" dimension is considered a maximum due to dimensional constraints on the MPP to fit between the existing test fixture side rails as shown on Figure 2.

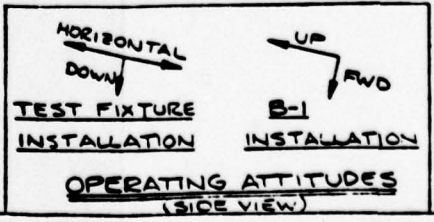
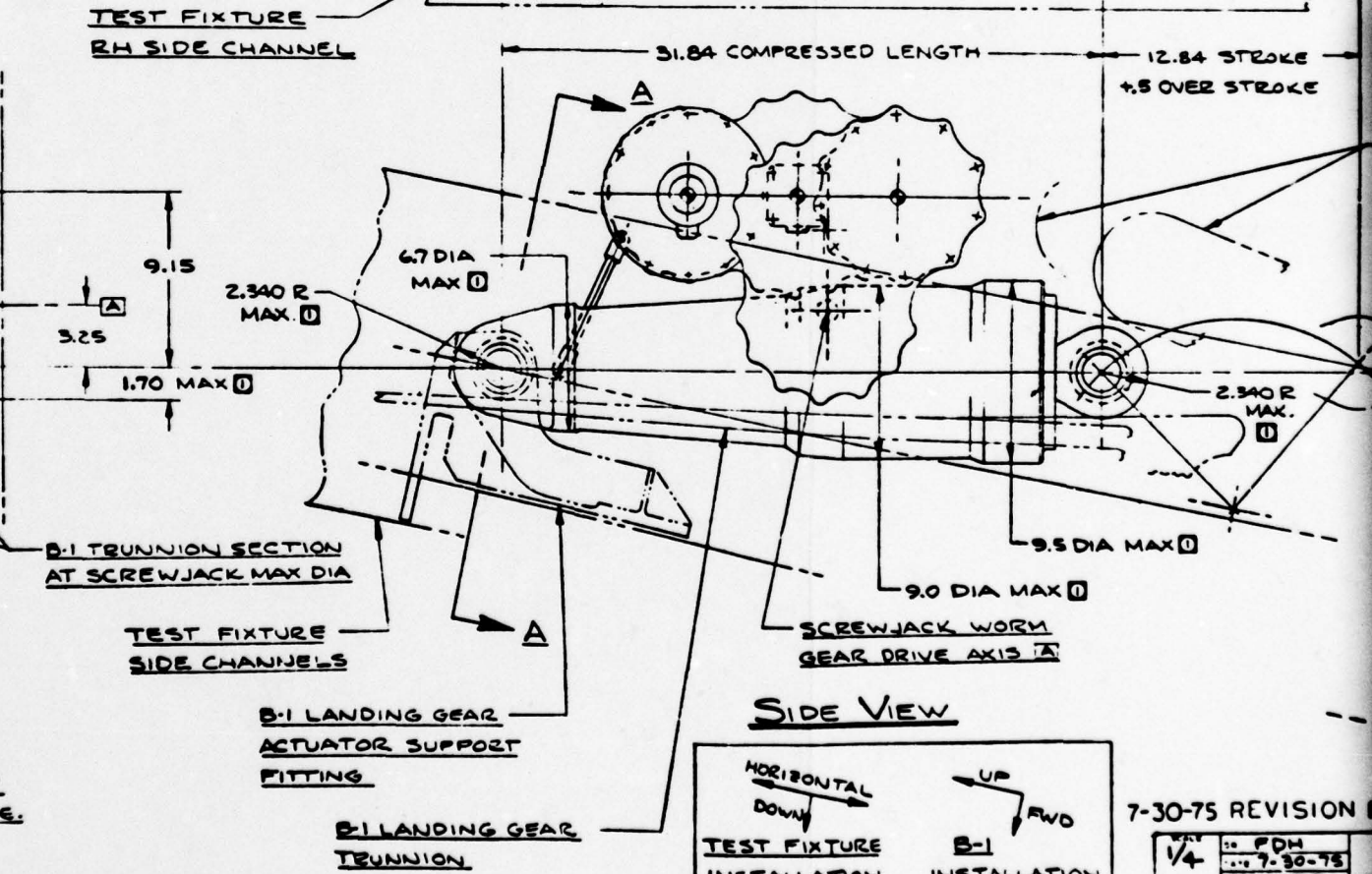
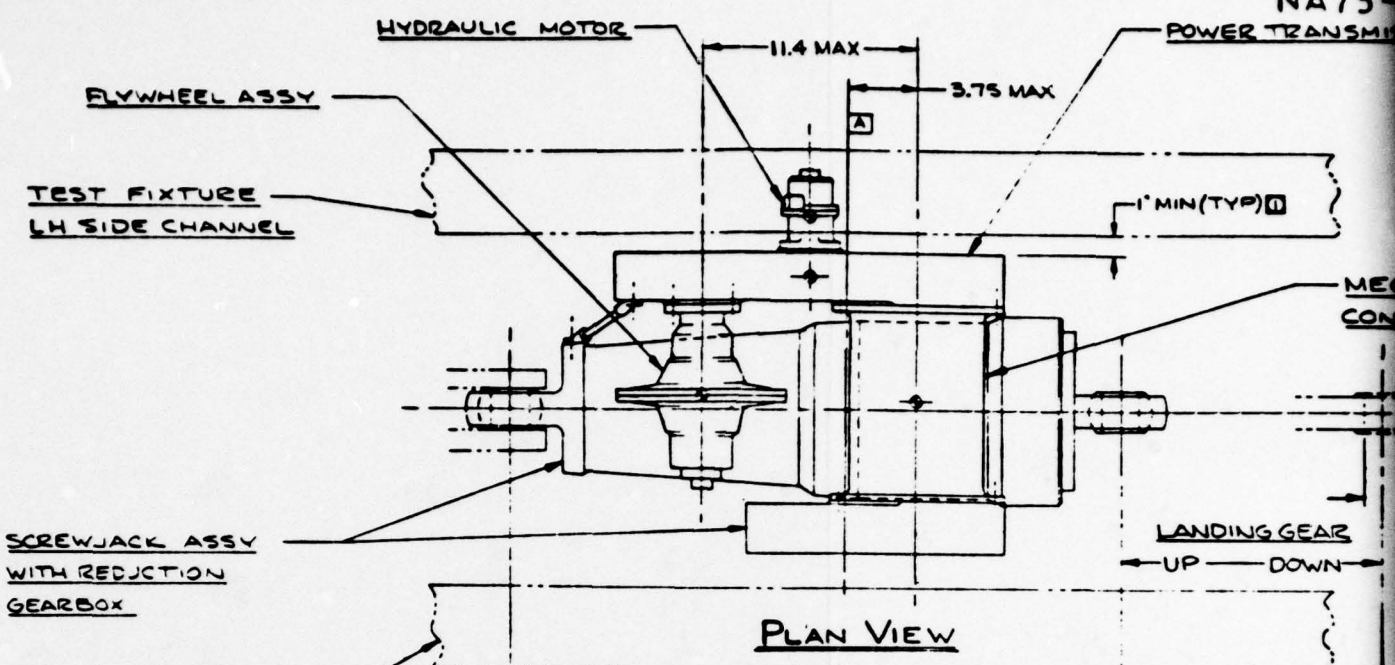
The input (gearbox) drive pad will be per AS968A-1 as modified per figure 3.

The output (screwjack) drive pad will be per AS965A - 12V.



2. DIMENSIONAL LIMITS CODED ① ARE  
REQUIRED TO MAINTAIN MINIMUM C  
BETWEEN THE MPP & ADJACENT  
1. APPROXIMATE CGS OF COMPONENTS  
SHOWN

NOTES



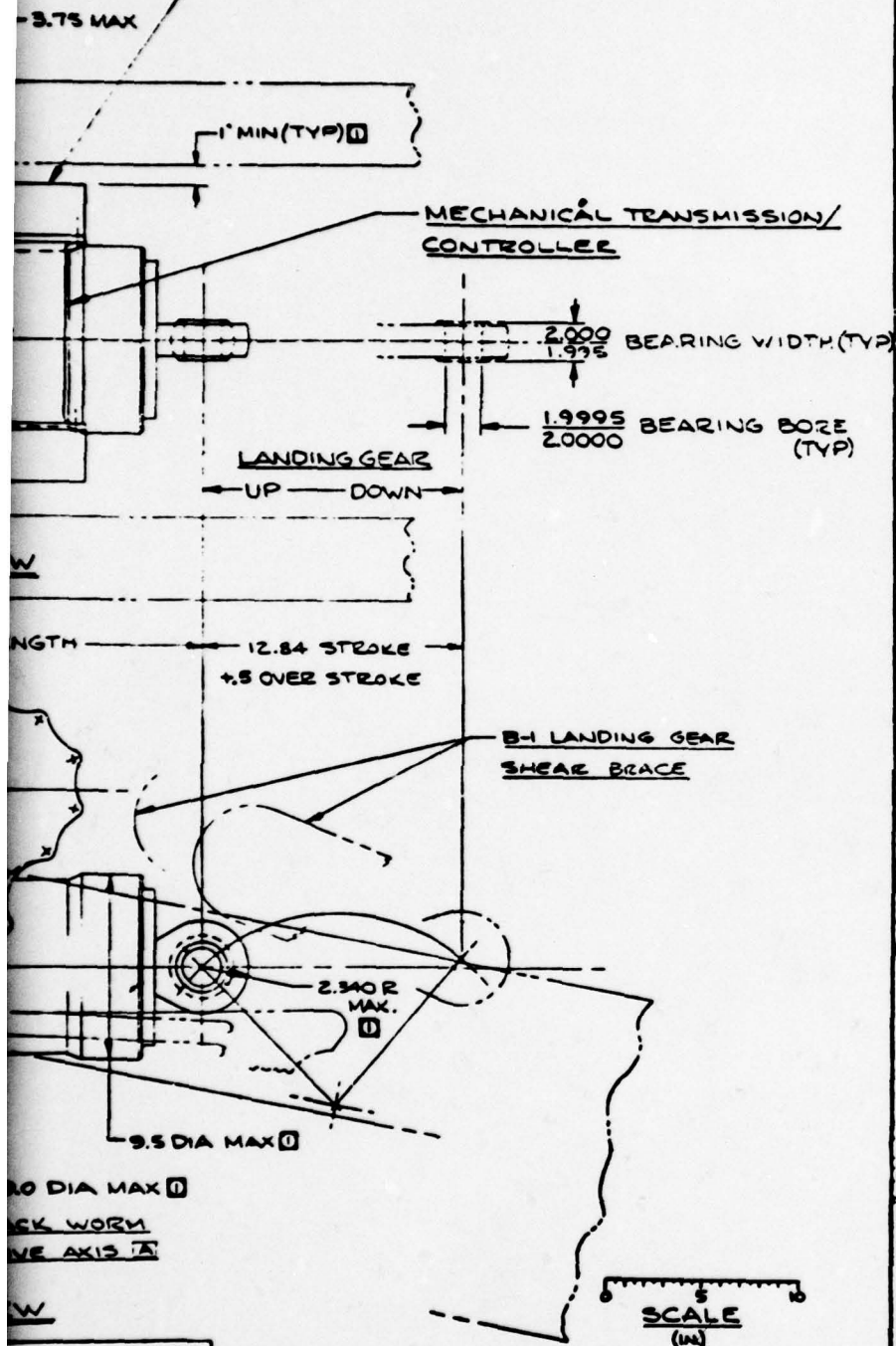
7-30-75 REVISION

|                             |     |
|-----------------------------|-----|
| 1/4                         | FDH |
| 7-30-75                     | MPP |
| MECHANICAL PO<br>GENERAL AR |     |



NA75-401.B. FIG. 2

## POWER TRANSMISSION GEARBOX



7-30-75 REVISION B - REVISED &amp; REDRAWN

|   |                              |                    |                    |                    |
|---|------------------------------|--------------------|--------------------|--------------------|
| REV<br>1/4  | BY<br>FDM<br>DATE<br>7-30-75 | DESIGNED BY<br>MPP | DESIGNED BY<br>MPP | ADVANCED<br>DESIGN |
| MECHANICAL POWER PACKAGE -<br>GENERAL ARRANGEMENT |                              |                    |                    | D589-200           |

NA75-401 B

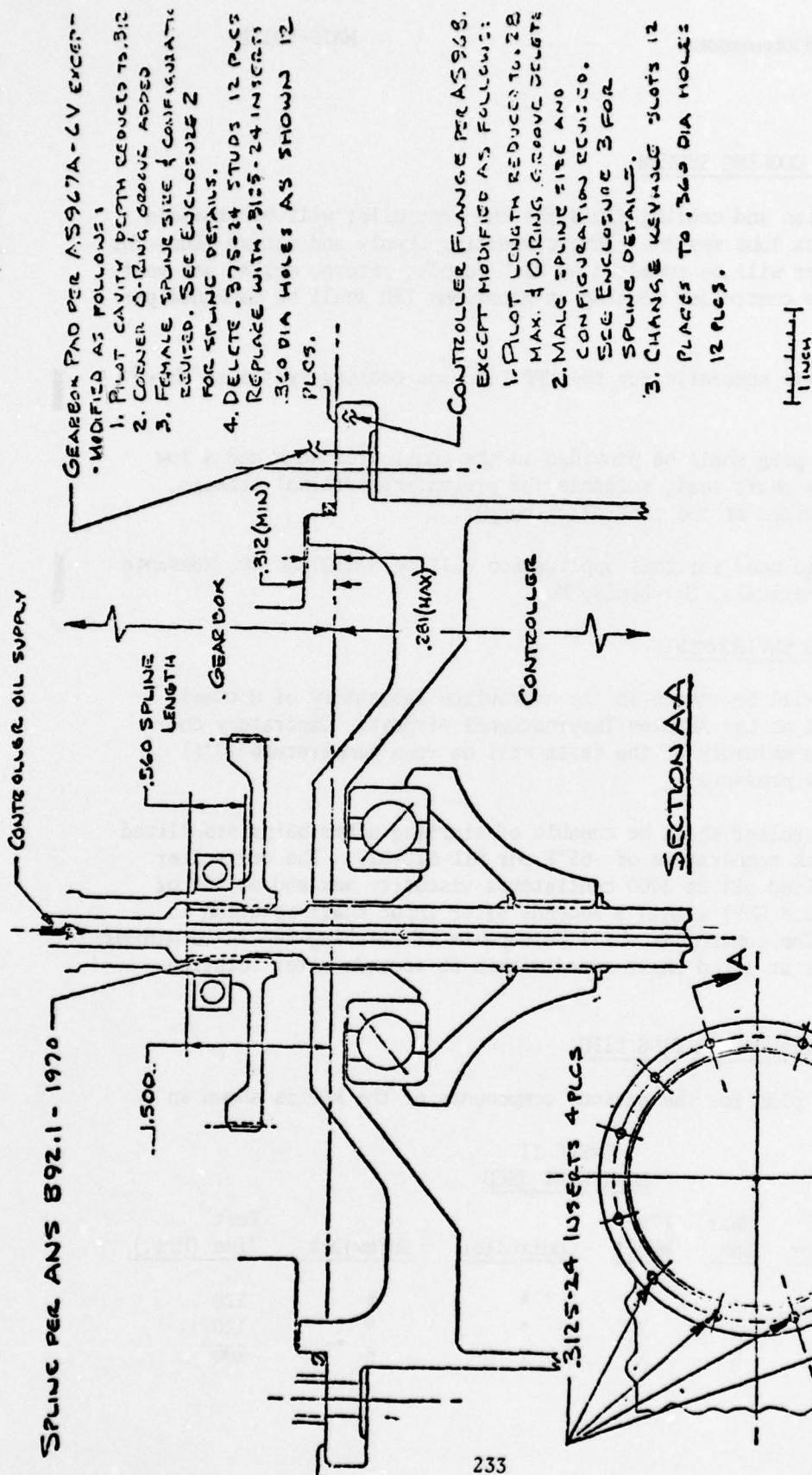


FIGURE 3  
GEARBOX/CONTROLLER  
INTERFACE DEFINITION

#### E. LUBE AND COOLING SYSTEM

Lubrication and cooling fluid for the controller will be provided by the gearbox lube system. Interconnecting supply and return lines for the controller will be supplied by RI. Supply, return, drain, and vent bosses on the controller housing at locations TBD shall be machined per MS33649.

A tentative schematic for the MPP lube and cooling system is shown in Figure 4.

A drain plug shall be provided in the controller sump and a low friction loss shaft seal, suitable for preventing external leakage, shall be provided at the controller output.

The fluid used for this application will be SANTOTRAC 30, Monsanto Industrial Chemicals, St. Louis, Mo.

#### F. OPERATING ENVIRONMENT

The MPP will be tested in the hydraulics laboratory of Rockwell International at Los Angeles International Airport. Laboratory conditions for a majority of the tests will be room temperature (70°F) and sea level pressure.

The controller shall be capable of starting after being stabilized at a cold soak temperature of -65°F per MIL-STD-810. The controller will be supplied oil at 3000 centistokes viscosity max and at 50% of rated flow (0.8 GMP) within 5 seconds after input shaft rotation is initiated. The controller shall be capable of carrying 396 in-lb minimum output torque at rated input speed within 60 seconds after rotation initiation.

#### G. TEST PLAN AND OPERATING LIFE

The test plan for the various components of the MPP is shown in Table II.

TABLE II  
EQUIPMENT USED

| <u>Test Config.</u> | <u>Hyd Motor</u> | <u>Gear Box</u> | <u>Fly-Wheel</u> | <u>Controller</u> | <u>Screwjack</u> | <u>Test Time (Hrs.)</u> |
|---------------------|------------------|-----------------|------------------|-------------------|------------------|-------------------------|
| 1                   | X                | X               |                  | *                 | *                | 120                     |
| 2                   | X                | X               | X                | *                 | *                | 120                     |
| 3                   | X                | X               | X                | X                 | *                | 200                     |



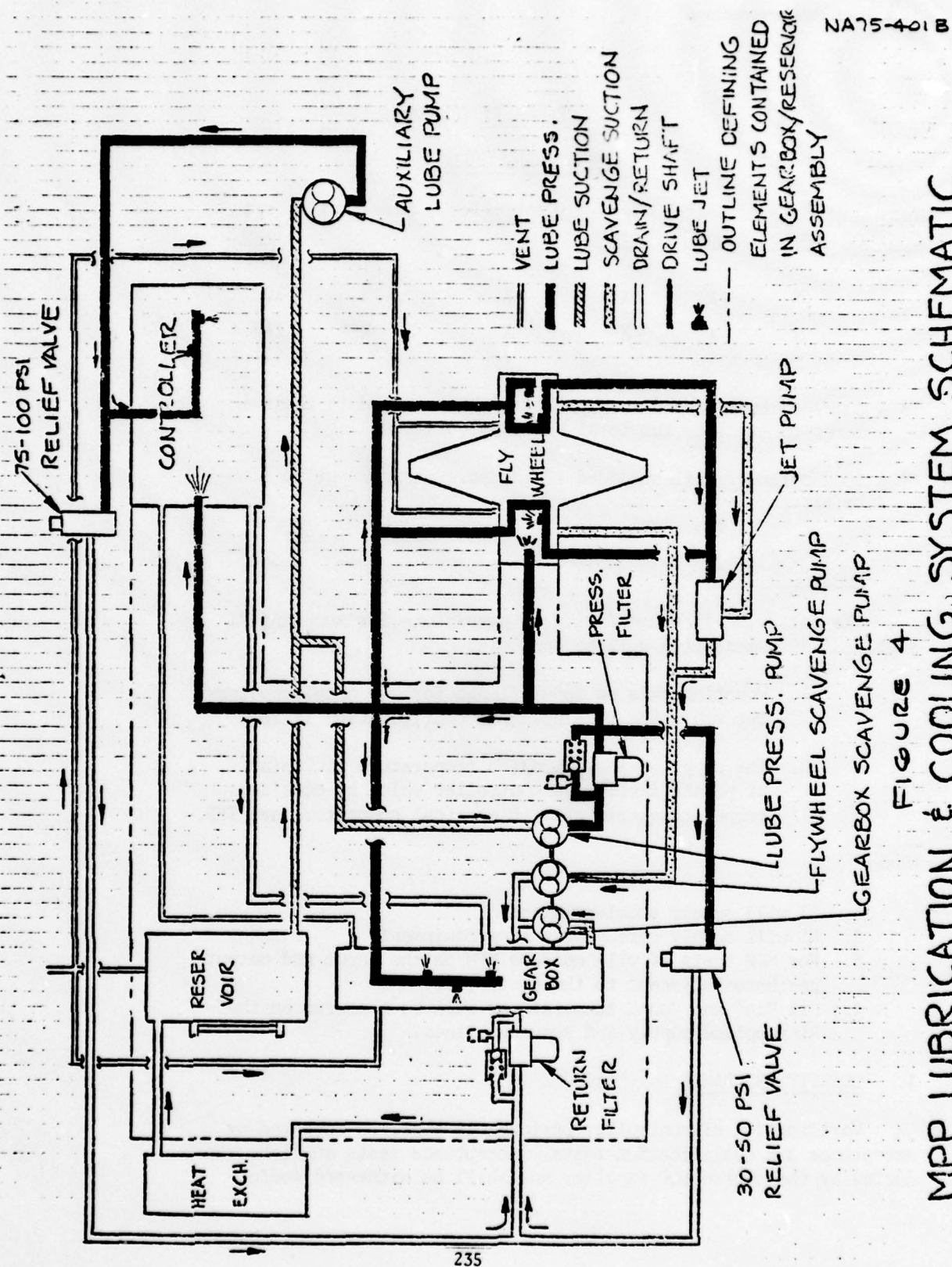


FIGURE 4  
MPP LUBRICATION & COOLING SYSTEM SCHEMATIC



TABLE II (Continued)

EQUIPMENT USED

| <u>Test Config.</u> | <u>Hyd Motor</u> | <u>Gear Box</u> | <u>Fly-Wheel</u> | <u>Controller</u> | <u>Screwjack</u> | <u>Test Time (Hrs.)</u> |
|---------------------|------------------|-----------------|------------------|-------------------|------------------|-------------------------|
| 4                   | X                | X               | X                | X                 | X                | 100                     |
| 5                   | X                | X               | X                | X                 | X**              | <u>111.4</u><br>651.4   |

\* A dummy controller and screwjack will be utilized in these instances to simulate the total MPP configuration.

\*\* A load cylinder will be added to the screwjack output to simulate aircraft system loads.

H. INSTRUMENTATION

The following instrumentation or provisions for mounting RI supplied instrumentation will be included:

1. Mounting pads on input flange for two accelerometers for vibration sensing. Pad configuration is TBD.
2. The supplier shall provide temperature pickup(s) at points inside the controller which he considers temperature critical. Electrical connectors are TBD.

Note:

1. RI will supply accelerometers.
2. RI will supply torque measuring equipment.
3. For MPP tests RI will measure RPM on the input and output gearboxes adjacent to the controller.
4. Oil "in" and "out" temperatures will be measured on the RI supplied supply and scavenge lines.

I. QUALITY ASSURANCE

Verification of controller performance shall be achieved by acceptance and qualification tests. Acceptance tests shall be conducted by the controller supplier and shall be witnessed and/or



approved by representatives of Rockwell International. Qualification tests shall be conducted at RI facilities by RI personnel and may be witnessed, at the suppliers discretion, by supplier personnel.

#### A. ACCEPTANCE TESTS

##### 1. Input speed range (zero output) tests

- a) The controller shall be started and accelerated gradually (250 RPM/SEC max.) to rated input speed (15000 RPM). With no load on the output and a neutral signal to the controller, the output speed shall not exceed 25 RPM in either direction.
- b) Operate the controller for five minutes at rated input speed. Oil out temperature and all other temperatures throughout the controller must stabilize. With an input oil flow of 1.3 GPM at 180°F output oil stabilization temperature shall not exceed 270°F.
- c) Accelerate and decelerate the controller input between zero RPM and rated RPM at least five times with the controller input signal at neutral and the controller unloaded. The characteristic wave form of the acceleration-deceleration cycle shall be of a generally sinusoidal nature with the maximum acceleration (or deceleration) during the cycle being  $1500 \pm 50$  RPM/SEC. There shall be no signs of skidding or other distress in the controller at any time during the test. Output speed shall be  $zero \pm 25$  RPM at all times during the test.

During the input speed range tests sensors and recorders shall be provided which adequately measure the performance of the controller. As a minimum the following parameters shall be measured.

- d) Input speed-recorded on an oscillograph type continuous recording.
- e) Input torque-recorded on an oscillograph type continuous recording.





- f) Case temperature-determined using a gage or recorded using a continuous recording.
- g) Output speed-recorded on an oscillograph type continuous recording.
- h) Case vibration-measured by an accelerometer mounted on the input flange and recorded on an oscillograph type continuous recording.

#### PERFORMANCE TEST

1. With a neutral signal applied to the controller start up and accel to 10,500  $\pm$  100 RPM at an acceleration of 2,250 RPM/SEC min. There shall be no signs of skidding or other distress in the controller.
2. Apply retract signal with output locked. Output torque shall fall within the limits of 395 in-lb min. to 425 in-lb max.
3. Remove the retract signal. Output torque shall drop to  $0^{+25}_{-5}$  in-lb biased in the retract direction.
4. Repeat steps 2 and 3 using an extend signal. Output torque values shall be the same except biased in the extend direction.
5. During tests 2 through 4 oil shall be supplied at 0.9 GPM min. and 180°F. At no time during these tests shall the oil out temperature exceed 240°F.
6. Repeat test 2 through 4 at 15,000 RPM. All output torques shall fall within the same limits as before. However, the oil shall be supplied at 1.3 GPM and the outlet oil temp shall not exceed 300°F.
7. At an input speed of 15,000 RPM min. apply retract signal with output free to rotate. The output shall accelerate to a speed of 7500  $^{+75}_{-0}$  RPM counterclockwise (looking at the controller output pad) within 1 second max.
8. Repeat test #7 applying an extend signal. The output requirements shall be the same except rotation shall be clockwise.



9. During test 7 and 8 oil shall be supplied at 1.3 GPM and 180°F max. The controller outlet temperature shall not exceed 300°F after 5 minutes operation at either the extend or retract condition.
10. At the end of the retract cycle (See Test #7) when the retract signal is removed the controller output speed shall decrease at a controlled rate of  $9500 \pm 500$  RPM/SEC.  
  
Note: Controlled rate deceleration is not required for the end of the extend cycle.
11. At an input speed of 15,000 RPM and when driving an output inertia load of  $0.50 \text{ in-lb-sec}^2$ , 2 retract and 2 extend signals shall be applied. The controller shall accelerate the load from rest to 7500 RPM in the appropriate direction in 1 second or less when either the retract or the extend signal is applied.

NA75-527 A

SERIAL NO.

SPECIFICATION  
SCREWJACK ACTUATOR AND REDUCTION GEARBOX,  
MECHANICAL POWER PACKAGE

F. W. Atkins  
Advanced Subsystems Design

*F. W. Atkins*

C. W. Helsley  
Program Manager  
Energy Systems

*C. W. Helsley*

REV. A 15 Dec. 1977  
DATE 2 April 1976  
NO. OF PAGES 11



**Rockwell International**

**Los Angeles Division**  
International Airport  
Los Angeles, California 90009  
(213) 670-9151





Rockwell International

#### A. GENERAL

This specification establishes the requirements for a screwjack actuator and reduction gearbox assembly, one component of a Mechanical Power Package (MPP) which will be developed and tested by the Los Angeles Aircraft Division (LAAD) of Rockwell International for the Air Force Systems Command, Aero Propulsion Laboratory, Wright-Patterson Air Force Base, Dayton, Ohio under contract F33615-75-C-2011.

The MPP, described schemetically in Figure 1, is intended to replace the high horsepower (high delivery) hydraulic actuation systems of certain intermittent duty aircraft functions with a low horsepower, stored energy system to eliminate the high peak demands which tend to size an aircraft hydraulic system.

As shown in Figure 1, the screwjack/gearbox assembly is the output device which converts moderate speed rotary motion from a reversible, infinitely variable mechanical transmission type, controller to low speed linear motion to accomplish the aircraft actuation function. The controller is mounted on a power transmission gearbox (PTG) and receives power through the gearbox from a PTG mounted flywheel.

Prior to initiation of the actuation function, the flywheel will have been accelerated to 88,235 rpm by a small PTG mounted hydraulic motor powered by the aircraft hydraulic system. During this energy storage phase the controller will be programmed to zero output. Upon initiation of the actuation function the controller will be programmed to the desired direction of output rotation and power will be transferred through the reduction gear train to the screwjack actuator. By the time actuation is complete, the controller will have been returned to zero output and the flywheel will be subsequently accelerated by the hydraulic motor to its peak energy storage rpm.

The direction of rotation and rated speeds of the various MPP components are shown in Figure 1.

Design of the screwjack and reduction gearbox will adhere to good aircraft design practice. Weight shall not exceed 145 pounds.

#### B. ENVELOPE AND ARRANGEMENT

The general arrangement of the MPP is shown in Figure 2.

During testing the MPP will be supported by the screwjack end bearings. The controller will be pad mounted on the reduction gearbox and the power transmission gearbox, with its flywheel assembly and hydraulic motor, will be pad mounted on the controller. A stabilizing

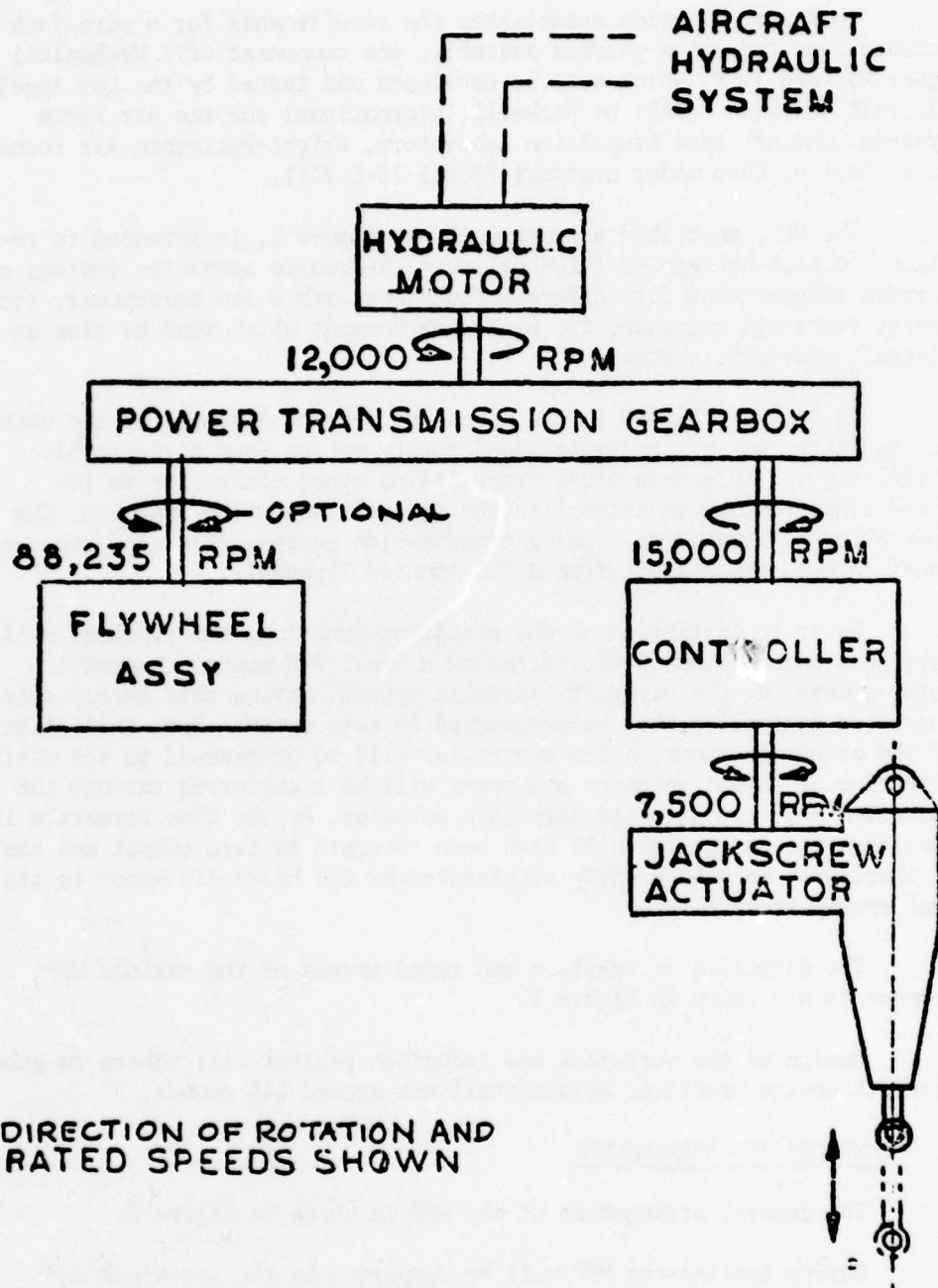
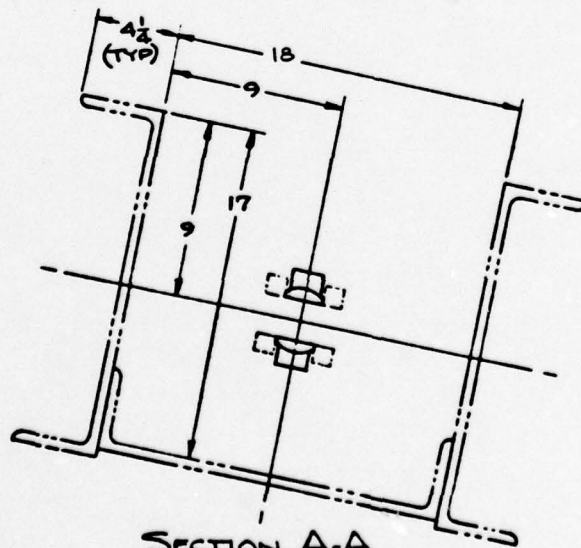
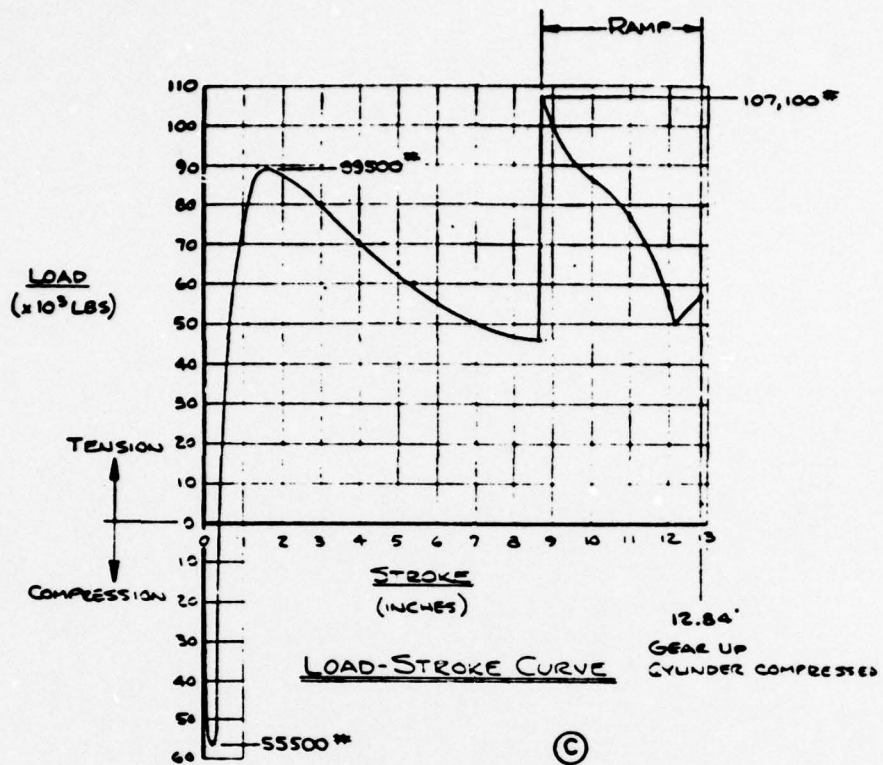
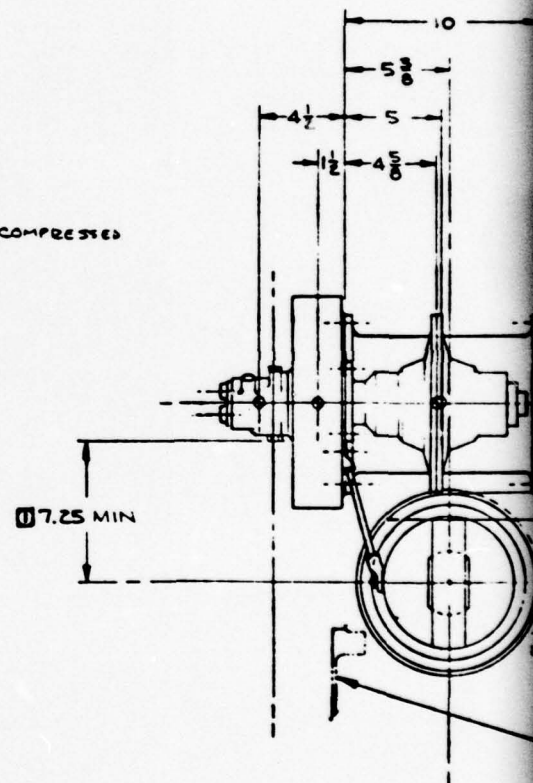


FIGURE 1  
SCHEMATIC - MECHANICAL  
POWER PACKAGE



SECTION A-A  
CROSS-SECTION OF  
TEST FIXTURE



2. DIMENSIONAL LIMITS CODED  $\square$  ARE  
REQUIRED TO MAINTAIN MINIMUM CLEARANCE  
BETWEEN THE MPP & ADJACENT STEEL

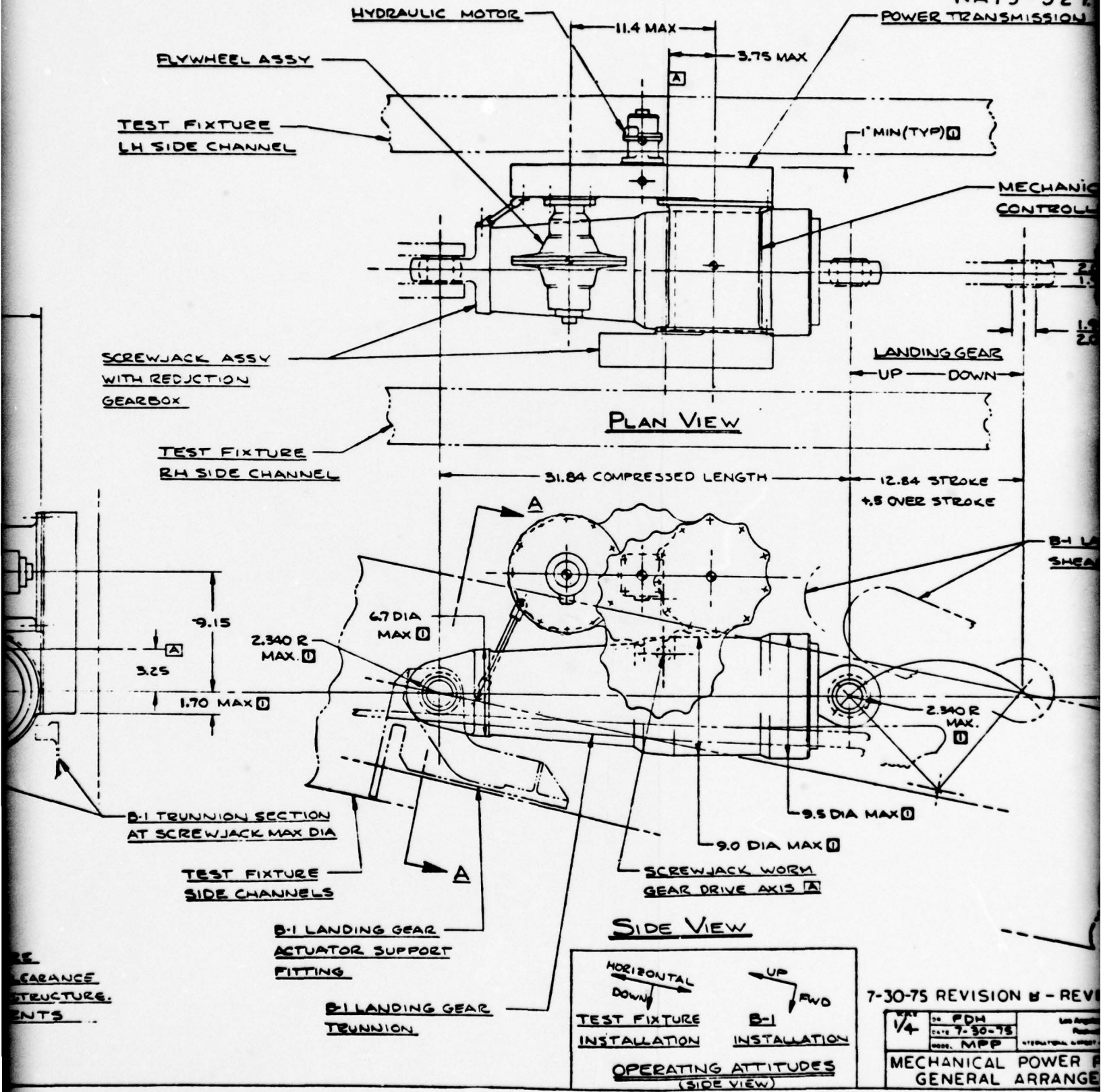
1. APPROXIMATE CGS OF COMPONENTS  
SHOWN  $\diamond$ .

NOTES



2

NA75-527



NA75-527.A. FIG. 2

POWER TRANSMISSION GEARBOX

3 MAX

1" MIN (TYP) [1]

MECHANICAL TRANSMISSION/  
CONTROLLER

2.000 BEARING WIDTH (TYP)  
1.995

1.9995 BEARING BORE  
2.0000 (TYP)

LANDING GEAR

UP DOWN

12.84 STROKE  
1.5 OVER STROKE

B-1 LANDING GEAR  
SHEAR BRACE

2.340 R  
MAX. [1]

9.5 DIA MAX [1]

1A MAX [1]

WORM  
WAS 1A

SCALE  
(IN)

7-30-75 REVISION B - REVISED & REDRAWN

|   |              |   |                    |
|---|--------------|---|--------------------|
| REV<br>1/4  | BY PDH       | Los Angeles Airport Division<br>Pasadena International<br>INTERNATIONAL AIRPORT - LOS ANGELES, CALIFORNIA 90009 | ADVANCED<br>DESIGN |
|   | DATE 7-30-75 |   |                    |
|   | CHKD MPP     |   |                    |
| MECHANICAL POWER PACKAGE -<br>GENERAL ARRANGEMENT |              |   | D589-200           |



link will be installed between the power transmission gearbox and the screwjack housing as shown in Figure 2. Weights of the components supported by the screwjack/gearbox are as follows:

|                            |             |
|----------------------------|-------------|
| Flywheel Assembly          | 17 pounds   |
| Power Transmission Gearbox | 20 pounds   |
| Hydraulic Motor            | 2 pounds    |
| Controller                 | 41.8 pounds |

Locations of the centers-of-gravity (CG) of the above components are noted in Figure 2.

The screwjack shall be capable of supporting the components when subjected to the vibration, acoustic noise, shock and acceleration environments of aircraft zones 2F and 3F as defined in B-1 prime item development specification CP621L2006B. The screwjack shall also be capable of reacting its own self-generated torque through its attach fittings while maintaining its ability to rotate freely about four critical axes. These axes are the rod and head bearing bore axes (Figure 2) and two axes normal to the plane of the bearing bore axes at the intersection of the actuator longitudinal axis and the two bearing bore axes. The self-generated torque shall not exceed 13,000 inch-pounds. The screwjack attach fittings (rod end and head end) shall be so designed that this maximum self-generated torque does not damage nor score the end clevises in which the screwjack is mounted.

#### C. SCREWJACK/GEARBOX CONFIGURATION

The screwjack/gearbox configuration will be generally shown, (dark outlined) in Figure 2. Critical dimensions relating to the adjacent test fixture and the landing gear components are shown to define and illustrate areas of limited clearance for the two installations.

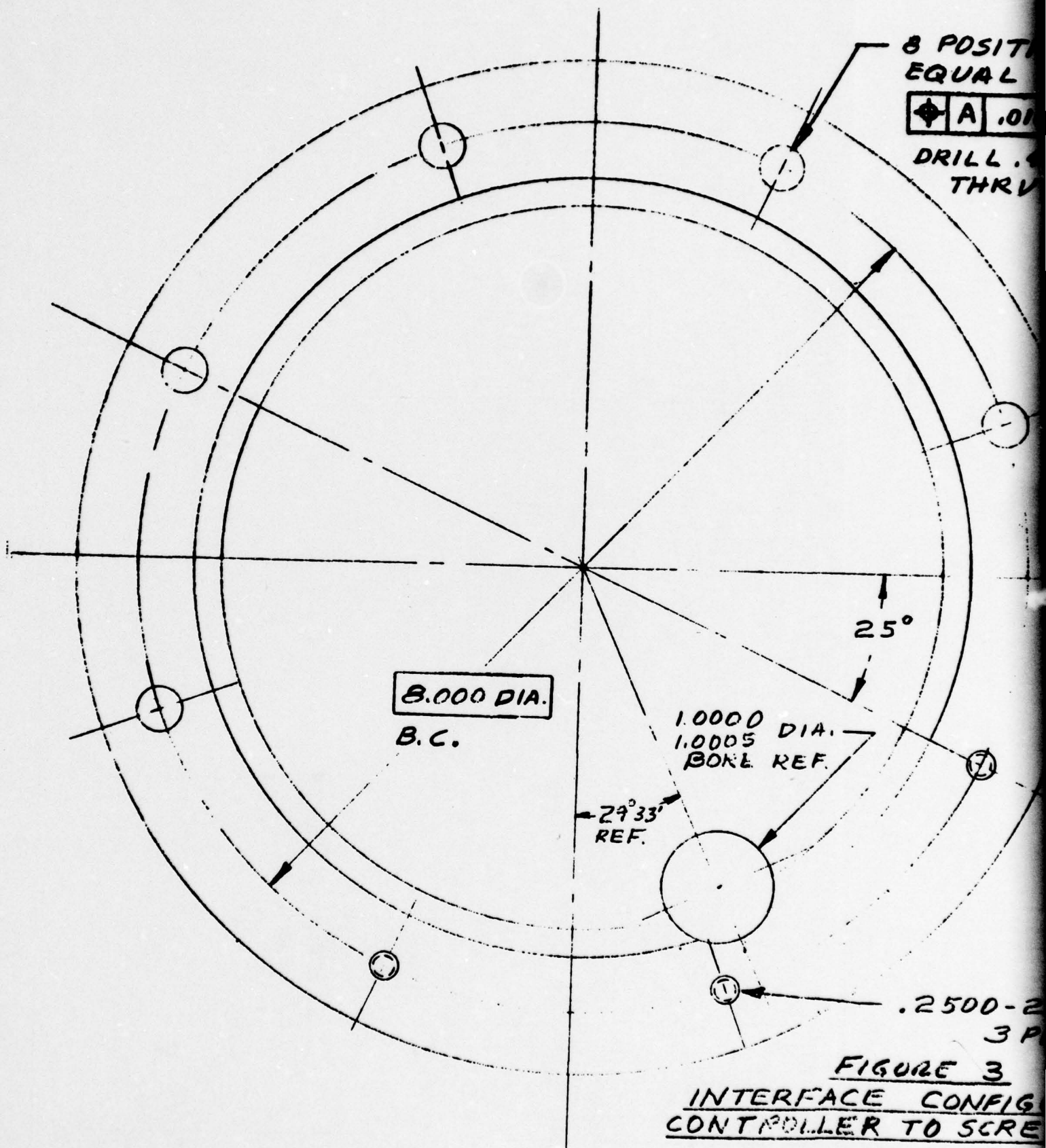
The controller mounting pad will be per AS966-1 as modified per Figure 3. The cylinder torque shield shall be a RI supplied washer as described in RI specification LD153-0029.

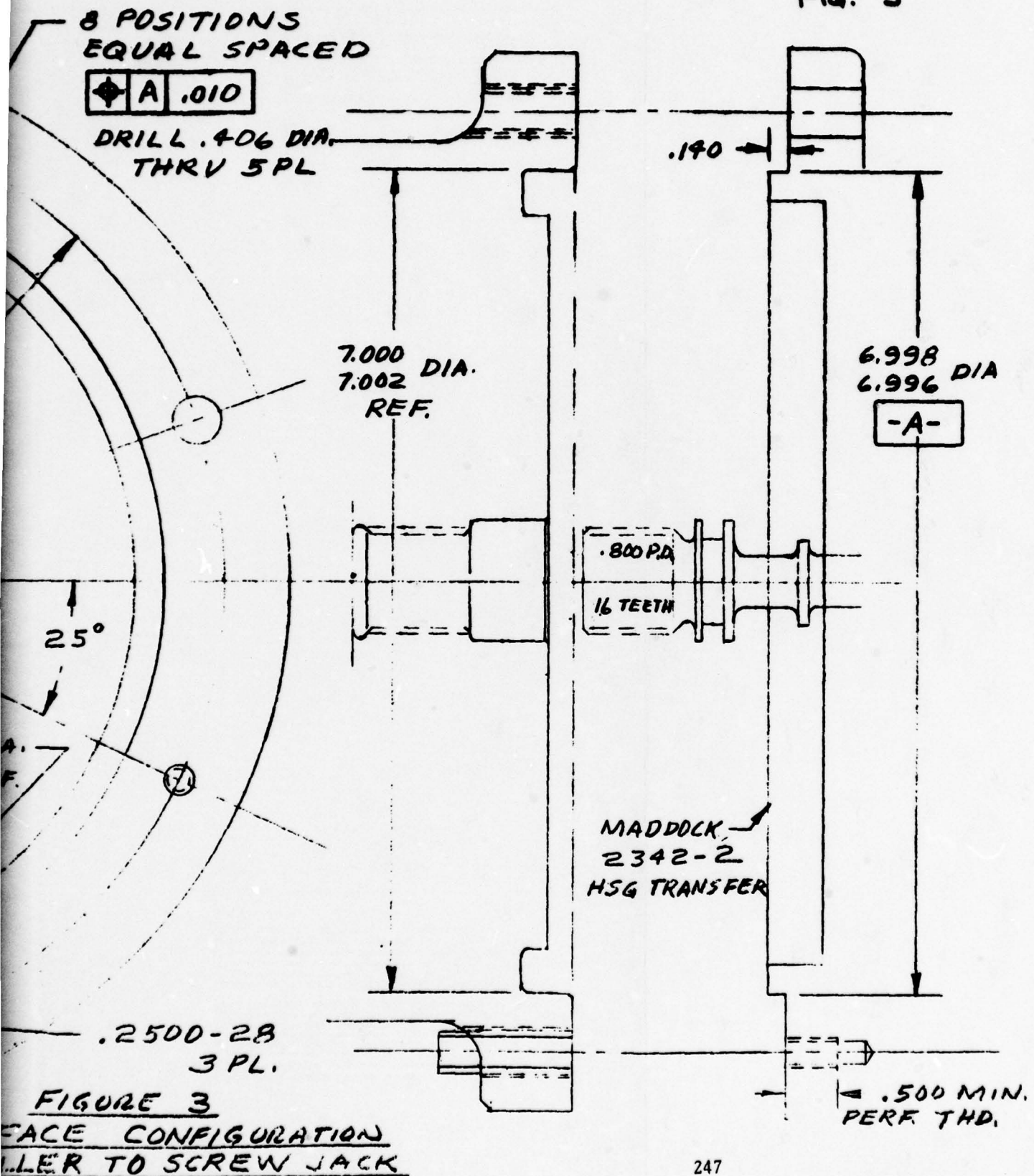
Location and configuration of the pad for attachment of the stabilizing link are shown in Figure 2.

#### D. OPERATING REQUIREMENTS

The limit output axial loads for screwjack operation are 107,100 pounds tension and -55,500 pounds compression. These limit loads occur





NA75-527 A  
FIG. 3



during the retract (tension) and extend (compression) cycles and are associated with a load stroke curve as shown in Figure 4A. The screwjack shall be designed to withstand 18,000 retract and extend load cycles per Figure 4A and 2,000 retract and extend load cycles per Figure 4B.

The input to the screwjack shall be accelerated from 0 to 7,875 rpm maximum (7500 rpm nominal) within one second after the retract or extend cycle is initiated and the screwjack output shall simultaneously accelerate from zero to 124.46 inches per minute of linear motion (118.53 inches per minute nominal). Actuation shall continue at this rate until snubbing begins. During snubbing, the screwjack input speed shall be reduced linearly to 750 rpm maximum before the actuator hits its external stop. The retract stop has a maximum spring rate of  $1 \times 10^6$  pounds per inch and the extend stop has a maximum spring rate of  $4 \times 10^5$  pounds per inch.

Microswitches (or equivalent) shall be provided by RI to send signals to the controller under the following conditions:

1. The screwjack is at the extend position.
2. The screwjack is at the retract position.
3. The screwjack is  $1.00 \pm .03$  inch from the retract and extend positions.

Total working stroke of the actuator shall be  $12.84^{+.5}_{-.0}$  inch with 0.3 inch overstroke at each end.

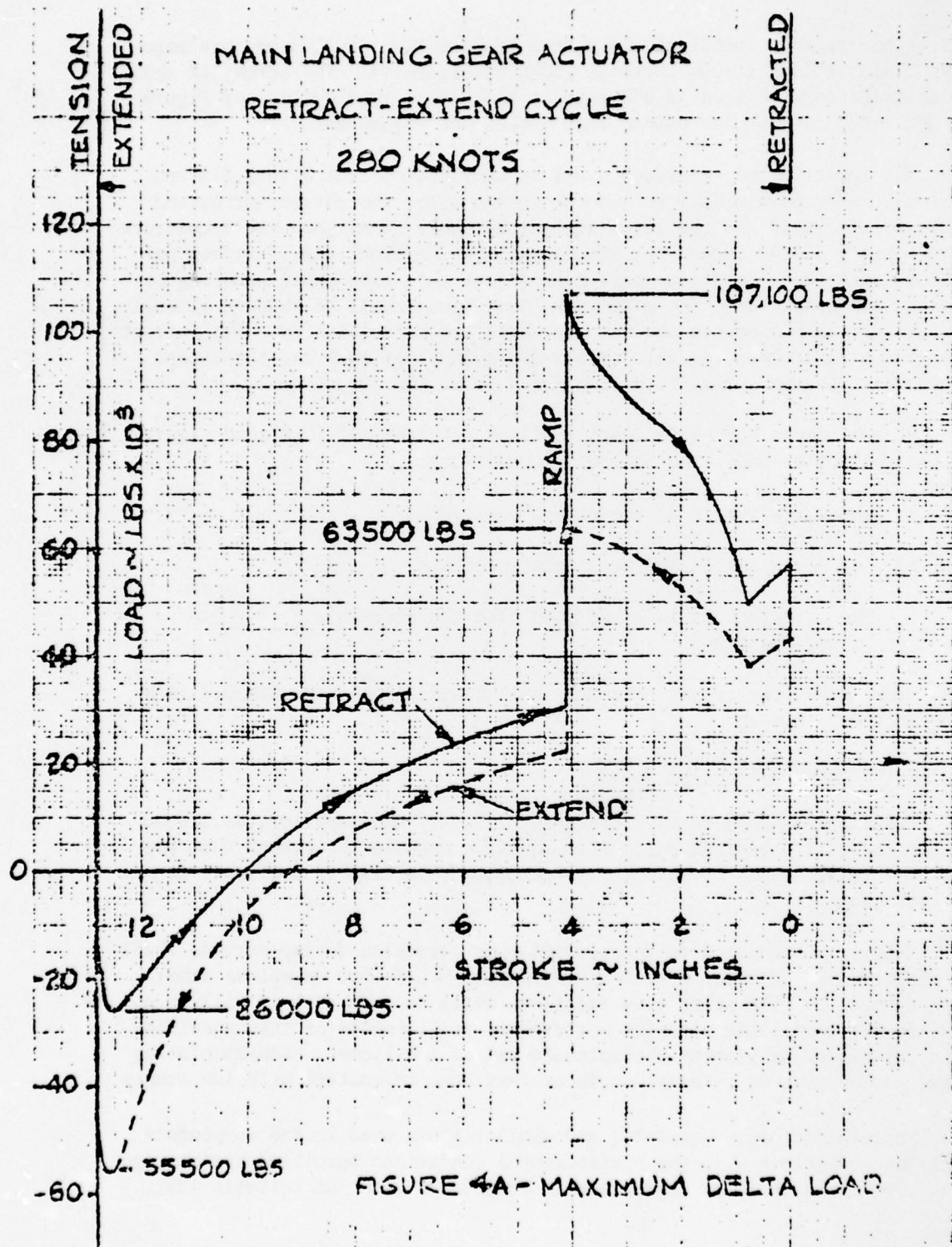
#### E. DESIGN AND CONSTRUCTION

Existing standard parts, Government industry and supplier, as listed in the Rockwell preferred parts list shall be used to the extent that they meet the requirements of this specification. This list is available to Rockwell suppliers.

Materials subjected to deterioration or corrosion during service shall be protected in accordance with Specification MIL-S-5002 except as otherwise agreed to. The protective treatment shall be such that it will in no way prevent compliance with the performance requirements of this specification, or hinder or prevent the intended use of the items. Cadmium plating shall not be used on internal surfaces that come in contact with lubricants.

Nonmetallic seals, gaskets, and similar items used in the components shall be compatible with the environmental conditions specified herein. Age sensitive items shall be controlled in accordance with ANA Bulletin 438.





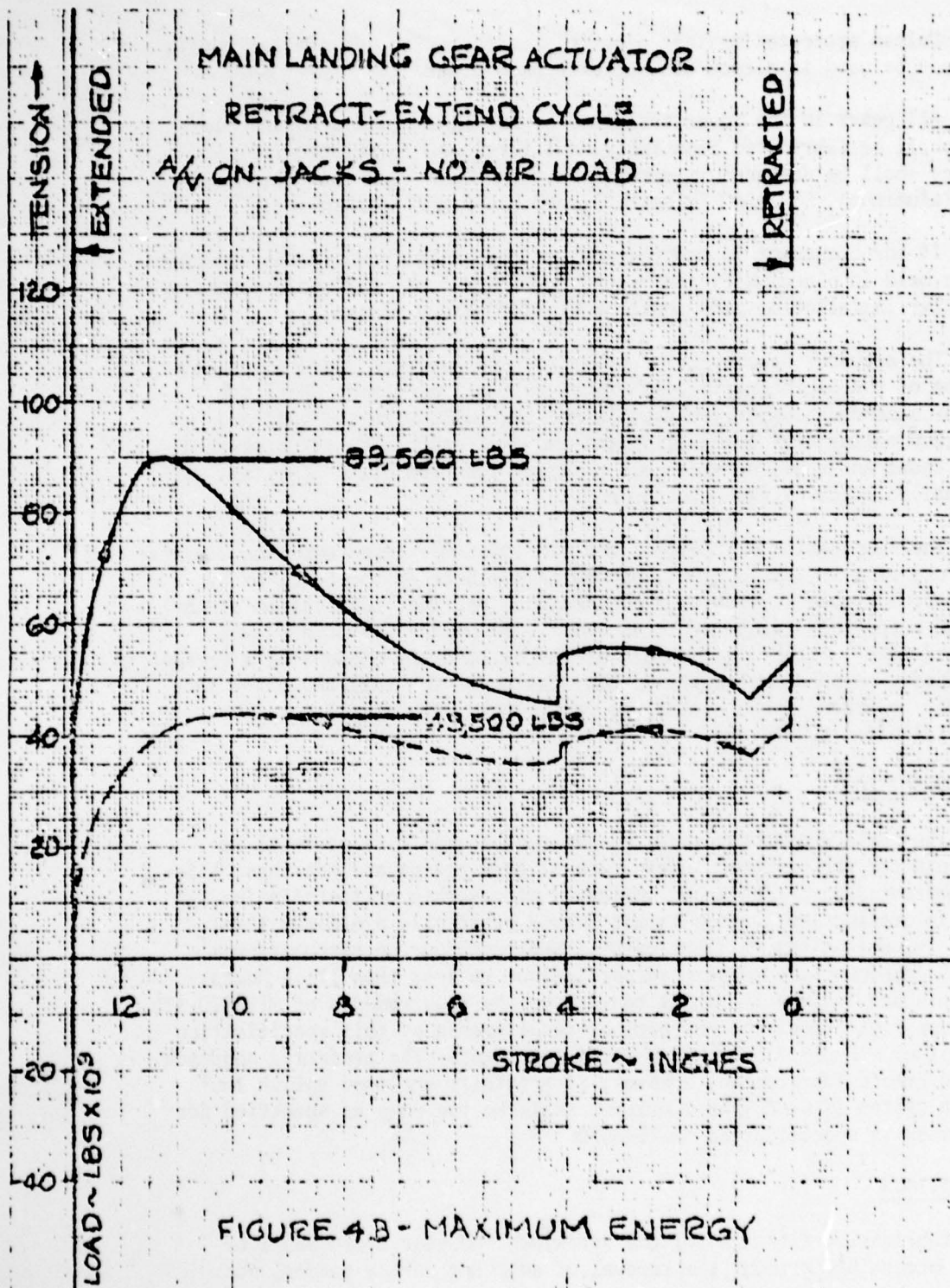


FIGURE 4B - MAXIMUM ENERGY



Unless protected against electrolytic corrosion, dissimilar metals shall not be used in direct contact with each other.

All gears in the power train and other highly loaded moving elements shall be fabricated from individual forgings, if practical. Forgings shall be designed in accordance with MIL-F-7190 (steel), MIL-A-22771 (aluminum), QQ-A-367 (aluminum), and MIL-F-8317 (titanium).

If any component is mounted and secured by bolts where the component must be held in place until the bolts are engaged, pilot keyhole mounting or similar installation aids shall be provided where possible.

The actuator bearings, and other rod end bearings, as applicable, shall be of the plain bearing, spherical self-aligning type. Rotation shall be accommodated between the pin and the ball, with the ball and outer race taking care of misalignment and deflection. The actuator shall be pin ended and shall provide self-aligning features while limiting torsional rotation of the actuator ends.

The lubrication of the ball and pin joint may be accomplished, either by the use of a TFE-based liner, bonded in the bore of the ball, or by the use of a grease lubricated type spherical bearing. Lubrication of the ball and outer race joint may be accomplished by the use of a bonded TFE-based liner, bonded in the bore of the ball, or by the use of a grease lubricated type spherical bearing. Lubrication of the ball and outer race joint may be accomplished by the use of a bonded TFE-based liner, per RI specification L20140-003.

#### F. LUBRICATION

The package assembly shall be designed to minimize or avoid requirements for the periodic lubrication of gear trains and bearings. Lifetime lubricated parts shall be lubricated at assembly or installation only. If lifetime lubrication is not deemed practical, a minimum time between relubrications shall be established but under no circumstances shall the minimum time between relubrications be less than 111.4 hours. Lubricants and lubrication shall conform to the requirements of MIL-STD-838. Gear trains shall meet the performance requirements of this specification using either MIL-G-81522 or MIL-G-21164 lubricants. The preferred approach shall be grease lubrication, however, if a totally enclosed splash lubrication system is used, the lubricant shall be the same as specified for the gearbox in specification NA-75-363B.

#### G. FITTINGS

Lubrication fittings for the screwjack and gear train shall be readily accessible without the removal of adjacent parts, covers, etc.





Provisions for drain plugs shall be such that all lubricants will drain satisfactorily with the MPP unit in its installed position(s).

#### H. INSTRUMENTATION AND SENSORS

Instrumentation shall be provided by Rockwell to measure surface temperature of the screwjack actuator. The instrumentation shall consist of a single iron-constantin pickup located at a spot on the actuator's surface determined by the supplier as being most representative of the critical temperatures occurring inside the actuator during repeated cycles of operation. The temperature pickup shall be capable of measuring temperatures throughout a range of  $-80^{\circ}\text{F}$  to  $300^{\circ}\text{F}$  with an accuracy of  $\pm 8^{\circ}\text{F}$  and shall withstand temperatures ranging from  $-80^{\circ}\text{F}$  to  $+500^{\circ}\text{F}$  without permanently affecting its ability to accurately measure temperatures in the normal operating range. The iron-constantin pickup shall be provided with lead-in wire at least 10 feet long. Instrumentation external to the actuator will be provided by Rockwell to measure input rpm and output linear position and travel speeds during tests conducted at Rockwell.

#### I. OPERATING LIFE

The following requirements are target values for design of the screwjack. The screwjack shall be designed for a total life of 13,500 hours which is broken down as follows:

1. Installed Life (10,694.7 hours) - Screwjack installed in an aircraft which is operating and thus is subject to aircraft induced vibrational, shock and acoustic inputs.
2. MPP Input Operating Life (2722.0 hours) - MPP input section operating but screwjack nonoperating. Thus, the screwjack is subject to both the aircraft and MPP vibrational shock and acoustic inputs.
3. Screwjack Operating Life (83.3 hours) - Screwjack operating extending and retracting the gear 20,000 times (15 second cycles) thus the screwjack is subject simultaneously to the aircraft and MPP vibrational, shock and acoustic inputs as well as the loads imposed by the landing gear load stroke curve.

The screwjack shall demonstrate at least 211.4 hours of operating life (items 4 and 5 of Table I) consisting of 203.07 hours under "MPP Input Operating Life" conditions (screwjack nonoperating) and 8.33 hours (2,000 cycles - 15 seconds each) under "Screwjack Operating Life" conditions. For the purposes of shortening the test time, successive operating cycles will be conducted as close together as possible, however, no test cycle will be started unless the outer housing temperature, as measured by the



Rockwell International

temperature sensor provided with the screwjack, is less than 200°F.

The screwjack shall demonstrate low temperature operating capability. The screwjack shall demonstrate the ability to perform at least two low temperature cycles, using the load stroke curve of Figure 3A, when the maximum input torque available is 396 inch-pounds and retract motion is initiated at a stabilized component temperature of -65°F.

#### J. TEST PLAN AND OPERATING LIFE

The test plan for the various components of the MPP is shown in Table I.

TABLE I  
EQUIPMENT USED

| <u>Test Config.</u> | <u>Hyd Motor</u> | <u>Gear Box</u> | <u>Fly-Wheel</u> | <u>Controller</u> | <u>Screwjack</u> | <u>Test Time (Hrs.)</u> |
|---------------------|------------------|-----------------|------------------|-------------------|------------------|-------------------------|
| 1                   | X                | X               |                  | *                 | *                | 120                     |
| 2                   | X                | X               | X                | *                 | *                | 120                     |
| 3                   | X                | X               | X                | X                 | *                | 200                     |
| 4                   | X                | X               | X                | X                 | X                | 100                     |
| 5                   | X                | X               | X                | X                 | X**              | <u>111.4</u>            |
|                     |                  |                 |                  |                   |                  | 651.4                   |

\* A dummy controller and screwjack will be utilized in these instances to simulate the total MPP configuration.

\*\* A load cylinder will be added to the screwjack output to simulate aircraft system loads.

#### K. ACCEPTANCE TEST

An acceptance test plan shall be developed mutually between the supplier and Rockwell International. Test requirements are TBD.

TFD-77-639

SERIAL NO.

APPENDIX B

MECHANICAL POWER PACKAGE TEST REQUIREMENTS

*C. W. Helsley Jr.*  
C. W. Helsley  
ENERGY SYSTEM PROGRAM MANAGER

DATE 6-20-77  
NO. OF PAGES 017



Los Angeles Aircraft Division  
Rockwell International  
International Airport, Los Angeles, California 90009, (213) 670-9151



# MECHANICAL POWER PACKAGE (MPP) TEST REQUIREMENTS

## OBJECTIVE

The objective of these tests is to evaluate the performance and endurance characteristics of an energy storing mechanical power package unit when applied to an aircraft utility function. The function selected is that of the B-1 aircraft's main landing gear actuation and the basic test rig which will be used is the main landing gear actuator qualification (MLGAQ) test rig. Using this test rig it is the objective of the test program to verify the performance of each individual component as it is received and as it is built up into a complete MPP. It is also the objective of the program to both performance test and endurance test the complete MPP assembly.

## Test Components and Fixtures

The basic components which will be tested individually and collectively as an MPP assembly are as follows:

| <u>Item</u>        | <u>Part No.</u> | <u>Supplier</u>     |
|--------------------|-----------------|---------------------|
| 1. Gearbox Assy    | 2341-00         | J. Maddock          |
| 2. Hydraulic Motor | AMOSC-25        | Abex                |
| 3. Flywheel        | D589-210        | Rockwell            |
| 4. Controller      | 1-76-2          | Traction Propulsion |
| 5. Screwjack       | TBD             | J. Maddock          |

With the exception of the flywheel (item 3 above) all components will initially be tested in the B-1 (MLGAQ) test rig. The flywheel will initially be tested in the IR&D bearing/seal test rig after which it will be phased into the sequential build up of the MPP as it is tested on the MLGAQ test rig.

The sequence of the testing will be as follows:

Test sequence "A"

Hydraulic Motor and Gearbox

Test sequence "B"

Add flywheel

Test sequence "C"

Add controller

Test sequence "D"

Add screwjack

Test sequence "E"

MPP performance

Test sequence "F"

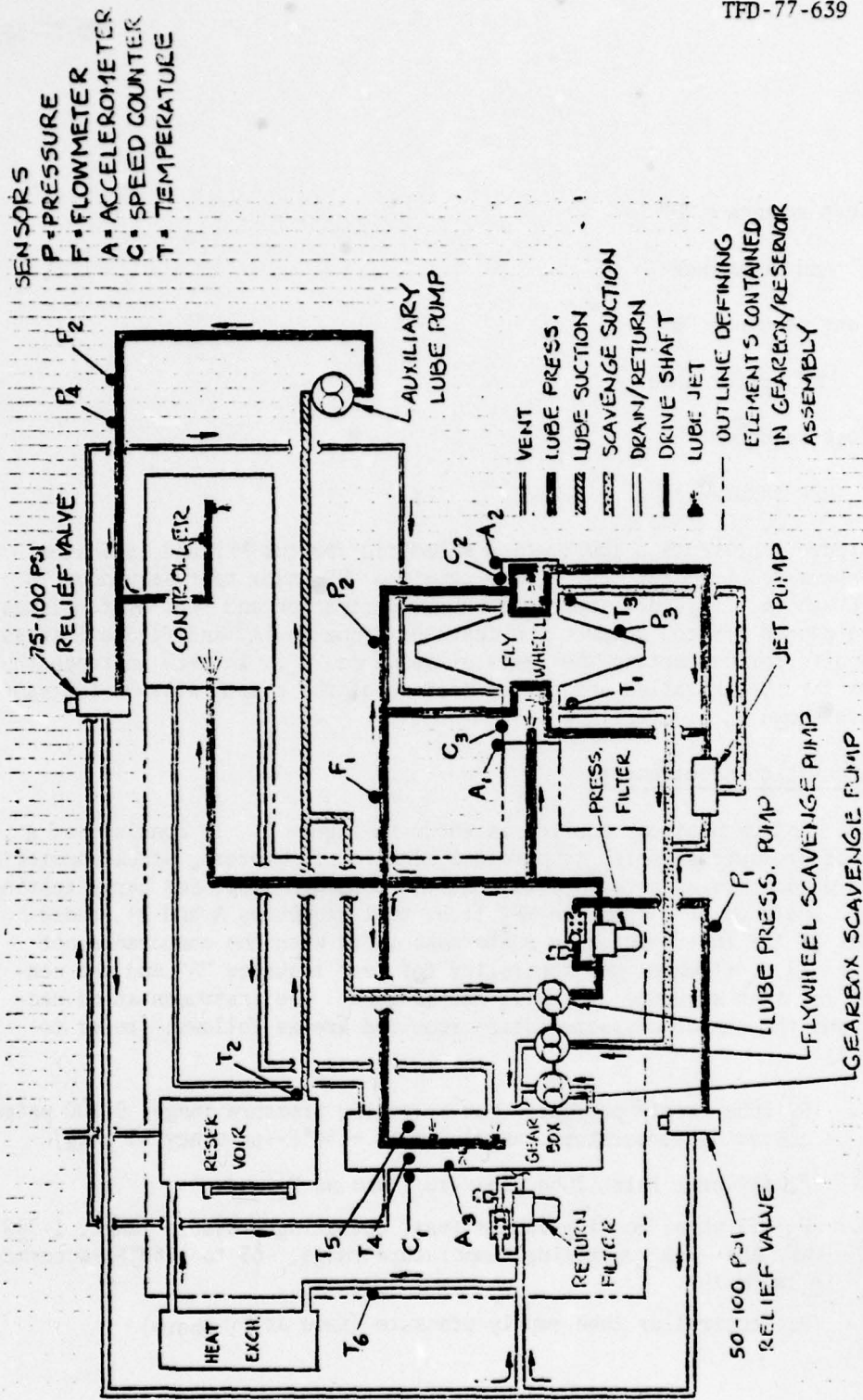
MPP endurance

Figure 1 presents a lubrication schematic for the MPP and indicates the sensors required for testing the complete MPP under test sequences "D" thru "F" above. Figure 2 indicates where lubrication and vent system lines must be capped off to conduct the tests of sequence "A" and figure 3 shows the capoffs for conducting the tests of sequence "B". In each instance the sensors for the installed and active portion of the system will be the same as those shown in figure 1.

#### Instrumentation Requirements

The instrumentation required is shown in figure 1. It consists of a series of pressure sensors, temperature sensors, flowmeters, accelerometers and speed counters as necessary to test the complete MPP. For early testing prior to build up of a complete MPP (i.e. test sequences A and B), those portions of the instrumentation suite associated with the components not installed (i.e. flywheel and controller for test sequence "A" and the controller for test sequence "B") will not be used. The instrumentation necessary and the sensor characteristics required are as follows: (refer to figure 1)

1. (P<sub>1</sub>) lube supply pressure (max operating pressure range, 0-100 psig--operating temperature range, -65 to +180°F--accuracy +1 psig)
2. (P<sub>2</sub>) flywheel inlet lube pressure (same as P<sub>1</sub> above)
3. (P<sub>3</sub>) flywheel housing vacuum (max. operating pressure range, 1-700 mmHg Abs--max. operating temperature range, -65 to +160°F--accuracy  $\pm$  1mmHg Abs.)
4. (P<sub>4</sub>) controller lube supply pressure (same as P<sub>1</sub> above)



**FIGURE 1**  
**MPP LUBRICATION & COOLING SYSTEM SCHEMATIC**



5. (T<sub>1</sub>) inboard flywheel bearing scavenge return temperature (operating temperature range, -65 to +400°F--accuracy +5°F)
6. (T<sub>2</sub>) reservoir suction temperature (operating temperature range -65 to +200°F--accuracy +4°F)
7. (T<sub>3</sub>) outboard flywheel bearing scavenge return temperature (same as T<sub>1</sub> above)
8. (T<sub>4</sub>) inboard gearbox high speed bearing temperature (same as T<sub>1</sub> above)
9. (T<sub>5</sub>) outboard gearbox high speed bearing temperature (same as T<sub>1</sub> above)
10. (T<sub>6</sub>) lube return temperature (same as T<sub>1</sub> above)
11. (A<sub>1</sub>) inboard flywheel bearing vibration acceleration (set of three triaxially mounted accelerometers--operating temperature range, -65 to +300°F--frequency measurement range, 0 to 5000 Hz--operational acceleration range, 0 to 100 G)
12. (A<sub>2</sub>) outboard flywheel bearing vibration acceleration (same as A<sub>1</sub>)
13. (A<sub>3</sub>) gearbox vibrational acceleration (same as A<sub>1</sub>)
14. (C<sub>1</sub>) hydraulic motor pad input speed count (operational speed range 0-12,600 RPM--operating temperature range, -65 to 300°F)
15. (C<sub>2</sub>) outboard flywheel bearing inner race speed count (operational speed range, 0-92647 RPM--operating temperature range, -65 to 300°F)
16. (C<sub>3</sub>) inboard flywheel bearing inner race speed count (same as C<sub>2</sub>)
17. (F<sub>1</sub>) flywheel bearing system lube flow (operating flow range, 0 to 5GPM--operating temperature range, -65 to 200°F-- accuracy + 0.1 GPM)
18. (F<sub>2</sub>) controller lube flow (same as F<sub>1</sub> above)

All data shall be presented to the test operator through suitable gages, traces or printouts on a real time basis. All data shall be recorded on suitable tapes, traces and printouts using a common time base so that they can be reviewed at a later time and/or can be included in reports.

#### Test Sequence "A"

Using a dummy mounting fixture, the gearbox and motor shall be mounted in the same approximate position in relation to the MLGAQ test rig, as it will have when it is part of the total MPP. The dummy mounting fixture shall attach to, and provide a capoff for, the controller mounting pad on the gearbox. Test Sequence "A" capoff requirements are shown in figure 2.

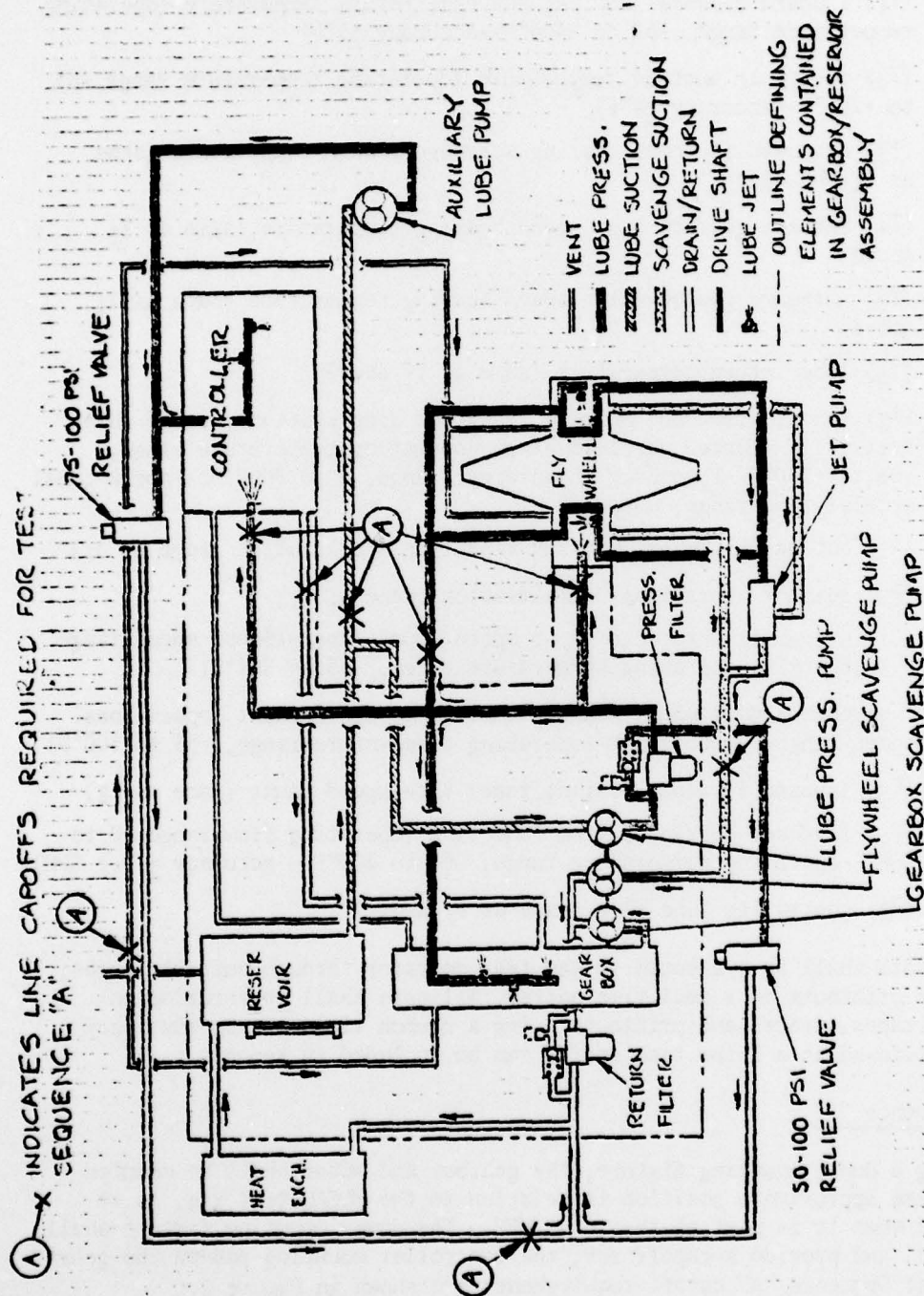


**FIGURE 2**  
MPP LUBRICATION & COOLING SYSTEM SCHEMATIC

An additional plate shall be provided to capoff the flywheel mounting pad on the gearbox. Both of the capoff devices will provide a centrally located port which will collect the lube oil (especially that oil which would normally be jetted from the gearbox into the controller and into the flywheel in the fully built up MPP) and direct it, through appropriate plumbing, to the inlet of the flywheel scavenge pump. A sleeve, or other suitable device, shall be provided to support the flywheel pad output shaft. Normally the outer end of the output shaft would be supported by the flywheel, however, in its absence, some other means of support will have to be created to prevent the shaft from whipping.

Prior to starting the test the lubrication reservoir shall be filled to the reservoir full level. The fluid used shall be Santotrac 30. The hydraulic motor shall be powered by a 4000 psi system using either MIL-H-5606 or M2V fluid.

For the test sequence, a series of gradual acceleration and dwell tests shall be run. During all tests the following parameters shall be monitored and recorded.

1. Gearbox input speed ( $C_1$  in figure 1)
2. Gearbox high speed shaft bearing temperatures ( $T_4$  and  $T_5$  figure 1)
3. Hydraulic motor "in" pressure
4. Hydraulic motor "out" pressure
5. Hydraulic motor input flow
6. Reservoir out temperature ( $T_2$  in figure 1)
7. Heat Exchanger in temperature ( $T_6$  in figure 1)
8. Vibration ( $A_3$  in figure 1)

For the lower end of the speed range, acceleration and dwells shall be made in increments of 1400 RPM up to 8400 RPM hydraulic motor pad speed ( $C_1$  in figure 1). Dwells shall be made at the end of each acceleration and shall be made at the following speeds:

1400  $\pm$  20 RPM  
2800  $\pm$  20 RPM  
4200  $\pm$  20 RPM  
5600  $\pm$  20 RPM  
7000  $\pm$  20 RPM  
8400  $\pm$  20 RPM



Each dwell shall be maintained until all measured parameters stabilize, or for 5 minutes, whichever comes first. The acceleration of shaft speed between dwells shall be conducted at  $200 \pm 50$  RPM/second.

At the higher end of the speed range (8400 to 11,968 RPM) smaller increments shall be used. In this speed regime the speed shall be increased in five increments of approximately 714 RPM/increment as follows:

9114  $\pm$  20 RPM  
 9828  $\pm$  20 RPM  
 10452  $\pm$  20 RPM  
 11256  $\pm$  20 RPM  
 11968  $\pm$  20 RPM

Each dwell shall be maintained until all parameters stabilize. Stabilization shall be deemed to have been achieved when the mean of the parameter value changes less than 0.1% per minute. Acceleration to the next dwell level shall be attempted only after stabilization has been achieved. The shaft speed acceleration between dwell levels shall be the maximum of which the hydraulic motor is capable when 2800 psi effective differential pressure exists between the motor's pressure and return ports.

All sequence "A" tests shall be conducted at an "oil in" temperature ( $T_2$  in figure 1) of  $170 \pm 10^\circ\text{F}$ . "Oil out" temperature ( $T_6$  in figure 1) shall not exceed  $275^\circ\text{F}$  and high speed shaft bearing temperatures ( $T_4$  and  $T_5$  in figure 1) shall not exceed  $300^\circ\text{F}$ . The exceedance of these temperatures shall be cause for shutdown of the test.

The tare power losses for the gearbox at each dwell speed shall be determined and plotted. This loss shall be determined by subtracting the known power loss of the hydraulic motor from the total power loss of the sequence "A" configuration as determined by the differential pressure and flow measurements taken at the motor inlet. The tare losses shall not exceed 1.5 H.P. at rated motor speed (11,968 RPM)

The vibrational characteristics of the sequence "A" test configurations as measured by the  $A_3$  accelerometers in figure 1, shall be recorded during all accelerations and dwells. Under no conditions shall the trace bandwidth as recorded by the  $A_3$  accelerometers exceed 20G. Accelerations greater than 20G shall be cause for shutdown of the test unit.

Upon completion of the 11968 RPM dwell the test unit shall be accelerated to 105% of rated speed (12,566 RPM max  $C_1$  speed) The unit shall be held at

the speed for one minute  $\pm$  0.1 minute and then decelerated to 100% rated speed in  $15 \pm 5$  seconds. During all accelerations and decelerations resonance points shall be noted and their approximate magnitude recorded.

Upon completion of the overspeed test and the return to 100% rated speed, a measurement shall be made to determine first; the controller pad lube jet flow and second; the flywheel pad lube jet flow. This may be accomplished by alternately redirecting the flow collected by each pad's capoff device through suitable valving to a measuring beaker. The flows, measured at 50 psig relief valve setting, shall be as follows:

|                   |                   |
|-------------------|-------------------|
| Flywheel Pad      | Controller Pad    |
| $.05 \pm .01$ GPM | $0.4 \pm .05$ GPM |

Upon completion of 100% rated speed testing the speed shall be reduced to 70% (8400  $\pm$  20 RPM  $C_1$  speed) and the test repeated. The flows, measured at 50 psig relief valve setting, shall be as follows:

|                   |                   |
|-------------------|-------------------|
| Flywheel Pad      | Controller Pad    |
| $.04 \pm .01$ GPM | $0.3 \pm .04$ GPM |

The test unit shall be shut down and allowed to coast to a stop. Speed temperature, flow pressure and acceleration data shall continue to be recorded during the shut down.

#### Test Sequence "B"

The cap covering the flywheel pad on the gearbox shall be removed and the flywheel added to the test unit and plumbed as shown in figure 3\*. With the addition of the flywheel, sensors A1, A2, C2, C3, T1, T3, P2, P3, and F1, (see figure 1) will become active and will provide data for monitoring and recording.

For this test sequence a series of acceleration and dwell tests plus an overspeed and a shutdown will be run which duplicates the tests in test sequence "A". The tare power losses for the flywheel under a particular test condition shall be determined by subtracting the total sequence "A" test unit configuration losses, from the sequence "B" test unit configuration losses under the same test conditions to determine the net losses.

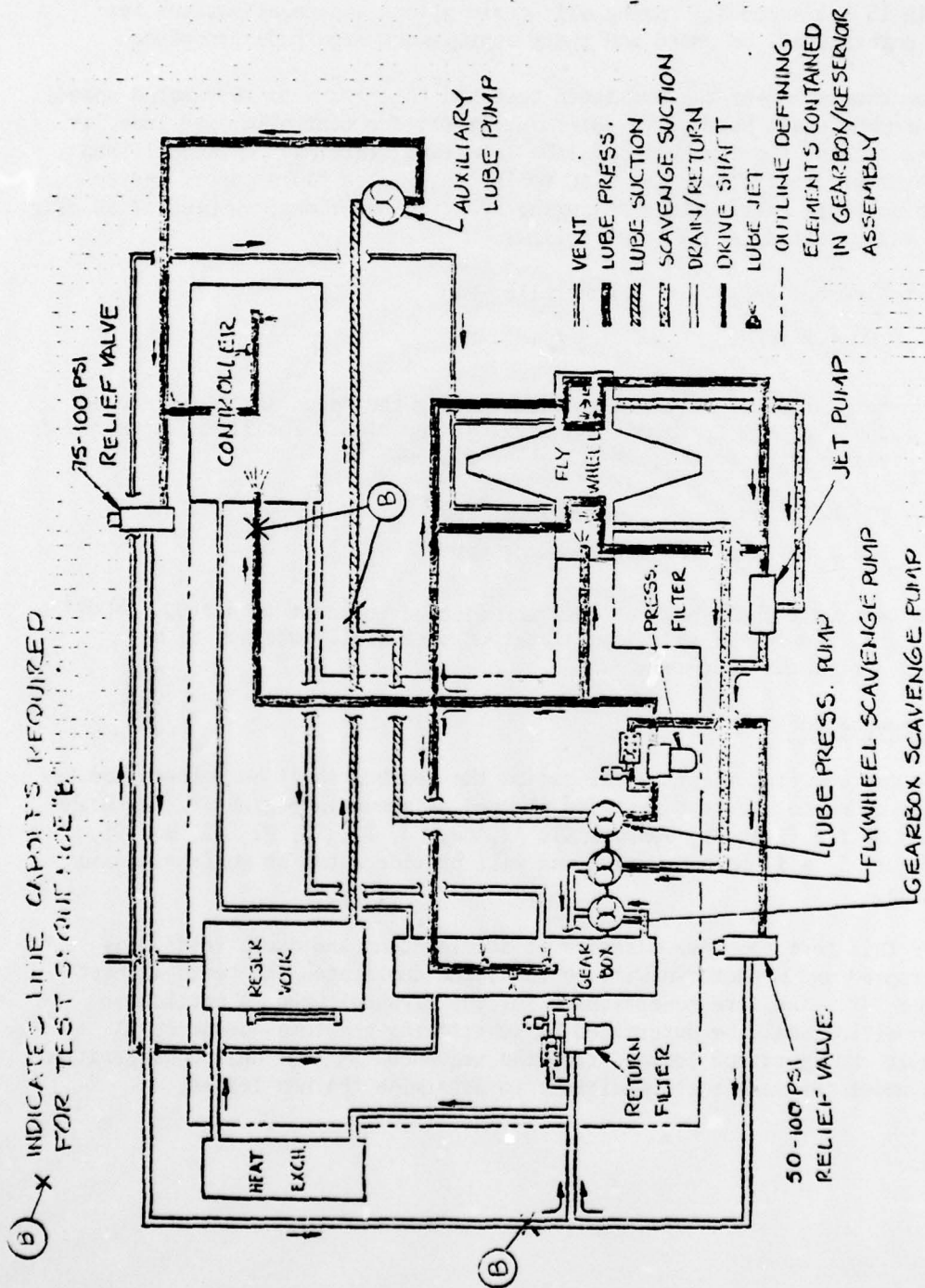


**FIGURE 3**  
MPP LUBRICATION & COOLING SYSTEM SCHEMATIC



During all test sequence "B" tests and all subsequent tests, the flow to the flywheel as measured by flow meter  $F_1$ , (figure 1) shall not exceed .4GPM at this flow, and, at an oil supply temperature of 180°F max as measured at  $T_2$ , the lube oil return temperatures as measured at  $T_1$ ,  $T_2$ , and  $T_6$  shall never exceed 300°F.

#### Test Sequence "C"

For test sequence "C" the controller shall be added to the test unit. The modular portion of the dummy mounting fixture which simulated the controller shall be removed and replaced by the actual controller. The plumbing shall be revised to the full MPP lubrication and cooling system configuration shown in figure 1. This means that all capoffs will be removed as well as the tee into the gearbox scavenge pump inlet lines. All scavenge lines will be routed as shown in figure 1.

In addition to the sensors shown in figure 1 provisions will be made for a bi-directional speed counter which will be attached to the output shaft of the controller. This counter will be capable of counting clockwise and counterclockwise shaft speeds up to 10,000 RPM with an accuracy of  $\pm 10$  RPM. Provisions will also be made so that the output shaft can be locked using a torque measuring device capable of measuring torques up to 500 in-lb with an accuracy of  $\pm 5$  in-lb.

#### Tests

1. With a neutral signal applied to the controller, start up the MPP and accelerate to  $8378 \pm 20$  RPM ( $C_1$  speed). This shall be done with 2800 psi differential pressure across the motor's ports unless acceleration exceeds 2,250 RPM/second, in which case the differential pressure shall be throttled back to maintain no more than 2,250 RPM/second. Under these conditions there shall be no signs of skidding or other distress in the controller. During the acceleration the output shaft may turn but shall not exceed 25 RPM in either direction at any time. Acceleration time shall not exceed 1.5 minutes max.
2. Lock the controller output with the torque measuring device and apply a retract signal. Static output torque shall fall within the limits of  $410 \pm 15$  in-lb. Note: The controller should not be operated with a locked output for more than 10 minutes at a time.
3. Remove the retract signal with the output still locked by the torque measuring device. Output static torque shall drop to  $0 \pm 25$  in-lb biased in the retract direction.

4. Repeat steps 2 and 3 using an extend signal. Output torque values shall be the same except biased in the extend direction.
  5. During tests 2 through 4 oil shall be supplied by the auxiliary pump at the rate of  $.65 \pm .05$  GPM (see figure 1) and oil shall be supplied by the gearbox lube jet through the central shaft at  $.3 \pm .05$  GPM. The auxiliary lube pump relief valve shown in figure 1 shall be set initially at  $75 \pm 3$  psi. It shall be the objective of these tests, and all subsequent tests, to set this oil flow rate and pressure at a value as low as feasible (but not less than 50 psi) while still meeting the controller response requirements. Another limitation on setting the oil flow rate and pressure shall be the requirements that the oil out temperature as measured at  $T_6$  shall not exceed  $240^\circ\text{F}$ . The oil in temperature, as measured at  $T_2$  shall not exceed  $180^\circ\text{F}$ . Figure 4 shows the maximum allowable temperature rise for fluid entering the MPP (leaving the heat exchanger) at other temperatures.
- \*Note: The lube scavenge lines which ran from the pad caps to the inlet of the flywheel scavenge pump shall be disconnected and the one coming from the flywheel cap shall be removed to the controller lube scavenge line shall be rerouted to "T" into the gearbox scavenge pump inlet.

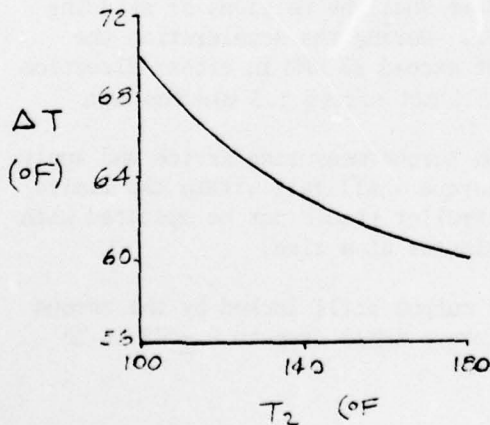


**FIGURE 4**  
**LUBE AND COOLING FLUID**  
**ALLOWABLE TEMPERATURE**  
**RISE**

6. Steps 2 through 4 shall be repeated at 11,968 RPM  $C_1$  speed. All output torques shall fall in the same limits as before. However, the oil shall be supplied by the auxiliary pump at a flowrate of  $.85 \pm 0.5$  GPM in conjunction with a gearbox lube jet flow through the controller's central shaft of  $.4 \pm .05$  GPM for a combined flow to the controller of approximately 1.3 GPM. At this flow, and with a lube oil supply temperature ( $T_2$ ) of 180°F, the MPP outlet lube oil ( $T_6$ ) shall not exceed 300°F. A ( $T_6$ ) temperature higher than 300°F shall be cause for shutdown of the test. The maximum temperature rise for conditions under which the lube oil is supplied at lower temperatures is shown in figure 5. The acceleration time from the 8378 RPM of step 1 to the 11,968 RPM of this step shall not be more than 2 minutes.

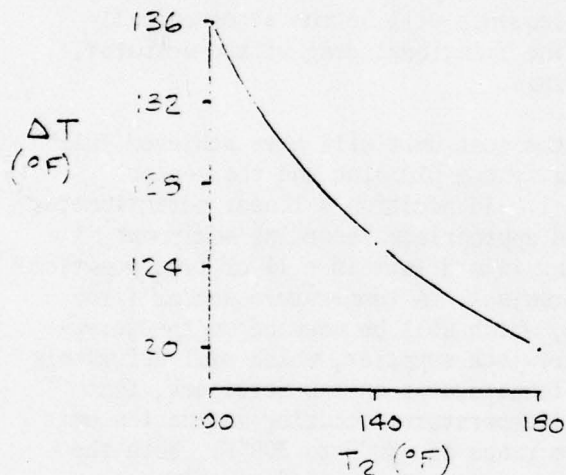


**FIGURE 5**  
**LUBE AND COOLING FLUID**  
**ALLOWABLE TEMPERATURE**  
**RISE**

7. At an input speed of 11,968 RPM ( $C_1$ ) speed, apply a retract signal with the output free to rotate. The output shall accelerate smoothly to a speed of  $7500 \pm 75$  RPM counterclockwise (looking at the controller output pad) within one second max. The controller shall be allowed to operate at this condition for five minutes, or until temperature stabilization, whichever occurs first. Upon removal of the retract signal the output shall decelerate smoothly and in a controlled manner at a rate of  $9500 \pm 500$  RPM/second to an output speed of  $\pm 25$  RPM.



8. Repeat test #7 at input ( $C_1$ ) speeds of  $10173 \pm 20$  RPM and  $8373 \pm 20$  RPM. The controller output shall accelerate smoothly to a speed of  $6375 \pm 64$  RPM and  $5250 \pm 53$  RPM respectively and when the retract signal is removed, shall decelerate smoothly at a rate of  $8075 \pm 500$  RPM/sec. and  $6650 \pm 500$  RPM/second respectively.
9. Repeat tests #7 and #8 except apply and remove an extend signal.

#### Test Sequence "D"

For test sequence "D" the screwjack shall be added to the test unit. The last remaining portion of the dummy mounting fixture (i.e. the segment which simulated the screwjack) shall be removed and replaced by the screwjack test unit. For all sequence "D" tests the MLGAQ load cylinder shall be unpressurized and vented and thus all tests for this sequence will be run at essentially no load except for load represented by the frictional drag of the actuator, the linkage, and the screwjack end bearings.

With the addition of the screwjack the test unit will have achieved full MPP status. The lubrication and cooling system plumbing and the sensor installation will be as shown in figure 1. In addition a linear potentiometer or other appropriate sensing device, and appropriate recording equipment shall be provided to accurately sense and record (within  $\pm 1\%$  of true position) the real time output position of the screwjack. A temperature sensor (iron constantin type) shall also be provided, which will be mounted on the screwjack at a location designated by the screwjack supplier, which will accurately measure ( $\pm 8^\circ\text{F}$  accuracy) those surface temperatures on the screwjack, that are most representative of the critical temperatures occurring inside the unit and will measure them over a temperature range of  $-80^\circ\text{F}$  to  $300^\circ\text{F}$ . Both the position and temperature data shall be continuously recorded at all times when the screwjack is actually operating.

The screwjack actuator will come equipped with microswitches (or equivalent) which will indicate when the actuator is at the extend position, the retract position, and at a point approximately one inch from the retract and extend positions. A functional and continuity check of these switches shall be conducted at a very low and controlled input speed (less than 10% rated  $C_1$  speed) to verify that the limit switches are properly rigged (44.68 in. screwjack extend length and 31.84 in. screwjack retract length) and that the snub switches actuate at the proper point along the screwjack stroke (43.68 in. screwjack extend length and 32.84 screwjack retract length.)

With the screwjack in the extend position the MPP input speed ( $C_1$  speed in figure 1) shall be increased to  $11,968 \pm 20$  RPM and held at this speed until temperatures and flows stabilize but shall not be held for more than 5 minutes. Alternate "Extend"-Retract" signals shall be applied to the controller. The rate of signal applications shall be increased from slow ( $\frac{1}{2}$  extend-retract cycle/min) to the maximum rate which can be achieved without dropping the flywheel speed below 70% rated (8378 RPM  $C_1$  speed) but not faster than 1 extend-retract cycles/min. Once the fastest cycling rate has been established cycling shall continue at this rate for 50 cycles or until oil return temperatures as measured at  $T_6$  (figure 1) tend to exceed  $275^\circ\text{F}$ . If the oil return temperature measured at  $T_6$  tends to exceed  $275^\circ\text{F}$ , or the scavenge oil temperatures measured at  $T_1$  and  $T_3$  tend to exceed  $300^\circ\text{F}$ , or the screwjack body temperature  $T_7$  tends to exceed  $200^\circ\text{F}$  at the start of the next cycle, the rate of cycling shall be reduced until the peak temperatures experience each cycle stabilize at a value at least  $10^\circ\text{F}$  below the limiting values stated above. Under all conditions the screwjack motion portion of the cycle shall be completed in 7.5 to 8.0 seconds.



### Test Sequence "E"

Test Sequence "E" differs from test Sequence "D" in that loads shall be applied to the load cylinder. The MLGAQ (load cylinder shall be set up to apply 4 load levels to the MPP. The loads applied shall have the general characteristics of the load versus stroke curve as shown in figure 3A of the Screwjack Actuator Specification NA75-527. For a particular load level, the absolute value of load at any stroke position shall be a certain percentage of the value shown in figure 3A. The load levels and their percentage of figure 3A loads are as follows:

- Load Level 1 - 25%
- Load Level 2 - 50%
- Load Level 3 - 75%
- Load Level 4 - 100%

Starting at load level 1, actuate the MPP through 10 "extend" - "retract" cycles at each load level in sequence. The actuation cycles may be run at any convenient rate up to 1/2 cycle/minute. The ambient temperature shall be  $80 \pm 15^\circ\text{F}$  during the tests. At no time during the tests shall the  $T_1$ ,  $T_3$  or  $T_7$  temperatures exceed the limits given for these temperatures in the preceding test sequence "D" writeup.

Upon completion of load level 4 tests the loads applied to the MPP shall be changed to match the characteristic load curve shown in figure 3B of specification NA75-527. Ten extend-retract cycles shall be conducted at this characteristic load. At no time shall the flywheel speed drop below 70% rated speed (i.e. below 61765 RPM) provided each specific cycle was initiated within 1% of rated speed (i.e. 89,117 to 87353 RPM). After the completion of ten retract-extend cycles the cycle rate shall be increased to the maximum practicable, but not more than 1 cycle/min, without overheating the unit or underspeeding the flywheel. Temperatures shall not exceed those listed as limits in the sequence "D" writeup and the flywheel shall have recovered to within 1% of rated speed prior to initiation of the next half cycle. Sufficient cycles (but not more than 50) shall be run to show that the temperatures and flywheel speed excursions have been stabilized and that the maximum practicable cycle rate has been achieved. The screwjack motion portion of each "extend" or "retract" half cycle shall be completed in 7.5 to 8.5 sec.

During all sequence "E" tests, the operation of the unit shall be smooth. At no time shall the load cell on the load cylinder show a peak load greater than 107,100 lbs during operations using figure 3A load characteristics nor greater than 89,500 lbs using figure 3B. At all other points along the load-stroke curve deviations from the curve chargeable to the MPP shall not be greater than  $\pm 5000$  lbs.

Attempts shall be made during sequence "E" testing to eliminate the auxiliary lube pump (see figure 1). This shall be done by increasing the relief setting of the MPP lube relief valve (50-100 psi) to equal that of the auxiliary lube relief valve (75-100 psi). The auxiliary lube relief valve setting will be that determined as the minimum practicable during test sequence "C" test #5 testing and verified (or modified) during subsequent testing. The increase in relief valve setting may cause excessive flow through the various





MPP lube jets and the jet pump. If this proves to be true certain selected lube jets, or all of the lube jets and the jet pump, shall be reworked to smaller orifice sizes. Appropriate flowmeters shall be installed in the MPP lube relief valve return line (F<sub>3</sub>) and the auxiliary lube relief valve return line (F<sub>4</sub>). When F<sub>3</sub> equals or exceeds the controller flow demand F<sub>2</sub> - F<sub>4</sub> (F<sub>2</sub> as shown on figure 1) as determined at the same pressure setting the auxiliary lube pump shall be deleted and the functions it serviced shall be plumbed into the MPP lube pressure system. The auxiliary lube relief valve shall be removed along with any surplus plumbing and its inlet and outlet lines shall be capped. At least 10 extend/retract cycles, at the maximum rate previously established, shall be performed after the auxiliary lube pump is removed to verify performance.

#### Test Sequence "F"

Test sequence "F" shall constitute the MPP endurance test. Using the cycle rate and the test configuration established during test sequence "E", 2000 endurance cycles shall be completed. The loads applied for 25 of these cycles shall be in conformance with figure 3B of NA75-527 and the balance (1975 cycles) shall be in conformance with figure 3A. The MPP shall be started up and shut down at least 20 times during the test. The following conditions shall prevail during this portion of the test:

|   |  |
|---|--|
| Flywheel Speed                                | 99,235 rpm max.<br>61,765 rpm min.<br>(except shutdowns)                                   |
| Hydraulic Motor Speed                         | 11,968 rpm max<br>8378 rpm min<br>(except shutdowns)                                       |
| Acceleration Time<br>(Startup to rated speed) | 3 min, max @ 80°F ambient  |
| Recovery time after half cycle                | 1.5 min max @ 160°F(T <sub>2</sub> )   |
| Maximum allowable temperatures                | T <sub>2</sub> = 180°F<br>T <sub>6</sub> = 275°F<br>T <sub>4</sub> &T <sub>5</sub> = 300°F |
| Ambient                                       | 95°F max   |
| Maximum Acceleration                          | A <sub>3</sub> = 20g Bandwidth   |



At the end of the endurance test, a low temperature test shall be conducted. The MPP shall be cold soaked to  $-40^{\circ}\text{F}$ . The unit shall be cooled until temperature sensor  $T_2$  (figure 1) has shown a temperature reading of  $-45^{\circ}\text{F}$  for at least one hour. The unit shall then be allowed to warm slowly until  $T_2$  reads  $-40 \pm 1^{\circ}\text{F}$  and the readings of the other temperature sensors in the unit ( $T_1$ ,  $T_3$ ,  $T_4$ ,  $T_5$  and  $T_6$ ) are within  $\pm 5^{\circ}$  of the  $T_2$  reading.  $T_2$  shall be held at  $-40 \pm 1^{\circ}\text{F}$  for at least one hour at which time the MPP unit shall be started. The hydraulic fluid supplied to the unit shall be warm ( $60^{\circ}\text{F min}$ ).

At the time of start initiation, the fluid in the lines close to the hydraulic motor shall be as warm as possible consistent with maintaining all temperature sensors at the required uniform low temperature. Under these conditions and with a 2800 psi differential pressure across the motor the hydraulic motor shall be capable of bringing the flywheel up to rated speed within 6 minutes. Using load curve of figure 3A NA75-527 cycle the test unit within  $8^{+0.5}_{-0}$  minutes after start initiation. The performance of the MPP shall be normal except that the screwjack motion time during the first half cycle (extend or retract) may take up to 12 seconds to complete instead of the normal 7.5 to 8.5 seconds and the flywheel may droop below 70% rated rpm. A complete extend-retract cycle shall be completed within 5 minutes.

Repeat the cold start test at  $-65^{\circ}\text{F}$ . All test conditions shall be the same except longer start up times and cycle times are acceptable as follows:

Time to rated speed = (18 minutes instead of 6 min.)

Time for start of first cycle after start initiation =  $(21^{+1.0}_{-0}$  minutes instead of  $8^{+0.5}_{-0}$  min.)

First half cycle motion = (16 seconds instead of 12 seconds) time of screwjack

Complete extend-retract = (8 minutes instead of 5 min.) cycle